Liposomal Drug Delivery to Brain Cancer Cells

Taahirah Boltman

UNIVERSITY of the
WESTERN CAPE

A thesis submitted in partial fulfilment of the requirements for the degree Master of Science in Nanoscience, in the Department of Medical Biosciences, University of the Western Cape

Supervisor: Dr Okobi Ekpo
Co-supervisor: Prof. Mervin Meyer

May 2015

ABSTRACT

Neuroblastomas (NBs) are the most common solid extra-cranial tumours diagnosed in childhood and characterized by a high risk of tumour relapse. Like in other tumour types, there are major concerns about the specificity and safety of available drugs used for the treatment of NBs, especially because of potential damage to the developing brain. Many plant-derived bioactive compounds have proved effective for cancer treatment but are not delivered to tumour sites in sufficient amounts due to compromised tumour vasculature characterized by leaky capillary walls. Betulinic acid (BetA) is one such naturally-occurring anti-tumour compound with minimum to no cytotoxic effects in healthy cells and rodents. BetA is however insoluble in water and most aqueous solutions, thereby limiting its therapeutic potential as a pharmaceutical product. Liposomes are self-assembling closed colloidal structures composed of one or more concentric lipid bilayers surrounding a central aqueous core. The unique ability of liposomes to entrap hydrophilic molecules into the core and hydrophobic molecules into the bilayers renders them attractive for drug delivery systems. Cyclodextrins (CDs) are non-reducing cyclic oligosaccharides which proximate a truncated core, with features of a hydrophophilic outer surface and hydrophobic inner cavity for forming host-guest inclusion complexes with poorly water soluble molecules. CDs and liposomes have recently gained interest as novel drug delivery vehicles by allowing lipophilic/non-polar molecules into the aqueous core of liposomes, hence improving the therapeutic load, bioavailability and efficacy of many poorly water-soluble drugs.

The aim of the study was to develop nano-drug delivery systems for BetA in order to treat human neuroblastoma (NB) cancer cell lines. This was achieved through the preparation of BetA liposomes (BetAL) and improving the percent entrapment efficiency (% EE) of BetA in liposomes through double entrapment of BetA and gamma cyclodextrin BetA inclusion complex (γ-CD-BetA) into liposomes (γ-CD-BetAL). We hypothesized that the γ-CD-BetAL would produce an increased % EE compared to BetAL, hence higher cytotoxic effects.

Empty liposomes (EL), BetAL and γ-CD-BetAL were synthesized using the thin film hydration method followed by manual extrusion. Spectroscopic and electron microscopic characterization of these liposome formulations showed size distributions of 1-4 μm (before extrusion) and less than 200 nm (after extrusion). As the liposome size decreased, the zeta-potential (measurement of liposome stability) decreased contributing to a less stable liposomal formulation. Low starting BetA concentrations were found to be more effective in

entrapping higher amounts of BetA in liposomes while the incorporation of γ-CD-BetA into liposomes enhanced the % EE when compared to BetAL, although this was not statistically significant.

Cell viability studies using the WST-1 assay showed a time-and concentration-dependent decrease in SK-N-BE(2) and Kelly NB cell lines exposed to free BetA, BetAL and γ-CD-BetAL at concentrations of 5-20 ug/ml for 24, 48 and 72 hours treatment durations. The observed cytotoxicity of liposomes was dependant on the % EE of BetA. The γ-CD-BetAL was more effective in reducing cell viability in SK-N-BE(2) cells than BetAL whereas BetAL was more effective in KELLY cells at 48-72 hours. Exposure of all cells to EL showed no toxicity while free BetA was more effective overall than the respective liposomal formulations

The estimated IC_{50} values following exposure to free BetA and BetAL were similar and both showed remarkable statistically significant decrease in NB cell viability, thus providing a basis for new hope in the effective treatment of NBs.

KEYWORDS:

Betulinic Acid (BetA)

Cyclodextrin (CD)

Liposomes

Neuroblastomas (NBs)

DECLARATION

I, Taahirah Boltman, declare that “Liposomal Drug Delivery to Brain Cancer Cells” is my own work and has not been submitted before for any degree or examination at this university or any other tertiary institute. This mini-thesis is being submitted in fulfilment for the Masters of Science in Nanoscience degree at the University of the Western Cape, Cape Town.

Signature.....

Date.....

TABLE OF CONTENTS

CHAPTER 2: MATERIALS AND METHODS

LIST OF FIGURES

LIST OF TABLES

LIST OF ABBREVIATIONS

AFM	Atomic Force Microscopy
AIF	Apoptosis inducing factor
ALK	Anaplastic Lymphoma kinase
ANS	Autonomic Nervous System
Apaf-1	Apoptotic protease activating factor 1
AZT	Azidothymidine
B1	Batch 1
B2	Batch 2

Bax	Bcl-2-Associated X Protein
BBB	Blood–Brain Barrier
Bcl-2	B-cell lymphoma 2
BCSFB	Blood–Cerebrospinal Fluid Barrier
BDNF	Brain-Derived Neurotrophic Factor
Bet	Betulin
BetA	Betulinic Acid
BetAL	Betulinic Acid Liposome
BMP	Bone Morphogenic Protein
BTB	Blood-Tumour-Barrier
CAD	Caspase-Activated DNAse
CARD	Caspase Recruitment Domain
Caspase	Cysteine Aspartic Acid-Specific Protease
CDs	Cyclodextrins
Chol	Cholesterol
CNS	Central Nervous System
CP	Choroid Plexus
Cryo-TEM	Cryo-Transmission Electron Microscopy
CSF	Cerebrospinal Fluid Brain Barrier
CT	Computed Tomography
CVOs	Circumventricular Organs
DISC	Death-Inducing Signalling Complex

DLS	Dynamic Light Scattering
DMEM	Dulbeco's Modified Eagles Medium
DMSO	Dimethyl Sulfoxide
DNA	Deoxyribonucleic Acid
DPPC	Dipalmitoylphosphatidylcholine
DSC	Differential Scanning Calorimetry
EE	Entrapment/Encapsulation Efficiency
EL	Empty Liposome
EPC	Egg Phosphatidylcholine
EPR	Electron Paramagnetic Resonance
EPR	Enhanced Permeability and Retention
EMT	Epithelial-to-Mesenchymal Transition
FADD	Fas-Associated Death Domain
GB	Glioblastoma
GUVs	Giant Unilamellar Vesicles
HR-TEM	High Resolution-Transmission Electron Microscopy
HtrA2	High Temperature Requirement Protien-A2
IAPs	Inhibitor of Apoptosis Proteins
IKK	Inhibitor of NF-Kb Kinase
INSS	International NBs Staging System
JAMs	Junctional Adhesion Molecules
LDE	Laser Doppler Electrophoresis

LUVs	Large Unilamellar Vesicles
MB	Medulloblastoma
MLV	Multilamellar Vesicles
MMV	Multivesicular Vesicles
MNPs	Magnetic Nanoparticles
MNS	Motor Nervous System
MRI	Magnetic Resonance Imaging
MRPs	Multidrug Resistance-Associated Proteins
NAC	N-acetyl-cysteine
NB	Neuroblastoma
NBs	Neuroblastomas
NC	Neural Crest
NF-kB	Nuclear factor- kB
NMR	Nuclear magnetic resonance
NPs	Nanoparticles
NS	Nervous System
P-gp	P-glycoprotein
PBN	N-tert-butyl-a- phenylnitrone
PBS	Phosphate Buffered Saline
PC	Phosphatidylcholine
PCS	Photon Correlation Spectroscopy
PE	Phosphatidylethanolamine

PEG	Polyethylene glycol
PG	Phosphatidylglycerol
PHOX2B	Paired-like homeo-box 2b
PI	Polydispersity Index
PL/PLs	Phospholipid(s)
PNS	Peripheral Nervous system
PS	Phosphatidylserine
PSNS	Parasympathetic Nervous System
PVP	Polyvinylpyrrolidone
PYSNS	Parasympathetic nervous system
SD	Standard Deviation
SENS	Sensory nervous system
SMAC	Second Mitochondrial-Derived Activator of Caspase
SNS	Somatic Nervous System
SUV	Small unilamellar vesicles
SYNS	Sympathetic Nervous System
RES	Recticular Endothelial System
ROS	Reactive Oxygen Species
Tc	Phase Transition Temperature
TLC	Thin Layer Chromatography
TNF	Tumour Necrosis Factor
TRADD	Receptor Associated Death Domain

UHPLC	Ultra-High Liquid Chromatography
ULVs	Unilamellar Vesicles
γ-CD	Gamma-Cyclodextrin
γ-CD-BetA	Gamma-Cyclodextrin Betulinic Acid Inclusion Complex
γ-CD-BetAL	Gamma-Cyclodextrin Betulinic Acid Liposomes
ζ-potential	Zeta-potential

DEDICATION

For my dearest family...

The Prophet Muhammad (Peace Be Upon Him) said, regarding knowledge:

"Acquire knowledge and impart it to the people...One who treads a path in search of knowledge, has his path to Paradise made easy by God" (Sunan Tirmidhi, Hadith 107; Riyadh us-Saleheen, 245).

ACKNOWLEDGEMENTS

First and foremost all praises and gratitude to my creator for sustaining me through this study, only through your strength and guidance was I able to persevere and complete my Masters! I would like to express my deepest gratitude to my supervisor Dr Okobi Ekpo and my co-supervisor Prof. Mervin Meyer for the knowledge gained, encouragement, support and motivation throughout the duration and the completion of this research. I would also like to express my heartfelt thanks to Dr Naushaad Ebrahim of the School of Pharmacy (UWC) for his invaluable advice, suggestions and assistance. I am grateful for the guidance provided to develop into a prospective researcher.

Also my sincere appreciation goes to Mr Yunus Kippie of the School of Pharmacy, for his technical assistance and insight with the ultra-high liquid chromatography and in the Physics department; I am once again thankful and appreciative to Mr Adrian Joseph for his technical assistance with scanning electron microscopy. May God reward you both for your generosity! I extend my sincere gratitude to Bridget Daniels, Valencia Jamalie and Chyril Abrahams for their helpfulness, motivation, and encouragement. The friendly and positive attitudes always displayed by these three women were an inspiration to me.

I forward my appreciation towards all my colleagues at the School of pharmacy, Department of Biotechnology and Medical Biosciences Department. To my wonderful classmates of the MSc Nanosciences class of 2013, I miss you all dearly and wish you success for the future! Many new friendships were established in the course of this research and I would like to extend my gratitude to all of these people for their kindness, generosity and support! A heartfelt thank you to my amazing friends and cousins for all your encouragement and support.

To my beloved family I love you all, thank you for being my support structure! Especially my sweet grandparents (Miriam and Omar) for always whispering words of encouragements in my ears and praying for me, my wonderful parents (Faizah and Ashraf) and my brothers (Thaabit and Zaheer)-*Shukraan!* Not forgetting my entertaining four-legged family member "Kitty", thank you for always trying to sit on my keyboard while I type and sipping my coffee. I would like to thank the National Nanoscience Teaching and training Platform, Department of Science and Technology and NIC for funding this research.

CHAPTER 1

INTRODUCTION AND LITERATURE REVIEW

1.1 Development of Cancer

The human body comprises of many different cells all proliferating and differentiating under the control of various related regulatory mechanisms. Some of these mechanisms involve several cell checkpoints which are responsible for detecting and correcting irregularities in deoxyribonucleic acid (DNA). In spite of these processes, DNA damage could occur through diet, hormonal imbalances, tobacco use, radiation exposure, environmental factors and certain infections (Cretney *et al.,* 2007). In the event of DNA damage, normal cells would trigger a DNA repair mechanism but failure to do this, results in genomic instability (Gotter, 2009).

Apoptosis or programmed cell death is initiated to ensure that cells are abolished and cannot multiply. A failure to execute apoptosis can cause the progression of abnormal cell proliferation which is one of the most prominent characteristics of cancer (Gotter, 2009). Cells can divide uncontrollably and out-compete the normal cells for nutrients thereby displacing normal cells and forming masses of purposeless tissues called tumours (Cooper, 2000; Quail and Joyce, 2013). Tumours could be benign (non-cancerous) or malignant (cancerous). Benign tumours lack the ability to invade other areas of the body whereas malignant tumours have the ability to metastasise to other parts of the body through the lymphatic system or the bloodstream (Maccauro *et al.,* 2011).

1.2 Tumour Vasculature

Tumour cells, similar to normal cells in the human body require nutrients, oxygen and the ability to eliminate harmful metabolic waste products and carbon dioxide. Stages involved in initial tumour growth depend on diffusion of nutrients; however when a tumour reaches a size of approximately 2 mm^3, diffusion from surrounding blood vessels becomes limited and may lead to hypoxia and nutrient deficiency (Rong *et al.,* 2006). This results in the development of vasculature within the tumour through recruitment of endothelial cells and angiogenic factors to construct new blood vessels from existing blood vessels to the site of the tumour; a process termed angiogenesis (Danhier *et al.,* 2010; Yoo and Kwon 2013). The increase in blood supply generates highly disorganised and abnormal vasculature marked with regions having a rich blood supply and others with low blood supply (Danhier *et al.,* 2010; Goel *et al.,* 2012). Poor vasculature results in dead end vessels with incomplete endothelial linings causing leaky

and highly permeable tumour vessels (Dudley, 2012; Goel *et al.*, 2012). Important hallmarks of malignant cell growth have been identified to include: self-sufficiency in growth signals, insensitivity to antigrowth signals, unregulated proliferation potential, an increase in blood supply to the tumour, metastasis, evading the immune system, reprogramming of energy metabolism and importantly, evasion of apoptosis (Hanahan and Weinberg, 2000; 2011).

1.3 The Nervous System

The nervous system (NS) is a highly sophisticated organ system comprising a network of specialised cells called neurons (Stahl, 2008). The brain is composed of approximately 86 billion neurons (Azevedo *et al*., 2009) which are the essential information-processing units of the NS, responsible for receiving and transmitting electrical and chemical signals between different parts of the human body (Stahl, 2008). They are categorized into three types (Figure 1.1): inter-neurons (which constitute the majority of neurons in the brain, conduct thought processes, vision and perception of surroundings); motor neurons (receive impulses from the brain to cause muscular contraction and gland secretion) and sensory neurons (receive information from sense organs and relay it to the brain) (Kandel *et al.*, 1995; Lodish *et al*., 2000; Martini, 2006).

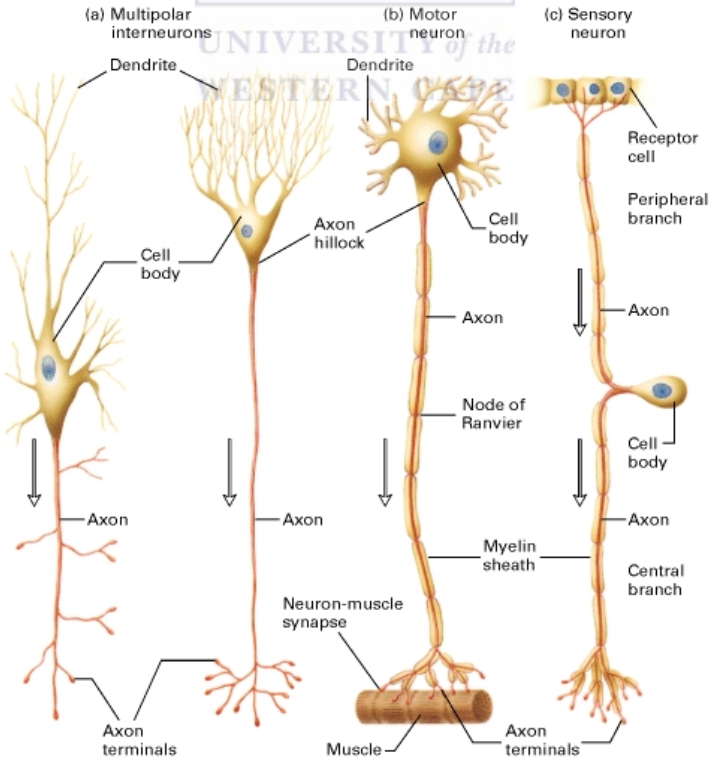

Figure 1.1 Schematic illustration of the structure of three different types of neurons*: a) Multi-polar inter-neurons, b) Motor neuron and c) Sensory neuron, with their major components. Arrows indicate the direction of the conduction of action potentials (Adapted from Lodish et al., 2000).*

A typical neuron constitutes three essential parts (Figure 1.1, p. 2): Cell body/soma (which contains the nucleus and cytoplasm), dendrites (which receive electrochemical stimulation from other neural cells) and axons (which conduct electrical impulses away from the soma, towards other neurons, muscles or glands) (Kandel *et al.*, 1995; Martini, 2006). Motor and sensory neurons have long axons covered by a myelin sheath, which assists in the speed of neural impulses (Morell and Quarles, 1999). The spaces in between myelin sheaths where axons are exposed are called 'Node of Ranvier' (Figure 1.1). Neurons can communicate in three different ways: electrical synapse, emphatic interaction and chemical synapse, with the latter being the most predominant form of communication within the brain (Kendal *et al* 1995). When a signal is received by dendrites, it is transmitted to the soma via an electrochemical signal and passes through the axon to the axon terminals, which form junctions with other cells (Figure 1.1). Pre and post synaptic neurons are in close proximity to each other and are separated by a gap junction called the synapse. Once signals arrive at the axon terminals of a pre-synaptic neuron, neurotransmitters (acetocholine, dopamine, serotonin, etc.) are released to transfer electrochemical signals to post-synaptic neurons (Purves *et al.*, 2001; Martini, 2006).

The NS is divided into two parts: the central nervous system (CNS) and the peripheral nervous system (PNS) (Figure 1.2):

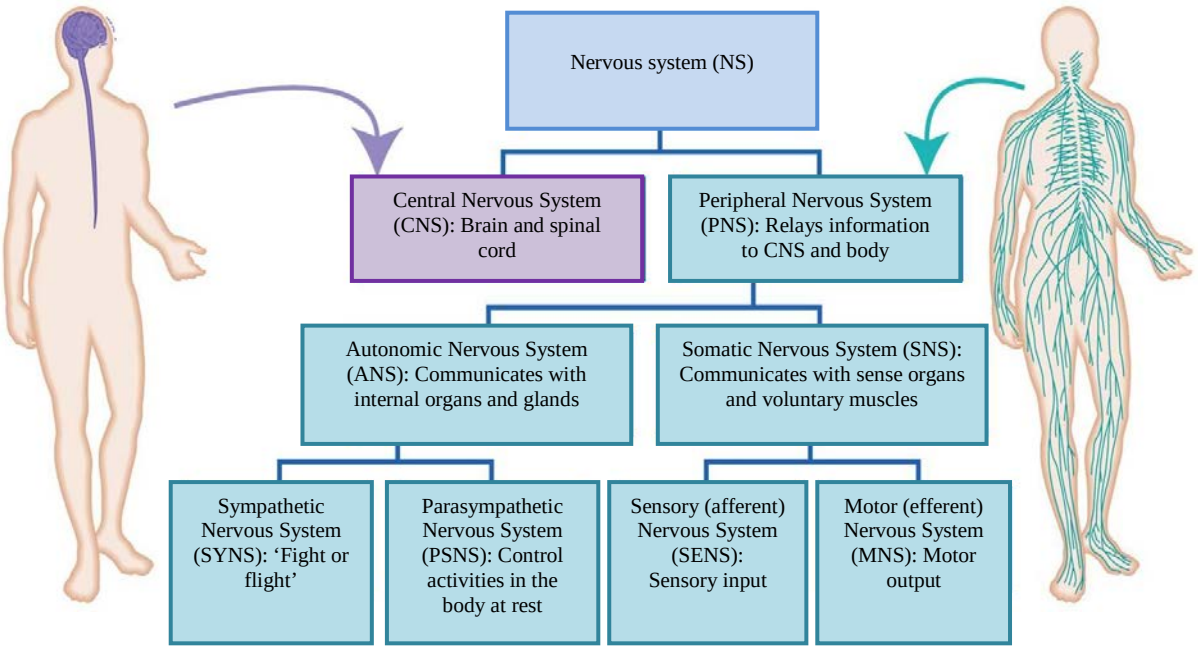

Figure 1.2 Flowchart representing the divisions and sub-divisions of the NS (*Adapted from http://classconnection.s3.amazonaws.com/420/flashcards/1094420/jpg/nervous_system_organization1328056081853.jpg with modifications).*

The CNS comprises of the brain and the spinal cord, located and protected by the skull and the vertebral column. The CNS receives information from the human body and coordinates sensory data and motor commands (Shepherd, 1987; Bear *et al*., 2006). The PNS constitutes all the nerves which relay information from the brain to the rest of the body (Shepherd, 1987; Bear *et al*., 2006). The PNS connects the CNS to sensory organs (e.g., eyes, ears, muscles, glands and blood vessels) and is further sub-divided into the somatic nervous system (SNS) and the autonomic nervous system (ANS) (Figure 1.2, p. 3) (Martini, 2006).

The ANS, also called the visceral NS or involuntary NS, consists of two main sub-divisions: the sympathetic nervous system (SYNS) and the parasympathetic nervous system (PSNS) (Figure 1.2, p. 3) (Martini, 2006; McCorry, 2007). The PSNS is responsible for control of digestion activities when the body is at rest, it also includes salvation, urination, defecation, sexual arousal and lacrimation (tear production) (McCorry, 2007). The SYNS allows the body to manage under stressful conditions and also controls the 'fight-or-flight' response (Martini, 2006). The SYNS consists of nerve fibres that run along the spinal cord, clusters of nerve cells called ganglia and nerve-like cells found at the medulla of the adrenal gland (Martini, 2006; McCorry, 2007). The main function of the SYNS is to allow the dilation of the pupils, inhibit salvation, relaxing of the bronchi of the lungs, acceleration of the heart, inhibits digestive activity, stimulates glucose by the liver, secretion of epinephrine and norepinephrine from the kidneys, relaxes the bladder and contracts the rectum (Bear *et al*., 2006; Martini, 2006; McCorry, 2007).

1.4 Central Nervous System (CNS) Cancers

More than 100 brain tumour types based on clinical presentation, genetics, histopathological features and malignancy have been recognized by the World Health Organization (WHO) (Fuller, 2008). Brain tumours are the second most common cancers in men (ages 20-39) and the fifth most common cancers in woman (ages 20-39). An estimated 23,380 new brain and other NS cancer cases were projected for 2014 in America, with more males being affected than females (12,820 men versus 10,560 females) (Siegal *et al.*, 2014). In the paediatric age group, tumours of the CNS account for 30% with the majority of other cases belonging to the groups of lymphomas, sarcomas, or embryonal tumours like nephroblastoma, hepatoblastoma, and neuroblastoma (Stiller, 2004). CNS embryonal tumours originate in embryonic cells that remain in the brain after birth and could potentially spread through the cerebrospinal fluid to other parts of the brain and spinal cord (Shalaby *et al*., 2014). The

global burden of CNS diseases is expected to increase to 14% in 2020 (Blasi *et al.*, 2007). Most NS tumours are difficult to treat with a low survival rate. They are known to grow aggressively, metastasize profusely and are resistant to current treatments (Van Meir *et al.*, 2010; Westphal and Lamszus, 2011). Any brain tumour is life-threatening because of its invasive and infiltrative nature within the limited intracranial cavity.

1.5 Neuroblastoma (NB)

Neuroblastomas (NBs) are the most common extra-cranial solid brain tumours to be diagnosed in infancy and childhood (Nuchtern, 2012), accounting for 7-8 % of all childhood cancers and affecting 10.2 per million children under the age of 15 years old in the USA (Cheung and Dyer, 2013). Approximately 75 % of diagnosed cases present with metastases, increased aggressiveness and chemo-resistance in children older than one year old (Kaatsch, 2010). Significant strides have been achieved in identifying prominent molecular and genetic markers for NB, however this disease remains one of the major challenges confronting paediatric oncology especially since the five year survival rate for patients presenting with high risk NB tumours remains below 40 % (Maris *et al*., 2007; Jiang *et al*., 2011). Children treated for high-risk NB also have the greatest risk of treatment-related complications, including severe hearing loss, infertility, cardiac toxicity, and secondary cancers related to the use of high-dose chemotherapy (Brodeur *et al*., 2011).

NB belongs to a group of embryonal tumours, which is characterised by a failure of precursor cells to exit from a proliferative phase and enter the differentiation process (Grimmer and Weiss, 2006). NB has been numerously reported to originate from the neural crest element of the SYNS during embryology (Acosta *et al*., 2009; Jiang *et al.*, 2011; Cheung and Dyer, 2013; Marshal *et al*., 2014).

1.5.1 NBs and Neural Crest Development

The formation of the CNS in embryology is called neurulation (Copp, 2005). The first step in neurulation is the formation of a neural plate which forms at the cranial end (the future brain region) of the embryo and grows towards the caudal end (the future spinal cord region). Neural crest (NC) development takes place in roughly the third week of embryogenesis, where the lateral edges of the neural plate border elevates and move together to form the neural fold which fuse together to form the neural tube (Figure 1.3, p. 6) (Copp, 2005; Bhatt *et al.*, 2013). The NC is masses of tissue located at the edges of the lateral plates of the

folding neural tube and constitutes multipotent NC cells (Simões-Costa and Bronner, 2013). Once the neural tube has completely fused, the process of neurulation is complete. NC cells start to populate the dorsal part of the neural tube (Figure 1.3) (Simões-Costa and Bronner, 2013).

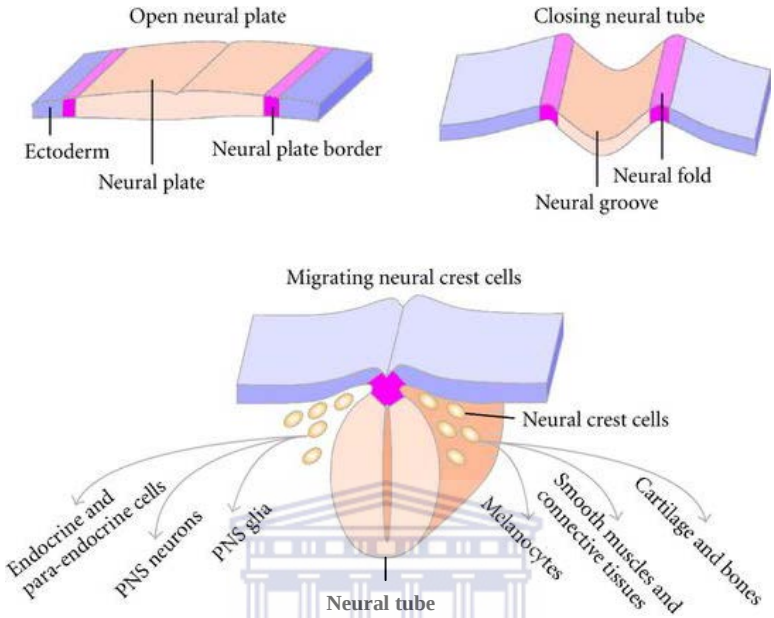

Figure 1.3 The process of neurulation. *The Neural crest (NC) development occurs in the third week of embryogenesis, where the lateral edges of the neural plate border elevate and form the neural fold which fuses together to form the neural tube. NC cells then migrate laterally along the sympaticoadrenal lineage of the SYNS and form a variety of diverse cell types (Adapted from Wislet-Gendebien et al., 2012).*

A group of NC cells are programmed to undergo an epithelial-to-mesenchymal transition (EMT) (Simões-Costa and Bronner, 2013). EMT is a process whereby polarised epithelial cells undergo multiple biochemical changes allowing it to acquire a mesenchymal cell phenotype, which includes improved migratory capacity, invasiveness and elevated resistance to apoptosis (Kalluri and Neilson, 2003; Kalluri and Weinberg, 2009). EMT is completed by the degradation of underlying basement membrane and the formation of mesenchymal cells that can migrate away from the neural tube (Figure 1.3) (Theveneau and Mayor, 2012). Migratory NC cells start to migrate laterally along migratory pathways and form a variety of diverse cell types, including PNS neurons, PNS glia, Schwann cells, cartilage and bones, melanocytes in the skin, smooth muscles and connective tissue (Figure 1.3) (Theveneau *et* Mayor, 2012; Wislet-Gendebien *et al*., 2012). Cells populate the primordia of the sympathetic ganglia and the adrenal gland, and finally differentiate into the sympathoadrenal lineage of

sympathetic neurons and adrenal chromaffin (endocrine) cells (Mora and Gerald, 2004; Park *et al.,* 2008; Taneyhill, 2008; Kulesa *et al*., 2009; Bhatt *et al.,* 2013).

The guidance of NC cells along migratory routes and the control of processes involved in cell proliferation and differentiation into sympathoadrenal lineage is highly dependent on extracellular signals from the microenvironment and intracellular signalling events that induce the complex process of NC formation (Gammill and Bronner-Fraser, 2003; Huber, 2006). Disturbances within these precisely controlled processes, especially the maintenance of proliferation and differentiation at specific points can initiate the transformation of NC cells to give rise to neuroblastic tumours (Mora and Gerald, 2004). The Sonic Hedgehog and Wnt signalling pathways, fibroblast growth factor and bone morphogenic protein (BMP proteins) are required for proper NC development and have been implicated in NB development (Schneider *et al*., 1999; Martinez-Morales *et al.,* 2005; Dupin *et al.,* 2007; Shahi *et al*., 2008).

Therefore NB can be considered as a malignant tumour of pre-cursor or undifferentiated neuroectodermal cells derived from the NC (Kamijo, 2012). Embryonic migration of NC cells relate the fact that NB can occur anywhere along the sympaticoadrenal lineage of the SYNS, however 65 % of primary NB tumours arise in the abdomen with the medulla of the adrenal gland being predominantly associated (Park *et al*., 2008). The paraspinal ganglia are also commonly associated with NB (Maris, 2010) and it can also develop in other nerve tissues such as PNS nerves, neck (5%), chest (20%), pelvis (5%) abdomen and from mental disorders such as Hirschsprung's disease, congenital central hypoventilation syndrome and neurofibromatosis type 1 (Rohrer *et al.,* 2002; Maris *et al.,* 2007). CNS NBs are rarer and occur in 5-10% of recurring NB cases (Matthay *et al*., 2003). CNS NB form in the nerve tissue of the cerebrum or the layers of tissue that cover the brain and spinal cord (Matthay *et al*., 2003; Yariş *et al*., 2004). CNS NBs may be large and spread to other parts of the brain or spinal cord (Kramer *et al*., 2001; Matthay *et al*., 2003). Presenting symptoms of NBs depend largely on the location of the primary tumour and presence of metastasis.

1.5.2. Genetics of NB

Familial (hereditary) NB is rare and heterogeneous, accounting for less than 5% of all NBs (Maris *et al*., 2002; Maris *et al.,* 2007; Jiang *et al*, 2011). Two of the most common genes associated with hereditary NBs are paired-like homeo-box 2b (PHOX2B) gene and anaplastic lymphoma kinase (ALK) oncogene (Jiang *et al.,* 2011). Germline mutations in the PHOX2B

gene on chromosome 4p13 was the first predisposition mutation gene identified in NB (Mosse *et al.,* 2004; Trochet *et al.,* 2004). PHOX2B encodes a homeo-domain transcription factor responsible for cell cycle exit and neuronal differentiation and is an important factor in the development of NC-derived autonomic neurons and proliferation of immature sympathetic neurons (Raabe *et al.,* 2008). PHOX2B has two polyalanine repeat sequences, but the non-polyalanine repeat mutations that are usually associated with NB-Hischsprung disease and congenital hypoventilation syndrome (Mosse *et al.,* 2004; Trochet *et al.,* 2004). Therefore a disturbance in PHOX2B-regulated differentiation pathway in the sympathoadrenal lineage of the NC is associated with NB tumour progression (Raabe *et al.,* 2008).

The lymphoma ALK gene is expressed in the developing sympathoadrenal lineage of the NC and regulates the balance between proliferation and differentiation through multiple cellular pathways (Motegi *et al.,* 2004, Schönherr *et al.,* 2010). Inherited changes in the ALK oncogene seem to account for most cases of hereditary NB (Mosse *et al.,* 2008 and Jiang *et al.,* 2011). Approximately 8% of all NB tumours are associated with ALK abnormalities, including the somatic cases (Cheung and Dyer, 2013). NB cell lines and primary tumours containing high expression levels of ALK showed high PHOX2B expression suggesting that PHOX2B can directly regulate ALK gene expression, showing a connection between these two pathways that are mutated in familial NB (Bachetti *et al.,* 2010).

LMO1 (LIM domain only 1) was recently linked to NB tumours (Wang *et al.,* 2011). Wang and colleagues over expressed LMO1 in SK-N-BE(2c) NB cell line which caused an increase in cell proliferation rate. Additionally, LMO1 copy number analysis in NB tumours showed copy number gain in 12.4 % of the tumours, which was shown to be associated with increased LMO1 expression (Wang *et al.,* 2011).

The majority of NB is non-familial (sporadic) (Cheung and Dyer, 2013). Three genetic subtypes: 1A, 2A and 2B are used based on their genomic outline. Low stage tumours (subtype 1) present with many abnormalities and a near triploid DNA content. Subtype 2A or 2B are characterized by an unbalance of chromosome 17, 17q gain, present in more than 50% of the cases. Subtype 2A contains 11q deletions, commonly together with 3p deletions (Cheung and Dyer, 2013). DNA alterations have been reported at chromosome arms 1q 160–162, 2q 163, 4p 164, 9p 165, 14q 166 and 19q 167 (Cheung and Dyer, 2013). Chromosomal deletions indicate tumour suppressor genes while chromosomal gains may cause presence of

oncogenes (Cheung and Dyer, 2013). Subtype 2B tumours present with MYCN amplification, often together with 1p deletions (Cheung and Dyer, 2013).

The proto-oncogene MYCN is a helix-loop-helix transcription factor that regulates growth, differentiation, angiogenesis, metabolism and apoptosis in the developing CNS (Wakamatsu *et al.*, 1997). Expression of MYCN is a strong intracellular stimulus for ventral migration of NC cells. It is present in moderate levels in the nuclei of all trunk NC cells before and during migration and several signalling pathways regulates its expression (Grimmer and Weiss, 2006). MYCN is most commonly associated with sporadic aggressive NB tumours and occurs in approximately 22-25% of NB tumours and is associated with poor outcome (Althoff *et al*., 2015).

1.5.3 Classification of NB Cancer

"International NBs Staging System" (INSS) (Table 1.1 and Figure 1.4, p. 10) was initiated to determine the stages of NBs according to its anatomical presence at diagnosis.

Table 1.1 International NBs Staging System (INSS) for NB with risk classification (Brodeur *et al.*, 1988; Brodeur, 2003; van Noesel and Versteeg *et al.*, 2004; Maris *et al.*, 2007):

INSS staging	Description	Risk classification
Stage 1	The tumour is confined to the area of origin.	Low risk
Stage 2A	The cancer remains localized to the area of origin, but NB cells may be present in the lymph nodes enclosed within the tumour. The lymph nodes outside the tumour may be free of cancerous cells.	Low risk/ Intermediate risk
Stage 2B	Cancer has spread from point of origin and lymph nodes surrounding the tumour. Surgery may be used remove the tumour.	Low risk/ High risk
Stage 3	Surgical intervention is often complicated as the tumour infiltrates across the midline with or without regional lymph node involvement; or unilateral tumour with contra-lateral lymph node involvement; or midline tumour with bilateral lymph node involvement.	Intermediate risk/High risk
Stage 4	The tumour has spread to distant sites such as distant lymph nodes, skin, bone marrow or other organs, however the criteria does not match that of stage 4S.	Intermediate risk/ High risk
Stage 4S	Stage 4S: The child is younger than one year old and the cancer originated from one side of the body but may disseminate to the lymph nodes on the same side but not on the opposite side. Less than 10% of the bone marrow cells are cancerous. The cancer can be disseminating to the other organs but it is limited to liver, skin or bone marrow.	Low risk/ High risk

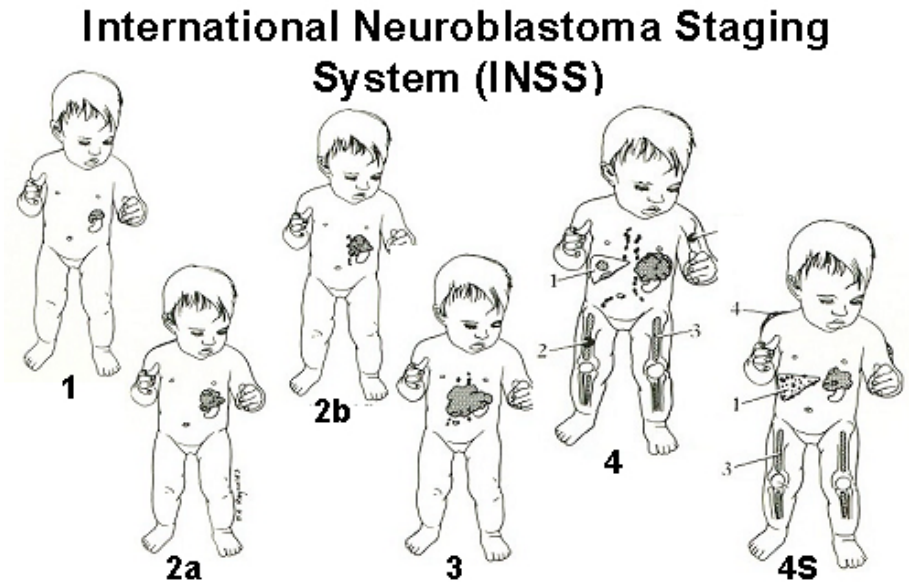

Figure 1.4 International Neuroblastoma Staging System (INSS) for NB based on anatomical presence
(Source: *http://www.nant.org/Patients_and_Families/neuroblastoma.php*).

1.5.4 Current Diagnosis and Treatment of NB Cancer

A multidisciplinary approach is commonly applied for the diagnosis and therapy of this cancer. Diagnosis is usually confirmed with imaging techniques such as magnetic resonance imaging (MRI) scan, computed tomography (CT) scan or positron emission tomography (PET) scan, with surgical tissue extraction for further lab analyses also done (Sharp *et al*., 2011).

A strong independent prognostic factor in NB is age. Children under the age of 18 months have localized tumours, allowing for easier diagnosis while in older children; NB has metastasized making diagnosis increasingly difficult, eluding to the fact that diagnosis of patients with high risk NB have a poor survival rate (Maris *et al*., 2007; Cohn *et al*., 2009).

Treatment usually involves a combination of chemotherapeutic drugs since removing the entire tumour is difficult however due to the high infiltrative nature, surgical intervention is necessary to assist in reducing the tumour size and radiotherapy usually follow shortly after (Wen and Kesari, 2008). Low risk groups such as NB stage 1 and stage 2 tumours are localized and can be treated successfully by surgical intervention followed by chemotherapy treatment (Jiang *et al.,* 2011). Stage 4S NBs risk group without MYCN amplification may regress spontaneously and require no treatment (Jiang *et al.,* 2011). The reported survival rate of patients with low risk NB is greater than 95% (Alvarado *et al.,* 2000; Simon *et al.,* 2004; Park *et al.,* 2008).

Intermediate risk groups such as stage 3 and 4 also rely on surgery and combination chemotherapy (Jiang *et al.*, 2011). Radiation may be used to remove residual tumours and patients who respond poorly to initial treatments and experience recurrence are treated with an aggressive form of chemotherapy (Jiang *et al.*, 2011). Approximately 70–90% cure rate is associated with this risk group (Matthay *et al.*, 1999; Schmidt *et al.*, 2000; Park *et al.*, 2008).

High risk groups with unfavourable biological features and those with MYCN amplification at stage 4S are more challenging to treat as the cancer has metastasized (Matthay, 1995; Castleberry *et al.*, 1997; Brodeur, 2003). At this late stage patients have poor prognosis and approximately 20-50% of high risk NB cases show a low response to high-dose chemotherapy and also demonstrates multi drug resistance (Maris and Matthay, 1999). High risk NB is treated with chemotherapy, surgery, radiation, bone marrow or hematopoietic stem cell transplant among other methods (Maris, 2010). Despite all these available treatments, the overall cure rate for high-risk patients was only about 30 % during the past two decades (Matthay *et al.*, 1999; Pearson *et al.*, 2008; Zage *et al.*, 2008).

Common chemotherapeutic drugs used singly or in combination for the treatment of NBs includes Cyclophosphamide/ifosfamide, Cisplatin/carboplatin, Vincristine, Doxorubicin (Adriamycan), Etopside, Topotecan, Busulfan and Melphalan (Simon *et al*., 2007; Kushner *et al*., 2010; Bagatell *et al*., 2011; London *et al*., 2011; DuBois *et al*., 2012; French *et al*., 2013; Kushner *et al*., 2013). Patients in the paediatric age group with high-risk NB can be treated with 13-cis-retinoic acid (isotretinoin) to reduce the risk of recurrence after high-dose chemotherapy and stem cell transplant (Veal *et al*., 2013; Sonawane *et al*., 2014). A monoclonal antibody called ch14.18 attaches to the ganglioside GD2, a substance found on the surface of many NB cells (Navid *et al*., 2010; Yang *et al*., 2010). This antibody can be given in conjunction with cytokines (immune system hormones) such as GM-CSF and interleukin-2 (IL-2) and is now part of the routine treatment for many children with high-risk NB also after a stem cell transplant (Navid *et al*., 2010).

Some of the drugs used to treat NBs are known to have toxic side effects. Short term side effects include hair loss, mouth sores, loss of appetite, diarrhoea, compromised immune system, nausea and vomiting. Cyclophosphamide and ifosfamide are known to damage the bladder and reproductive organs thereby affecting fertility (Emadi *et al*., 2009). Doxorubicin is frequently associated with cardiotoxicity, while cisplatin and carboplatin induce nephrotoxicity and hearing loss (Kumar *et al*., 2012; Schacht *et al*., 2012). The most common

side effect of 13-cis-retinoic acid is drying and cracking of the lips and nosebleeds (Scheinfeld and Bangalore, 2006). Vincristine may induce neuropathy and ch.14.18 cause severe nerve pain and leaking of fluid in the body which could lead to a decrease in blood pressure, increase in heart rate, shortness of breath, swelling and allergic reactions (Wang *et al*., 2000; Yang *et al*., 2010).

The long term toxic side effects to adjacent brain structures usually include cognitive deficits and epilepsy due to neuronal damage (Wen and Kesari, 2008), growth reduction, thyroid function disorders, learning difficulties and an increased risk of secondary cancers affecting survivors of high-risk NB (Brodeur *et al*., 2011).

Table 1.2 Therapeutic strategies for different risk groups of NBs (Maris, 2010)

Variable	**Category**			
	Stage 1	**Stage 2**	**Stage 3**	**Stage 4S tumours**
	Low risk	**Intermediate risk**	**High risk**	**High risk**
Treatment	Surgery	Moderate-intensity chemotherapy; Surgery	Multimodal therapy	Supportive care
Survival rate (%)	> 98	90-95	40-50	> 90

1.6 Challenges in Treating CNS and Brain Cancers

The delivery of drugs in CNS cancers is mainly limited by the presence of anatomical barriers: the blood–brain barrier (BBB), blood–cerebrospinal fluid barrier (BCSFB) and the cerebrospinal fluid brain barrier (CSF) (Engelhardt and Sorokin, 2009) (Figure 1.5, p. 13). These barriers are essential for the normal function of the CNS as it separates brain extracellular fluids in the CNS from circulatory blood and provides transport processes for essential nutrients, ions and metabolic waste products (Redzic, 2011; Khanbabaie and Jananshahi, 2012). Other specialized barriers such as the blood-tumour-barrier (BTB) also hamper CNS drug delivery.

1.6.1 Blood-Brain Barrier (BBB)

The BBB is located at the blood capillaries of the brain and is formed by capillary endothelial cells (Figure 1.5, p. 13), astroglia, pericytes and perivascular mast cells (Schulz and Engelhard, 2005; Abbott *et al*., 2006). This barrier is approximately 200 nm thick separating

over a billion capillaries from the brain tissue, the surface area of these capillaries being approximately 20m² (Pardridge, 2005).

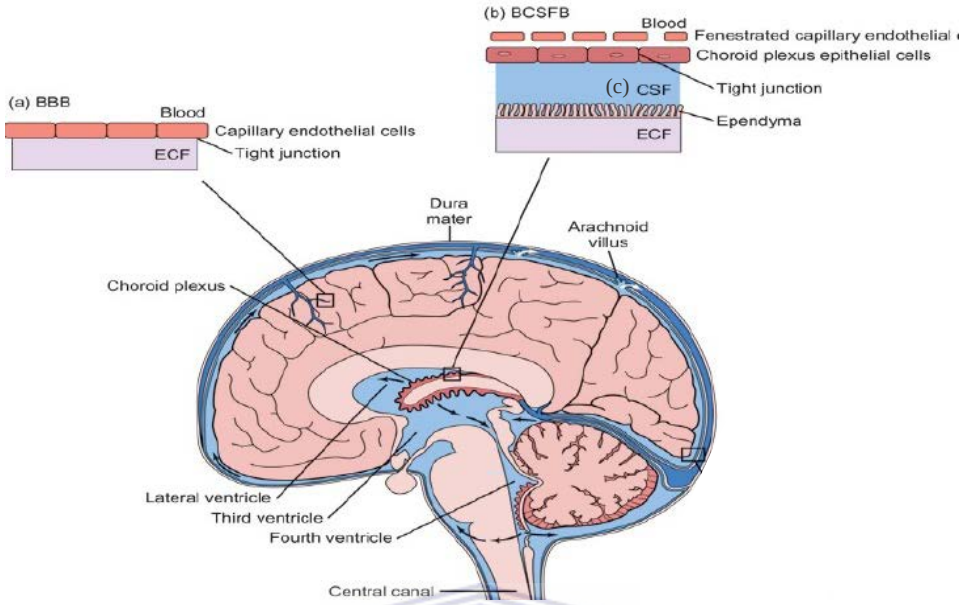

Figure 1.5 Sagital section of the brain indicating the location of anatomical barriers. *The specialized barriers of the CNS include: (a) Blood-brain-barrier (BBB), (b) blood–cerebrospinal fluid barrier (BCSFB) and the (c) cerebrospinal fluid brain barrier (CSF) (Saim, 2012).*

The capillary endothelial cells are held together by complex tight junctions which are interconnected side-by-side by tight adherens junctions (Figure 1.5) thereby preventing the passage of small molecules and ions through spaces between cells by diffusion or active transport (Martini, 2006; Stamatovic *et al*.,. 2008). The main integral proteins present at tight junctions include: occludin, claudins and junctional adhesion molecules (JAMs) (Stamatovic *et al*., 2008). The compact network of interconnections confers the highest trans-endothelial electrical resistance (approximately 500 Ωcm²), higher than that of systemic endothelia (3-33 Ωcm²) (Butt *et al*., 1990; Burke *et al*., 1999).

Nutrition transport of ions, amino acids, vitamins and proteins through the brain endothelium is induced by several molecular transport systems in the plasma membrane (Visser *et al*., 2005). This barrier is highly selective and controls the entry of compounds into the brain (Upadhyay, 2014). Crossing of any molecule through the BBB is dependent upon its physicochemical properties and pharmacokinetic profile in plasma (Balda and Matter, 1998; Upadhyay, 2014). A large amount of drugs or molecules such as nucleic acids, peptides, proteins and antibiotics fail to cross the BBB, but substances such as alcohol, caffeine, nicotine, anaesthetics and glucose can cross rapidly (Martini, 2006). Only molecules with a

mass lower than 400–600 Da and hydrophilic compounds with a mass lower than 150 Da, can cross the BBB via passive diffusion (Visser *et al.*, 2005; Santaguida *et al*., 2006). Most molecules cannot cross the BBB due to these factors, including the majority of anti-cancer drugs; however drugs such as anxiolytics, antipsychotics selective serotonin reuptake inhibitors and opiates can cross (Pardridge, 2005; Upadhyay, 2014). Even drugs, small molecules or solutes that can cross the BBB are confronted with many degrading enzymes present inside endothelial cells. These enzymes recognize and rapidly degrade most peptides, including naturally occurring neuropeptides (Misra *et al*., 2003). In addition, capillary endothelial cells have a high concentration of drug efflux transporter proteins such as P-glycoprotein (P-gp) (Thuerauf and Fromm, 2006) and multidrug resistance-associated proteins (MRPs) (Borst *et al*., 2000) which hampers penetration of many therapeutic agents into the brain parenchyma.

1.6.2 Blood-Cerebrospinal Fluid Barrier (BCSFB) and CSF-Brain Barrier

Regions of the CNS located adjacent to the cebral ventricles of the brain called the circumventricular organs (CVOs) do not possess the BBB. These regions comprise the pineal gland, median eminence, organum vasculosum of the lamina terminalis, neurohypophysis, the area postrema, subfornical organs, the subcommisural organ and choroid plexus (CP) (Khanbabaie and Jahanshahi, 2012). The BCSFB is situated at the CP epithelial cells which are responsible for secreting cerebrospinal fluid (CSF). Unlike BBB capillaries, BCSFB capillaries are fenestrated and have no tight junctions (Figure 1.5, p.13); therefore there are no astrocytes in contact with endothelial cells. The endothelium does not form a barrier for the movement of small molecules; instead the BCSFB at the CP is formed by epithelial cells and tight junctions that connect them (Redzic, 2011; Khanbabaie and Jahanshahi, 2012).

Similar to the BBB, transport across the BCSFB is selective with only small molecules such as ions, potassium, calcium and chloride crossing in a controlled environment (Martini, 2006). Diffusion, facilitated diffusion and active transport into CSF from CSF to blood occur in the CP (Johanson *et al*., 2008). The CP epithelial cells offer low resistance (150–200 Ωcm^2) in comparison with capillary endothelial cells from the BBB (Saito and Wright, 1983). Consequently, substances move from the blood into the CSF in a molecular weight-dependent manner and irrespective of their movement across the BBB such as azidothymidine (AZT), which rapidly enters CSF across the CP epithelium but cannot cross the BBB easily (Dykstra *et al*., 1993). Therefore the presence of drugs in the CSF

compartment does not neccsearily guarantee penetration into the brain parenchyma. Unlike at the BBB, where solutes that have crossed the capillary barrier undergo rapid distribution throughout the brain parenchyma, the penetration of solutes from CSF to brain parenchyma is accomplished through diffusion which decreases rapidly with distance, e.g., the highest penetration of brain-derived neurotrophic factor (BDNF) is approximately 0.3 mm from the ependymal surface of the brain (Mak *et al*., 1995). The estimated volume of CSF in the human brain is 140 ml and in a healthy adult the CSF is replaced 4–5 times a day (Mak *et al*., 1995). CSF produced by the CP progresses from the lateral ventricles to the third ventricle and then into the fourth ventricle of the brain. The CSF then passes from the foramina of Luschka and Magendie to the cisterna magna and then into the cranial and spinal subarachnoid spaces and is finally absorbed into the bloodstream across the arachnoid villi. Therefore drugs that are injected into the CSF are removed quickly via bulk flow through the CSF flow pathway as a result of the high turnover rate of CSF (Johanson *et al*., 2008).

One of the most challenging steps in neuroscience researches and therapy is the ability to penetrate these permeability barriers for delivering anti-cancer drugs to the CNS (Khanbabaie and Jahanshahi, 2012).

1.6.3 Challenges Associated with Chemotherapeutic Drugs

In addition to the anatomical barriers presented by the CNS, which contributes largely to the diminished therapeutic value of many potent anticancer drugs, in comparison with normal brain vasculature, tumour vasculature of the brain comprises abnormal blood vessels; distended capillaries with leaky walls, leading to inconsistent drug delivery into the brain (Van Meir, *et al.,* 2010). Localized hypoxia can lead to tumour resistance as a result of irregular blood flow. Drug metabolizing enzymes that are situated in the cerebral microvasculature mainly provide a protective role aginst exogenously administered molecules (Borst *et al*., 2000; Thuerauf and Fromm, 2006).

The difficulty in NS and CNS tumours therapy is also greatly impacted by the lack of specificity of anticancer drugs to pathological diseased sites, resulting in very low amount of administered drug that can ultimately reach the brain (Begley and Brightman, 2003). This also contributes to the systemic toxicity associated with chemotherapeutic agents. Drugs with short distribution half-lives can lead to sub-therapeutic levels of chemotherapy and may result in a minimal probability of circulating the drug through the tumour vascular bed (Medina *et al*. 2004). For the anticancer agent anthracycline, drug-induced congestive heart failure,

alopecia, mucositis, nausea and vomiting are the major concerns due to its very poor prognosis (Drummond *et al*. 1999). Myelosupression and cardiotoxicity are considered dose-limiting factors in conventional cancer treatment with free doxorubicin (Drummond *et al*. 1999). Tumour cells may become resistant to conventional treatments and the brain becomes susceptible to damage, also the brain has a limited ability for self-repair which decreases with age (Wang *et al*., 2013). Avoidance of systemic toxicity through chemotherapeutic drugs and radiation is crucial especially in the paediatric age group; combating drug resistance, improving drug delivery to the diseased sites thereby reducing side effects are essential in combating NB. The importance of anti-cancer drug delivery to patients with NB especially in CNS related NB, is important as the neurons in the CNS shows limited regenerative capacity. Therefore damaged neurons are not capable of dividing and replacing themselves under normal circumstances and as a result this comprises the CNS greatly (Buga *et al*., 2011).

Consequently, there has been little advancement in the development of effective therapeutic agents for NB cancer in the past decades. However, a great deal of research has aided in our molecular understanding of the pathogenesis involved in NB cancer. Most antitumor therapies such as chemotherapy, radiation or immunotherapy act through the induction of apoptosis in cancer cells (George *et al*., 2010). It has been proposed that one of the mechanisms contributing to the aggressive behaviour of advanced-stage NB in older children is resistance to the extrinsic apoptosis pathway activation (George *et al.*, 2010). Hence, recent years has focused on assessing the mitochondrial pathway for drug-induced apoptosis treatments for cancers such as NB (Ferrin *et al*., 2011; Posadas *et al*., 2012).

1.7 Apoptosis (Programmed Cell Death)

Apoptosis is a highly specialized form of controlled cell death which is executed in an orderly manner (Palai and Mishra, 2015). It occurs during development and aging of cells to maintain cell proliferation in tissues. It differs to necrosis which is also a type of cell death but occurs after cell injury, whereas apoptosis is constant and required to maintain the homeostasis of cell proliferation and cell death (Sankari *et al.*, 2012).

Apoptosis occurs through two main pathways the intrinsic (mitochondrial pathway) and extrinsic (death receptor pathway). A third pathway involving T-cell mediated cytotoxicity called the perforin/granzyme pathway also exists (Thornberry and Lazebnik, 1998; Fischer and Schulze–Osthoff, 2005). The intrinsic and extrinsic pathways depend on the specific triggering by signals to begin an energy-dependent cascade of molecular events, while

Granzyme A works in a caspase-independent fashion in the perforin/granzyme pathway (Elmore, 2007). All the pathways converge at the execution pathway resulting in the characteristic biochemical and physical changes such as membrane blebbing, cell shrinking, nuclear fragmentation, condensation of the chromatin network and chromosomal DNA fragmentation (Figure1.6 and Figure 1.7). The final stages of apoptosis are marked by the formation of apoptotic bodies which are engulfed by phagocytes (Gotter, 2009).

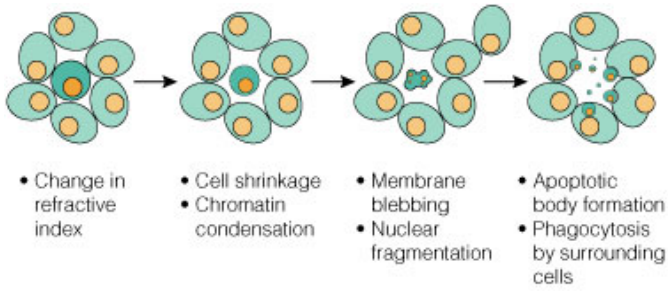

Figure 1.6 Characteristic cellular changes that normally occur during apoptosis. *This includes changes in reactive index, cell shrinkage, chromatin condensation, membrane blebbing and DNA fragmentation. Apoptotic bodies form and are phagocytised by neighbouring cells (https://www.promega.com/resources/product-guides-and-selectors/protocols-and-applications-guide/apoptosis/).*

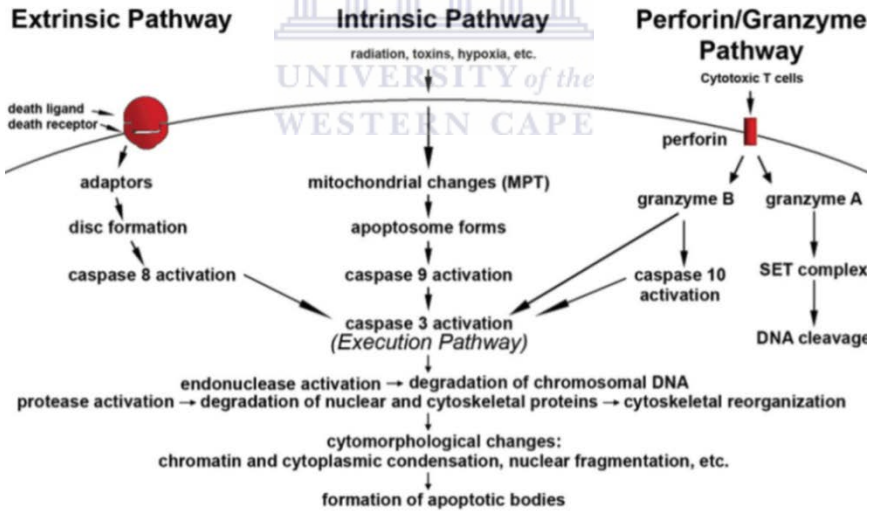

Figure1.7 The three main pathways involved in apoptosis*: Extrinsic Pathway (death receptor), Intrinsic Pathway (mitochondrial pathway) and Perforin/Granzyme Pathway (Adapted from Elmore, 2007).*

1.7.1 Extrinsic Pathway

The extrinsic pathway is activated by the binding of death ligands to death receptors (Rubio-Moscardo *et al*., 2005; Elmore, 2007). The death receptors possess an intracellular domain which causes the recruitment of adaptor proteins, such as tumour necrosis factor (TNF)

receptor associated death domain (TRADD), Fas-Associated death domain (FADD) adaptor molecule and cysteine proteases like caspase-8 (Schneider and Tschopp, 2000; Wong, 2011). When the death ligand binds to its death receptor, it forms a death-inducing signalling complex (DISC). This activates pro-caspase-8 which then processes downstream effector caspases and cleaves specific substrates causing cell death (Elmore, 2007; Wong, 2011; Sankari *et al.*, 2012).

1.7.2 Intrinsic Pathway

Stimuli such as cell damage by toxins, free radicals, radiation, DNA damage, the absence of certain growth factors, hormones and cytokines that lead to failure of suppression of death programs, causes changes in the inner mitochondrial membrane (Elmore, 2007). Consequently, this causes the opening of the mitochondrial permeability transition pore resulting in the loss of the mitochondrial transmembrane potential and the release of pro-apoptotic proteins from the intermembrane space into the cytosol (Saelens *et al.*, 2004). These pro-apoptotic proteins are cytochrome c, Smac/DIABLO and HtrA2/Omi (Du *et al.*, 2000; van Loo *et al.*, 2002; Garrido *et al.*, 2006).

Apoptotic events occurring in mitochondria are regulated by the activity of members of the B-cell leukemia/lymphoma 2 (Bcl-2) families of proteins and tumour suppressor protein p53 (Cory and Adams, 2002). Bcl-2 family members are divided into three groups based on the presence of 1-4 Bcl-2 homolog domains. Proteins containing all four domains are anti-apoptotic e.g. Bcl-2, Bcl-x, Bcl-XL, Bcl-XS, Bcl-w and BAG. They reside in the outer mitochondrial membrane and control cytochrome c release from the mitochondria via alteration of mitochondrial membrane permeability. The other groups are pro-apoptotic proteins such as Bax, Bak, and BH-only proteins such as Bid, Bad, Noxa, Puma and Bim (Ola *et al*., 2011).

When cytochrome c is released into the cytosol, it binds to the C-terminal of Apaf-1, a cytosolic protein with an N-terminal-recruitment domain (CARD) (Zou *et al.*, 1997), thus facilitating the association of dATP with Apaf-1, exposing the N-terminal CARD through which caspase-9 is recruited, creating an “apoptosome”. Caspase-3 is then recruited to the apoptosome, where it is activated by caspase-9 (Bratton *et al.*, 2001). Caspase-3 cleaves key substrates and promotes the execution phase (Chinnaiyan, 1999; Hill *et al.*, 2004).

Second Mitochondrial-Derived Activator of caspase (Smac)/DIABLO and High Temperature Requirement Protien-A2 (HtrA2)/Omi indirectly promote apoptosis by inhibiting inhibitors of apoptosis proteins (IAP) activity (Salens *et al.,* 2004; Schimmer, 2004). The IAP family of proteins are important apoptosis regulators because they can regulate both the intrinsic and extrinsic pathways (Deveraux and Reed, 1999; Silke *et al.*, 2002; Elmor, 2007).

Apoptosis Inducing Factor (AIF), endonuclease G and Caspase-Activated DNAse (CAD) are a second group of pro-apoptotic proteins released from mitochondria. AIF causes DNA fragmentation into approximately 50-300 kilobase pieces and condensation of peripheral nuclear chromatin referred to as "stage I" condensation (Susin *et al.,* 2000; Joza *et al.,* 2001). The endonuclease G cleaves nuclear chromatin to produce oligonucleosomal DNA fragments (Li *et al.,* 2001). CAD is then released from the mitochondria and translocates to the nucleus where it causes oligonucleosomal DNA fragmentation and more pronounced chromatin condensation, called "stage II" condensation, after cleavage by caspase-3 (Enari *et al.,* 1998; Susin *et al.,* 2000).

A sensor of cellular stress and a critical activator of the intrinsic pathway is p53. This protein could lead to the expression of BH3-only molecules Puma and Noxa (Villunger *et al.,* 2003) or could directly activate Bax transcriptionally or functionally (Johnstone *et al.,* 2002; Chipuk *et al*., 2004).

1.7.3 Cancer and Apoptosis

As seen in Figure 1.7 (p. 17) the different pathways occur simultaneously and overlap at certain stages, showing cross-talking between pathways. Therefore these pathways are dependent on each other and an imbalance in the expression of genes in the apoptotic pathways can promote the transgression of cellular homeostasis, resulting in diseases such as cancer (Cory and Adams, 2002; Elmore, 2007; Sankari *et al.,* 2012). Drugs inducing apoptosis remain the principal chemotherapeutic choice in medical oncology, with more than half of anti-cancer drugs coming from natural origins, such as plants (Gotter, 2009). These therapies usually induce apoptosis by inducing cellular stress leading to the intrinsic activation of apoptosis through p53 or upstream of the mitochondria.

The pathways involved are complex and cancer cells often become resistant to conventional therapies through developing escape-mechanisms in the signalling cascade (Bouillet *et al.,* 1999; Puthalakath *et al.,* 1999; Orr *et al.,* 2003). Approximately half of all human tumours

have acquired p53 mutations and the rest have deactivated the p53 pathway such as increasing p53 inhibitors or decreasing its activators (Green and Kroemer, 2009). Therefore, treatments that rely solely on p53-dependent apoptosis might not function and a novel class of anti-cancer agents directly targeting the mitochondria and not just depending on p53 may hold great promise in overcoming drug-resistance in tumours. Betulinic Acid (BetA) is potentially one such anti-cancer agent (Mullauer *et al.*, 2010).

1.8) Betulinic Acid (BetA)

Natural products have been used to combat human diseases for decades and play an increasing role in drug discovery and development (Ji *et al*., 2009). Two important known classes of naturally-derived compounds used in clinical settings and research are vinca alkoids and taxanes, with products such as Velban and Navelbine already on the market (Risinger *et al.*, 2009; Mullauer *et al*., 2010). Taxanes and triterpenoids belong to the terpenoids class of successful naturally-derived compounds approved in 1992 by the US Food and Drug Administration (FDA) and is used for various cancers including ovarian, lung and breast cancers (McChesney *et al.*, 2007). Triterpenoids (also referred to as isoprenoids), are the largest group of natural compounds consisting of six isoprene units and can be isolated from many different plant sources (Hill and Connolly, 2013). They can be sub-classified into several groups and many of them or their synthetic derivatives are currently being investigated for various diseases, especially the anti-cancer agents (Bishayee *et al*., 2011).

One highly promising class of natural compounds from the triterpenoids is BetA (3β-hydroxy-lup-20(29)-en-28-oic acid) which is the oxidized derivative of Betulin (Bet) (Figure 1.8, p. 21). BetA is a natural plant-derived pentacyclic triterpenoid present in a large diversity of plants (Dehelean *et al*., 2012). Both Bet and BetA have been studied extensively and have shown a great number of pharmacological benefits, with BetA being more effective (Șoica *et al*., 2012). BetA is most commonly found in the bark of the white birch tree (*Betula alba*), due to the high betulin content of up to 22% (Fulda and Kroemer 2009). Other known sources of BetA include trees and shrubs such as *Ziziphus spp*. (Rhamnaceae), *Syzygium spp.* (Myrtaceae), *Diospyros spp.* (Ebenaceae) and *Paeonia spp.* (Paeoniaceae) (Cichewicz and Kouzi, 2004).

The chemical structures of Bet and BetA differ at the C-28 position (Figure 1.8, p. 21) and many different extraction techniques have been proposed to isolate BetA from Bet. After extraction, the white crystalline solid form of BetA has a molecular formula of $C_{30}H_{48}O_3$

with a molecular mass of 456.3603 g mol−1 and demonstrates limited solubility in organic alcohols (Tolstikov *et al.,* 2005; Cheng *et al.,* 2011; Dehelean *et al.,* 2012). It has low solubility in water, petroleum ether, dimethylformamide, dimethyl sulfoxide, and benzene; however it is highly soluble in pyridine and acetic acid and has a melting temperature of between 316-318 °C (Cichewicz and Kouzi, 2004; Cheng *et al*., 2011).

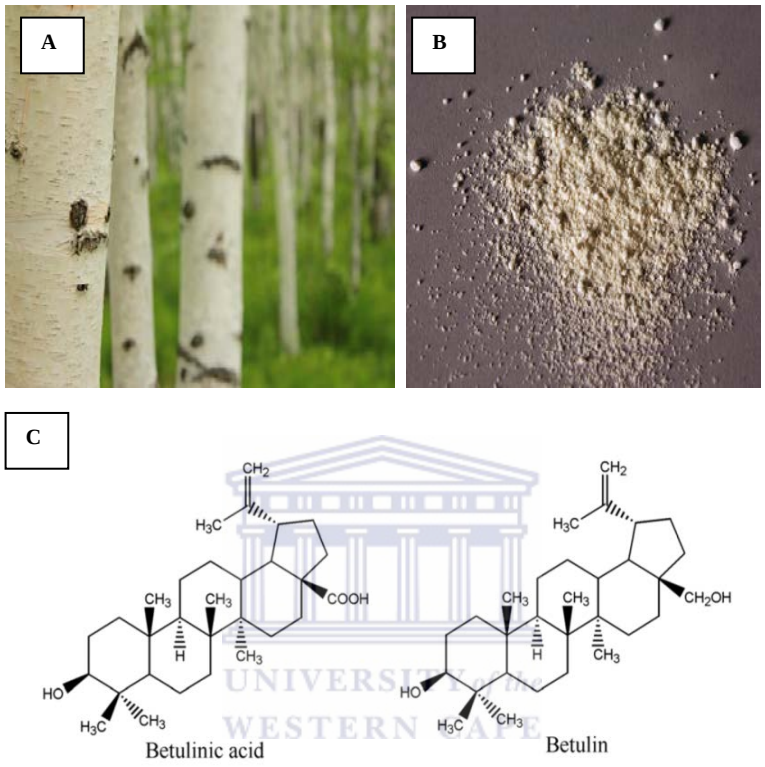

Figure 1.8 Birch trees (A) from which BetA is commonly extracted to give a white crystalline solid (B) and the chemical structures of BetA and Bet (C)

(http://plantextract8988.en.ec21.com/Birch_Bark_Extract_Powder_Betulin--5520266_5520364.html; Moghaddam et al., 2012).

1.8.1 Medicinal Properties of BetA

BetA extracted from the white birch bark has a long tradition in folk medicine for treatment of stomach and intestinal problems by Native Americans and in certain parts of Russia (Yogeeswari and Sriram, 2005; Alakurtti *et al.,* 2006; Dehelean *et al.,* 2012). It is a unique compound as it demonstrates many different biological activities and medicinal properties such as anti-inflammatory (Alakurtti *et al.,* 2006; Moghaddam *et al.,* 2012), anti-bacterial (Chandramu *et al.,* 2003; Eiznhamer and Xu, 2004; Fontanay *et al.,* 2008), anti-malarial (Bringmann *et al.,* 1997; Steele *et al.,* 1999; de Sá *et al.,* 2009), antheminitic (Enwerem *et al.,* 2001), antinociceptive (Kinoshita *et al.,* 1998), anti-HSV-1 and inhibition of human immunodeficiency virus (HIV) (Dang *et al.,* 2009; Moghaddam *et al.,* 2012). BetA has also

demonstrated anti-cancer abilities (Chintharlapalli *et al.*, 2007; Fulda and Kroemer, 2009; Mullauer *et al.*, 2010; 2011; Moghaddam *et al.*, 2012).

1.8.2 BetA Anti-tumour Effects and Effects on Healthy Cells

BetA only gained attention in cancer research in 1995, when Pisha *et al.*, (1995) identified it as a specific inducer of apoptosis in melanoma cells. Since then, the capacity of BetA to induce apoptosis has been demonstrated *in vitro* for a wide variety of prevalent cancers such as leukaemia (Ehrhardt *et al*., 2004; Raghuvar *et al.*, 2005), ovarian cancer (Zuco *et al*., 2002), cervix cancer (Xu *et al*., 2014), prostate cancer (Reiner *et al*.,2013), lung cancer (Hsu *et al*., 2012), breast cancer (Damle *et al*., 2013), colorectal cancer (Chintharlapalli *et al*., 2011), glioblastoma (GB) cancer as well as other head and neck cancers including NB (Thurnher *et al*., 2003; Fulda and Kroemer, 2009; Mullauer *et al*., 2010). BetA shows little to no toxicity to healthy cells (Zuco *et al*., 2002; Mullauer *et al.*, 2010).

1.8.3 Apoptotic Effects of BetA

Numerous studies have attempted to elucidate the molecular mechanisms of BetA-mediated antitumor activity and have shown that BetA-induced apoptosis differs from that caused by other anticancer agents (Figure 1.9, p. 23). Common anti-cancer agents activate the death receptor pathway of apoptosis or induce cellular stress such as cytokine withdrawal or DNA damage, resulting in activation of the apoptotic signalling cascade via p53 and/or BH3-only proteins. BetA does not involve p53 or death ligands but directly induces mitochondrial damage (Figure1.9, p. 23), leading to Bax/Bak independent release of cytochrome c (Fulda and Kroemer, 2009; Mullauer *et al.*, 2010) overcoming resistance that a tumour cell could have gained upstream of the mitochondria. The formation of the mitochondrial transition pore complex causes inhibition of STAT3, JAK1 and JAK2 (Shanmugam *et al*., 2012). BetA also causes the inhibition of topoisomerases 1 and 2 and the activation of nuclear factor-kB (NF-kB) (Mullauer *et al.*, 2010; Pandey *et al.*, 2010).

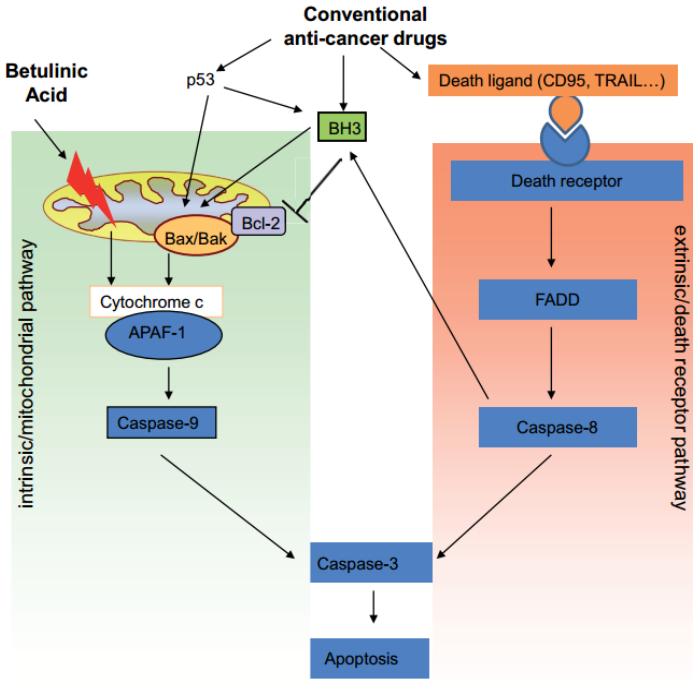

Figure 1.9 Comparison of the induction of apoptosis by conventional anti-cancer drugs compared to BetA. *The majority of anti-cancer agents induce cellular stress such as cytokine withdrawal or DNA damage, resulting in activation of the apoptotic signalling cascade via p53 and/or BH3-only proteins. BetA induces apoptosis independently of p53, by directly inducing mitochondrial damage resulting in the release of cytochrome C (Adapted from Mullauer et al., 2010).*

1.8.4 BetA Induces Apoptosis in Brain Cancer Derived Cell Lines

Fulda *et al.*, (1997) first identified BetA as a new cytotoxic agent against neuroectodermal tumour cells including NB, medulloblastoma (MB), GB and Ewing's sarcoma cells. They showed that BetA exerted a cytotoxic effect on different NB and GB cell lines that was independent of p53 and caused the release of cytochrome c or AIF from mitochondria into the cytosol induced activation of caspases and nuclear fragmentation leading to cell death (Fulda *et al.*, 1997; 1998; 1999).

BetA regulates Bcl-2 family proteins in a context-dependent manner (Fulda, 2008; Fulda and Kroemer, 2009). Treatment with BetA resulted in up-regulation of the pro-apoptotic Bcl-2 family protein Bax in NB, GB and melanoma cells, whereas Bcl-XS was found at high levels in BetA-treated NB cells. The alterations in the balance of Bax/Bcl-2 proteins were suggested to have caused apoptosis in NB, GB and melanoma cells treated with BetA (Fulda *et al.*, 1997; Wick *et al.*, 1999). Expression levels of anti-apoptotic Bcl-2 remained unchanged upon incubation with BetA in NB cells while an increase in Bcl-2 protein levels was reported in GB cells (Fulda *et al.*, 1997; Wick *et al.*, 1999).

Generation of reactive oxygen species (ROS) upon treatment with BetA has been reported to be involved in initiating mitochondrial membrane permeabilization (Fulda *et al*., 1999; Fulda and Kroemer, 2009). Glioma cells exposed to BetA induced ROS generation, which was blocked by Bcl-2 or the antioxidants N-tert-butyl-a-phenylnitrone (PBN) and N-acetyl-cysteine (NAC). Expression levels of Bcl-2 and Bax increased after BetA application; however levels of Bcl-Xs and Bcl-XL were not affected. Furthermore, ROS formation was dependent on new protein synthesis and was crucial for caspase activation (Wick *et al.,* 1999).

BetA has also been reported to modulate activity of the transcription factor NF-kB (Fulda, 2008). BetA was identified as a potent activator of NF-kB in a number of cancer cell lines including SHEP neuroblastoma cell line (Kasperczyk *et al.,* 2005). The activation by NF-kB has been found to be involved in decreased phosphorylation of inhibitor of NF-kB kinase (IKK) with subsequent proteasome degradation as well as increased translocation of the NF-kB subunit p65 to the nucleus (Takada and Aggarwal, 2003).

Interestingly, NB cells that showed resistance to CD95-or doxorubicin-triggered apoptosis remained sensitive to treatment with BetA, and BetA exhibited potent antitumor activity on primary tumour cell cultures from all NB (4/4) and all MB (4/4) (with an ED_{50} of 3-15µg/ml for both) and most GB patients (20/24) (with an ED_{50} of 5-16 µg/ml) *ex vivo* (Fulda *et al*., 1998b).

1.8.5 Use of BetA for Drug Delivery

BetA has demonstrated the ability to initiate apoptotic pathways in cancer cells and show a favourable therapeutic window in which it could even overcome anticancer drug resistance or used in combination treatments, which could improve the efficacy of anticancer therapy, especially since it shows low cytotoxicity in normal cells (Zuco *et al*., 2002; Mullauer *et al.,* 2010).

Pisha *et al.,* (1995) published the first *in vivo* study of BetA which described a method for enhancing its solubility by co-precipitating BetA with polyvinylpyrrolidone (PVP) and intraperitonally delivering it to nude mice bearing subcutaneous human melanoma xenografts. Complete lack of toxicity was observed with tumour regression using a 500 mg/kg body weight dose, indicating a broad therapeutic window (Pisha *et al.,* 1995). A few other studies addressing the *in vivo* efficacy of BetA have since followed, all indicating a

potent anti-tumour effect with no systemic toxicity (Zuco *et al.*, 2002; Chintharlapalli *et al.*, 2007; Rajendran *et al.*, 2008; Mullauer *et al.*, 2011).

Due to its lipophilic properties, BetA cannot be dissolved and administered in most aqueous solutions (Mullauer *et al.*, 2011), posing a difficulty in its *in vivo* efficacy and hampering its formulation into a pharmaceutical product. Many studies have tried to modify BetA derivatives to enhance their solubility such as modifications at the C-3 and C-28 positions which demonstrated potential in addressing the solubility challenges (Liu *et al*., 2004; Huang *et al.*, 2007; Rajendran *et al.*, 2008). However, since the lipophilic character of BetA is likely to be crucially involved in its pluripotent mechanism of action, permitting its broad activity profile, newer formulations of BetA are needed (Mullauer *et al.*, 2011). With the advent of nanotechnology, nanoscale drug delivery systems for cancer have greatly improved the efficacy of many anti-cancer drugs.

1.9 Nanotechnology for Cancer Treatment

Considered as one of the key technologies of the 21st century, nanotechnology holds many promises for the future in various scientific disciplines including offering numerous novel possibilities for the treatment of cancer. Nanotechnology employ particles in the 1-100 nm size range in at least one dimension making them attractive for medical purposes (Khanbabaie and Jananshahi, 2012; D'Souza, 2014). The size of nanoparticles (NPs) offers unique and important features such as surface to mass ratio which is much larger compared to that of their bulk size (Parveen *et al.*, 2012). NPs based on their size can cross biological barriers through small capillaries and into individual cells (Fisher and Ho, 2002; Lockman *et al.*, 2002). Most importantly, NPs can be surface-functionalized with targeting moieties such as antibodies, aptamers, peptides, etc, for surface proteins on diseased cells, thereby allowing efficient drug accumulation at the target site and reducing unwanted side effects and the toxicity posed by most anti-cancer therapeutic agents (Parveen *et al.*, 2012). Cancer nanotherapeutic systems are being implemented to decrease the limitations associated with conventional cancer drugs, most importantly the lack of specificity as nanotherapeutics offers a safer platform than using viral vectors to deliver therapeutic agents directly to diseased cells (Mamo *et al*., 2010). Other advantages associated with NPs for cancer drug delivery include: improving hydrophobic drugs and molecules, increased aqueous solubility of drugs, protecting of drugs from degradation, sustained drug release, improving drug bioavailability,

improving pharmokinetic and pharmocodynamic properties and offering appropriate form for all routes of administration (Parveen *et al.*, 2012).

1.9.1 Drug Delivery to Cancer Cells Using Nanoparticles (NPs)

To deliver anticancer drugs through NP systems, two main approaches exist: Passive targeting and active targeting (Figure 1.10) (Parveen *et al.*, 2012). Passive targeting takes advantage of the leaky vasculature in tumour tissues caused by angiogenesis as blood vessels are known to be poorly defined (Alexander-Bryant *et al*., 2013). Blood vessels in tumours are irregularly shaped, leaky and show abnormal blood flow (Peer *et al*., 2007). Endothelial junctions are gaps in the endothelium which control the passage of macromolecules from the blood to tissue (Alexander-Bryant *et al*., 2013). In normal vasculature, endothelial junctions range from approximately 5-10 nm in width (Haley and Frenkel, 2008), however in tumour tissues, this size increases to a range of 100-780 nm depending on the tumour type (Folkman and Shing, 1992; Baban and Seymour, 1998). NPs are naturally attracted to this localized area compared to normal cells and due to their small size; they can easily enter these gaps into the extracellular vascular space. This phenomenon is referred to as the enhanced permeability and retention (EPR) effect and can be exploited for passive drug targeting (Figure 1.10) (Maeda *et al*., 2000; Peer *et al*., 2007).

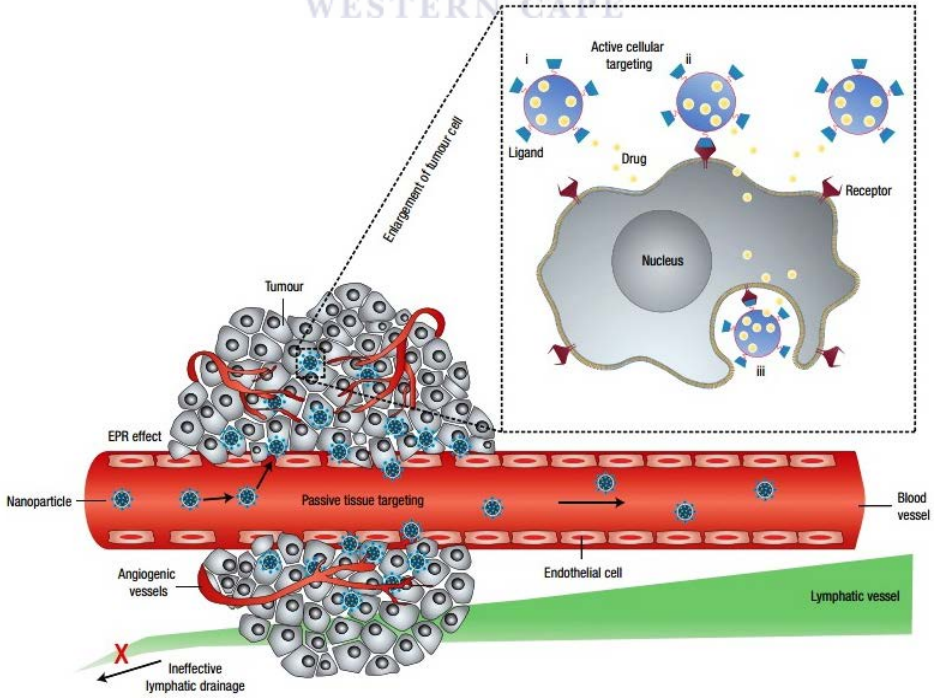

Figure 1.10 Schematic diagram showing passive and active targeting approaches for NP drug delivery*. Active targeting requires surface functionalization for cell-specific recognition binding while passive targeting takes advantage of the diseased leaky tumour vasculature for EPR effect (Adapted from Peer et al., 2007).*

Active targeting requires surface functionalization of receptor specific ligands that can promote cell-specific recognition binding (Thorpe, 2004). This is dependent on the targeting moiety of the NPs which should be abundant and show high specificity for the diseased cells. The active targeting can be accomplished by molecular recognition of the diseased cells by different molecules that are over expressed at the surface of diseased site via the ligand-receptor, antigen-antibody interactions, and peptides or by targeting through aptamers etc., (Parveen *et al.*, 2012).

Numerous biological barriers exist for NPs to successfully reach the intended disease sites such as extracellular and intracellular barriers (Desai, 2012). Extracellular barriers are primarily concerned with stability of the NPs as the innate immune system destroys all foreign objects. Therefore, stabilization of these NPs with biocompatible proteins such as human serum albumin or polymers such as polylactide or polycaprolactone etc. is fundamental in offering a 'stealth mode' for targeted or non-targeted drug delivery systems and assists in preventing agglomeration of NPs when inside the human body. Aggregates or clusters usually form if NPs are not steric stabilized or bio-functionalized for human applications. Intracellular barriers pose a difficulty for drug delivery systems through endosome entrapment and the ability to escape the recticular endothelial system (RES) (Guo and Huang, 2011). Smaller-sized NPs have a relatively long circulation time because they can avoid the RES uptake more easily and can penetrate deep into tissues through fine capillaries, thus allowing for better control of therapeutic drug delivery (Gupta *et al.*, 2006).

1.9.2 Nanocarriers for Therapeutic Delivery

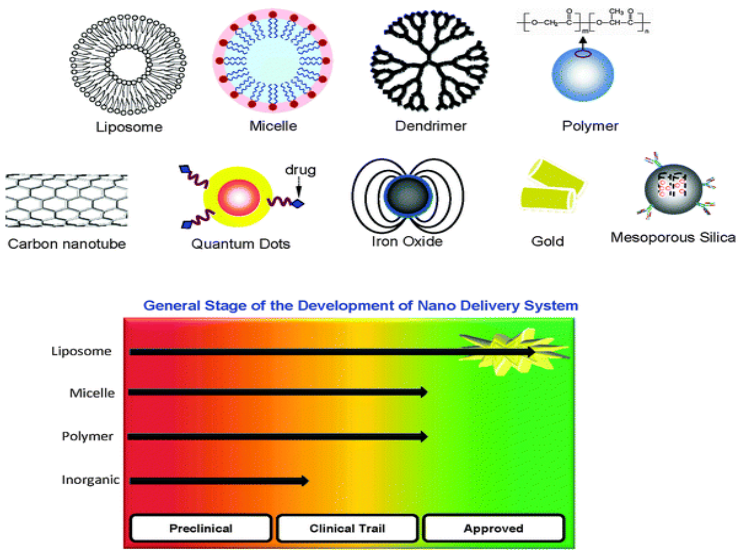

Figure 1.11 Different types of nano-drug delivery systems *(Mai and Meng, 2013).*

Many different types of nanocarriers have been developed over the past decades and some of these are shown in Figure 1.11 (p. 27). The main requirements for these carrier systems are: stability, biocompatibility, biodegradability, low toxicity, and the ability to protect drugs or nucleic acids from rapid degradation or excretion as well as high target specificity for targeted drug delivery (Markovsky *et al.,* 2012). Based on their classification, some of the types shown in Figure 1.11 will be discussed below in detail (Table 1.3):

Table 1.3 Different types of nanocarrier systems

Nanocarrier system	Structure	Characteristics	Examples
Polymeric NP (polymeric drug conjugates)	Drugs are conjugated to the side chain of a linear synthetic or semi synthetic polymers with a linker (cleavable bond) (Sanchis *et al*., 2010)	Biodegradable, passive and active drug delivery, controlled release polymer technologies where natural or synthetic polymers combines with a drug in such a way that the drug is encapsulated within the polymer system for release in a predetermined manner e.g. by temperature, pH or the presence of specific biological analytes	Opaxio (Li and Wallace, 2008, Sanchis *et al*., 2010)
Polymeric Micelles	Amphiphillic block co-polymers self-assemble and form micelles with a hydrophobic core and a hydrophilic shell (Adams *et al.,* 2003).	Self-assembling, biocompatible, non-toxic, carrier for non-polar drugs, controlled drug release and targeting capabilities and high cargo loading (Nakanishi *et al*., 2001; Al-Zubaidi *et al.,* 2014).	Genexol-PM (PEG-poly (D, L-lactide) (Nasongkla *et al.,* 2006).
Dendrimers	Monodispersed symmetric macromolecules with nm size dimensions constructed around an internal cavity surrounded by many hyper-branched structures of reactive end groups (Malik *et al.,* 1999).	Multifunctional-dendrimers can be modified with several molecules such as imaging contrast agents, targeting ligands, or therapeutic drugs, rendering a dendrimer-based multifunctional drug delivery system (Svenson and Tomalia 2005). The internal cavity can also encapsulate drugs (Svenson and Tomalia 2005).	PAMAM-platinate (Malik *et al.,* 1999).
Magnetic NPs (MNPs)	Nm sized particles with magnetic properties which can be manipulated using magnetic fields	Gold NPs and supramagnetic NPs (e.g. ferrite-or magnetite (Fe3O4)-based spherical particles) can be applied to improve MRI imaging, magnetic drug delivery and localized photo-thermal induced therapy by heating the specific area where these NPs accumulate and consqeuntly leading to the destruction of diseased cells (Mody *et al.,* 2014).	MNPs for improving imaging for cancer diagnosis and hyperthermia treatment of cancer treatment (Kumar and Mohammad, 2011; Yigit *et al*., 2012).
Carbon nanotubes (CNTs)	NPs composed of benzene rings forming graphene sheets folded to produce a tube. It can be single walled or double walled depending on their application (Rastogi *et al*., 2014).	CNTs can be made biocompatible through chemical modifications. Sidewall or tips of CNTs allows attachment of several molecules at once, therefore a higher therapeutic load compared to the other NPs. It also has similar applications as the MNPs in terms of drug delivery and photo-thermal therapy (Rastogi *et al*., 2014).	Antifungal agent or anticancer drugs have been covalently linked to CNTs (Parveen *et al.,* 2012).
Quantum dots (QDs)	Semi conductor crystals with nm size dimensions possessing conductive properties based on size (Cho *et al*., 2007)	QDs are imaging modalities due to their quantum size characteristics which lead to size-tuneable band gaps thereby enhancing the photonic function (Yong *et al*., 2012).	QDs are capable of detecting cancer biomarkers (Wagner *et al*., 2010).

1.9.3 Toxicity Associated with NPs

The predicted benefits of NP drug-delivery systems are numerous as they are already resolving most of the common problems experienced with conventional drugs and beginning to replace them (Table 1.3, p. 28). However, to exploit the full potential of nanotechnology in nanomedicine, attention should also focus on safety and toxicity issues regarding these carrier systems. The toxicity factor surrounding most of these NPs, especially the non-degradable NPs are an uncertainty which hampers clinical success.

Non-degradable NPs used for drug delivery may show persistence and localization at the site of the drug delivery, but in some many cases it results in chronic inflammatory response (De Jong and Brom, 2008). Cationic NPs including gold and polystyrene have been shown to cause haemolysis and blood clotting (Gupta and Gupta, 2005; De Jong and Brom, 2008). Studies with carbon nanotubes (CNTs) showed that platelet aggregation was induced by both single and multi-walled CNTs (Radomski *et al.*, 2005). Quantum dots (QDs) composed of heavy metal compounds may prove difficult for the body to degrade and the accumulation in the body may lead to cytotoxic effects (Sahoo and Labhasetwar, 2005).

The efficiency of NP carriers is dependent on their design, application and materials used. Overloading of the NPs may cause problems and hydrodynamic size also affects NP clearance rate from circulation (Moghimi *et al.*, 2001). Materials, used for coating and immobilization approaches are important as many studies show that the coating thickness and hydrophobicity can significantly affect the magnetic properties of magnetic NPs (MNPs) (LaConte *et al.*, 2007; Duan *et al.*, 2008). It has been reported that small NPs (20 nm) are excreted by the renal system (Banerjee *et al.*, 2002), medium sized NPs (30–150 nm) accumulate in the bone marrow, heart, kidney and stomach while large NPs (150–300 nm) have been found in the liver and spleen (Veiseh *et al.*, 2010). These results require a novel way of handling the toxicology of NPs.

Liposomes are the first drug-carrying nano-carriers to reach cancer clinics (Figure 1.11). The first liposomal drug to gain approval by the FDA in 1995 was Doxorubicin (Doxil/Caelyx) and has since been used to treat a wide variety of advanced stage cancers such as ovarian cancer, metastatic breast cancer and AIDS-related Kaposi's sarcoma (Perche and Torchilin, 2013). Other approved liposome encapsulated anti-cancer drugs include Vincristine (Marqibo) and Paclitaxel (Lipusu), with many ligand targeting liposomes for targeted drug delivery being in phases I, II and III of drug development stages (Perche andTorchilin, 2013).

1.10 Liposomes

Since the discovery of liposomes by Dr Bangham and colleagues in 1965, liposomes have generated much enthusiasm due to their unique potential to improve the delivery of current drugs (Paliwal *et al.*, 2011; Monteiro *et al.*, 2014). They are self-assembled, closed colloidal structures composed of one or concentric phospholipid bilayers surrounding a central aqueous core (Parveen *et al.*, 2012). Liposomes offer simultaneous loading of hydrophobic (non-polar) molecules/drugs into the phospholipid bilayer while hydrophilic (polar) molecules/drugs can be encapsulated in the aqueous space (Figure 1.12), thus allowing unlimited therapeutic cargo loading (e.g., anti-cancer drugs, DNA, peptides vaccines, enzymes and imaging agents to be loaded into this assembly) (Perche and Torchilin, 2013).

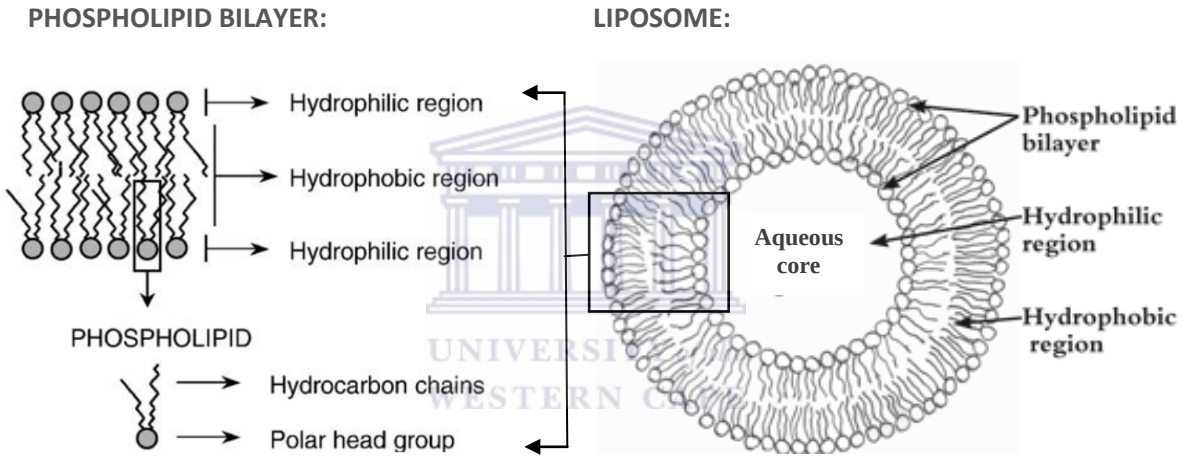

Figure 1.12 Schematic illustration of a liposome. *The phospholipid bilayer creates a hydrophobic region for entrapping non-polar molecules/drugs, while the aqueous core creates the hydrophilic region for encapsulating polar molecules/drugs. Liposomes may have one or more than one phospholipid bilayer, depending on the size, type and method of preparation of the liposome (Adapted from Lopes et al., 2013 with a few modifications).*

Liposomes have been reported to be biocompatible, degradable *in vivo*, have low immunogenicity and excellent safety profiles in humans. They offer increased pharmokinetic and pharmodynamic properties and it is relatively inexpensive for mass production, which makes them superior as a NP for therapeutics (Allen and Cullis 2013; Ait-Oudhia *et al*., 2014). Additionally, liposomes can be surface coated with targeting agents for targeted drug delivery (Kelly *et al*., 2011; Tiwari *et al*., 2012; Allen and Cullis 2013; Monteiro *et al*., 2014)

Some of the advantages of liposomes include:

- Passive and active targeting to tumour tissues (Torchilin, 2010)

- Increased efficacy and therapeutic index (Chuang *et al*., 2011)
- Increased drug loading and stability of encapsulated agents (Nallamothu *et al*., 2006; Gubernator, 2011)
- Improved pharmacokinetics and pharmocodynamics (Drummund *et al*., 1999; Gubernator, 2011)
- Decreased toxicity due to biodegradability (Mufamadi *et al*., 2011; Akbarzadeh *et al*., 2013)

1.10.1 Phospholipolipids and Liposomes

Phospholipids (PL) are a class of amphipahtic molecules composed of hydrophilic (polar) head groups and hydrophobic (non-polar) hydrocarbon tail groups (Figure 1.12, P. 30) and can have a structural backbone such as glycerol or sphingomyelin (Cooper and Hausman, 2009). They are present in high levels of all cell membranes of living matter and can orient in a variety of supramolecular structures in aqueous solutions through the hydrophobic interactions of the hydrocarbon chains (Kent, 1995; Monteiro *et al*., 2014).

Biocompatible phospholipids and sphingolipids are mainly used to prepare liposomes. Phospholipids could comprise of different head and tail groups that can influence the surface charge and bilayer permeability of liposomes (Perrie and Rades, 2010). Common phospholipids used in liposome preparations are provided in Table 1.4.

Table 1.4 Examples of common phospholipids used in the preparation of liposomes

Name of phospholipid	The esterfied group	Net charge at pH 7
Phosphatidylcholine (PC)	$CH_2CH_2N^+(CH_3)_3$	Zwitterionic
Phosphatidylethanolamine (PE)	$CH_2CH_2NH_3^+$	Zwitterionic
Phosphatidylglycerol (PG)	$-CH_2CHOHCH_2OH$	Negative
Phosphatidylserine (PS)	$CH_2CHNH_3^+COO$	Negative

PLs could be naturally-occurring such as egg/ soy phosphatidylcholine (EPC) or synthetic such as dipalmitoylphosphatidylcholine (DPPC) (Monteiro *et al*., 2014) shown in Figure 1.13. Synthetic PLs are more stable than natural PLs because they can be produced from natural PLs with improved features. Modifying the non-polar and polar-regions of PLs permit

the formation of an unlimited variety of well-defined and characterized PLs (Monteiro *et al*., 2014).

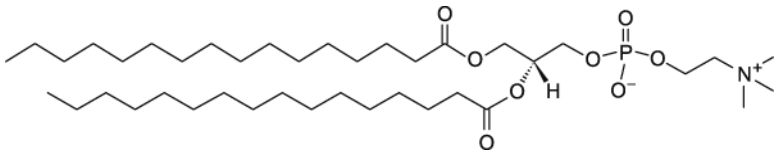

Figure 1.13 Chemical structure of dipalmitoylphosphatidylcholine (DPPC) lipid*. DPPC is a16 alkyl chain lipid which consists of a hydrophilic head group with a quaternary ammonium moiety choline linked to a glycerol via a phosphoric ester (Brandl, 2001). The permanent positive charge on the choline of the head group counteracts the negative charge of the phosphate to produce a neutral hydrophilic head group (Philippot and Schuber, 1994).*

Natural or synthetic phosphatidylcholine (PC) is the most widely employed phospholipid for preparing liposomes due to its stability and capacity to act against changes in pH or salt concentrations in the product and or the biological environment (Perrie and Rades, 2010). It is also the most predominant PL found in natural membranes, located in the outer leaflet of the cell membrane and accounting for 50-90% of cell membrane phospholipids (Kent 1995; Li and Vance 2008). PCs in mammals are usually synthesized from the DAG branch of phospholipid synthetic pathway and transferred to carbon-3 via the action of the choline: 1, 2-diacylglycerol cholinephosphotransferase (Li and Vance, 2008). It consists of a hydrophilic head group with a quaternary ammonium moiety choline, which is linked to a glycerol via a phosphoric ester (Brandl, 2001). The permanent positive charge on the choline of the head group counteracts the negative charge of the phosphate to give neutral hydrophilic head group (Philippot and Schuber, 1994).

1.10.2 Phase Transition Temperature (Tc)

Phase transition temperature (Tc) is the temperature above the lipid boiling point, which is required to change the lipid from an ordered gel phase, where the hydrocarbon chains are closely packed and extended, to a disordered liquid crystalline phase, where the hydrocarbon chains are randomly oriented (Mozafari *et al.,* 2008; Monteiro *et al*., 2014).

Factors affecting the Tc include hydrocarbon chain length, degree of saturation of the hydrocarbons, charge and polar head group species (Mozafari *et al.,* 2008). When a double bond exists between two carbon atoms in a hydrocarbon chain, the chain is said to be unsaturated, whereas hydrocarbon chains without double bonds are said to be saturated. The

length and degree of saturation of the lipid chain influence the gel liquid-crystalline Tc. As the hydrocarbon length is increased, van der Waals interactions become stronger requiring more energy to disrupt the ordered packing, therefore the phase Tc increases (Monteiro *et al*., 2014). Tc is lowered by decreased chain length and by unsaturation of the hydrocarbon chains and the presence of branched chains and bulky head groups (e.g., cyclopropane rings) (Szoka and Papahadjopoulos, 1980; Small, 1986). Liposomes cannot form at temperatures below Tc of the lipids and selecting a high transition lipid where the lipid vesicle would always be in the gel phase would contribute to an ideal non-leaky packaging system (Patel and Panda, 2012).

Tc of liposomes is crucial as it determines the permeability, fusion, aggregation, deformability and protein binding which all contributes to stability of liposomes and behaviour *in vitro* and *in vivo* (Mozafari *et al.*, 2008).

1.10.3 Characteristics of Liposomes

1.10.3.1 Liposomal Size

The size of a liposome usually ranges from approximately 20 nm upwards and may be composed of one or numerous bilayers, each with a thickness of approximately 4 nm (Maherani *et al.*, 2011) or 20-100 nm (Yang *et al*., 2011) as reported in literature. Size characteristics of liposomes and the number of bilayers present, depend on the method of preparation (Cornell, 2000).

Table 1.5 Classification of liposomes based on size and number of bilayers (Elhissi *et al*., 2006; Raman *et al*., 2010; Swaaya and deMello, 2013) as shown below:

Vesicle Types	Abbreviation	Diameter Size	Number of lipid bilayers
Small unilamellar vesicles	SUV	Diameter of 20-100 nm	One lipid bilayer
Large unilamellar vesicles	LUV	Diameter of > 100 nm	One lipid bilayer
Giant unilamellar vesicles	GUV	Diameter of > 100 nm	One lipid bilayer
Multilamellar vesicles	MLV	Diameter of 0.1-20 μm.	Four to twenty lipid bilayers
Multivesicular vesicles	MVV	Diameter of > 1 μm.	Multicompartmental structure

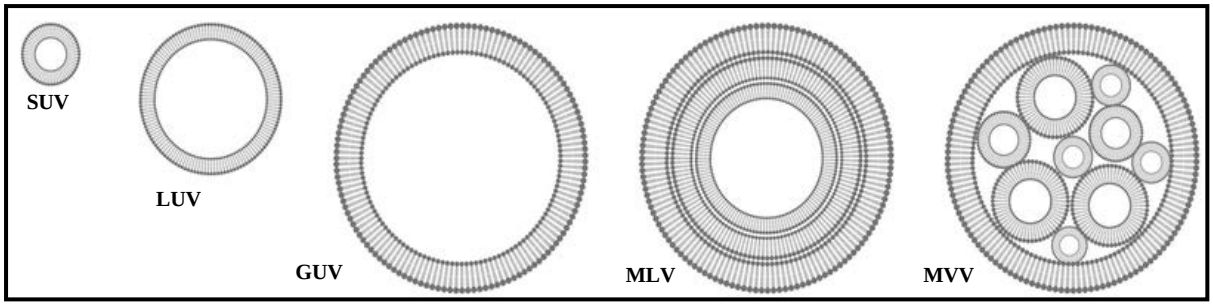

Figure1.14 Schematic illustration of the classifictaion of different liposomes based on size and number of bilayers *(Adapted from Swaaya and deMello, 2013 with a few modifications).*

The size of a liposome is crucial, as it will influence the rate of the opsonisation (process whereby the immune system recognises foreign particles and recruits immune cells called phagocytes to engulf and destroy these foreign particles) and clearance by the RES after intravenous administration and their ability to remain in blood vessels and exploit the EPR effect for delivering anti-cancer drugs (Liu *et al.,* 1995). Liposomes with a diameter of less than 150 nm have been reported to be suitable for efficient drug delivery (Takeuchi *et al.,* 2001). Lamellarity refers to liposomes that have more than one lipid bilayer and the number of lipid bilayers present in liposomes influences the encapsulation efficiency and drug release kinetics, therefore intracellular fate is affected by the size and lamellarity (Laouini *et al.,* 2012). Based on their composition and size, liposomes have the potential of transporting drugs or small molecules through blood vessels and biological barriers promoting efficient transport. Liposomes with a diameter of 100 nm or less can undergo free diffusion through the BBB by receptor mediated or absorptive mediated transcytosis (Prathyusha *et al.,* 2013).

If the size and composition of liposomes are not considered thoroughly before intravenous administration, larger liposomes (> 200 nm in diameter) can become coated by serum proteins such as opsonins, which would result in opsination and ultimately phagocytosis by the RES and would most likely accumulate in the liver (> 300 nm) and spleen (< 40 nm) (Maurer *et al.,* 2001; Immordino *et al.,* 2006). Small liposomes would have a lower density of opsonins on the membrane surface which would result in lower uptake by the macrophages and a greater chance to evade the RES and remain in the circulation longer before reaching the target site (Liu *et al.,* 1995), however NPs less than 10 nm have a greater propensity for renal clearance (D'Souza, 2014).

1.10.3.2 Liposomal Stability

Liposome stability consists of physical, chemical and biological stability. Physical stability indicates mostly the quality of the size and the charge present on the surface of liposomes as this should be considered for aggregation (Popovska *et al*., 2013). The ability of liposomes to maintain the surface charge for extended durations during storage adds to the high physical stability of the formulation and shelf life. Cationic liposomes can be stable at 4°C for long periods of time, if properly sterilized (Laouini *et al.,* 2012). Chemical stability entails the prevention of both the hydrolysis of ester bonds in the phospholipids bilayers and the oxidation of unsaturated sites in the lipid chain (Prathyusha *et al.,* 2013). Oxidation of phospholipids in liposomes occurs in unsaturated fatty acyl chain-carrying phosphlipids. The chains are oxidised via a free radical chain mechanism in the absence of particular oxidants. The ester groups of the phospholipids can be hydrolyzed in the presence of water, producing lysophospholipids, a high concentration of which commonly leads to an increased permeability of the lipid bilayer and a destabilization of the system (Prathyusha *et al.,* 2013). Chemical instability can lead to physical instability and leakage of encapsulated drug from the bilayers and fusion and aggregation of vesicles.

Approaches that can be taken to increase liposomal stability (Akbarzadeh *et al.,* 2013) are as follows:

a) Storing liposomes at low temperatures, protection from light and adding antioxidants such as α-tocopherol and butyl hydroxy toluene in order to minimize oxidation of liposomes.
b) Avoidance of high temperature and excessive shear forces.
c) Working under nitrogen or argon will minimize the oxidation of lipids during the preparation process and maintain low oxygen potential.
d) The hydrolysis of ester bonds can be reduced by optimising the pH, temperature, ionic strength, chain length and the amount of cholesterol incorporated into the bilayers.

1.10.3.3 Addition of Cholesterol (Chol) in Liposome Formation

The addition of the cholesterol (Chol) in the lipid bilayer improves the overall structural integrity and stability, and forms a highly ordered rigid membrane with fluid-like characteristics (Lee *et al.,* 2005; Monteiro *et al*., 2014). It does this by filling up holes present in the membrane, by reducing the permeability of the membrane to water soluble molecules

and decreasing the fluidity or increasing the microviscosity of the bilayer making it less permeable, thereby preventing drug leakage from the liposome and creating a more hydrophobic region (Monteiro *et al*., 2014). This could reduce binding of opsonins on the liposomes and may improve stability and retention of liposomes *in vivo* (Maurer *et al.*, 2001). Liposomal formulations containing Chol and phospholipids are referred to as 'conventional liposomes' (Monteiro *et al*., 2014).

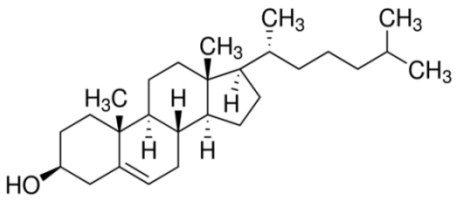

Figure 1.15 Chemical structure of cholesterol (Chol). *Chol consists of four hydrocarbon rings, making it strongly hydrophobic and hydroxyl (OH) group attached to the end of the Chol makes that part weakly hydrophilic (http://www.sigmaaldrich.com/catalog/product/sigma/c8667?lang=en&region=ZA).*

Chol molecular structure (Figure 1.15) consists of four hydrocarbon rings which aids in making it strongly hydrophobic. The presence of the hydroxyl (OH) group attached to the end of the Chol makes that part weakly hydrophilic therefore it inserts itself in the bilayer of liposomes with its OH-group towards the aqueous core, and the rigid hydrophobic tail toward the phospholipid bilayers (Cooper and Hausman, 2009; Perrie and Rades, 2010). Chol can be added to the lipid bilayers at concentrations up to 1:1 molar ratio, however Chol at higher molar ratios causes low encapsulation of drugs and the fact that it is readily oxidized could create problems for lipid based drug products (Nallamothu *et al.*, 2006; Torchilin and Weissig, 2003).

1.10.3.4 Surface Charge and Membrane Characteristics

Surface charge of the liposome is influenced by the lipids used in the liposome formation. The surface charge can be modified to suit applications; an example would be to use negatively or positively charged phospholipids which induce electrostatic repulsion and stabilization against liposome aggregation (Ogihara *et al.*, 2010).

Most biological cell membranes, including cancer cells exhibit a negative charge; neutral-charged liposomes with tightly packed membranes seem to remain in circulation for longer periods of time and display higher drug retention when compared to charged systems

(Honary and Zahir, 2013). Certain plasma proteins have an affinity for liposomes, and the affinity is enhanced if the liposome is charged.

Cationic systems interact quickly with various components in systemic circulation and thus have shorter half-lives *in vivo* (Maeda, 2000). Cationic liposomes can be more cytotoxic than neutral or anionic liposomes. This is due to the positive charge of the liposomes which allows non-specific interactions with cell membranes. However, anionic liposomes activate platelets but cationic or neutral liposomes do not (Ilinskaya and Dobrovolskaia, 2013). Cationic liposomes are less toxic *in vitro* than *in vivo*; studies suggest that reactive oxygen intermediates may be involved in the toxicity (Dokka *et al*., 2000; Audouy *et al*., 2002; Wu *et al*., 2004; Chien *et al*., 2005). Studies indicate that anionic liposomes containing negatively charged lipids such as PS and PG are quickly taken up by macrophages and thus disappear from the circulation in a short time (Liu *et al.,* 1995; Massing and Fuxius, 2000).

Therefore liposomes for drug delivery systems must maintain stability while in circulation for a prolonged period of time before reaching the intended site and avoid the RES in the process. In order to achieve this, liposomes can be coated with the commonly used polyethylene glycol (PEG) (Torchilin, 2005). PEG is a FDA approved hydrophilic polymer varying in molecular weight due to the number of monomer repeat units. Sterric stabilization of liposomes with PEG was one of the main advances in liposome development (Monteiro *et al*., 2014). PEG serves as a steric barrier with the flexible chains forming “brushes” which extends out from the surfaces of liposomes and changes the surface properties of liposomes. This prevents interaction of phagocytes and creates the desired “stealth layer” to produce the so-called ‘stealth liposomes’ or ‘PEGylated liposomes’ (Monteiro *et al*., 2014). PEG has good solubility properties in aqueous media and has been used to coat many NP, as it does not form any metabolites, has a low toxicity profile and does not accumulate in the RES (Perrie and Rades, 2010).

1.10.4 Liposomal Release of Contents

Liposomes have evolved since their discovery with many different stimuli being exploited to trigger the release of the encapsulated cargo from liposomes into cells, including temperature (Torchilin, 2005, Ponce *et al.,* 2006), pH (Simões *et al.,* 2004), light (Troutman *et al.,* 2009), redox potential (Ong *et al.,* 2008), magnetic fields (Amstad, *et al.,* 2011), near infra-red and ultrasound (Hagtvet *et al.,* 2011 and Nappini *et al.,* 2011) and targeting molecules each with its own specific advantage depending on the applications (Torchilin, 2005).

1.10.5 Liposome Interaction with Cells

Liposomes can enter cells via different mechanisms or a combination of mechanisms (Vyas and Khar, 2002). The entry of liposomes or their contents into cells is dependent on the type of liposomes as shown in Figure 1.16. They can be 1) non-targeting liposomes or 2) targeting liposomes:

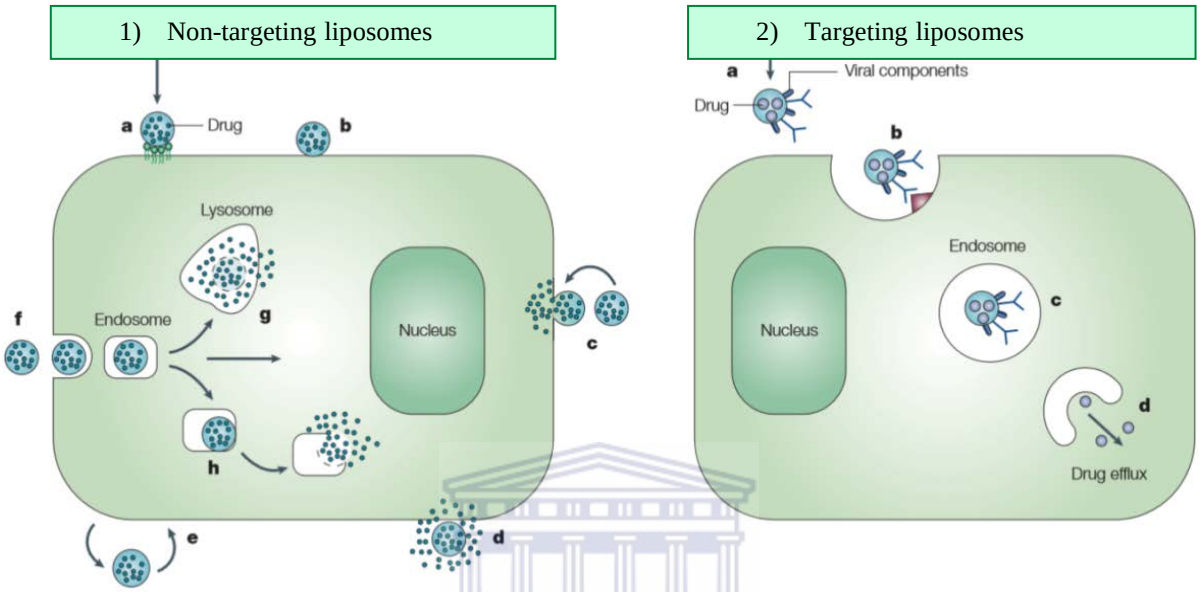

Figure 1.16 Different mechanisms of liposome-cell-interaction for non-targeting liposomes and targeting liposomes *(Adapted from Torchilin, 2005).*

1.10.5.1 Non-targeting Liposomes

Liposomes containing drugs can adsorb onto the cell surface (Figure 1.16, a and b). Adsorption on the surface of the cell can occur by physical attractive forces which causes the release of liposomal contents into the cells. This process may or may not involve internalisation of the liposome into the cell. In fusion (fusogenic liposomes), liposomes come into close proximity with the cell membrane and mixing of plasma membrane cell lipids occurs (Figure 1.16, c). This causes liposomal contents to automatically be released into the cell cytoplasm. Drugs can be released into the cytoplasm or can be destabilized by certain membrane components when adsorbed on the cell surface so that the released drug can enter the cells via micropinocytosis (Figure 1.16, d). Due to similar lipids found in the bilayer of liposomes, cell membranes can recognise these lipids, leading to lipid exchange (Figure 1.16, e). Internalisation by endocytosis (Figure 1.16, f) occurs when liposome come into close contact with the cell surface, cells form endosomes (Figure 1.16, g) through invagination of the plasma membrane, taking up the liposome which would then fuse with the lysosome to

form secondary lysosomes, allowing for cellular digestion of the lipids and release of its contents into the cytoplasm, where they are reduced by oxy-redoxy systems inside the cell (Figure 1.16, h) (Torchilin, 2005).

1.10.5.2 Targeting Liposomes

Liposomes loaded with drugs and accessorised with targeting molecules such as antibodies, peptides, aptamers etc (Figure 1.16, a, p. 38) can be cell-specific and interact with a specific recognition sites present on the surface of the diseased cell (Figure 1.16, b). Endocytosis occurs and the liposome is encapsulated into an endosome (Figure 1.16, c) to allow the drug to be released into the cytoplasm (Figure 1.16, d) (Torchilin, 2005).

1.10.6 Production Process of Liposomes

The production process of liposomes includes (Akbarzadeh *et al*. 2013):

1) Method of liposome preparation
2) Liposome size reduction
3) Purification
4) Characterization

1.10.6.1 Methods of Liposome Preparation

A number of different methods have been established based on the scale of the production, drug encapsulation, administration route and drug physiochemical properties, etc. (Akbarzadeh *et al*., 2013). Based on the different drug loading methods of preparing liposomes, two main approaches are used: passive loading methods and the active loading methods (Figure 1.17, p. 40) (Akbarzadeh *et al*. 2013; Popovska *et al.,* 2013).

In the passive loading method the drug is encapsulated by introducing an aqueous phase of a water-soluble drug or an organic phase of lipid-soluble drug before or during the steps involved in the manufacturing of liposomes (Popovska *et al.,* 2013). In this process, owing to the same drug concentration across the bilayer of the liposomes, the percentage of encapsulation depends on the affinity of the drug to the lipid membrane, the lipid composition of the membrane, the volume of internal aqueous phase, the concentration of the liposomes formed and the drug-to-lipid ratio (Muppidi *et al.,* 2012). For lipid-soluble drugs with high affinity to the lipid membrane, the passive loading method can yield a high entrapment efficiency of drugs (Akbarzadeh *et al*. 2013).

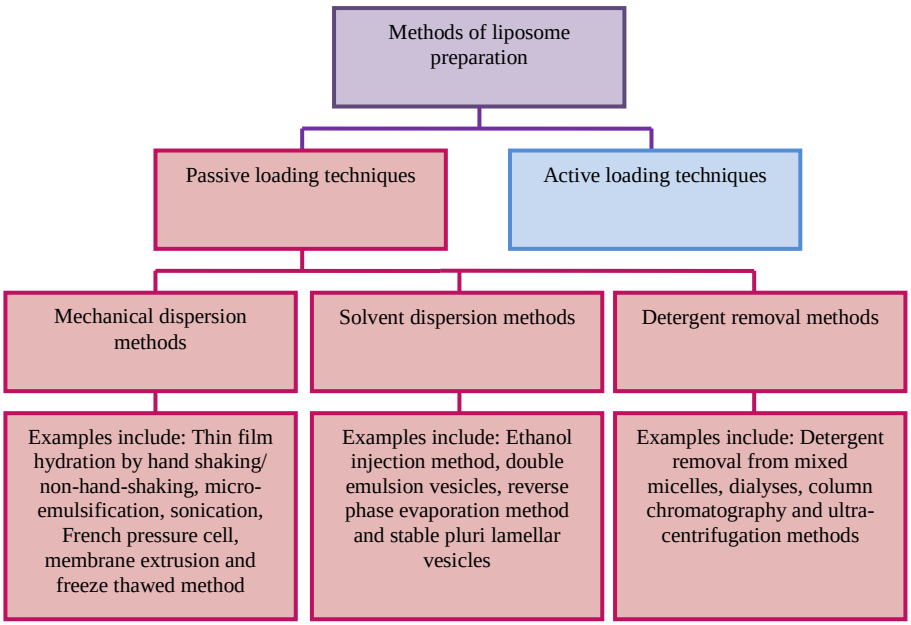

Figure 1.17 Different methods of liposome preparation. *Liposomes can be entrapped with drugs/molecules through passive loading techniques (drug/molecules are loaded during the process of preparation) or active loading techniques (drug/molecules are loaded after the liposome has been prepared**)** (Prathyusha et al., 2013).*

In active loading technique, the drugs are loaded after the liposome has been formed by creating diffusion gradients for ions or drugs across the external and internal aqueous phases such as K^+-Na gradient and H^+ gradient (Popovska *et al.*, 2013). The drug is able to permeate through the lipid bilayers into the liposome following the concentration gradient until equilibrium between the interior and the surrounding medium is attained (Gregoriadis, 2007). The amount of hydrophobic drug that can enter into a liposome depends on the packaging arrangement of lipids in the lipid bilayer. Polar drugs interact with the polar head groups of phospholipids and are sequestered by the liposomes but amphiphilic molecules are difficult to retain inside liposomes as they can rapidly permeate through lipid bilayers (Maherani *et al.*, 2011). Active loading has certain advantages since the active agent is not yet present during the preparation of the liposome but the method is restricted to a small range of drugs that behave as weak amphipathic bases or acids and can permeate bilayers in the uncharged state, but not in the charged state (Maherani *et al.*, 2011).

1.10.6.1.1 Thin Film Hydration Method

Thin film hydration method is the original method proposed by Bangham and is the simplest method for preparing liposomes on a research scale (Wagner and Vorauer-Uhl, 2011).

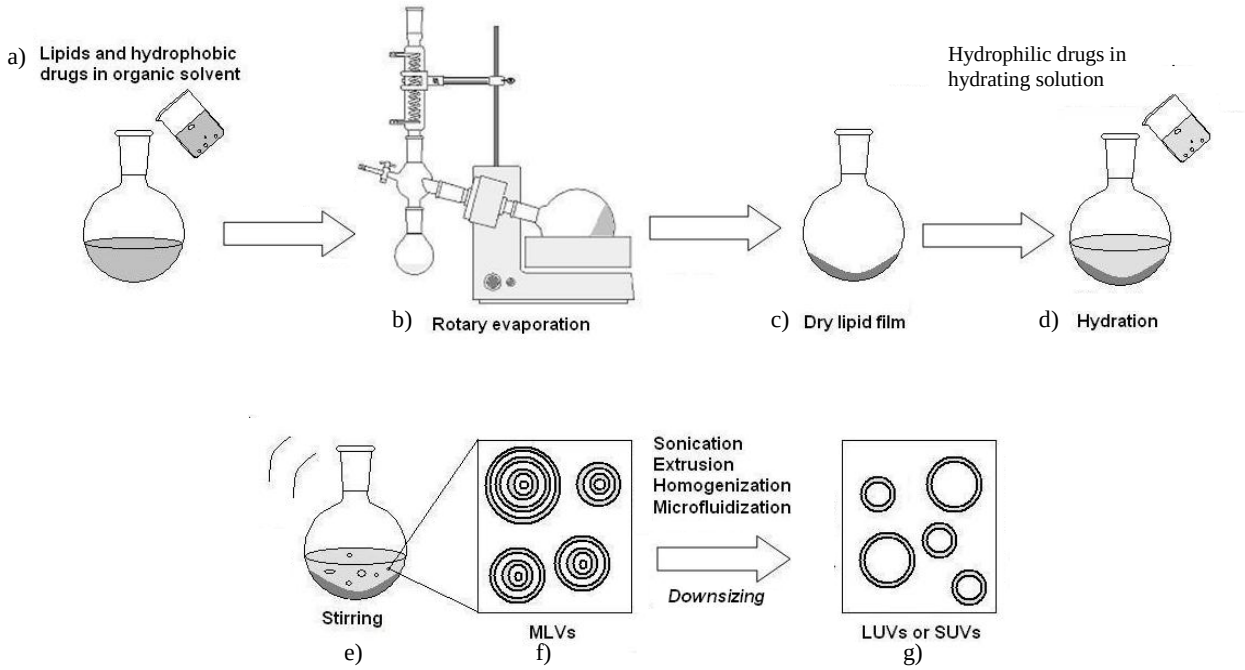

Figure 1.18 Flow diagram of liposome formation using thin film hydration method *(Adapted from Lopes et al., 2013, with a few modifications).*

The method (Figure 1.18) involves dissolving lipid compositions, with or without hydrophobic drugs in an organic solvent (chloroform only or chloroform: methanol mixtures) in a round bottom flask. The solvent is removed by a rotary evaporation at above Tc to produce a thin dry lipid film on the wall of the round-bottom flask (Figure 1.18, a, b, c). The thin film is hydrated by adding a hydration solution with/without the hydrophilic drugs to be encapsulated (Figure 1.18, d). The flask is then heated above Tc and stirred or vigorously shaken for a few hours (Figure 1.18, e). Liposomes are formed when thin lipid films are hydrated and detach during agitation and self-close into vesicles to form large MLVs (over 1 μm in diameter) (Figure, f). This method can yield an entrapment efficiency of approximately 40% and a heterogeneous sized population of multilamellar vesicles (MLVs) (Akbarzadeh *et al.*, 2013; Lopes *et al.*, 2013; Prathyusha *et al.*, 2013). Further sizing techniques are employed to create the desired size (Figure 1.18, g).

1.10.6.2 Size Reduction Methods

Sizing of liposomes requires energy input such as sonic energy (sonication) or mechanical energy (extrusion). The sonication method is a common method used for producing small unilamellar vesicles (SUVs) with diameters of roughly 15-25 nm. Two sonication techniques that exist are probe sonication and bath sonication (Akbarzadeh *et al.*, 2013). The disadvantage of sonication is the low internal encapsulation efficiency caused by damage to

the phospholipid structure, metal pollution from the probe tip as well as heterogeneous size distribution (presence of MLV along with SUVs) (Dua *et al.*, 2012; Akbarzadeh *et al.*, 2013; Popovska *et al.*, 2013).

Extrusion methods are based on the principle of passing MLV through filters with specific sizes to obtain a liposome population with a mean diameter size the same as the filter pore size. It was first introduced in the 1970s in order to reduce the size of liposomes for biological applications (Johnson *et al.*, 1971). It is the most common method of sizing liposomes and producing unilamellar vesicles (ULVs) on a research scale (Mokhtarieh *et al.*, 2013). Extrusion is more advantageous than sonication as a variety of lipid mixtures can be extruded without lipid degradation; it's possible to eliminate organic solvents or detergents from the final preparations and to produce homogenous populations of SUVs in the size range of 50-150 nm (Akbarzadeh *et al.*, 2013). There are many commercial products available for extruding liposomes but the most common extruder used is the *Avanti* large and mini extruders (Figure 1.19).

Figure 1.19 Avanti® Mini-Extruder. *Extruder compartments include two gas-tight glass syringes, membrane compartment and a heating block* ***(A)***. *The more times the lipsome suspension passes though the membrane, the more homogenous the lipid solution becomes, as noted by the whitish colour of liposome suspension before extrusion and the more transparent liposome suspension after extrusion (B) (http://www.avantilipids.com/index.php?option=com_content&view=article&id=533&Itemid=297).*

The extruders is made of stainless steel and Teflon, and has two glass gas tight syringes on either ends, one syringe is loaded with the liposome suspension and when pressure is applied the liposome suspension passes through the size specific filter pores for the required amount of passes to obtain a mean distribution of SUVs at a specific size range (Figure 1.19, A). An odd number of passes is used to finish on the opposite side, leaving everything that never made it through the filter in the first syringe. As the liposome suspension passes through the membranes repeatedly, the colour will become more transparent (Figure 1.19, B). The extruding process takes place on a heating block at above the Tc.

1.10.6.3 Purification Methods

Purification of liposomes is an important step as it removes low molecular weight material that was not entrapped into liposomes. Liposomes are normally purified by size exclusion chromatography, gel filtration chromatography, dialysis and centrifugation methods (Akbarzadeh *et al.*, 2013).

1.10.6.4 Characterization of Liposomes

Characterization of liposomes focuses on the evaluation of certain physio-chemical and biological parameters (Table 1.6). Taking the physical and chemical parameters into account, determines the safety profiles and final behaviour of liposomes both *in vitro* and *in vivo.*

Table 1.6 Different characterization techniques for liposomes

Characterization	Some of the methods/instrument used for characterization
Size, shape and surface morphology	Photon correlation spectroscopy (PCS) using Zetasizer NanoZS, Transmission electron microscopy (TEM), cryo-TEM, atomic force microscopy (AFM) and scanning electron microscopy (SEM)
Surface charge	Free flow electrophoresis, zeta potential measurement using a Laser Doppler electrophoresis (LDE) or Zetasizer NanoZS
Lamellarity	Nuclear magnetic resonance (NMR), Electron paramagnetic resonance (EPR) TEM and small angle X-ray scattering
Tc	Differential scanning calorimetry (DSC) and NMR
Phospholipid quantification	Lipid phosphorus content (Bartlett method)
Lipid oxidation	Spectroscopy, thin layer chromatography (TLC), high-performance liquid chromatography (HPLC), gas-liquid chromatography
Encapsulation percentage	Mini column centrifugation, gel exclusion, spectrophometry, fluorescence spectroscopy, enzyme based methods, HPLC, fluorescence spectrophotometer
Drug release	Diffuse cell/ dialysis and HPLC

1.10.7 Liposomal Encapsulation of Lipophilic Drugs

The water solubility of lipophilic drugs or compounds incorporated into the conventional liposome bilayer is often limited in terms of drug-to-lipid ratio (Dhule *et al.*, 2012). It has also been reported that some lipophilic drugs may interfere with the bilayer formation, limiting the dose which can be incorporated into the liposome (Chordiya and Senthilkumaran *et al.*, 2012). Furthermore, both incomplete and rapid release has been reported for lipophilic drugs entrapped within liposomes (Otero-Espinar *et al.*, 2010). In recent years, many different strategies have been employed to increase the overall entrapment of lipophilic drugs or molecules for aqueous encapsulation into liposomes, one such strategy is the use of cyclodextrins and liposomes.

1.11 Cyclodextrins (CDs)

Cyclodextrins (CDs) are torus-shaped supramolecular crystalline cyclic oligosaccharides with at least 6 D-(+) glucopyranose units attached by glucosidic bonds allowing amphoteric properties of a hydrophophilic outer surface and a lipophilic interior (Laza-Knoerr *et al.*, 2010).

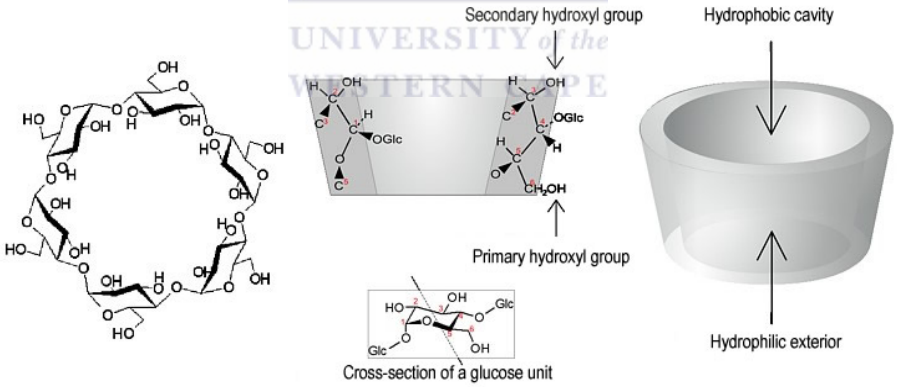

Figure 1.20 Molecular structure of β-cyclodextrin. *Cross-section of a cyclodextrin molecule is provided, showing the arrangement of a glucose unit and conical representation showing the hydrophilic exterior and hydrophobic cavity (http://www.chemiedidaktik.uni-wuppertal.de/disido_cy/cyen/info/03_physical_cy.htm).*

The glucopyranose units are present in a chair conformation and the hydrophilicity of the outer surface of CDs is due to the presence of hydroxyl groups orientated to the cone exterior with the primary hydroxyl groups of the sugar residues at the narrow and wider edges (Figure 1.20). The central cavity is formed by the skeletal carbons and ethereal oxygen's of glucose residues, which gives the CD molecule a hydrophobic inner cavity for appropriately sized non-polar molecules for forming host-guest complexes. The van der Waals, hydrogen bonds

and hydrophobic effects facilitate the formation of stable complexes of lipophilic/poorly water-soluable drug molecules in the non-polar cavity of CDs (Nasir *et al*., 2012). Consequently, CDs has been employed in numerous applications in a variety of fields, including the pharmaceutical industry and novel drug delivery systems (Nasir *et al*., 2012).

1.11.1 Advantages of CD Complexation

It is estimated that 30 different pharmaceutical products containing drug CD complexes is available worldwide (Tiwari *et al*., 2010). Some of the advantages of CDs complexation in pharmaceutical products (Otero-Espinar *et al*., 2010; Nasir *et al*., 2012) include:

- Improved aqueous solubility of many poorly water soluble drugs
- Enhanced bioavailability of drugs and decreased toxic effects associated with drugs
- CDs inclusion complexation helps to alleviate the irritancy of the drugs that normally irritate the stomach, skin or eye
- CDs conceal the unpleasant odour and bitter taste of drugs

1.11.2 Types of CDs

CD is usually classified based on several parameters such as the amount of glucopyranose units present, internal cavity diameter and molecular mass etc. There are over 1500 types of CD derivatives mentioned in literature (Szejtli, 1998; Blanford, 2014); common parent CDs is highlighted in Figure 1.21 and Table 1.7 (p. 46).

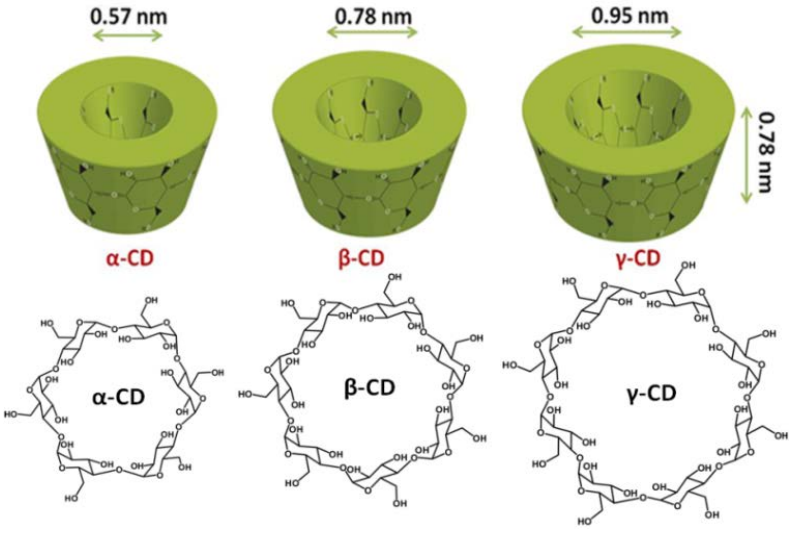

Figure 1.21 Three of the most common types of cyclodextrins (CDs). CDs are often classified based on the glucose units present: α-, β-, and γ-CDs (with 6, 7 or 8 glucose units respectively) (http://unam.bilkent.edu.tr/~uyar/images/Research_fig2.png).

Table 1.7 Characteristics of natural cyclodextrins (CDs) (Nasir *et al*., 2012).

Parameters	A-CD (α-CD)	B CD (β-CD)	γ-CD (γ-CD)
Empirical formula	$C_{36}H_{60}O_{30}$	$C_{42}H_{70}O_{35}$	$C_{48}H_{80}O_{40}$
Glucose units	6	7	8
Molecular mass	973	1135	1297
Cavity diameter	0.47-0.53 nm	0.60-0.66 nm	0.75-0.83 nm

The parent CDs are natural, non-reducing, crystalline, homogeneous, and non-hygroscopic having limited aqueous solubility due to strong intermolecular hydrogen bonding in the crystal lattice (Hakkarainen *et al.*, 2005). To improve their physiochemical properties and inclusion capacity, chemically modified derivatives of these parental CDs have been prepared which are amorphous, non-crystallisable with enhanced aqueous solubility, physical stability, and microbiological stability and reduced parent toxicity (Szente and Szejtli, 1999).

1.11.3 CD Complexation Techniques

The complexes are formed when a "guest" molecule (non-polar drug/molecule) is partially or fully included inside a "host" molecule (CD) with no covalent bonding (Astraya *et al*., 2009; Anjana *et al*., 2013). Some common techniques used include: solid dispersion or co-evaporated dispersion, neutralization method, kneading method, precipitation method, spray drying or automization method and certain melting techniques (Anjana *et al*., 2013).

1.11.4 BetA and CDs

The water solubility of BetA is poor (0.02µg/ml) (Jäger *et al.*, 2007), however the solubility of Bet and BetA was recently greatly improved by CD complexation, which created a stable complex, improving the *in vitro* and *in vivo* properties of the active compound (Dehelean *et al.*, 2011a; Şoica *et al.*, 2014). Natural and semi-synthetic CDs have been involved in triterpene complexation with good solubility and the best results were obtained with γ-CD derivatives (Dehelean *et al.*, 2008). Glucose derivatives have the added benefit of being able to cross the BBB actively, through saccharide receptors and channels; in particular glucose channels (Upadhyay, 2014). Therefore, the derivatives shown have additional advantages for the treatment of tumours located in the brain.

1.11.5 Liposomes and CDs

It has been reported that some lipophilic drugs may interfere with the lipid bilayer formation during the preparation of liposomes, limiting the dose which can be incorporated into the liposome. Furthermore, both rapid release and incomplete release have been reported for lipophilic drugs formulated in liposomes (Otero-Espinar *et al*., 2010). CDs and liposomes have been used in recent years as drug delivery vehicles (Table 1.8). By forming water soluble complexes, CD would allow insoluble drugs to accommodate in the aqueous phase of liposomes, thereby increasing the amount of insoluble drugs entrapped in liposomes improving the bioavailability and therapeutic efficacy of many poorly water solube drugs and may also offer a prolonged or controlled drug release (Arun *et al.,* 2008; Chordiya and Senthilkumaran, 2012; Nasir *et al.,* 2012). Problems associated with intravenous administration of CD complexes such as their rapid removal into urine can be avoided by their entrapment in liposomes (Arun *et al.,* 2008).

Table 1.8 CDs and liposomes as drug delivery vehicles

Drug/ anti-cancer agent	**Type of CD**	**Effect**	**Reference**
Asialofetuin	γ-CD	Increased gene transfer activity	Motoyama *et al.,* 2011
Benzocaine, Butamben	HPβCD	Enhanced intensity and duration of anesthetic effect	Maestrelli *et al.,* 2010
Curcumin (water insoluable chemical compound)	2HP-γ-CD	Increased efficiency and potential drug delivery vehicle for the treatment of various cancers	Dhule *et al.,* 2012
Colchicine	βCD	Sustained drug release and improved target specificity	Singh *et al.,* 2010
Fluocinolone acetonide	Several different CDs	Sustained-release profile over prolonged periods of time for ocular inflammatory disease	Vafaei *et al.,* 2014
Irinotecan	SBECD	Improved irinotecan retention resulting in a highly active liposomal irinotecan formulation demonstrating prolonged release and protection against hydrolysis	Li *et al.,* 2011
Prilocaine (anesthetic)	HPβCD	Efficient encapsulation of prilocaien (PRL) base in aqueous vesicle core, increased anesthetic effect duration and reduced initial lag time in comparison with PRL in the lipophilic phase or PRL hydrochloride in aqueous core.	Bragagni *et al.,* 2010

1.12 Justification of Current Research

Despite the best available treatment, tumour relapse is often observed in most patients diagnosed with high grade NBs. Treatment for NB cancer in the paediatric age group is crucial due to the developing brain as it is expected that two out of three survivors of the childhood cancer will ultimately develop at least one serious health problem within 20 to 30 years after the initial cancer diagnosis (Modak and Cheung, 2010). More than half of children diagnosed with high-risk NB will either not respond to conventional therapies or relapse after treatment, necessitating the development of novel treatments (London *et al*., 2011).

Cancer nanotechnology research is the most expanding interdisciplinary research that is using state of the art techniques to overcome limitations associated with early diagnosis and effective drug delivery systems for cancer. Liposomes are the first nano drug-delivery systems to reach cancer clinics, making them the most superior NP for nano-based drug delivery systems and are continuously being improved to better suit applications. They have the potential revolutionary impact into the understanding, visualization and therapeutic applications for NB cancer.

1.13 Aims

The aim of the study was to develop a NP drug delivery system for treating NB brain cancer cell lines with BetA. We proposed that BetA be incorporated into liposomes (BetAL) (Figure 1.22, p. 49), but due to its lipophilic nature, entrapment will occur only in the bilayers and this could pose a limitation when downsizing liposomes as the remaining entrapped BetA could be too poor to have potent cytotoxic efficacy. To improve BetA encapsulation within the aqueous core, BetA complexation with γ-CD was suggested to produce a γ-CD-BetA inclusion complex (Figure 1.24, p. 50). Double loading of BetA and the γ-CD-BetA inclusion complex into liposomes was expected to create a novel drug delivery system for BetA (γ-CD-BetAL) (Figure 1.25, p. 50).

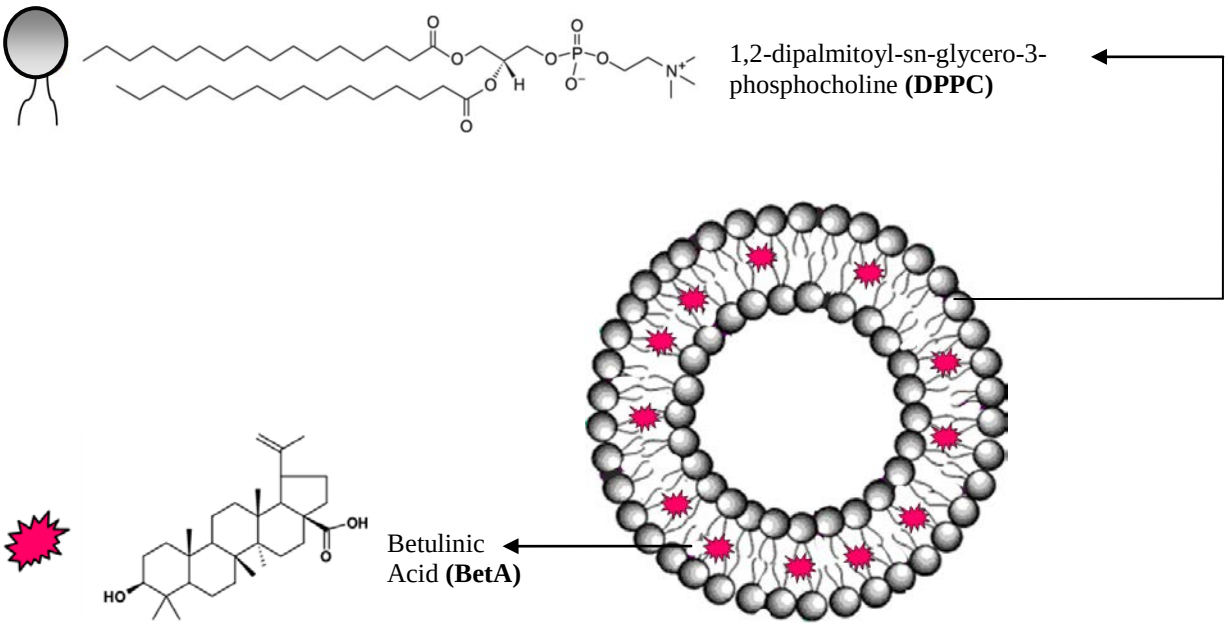

Figure 1.22 Schematic illustration of the BetAL delivery system

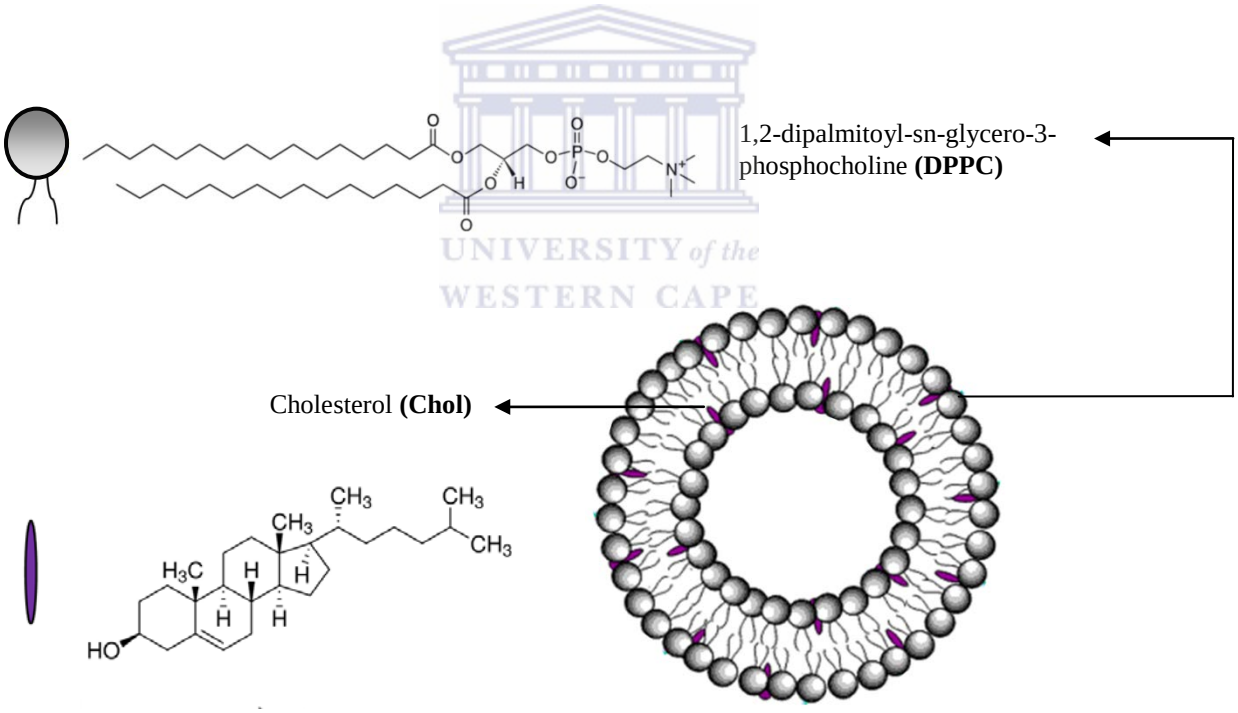

Figure 1.23 Schematic illustration of the Empty liposome (EL) delivery system.

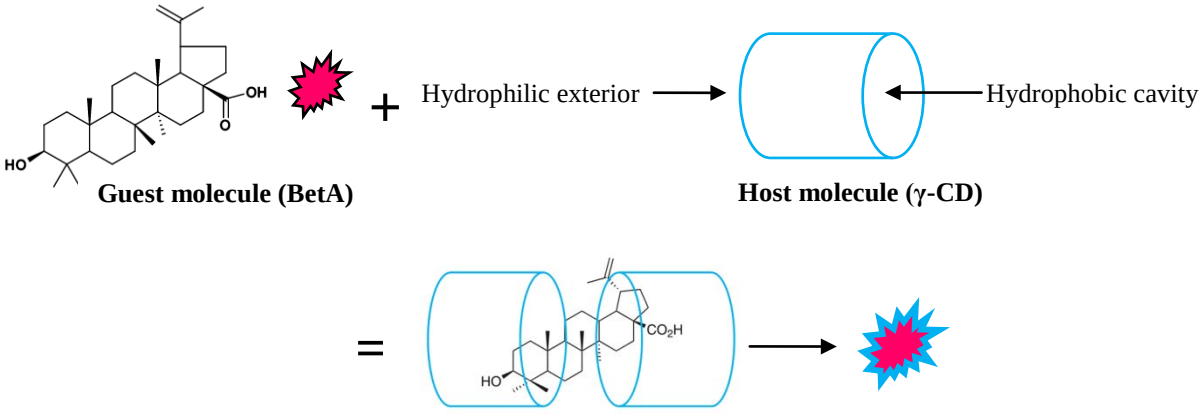

Figure 1.24 Schematic representation of γ-CD-BetA inclusion complex.

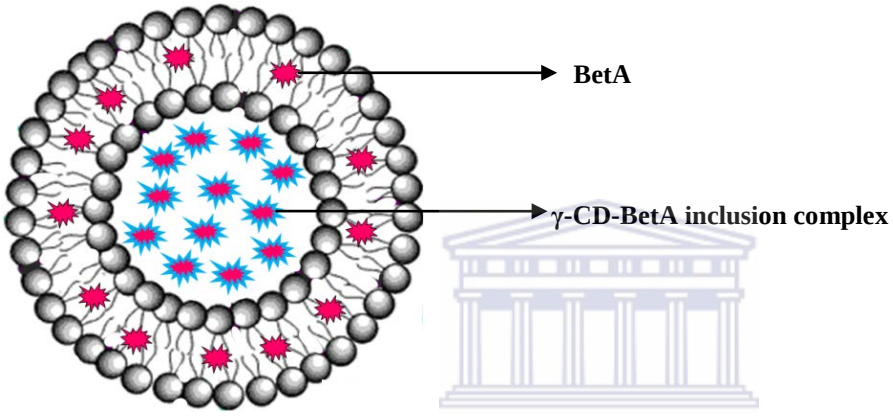

Figure 1.25 Schematic illustration of the γ-CD-BetAL delivery system.

1.14 Objectives

The objectives of the study were to prepare free BetA, empty liposomes (EL), BetAL and γ-CD-BetAL and evaluate:

1) Physical and chemical characteristics of the liposome designs
2) Effects on cell viability in SK-N-BE(2) and Kelly NB cell lines *in vitro*

1.15 Hypothesis

We hypothesize γ-CD-BetAL would produce a higher entrapment efficiency compared to BetAL and therefore a higher cytotoxic effect in comparison to BetAL.

CHAPTER 2

MATERIALS AND METHODS

2.1 Materials

2.1.1) Materials used in the preparation and characterization of liposomes with respective manufacturers:

1,2-Dipalmitoyl-Sn-Glycero-3-Phosphocholine	Sigma- Aldrich
Acetonitrile (HPLC grade)	Sigma- Aldrich
Betulinic acid (>98%, HPLC grade and 90% grade)	Sigma-Aldrich
Chloroform (HPLC grade)	Sigma- Aldrich
Cholesterol (Sigma Grade, ≥ 99%) (Chol)	Sigma-Aldrich
Disposable folded capillary cell	Malvern Ltd., Germany
Disposable plastic cuvette 12mm Square Polystyrene	Malvern Ltd., Germany
Methanol (HPLC grade)	Sigma- Aldrich
OptiSeal polypropylene tubes (4.9 ml, 13 x 51 mm)	Beckman Coulter, USA
Whatman nuclepore track-etched polycarbonate membrane (0.1µm**,** 19 mm)	Sigma-Aldrich
Whatman nuclepore track-etched polycarbonate membrane (0.2µm**,** 19 mm)	Sigma-Aldrich
γ-cyclodextrin (powder, BioReagent, suitable for cell culture, ≥ 98%)	Sigma-Aldrich

2.1.2) Materials used in cell culture experiments with respective manufacturers:

25 cm² Tissue culture flask	Biosmart
75 cm² Tissue culture flask	Biosmart
96-Well tissue culture treated plates	Biosmart

Cell proliferation reagent WST-1 (25 ml)	Roche
Centrifuge tubes (15 ml and 50 ml)	Biosmart
Cryovials	Biosmart
Dimethyl sulfoxide (DMSO)	Sigma
Dulbeco's modified eagles medium (DMEM)	Life Technologies
Ethanol	Kimix
Fetal bovine serum	Biochrome
Penicillin-streptomycin solution	Sigma-Aldrich
Phosphate buffered saline (1X, without calcium or magnesium and pH 7.4)	Whitehead Scientific
Pipette tips (white tips: 2-10 µl, yellow tips: 10-200 µl and blue tips: 200-1000 µl)	Biosmart
SK-N-BE(2) and KELLY Neuroblastoma cell lines	Radiobiology Department Stellenbosch University (gift)
Sterile 1 ml syringes and Sterile needles (0.70 x 32 mm)	Lasec
Sterile serological pipettes (5ml single-piece extrusion)	Biosmart
Sterile syringe filters (0.20µm)	Lasec
Trypan blue	Whitehead Scientific
Trypsin-Versene (EDTA) Mixture	Life Technologies

2.2 Experimental Design

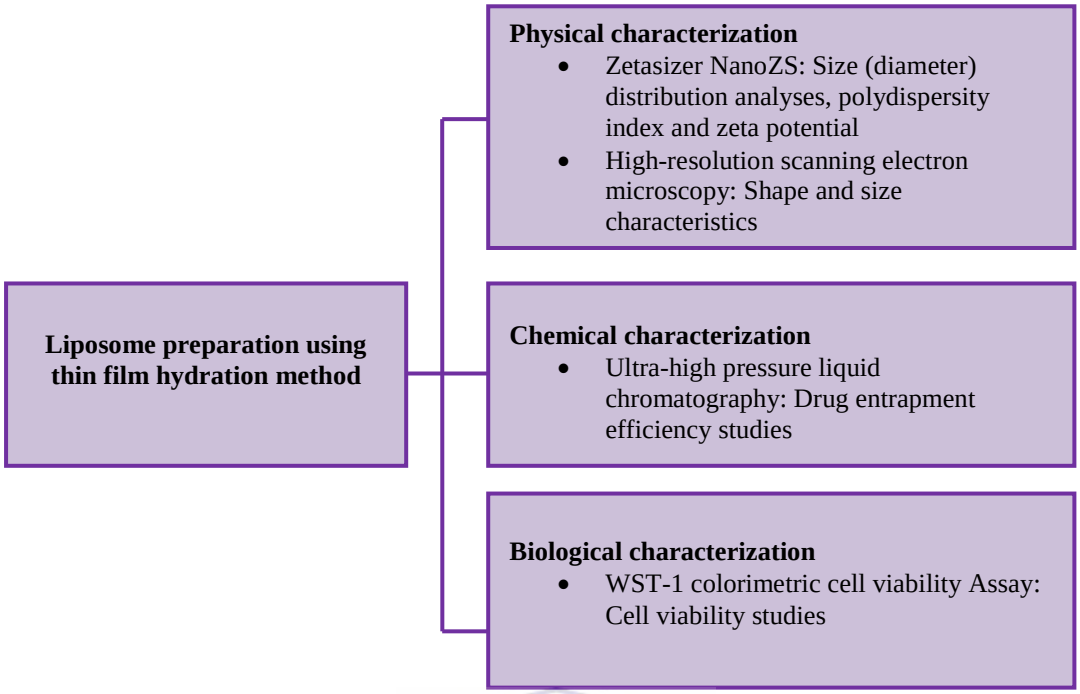

Figure 2.1 Schematic overview of the experimental design.

2.3 Methodology

The preparation and characterisation of liposomes was performed at the University of the Western Cape (UWC). Liposomes were prepared in the School of Pharmacy and the Department of Biotechnology. Characterization of liposomes occurred at the South African Institute for Advanced Materials Chemistry (SAIMC), the Department of Biotechnology and the Department of Physics (UWC). Cell culture study was completed at the Department of Biotechnology and Medical Biosciences.

2.3.1 Preparation of BetAL

Liposomes containing BetA were prepared by the passive drug encapsulation method as previously described (Csuk *et al*., 2011; Mullauer *et al.*, 2011) with a few alterations (Figure 2.2, p. 55). A lipid phase was prepared by dissolving accurately weighed quantities of BetA and 1,2-Dipalmitoyl-Sn-Glycero-3-Phosphocholine (DPPC) lipid (Table 2.1, p. 55) in 10 ml of chloroform and placed in a 250 ml round bottom flask. The solvent mixture was evaporated using a rotary evaporator (Lasec, South Africa), with the water bath set at above the phase transition temperature (Tc = 55 ˚C) until a whitish thin film of lipids was obtained on the surface of the flask. To ensure the complete evaporation of the solvent, the thin film was left overnight for complete dryness. The lipid film was then hydrated for 3 hours with 5

ml of 1 X phosphate buffered saline (PBS) (pH 7.4) at 55 ˚C in a shaking water bath (Labtec, Germany) allowing 10 minutes cooling cycles after each hour (Figure 2.2, p. 55). Empty liposomes (EL) were prepared using the same procedure, but excluding BetA (Table 2.1). The EL was used as a control to study the effects of the phospholipids and cholesterol (Chol) on the selected cell lines.

2.3.2 Entrapment of γ-CD-BetA (Inclusion Complex) into Liposomes (γ-CD-BetAL)

The γ-CD-BetAL was prepared as above; however in the hydration step when 1X PBS was added, the PBS contained the γ-CD-BetA inclusion complex (Figure 2.2, p. 55). Batch 1 (B1) was selected to be rehydrated with γ-CD-BetA inclusion complex in 1X PBS (pH 7.4) (Table 2.1, p. 55) as this batch demonstrated a higher entrapment efficiency when compared to Batch 2 (B2) (Chapter 3, section 3.4).

2.3.3 Preparation of the γ-CD-BetA

The preparation of the γ-CD-BetA inclusion complex was prepared as previously described (Şoica *et al*., 2014). Briefly, γ-CD and BetA powdered form was mixed, using a mortar and a pestle and kneading with ethanol and double distilled water (1:1 v/v) until most of the solvent was evaporated; the paste-type mixture was then dried at room temperature for 24 hours and placed in an oven at 105 ºC for nine hours. The final product was pulverized and sieved using a 100μm sieve. The binary products were prepared using 1:1 molar ratios. The γ-CD-BetA inclusion complex was dissolved in 1X PBS (pH 7.4) to produce a final volume of 0.5 mg/ml.

2.3.4 Size Reduction of Liposomes

Liposomes with a size of approximately less than 200 nm were designed by manual extrusion using an Avanti-mini extruder (Avanti Polar Lipids, Inc., USA). The hydrated solution was extruded 11 times through a 200 nm polycarbonate membrane followed by 5 times through a 100 nm polycarbonate membrane at 55 ˚C. Separate batches of BetAL (B1 and B2) and γ-CD-BetAL was not extruded to compare un-extruded liposomes with extruded liposomes. Triplicate batches were prepared for each liposomal formulation.

2.3.5 Purification

Prepared BetAL and γ-CD-BetAL were a mixture of encapsulated and un-encapsulated products. The resulting liposomes were transferred to 4.9 ml Beckman Coulter Optiseal tubes and then purified using ultracentrifugation (Beckman Coulter Optima L-80,

Beckman, USA) at 30 000 rpm at 4 °C for two hours to remove un-encapsulated products. The supernatant was removed and the tubes were then either characterized or capped and stored at 4 °C until use.

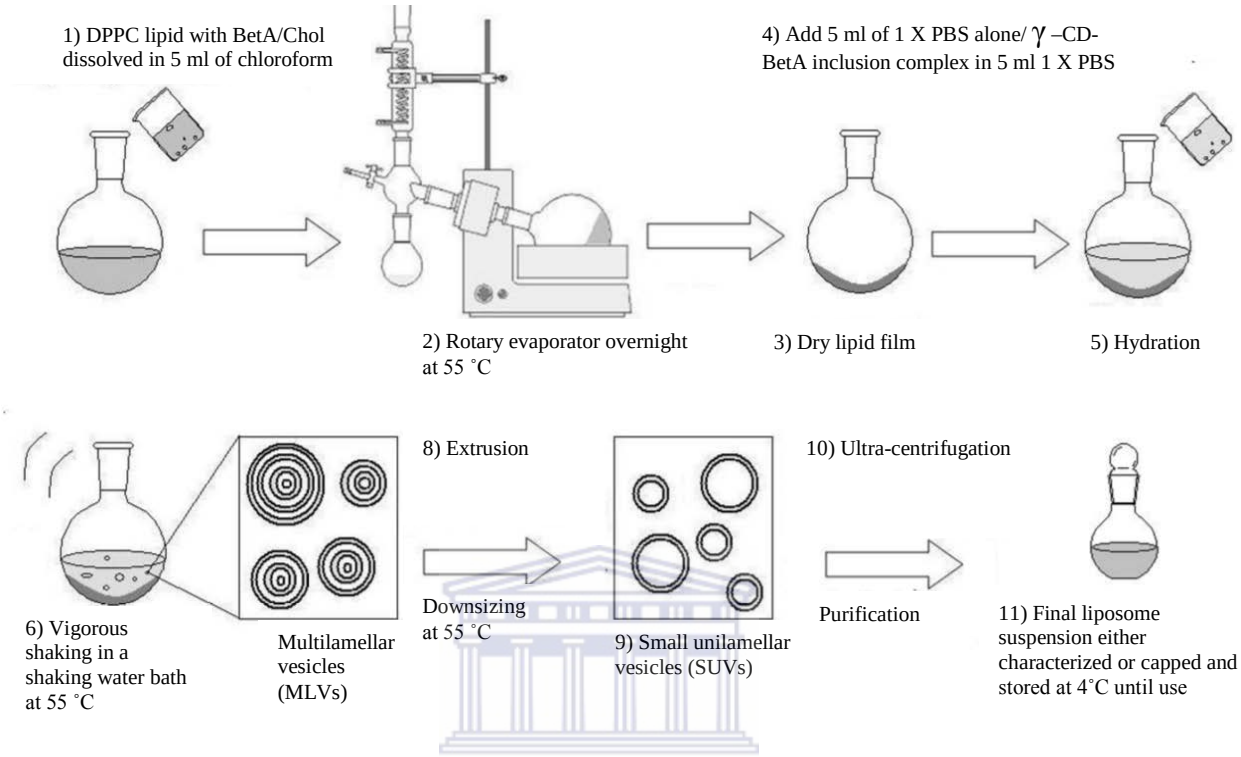

Figure 2.2 Schematic illustration of liposome preparation using thin film hydration method followed by downsizing and purification techniques *(Adapted from Lopes et al., 2013 and modified).*

Table 2.1: Drug-lipid ratio of BetA, DPPC and Chol (Triplicate batches were prepared for each liposomal formulation)

Batch	**BetA: DPPC: Chol (Weight ratio in mg)**
EL	X : 50 : 10
Batch 1 (B1)	2.5 : 50 : 0
Batch 2 (B2)	5 : 50 : 0
γ-CD-BetA L	2.5: 50: 0

2.4. Characterization Techniques

Characterization of liposomes is important as it will reveal the fate of the drug-delivery system *in vivo* and *in vitro*. In this study, synthesized liposomes underwent physical characterization, chemical characterization and biological characterization.

2.4.1 Physical Characterization

2.4.1.1 Determination of Size and Polydispersity Index

Photon correlation spectroscopy based on dynamic light scattering (DLS) technology and can be used to determine the particle size and polydispersity index (PDI). PDI refers to the width parameter derived from the cumulants analyses and provides information about uniformity in NPs size (Kale *et al*., 2012). This is important to consider, as particles with a PDI value close to 0.7 indicate that the sample has a very broad size distribution and is not suitable for DLS measurements. DLS measures the time-dependent fluctuations of light scattered from particles undergoing Brownian motion. When a particle is suspended in a solution and illuminated by light, it scatters light given that its index of refraction differs from that of the suspending solvent. Therefore DLS provides information about the size and the size distribution of NPs in solutions. Advantages of using this method include its sensitivity and minimal sample requirement (Laouini *et al.*, 2012).

The liposome size (diameter) distribution and polydispersity index (PDI) was measured using photon correlation spectroscopy techniques on a Malvern Zetasizer NanoZs (Malvern instruments, Ltd., UK) at 25 ºC using DLS at an angle of 173 ˚C to the laser beam. A sample of 1 ml was transferred to a 12 mm disposable plastic cuvette and placed into the instrument. The intensity-weighted mean value was measured and the average of three measurements was taken. DLS does not yield information about the shape of liposomes; hence other techniques were applied for this purpose.

2.4.1.2 Determination of Zeta Potential (ζ-Potential)

The presence of a net charge on a particle in solution will affect the distribution of ions around it; causing an increase in the concentration of counter ions. The area over which this layer extends is referred to as the electrical double layer (Hunter, 1981). This layer has two separate regions: the stern layer (inner layer of strongly bound ions) and the diffuse layer (outer layer of loosely associated ions) (Figure 2.3, p. 57). As particles move in solution as a

result of an applied voltage or gravity, the ions move as well. A boundary exists at some distance from the particle in which ions are stationary; this is referred to as the slipping plane (Figure 2.3). The potential that exists at the slipping plane of a particle in an aqueous solution is called the zeta potential (ζ-potential) (Domingues *et al*., 2008; Kaszuba *et al*., 2010).

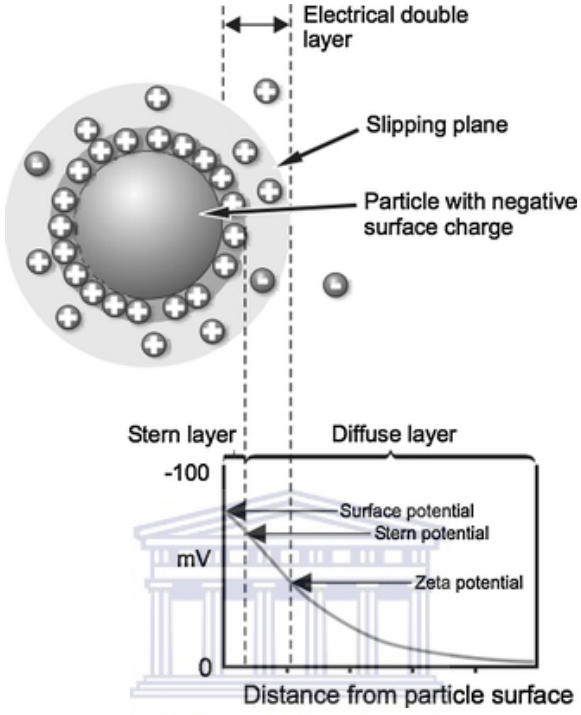

Figure 2.3 Schematic illustration of ions around a charged particle in solution, indicating the slipping plane. *The potential present at the slipping plane is defined as the zeta potential (ζ-potential) (Adapted from Malvern, 2007).*

The ζ-potential is a physical property which is exhibited by any particle in suspension and is a very good index of the interaction magnitude between colloidal particles (Popovska *et al*., 2013). Measurements of ζ-potential are commonly used to predict the stability of colloidal systems (Freire *et al*., 2011). Colloidal particles are measured using a folded capillary cell containing gold electrodes on either side. A voltage is applied and charged particles are attracted to the oppositely charged electrode on the folded capillary cell. The particles move in a known electric strength in the interference pattern of two laser beams and produce scattered light which depends on the speed of the particles, from this the ζ-potential can be recorded (Popovska *et al*., 2013). If all the particles in suspension have a large negative or positive ζ-potential then they will tend to repel each other and there will be no tendency to aggregate. However, if the particles have low ζ-potential values, then there will be no force to prevent the particles from aggregating (Popovska *et al*., 2013). Particle suspension with ζ-potentials > +30 mV or < −30 mV are normally considered stable (Hunter *et al*., 2001).

For this characterization technique, Malvern Zetasizer NanoZs was employed. A disposable folded capillary cell was rinsed with distilled water using a 1 ml syringe prior to analyses as recommended by the manufacturer and 700 µl of liposome solution was added to the cell. The samples were then analyzed with a voltage of 4 mV at 25 ºC at an angle of 173 ˚C to the laser beam. The intensity-weighted mean value was measured and the average of three measurements taken.

2.4.1.3 Determination of Shape and Size Characteristics of Liposomes

Scanning Electron Microscopy (SEM) is often used to study the surface morphology and shape characteristics of NPs (Charurvedi and Dave, 2012). An electron beam is generated by an electron gun and passes through the electromagnetic lenses of a column and across the surface of a sample. Electrons interact with atoms on the surface of the sample, producing various signals that can be detected to create an image, providing information about the sample size topography and composition. In this study, the shape and size characteristics of liposomes were investigated based on a previous method with a few alterations (Odeh *et al.,* 2012).

A drop of un-extruded or extruded liposomes was dispersed on carbon adhesive tape applied on an aluminium stub, then dried completely under fume hood. The dried liposomes was coated with gold palladium for 30 seconds using Emitech K550X (England) sputter coater and viewed with the Auriga HR-SEM F50 (Zeiss, South Africa) with a voltage of 5 KV.

2.4.2 Chemical Characterisation

2.4.2.1 Determination of the Concentration of BetA (in mg/ml) Entrapped in Liposomes and the Percentage Entrapment Efficiency (% EE) of BetA in Liposomes

Standard solutions of BetA (0.005, 0.01, 0.04, 0.06, 0.0625, 0.08, 0.1, 0.125, 0.25, 0.5 and 1 mg/ml) were prepared in methanol. Following ultra-centrifugation in the purification step, the pellet was lysed in methanol and vortexed for 10-15 minutes and diluted suitably for analyses with ultra-high performance liquid chromatography (Perkin Elmer Flexar FX-15 UHPLC, USA). All standards as well as samples were filtered through 0.2 µm filters. The HPLC method was adapted from Taralkar and Chattopadhyay (2012) with a modification in the detection time due to the use of a shorter C-18 column and an UHPLC system which offered a more robust and sensitive system and allowed for earlier detection of BetA (refer to appendix for chromatographs, section 7.2). The UHPLC experimental conditions was carried

out at 35 °C using a C-18 (4.5 mm x 150.5 µm) column (Phenomenex Kinetex, USA), a mobile phase of acetonitrile : methanol (80:20 v/v), an injection volume of 10 µl, at 0.5 ml/min flow rate and detection at a wavelength of 205 nm at 2.5 minutes. Triplicate injections were performed for standards and using the averaged area under the curve/peak, a calibration curve was constructed (Figure 2.4) and the concentration in mg/ml of BetA in liposomes was determined using the linear equation. The percentage entrapment efficiency (% EE) of BetA in liposomal formulations was determined as previously described (Ramana *et al.*, 2010 and Begum *et al.*, 2012):

$$\% \text{ EE} = \frac{\text{Amount of drug in liposomes (pellet) (mg/ml)}}{\text{Total amount of drug used (mg/ml)}} \text{ X } 100$$

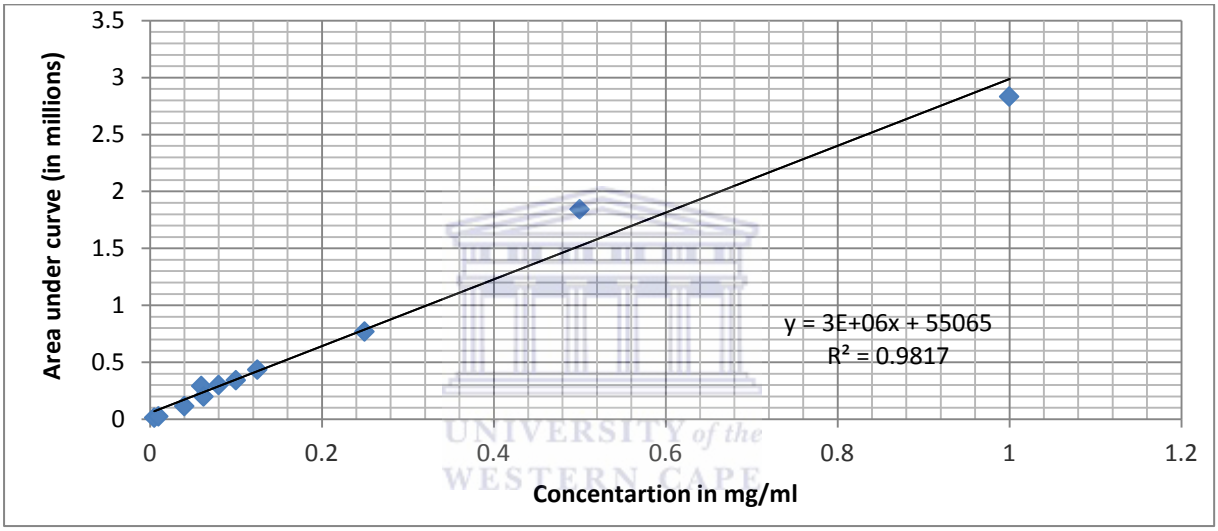

Figure 2.4 UHPLC calibration curve of BetA. *BetA standards (0.005-1 mg/ml) were dissolved in methanol and analysed using ultra high performance liquid chromatography (Perkin Elmer Flexar FX-15 UHPLC, USA). The average area under the curve/peak for each concentration was obtained and used to construct a calibration curve (refer Appendixes, section 7.2). The linear equation was used to determine the concentrations (in mg/ml) and % entrapment efficiency (% EE) of BetA in liposomes (n = 3 for each liposomal formulation).*

2.4.3 *Biological Characterization*

2.4.3.1 Cell Culture Procedures

Established human NB brain cancer cell lines SK-N-BE(2) and KELLY were a gift from the Radiobiology Department at the University of Stellenbosch. The same standardized cell culture protocol was used to grow SK-N-BE(2) and KELLY NB cells in Dulbeco's Modified Eagles Medium (DMEM) supplemented with 1% penicillin/streptomycin and 10% Fetal Bovine Serum (FBS).

SK-N-BE(2) NB cell line is a sub clone from the parental cell line which was established in 1972 from the bone marrow of a two year old Caucasian male biopsy with disseminated stage

4 NB after repeated courses of chemotherapy and radiotherapy (Lee and Kim, 2004). The morphology presents as epithelium-like cells that are mixed adherent and suspension growth. They are known to exhibit moderate levels of dopamine bet hydroxylase and tyrosine hydroxylase activity.

The KELLY NB cell line is derived from human brain and shows a predominantly neuronal morphology with adherent cell growth. The cells have a genomic amplification of the N-myc gene and express elevated levels of N-myc RNA or protein (nuclear DNA binding protein) (Beierle *et al*., 2007). The following procedures were followed:

i) Thawing of Cells

When required, frozen vials of SK-N-BE(2) NB cell line (passage number 4) and KELLY NB cell line (passage number 82) were removed from storage at -80 °C and quickly thawed. The contents of the cryovial were slowly mixed with 9 ml of growth medium in a 15 ml centrifuge tube. The cells were centrifuged at 2500 rpm for 5-7 minutes; the supernatant was decanted and the pellet was re-suspended in 10 ml of complete media and 5 ml each was transferred into two 25 cm^2 tissue culture flasks and placed in a water jacketed CO_2 incubator (Labtec, Germany) at 37 °C with 5% CO_2 until 70–80% confluency was reached.

ii) Sub-culture and Trypsinization Procedure

When the cells reached the desired confluency, the media was discarded and the cells were rinsed with 1 ml of 1X PBS (pH 7.4). The PBS was discarded and 1–2 ml of 2X trypsin EDTA was added to the flask to detach the monolayer. The flask was placed in a water jacketed CO_2 incubator at 37 °C with 5% CO_2 for 3-5 minutes. After incubation the cell suspension was removed and 5 ml of DMEM was added to deactivate trypsin. To remove traces of trypsin, the cells were centrifuged at 2500 rpm for 5-7 minutes and the supernatant was discarded. The cell pellet was then re-suspended in 5 ml growth medium and the cells counted using trypan blue and a Countess™ automated cell counter (Invitrogen, USA). Cells were seeded into 25 cm^3 or 75 cm^3 tissue culture flasks and placed in the water jacketed CO_2 incubator at 37 °C with 5% CO_2. Cells were seeded in a ratio of 1:6/1:10 for SK-N-BE(2) and 1:4 for KELLY NB cells with media renewal occurring every 3-4 days.

iii) Trypan Blue for Cell Viability and Cell Seeding

Live cells have intact cell membranes that exclude certain dyes, such as trypan blue whereas dead cells do not. Therefore trypan blue stains non-viable cells blue and viable cells will remain opaque or clear.

Cell viability and cell counting for seeding into plates was conducted using trypan blue by mixing 10 µl cell suspension and 10 µl trypan blue and pipetting it into the countess chamber slide (Invitrogen) which was analysed using the Countess Automated Cell Counter (Invitrogen, USA). The required cell suspension and media was added and seeding for experimental use took place one day before exposure to dimethyl sulfoxide (DMSO), free BetA, free γ-CD and liposomal formulations. Only cells with a viability of 80% and higher were seeded.

iv) Cryopreservation

Once cells reached the desired confluency, cells were trypsinized as described above (section ii); but the final cell pellet was re-suspended in cryo-media consisting of 90% FBS and 10% DMSO. The resultant suspension was stored in cryovials containing 1 ml aliquots. These vials were stored at -80 °C for short term storage and -150 ˚C for long term storage.

2.4.3.2 Cell Viability Studies Using the WST-1 assay

Agents that disrupt cell membranes and destroy the respiratory chain will affect cell proliferation and can be detected with a cell proliferation reagent such as WST-1 proliferation assay. WST-1 is a stable tetrazolium salt cleaved to a soluble formazan by a complex cellular mechanism that occurs at the cell surface. This bioreduction depends on the glycolytic production of NAD(P)H in viable cells. Therefore, the amount of formazan dye formed is directly proportional to the number of metabolically active cells in the culture. WST-1 cell viability assay is considered to be more favourable when compared to other cell viability assays such as MTT and XTT assays as it has several advantages over older cell viability assays. WST-1 does not have the additional solubilisation step as MTT, but can be measured after 2-4 hours incubation. WST-1 is more stable than XTT and MTS and can be stored at 2 to 8˚C for several weeks without degradation (CytoSelect™ WST-1 Cell Proliferation Assay Reagent Product Manual, 2013-2014).

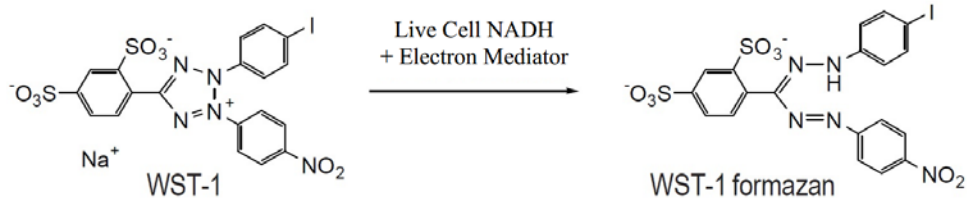

Figure 2.5 The principle of WST-1 colorimetric cell viability assay. *This assay is based on the conversion of the metabolically active/live cells from WST-1 to formazan in the presence of cellular NADH and electron mediator. Live cells can be detected by the observable orange colour change and can be measured with a spectrophotometer with an absorbance at 450 nm and the reference absorbance at 620 nm (http://www.cellbiolabs.com/sites/default/files/CBA-253-cell-proliferation-assay-colorimetric.pdf).*

i) DMSO Tolerance Test for SK-N-BE(2) and KELLY NB Cells

Following the trypsinization and cell counting procedure, 100 µl of cells were seeded into the inner columns and rows of 96-well plates (where n = 6 for each column treated) while 100 µl of 1X PBS (pH 7.4) was added to the outer rows and columns to avoid evaporation around the perimeter. Cells were seeded at a cell density of 1 x 10^3 and 5 x 10^3 for SK-N-BE(2) and KELLY NB cells respectively (Baik *et al*., 2012; Gogolin *et al.*, 2013). Cells were allowed 24 hours for attachment in a water jacketed CO_2 incubator at 37 °C with 5% CO_2 after which the media was removed and replaced with 100 µl of fresh media or DMSO concentrations (0.1%, 0.4%, 1% and 2%) and placed back into the incubator for 24, 48 and 72 hours exposure. DMSO concentrations were prepared in DMEM (1% penicillin/streptomycin and 10% FBS) in order to obtain increasing concentrations of 0.1%, 0.2%, 1% and 2% DMSO and stored at 4 ˚C. Following incubation, on the day of 24, 48 and 72 hours exposure the WST-1 colorimetric assay was performed according to the manufacturer's protocol; briefly 10 µl of WST-1 reagent was added to all the occupied wells, except PBS occupied wells. The plates were incubated in the water jacketed CO_2 incubator at 37 °C with 5% CO_2 for 4 hours. After incubation, the plates were gently shaken for a minute and read with a spectrophotometer (BMG labotec, Germany) with an absorbance wavelength set at 450 nm and the reference absorbance wavelength set at 620 nm. The parameters for the plate were set as follows: Blank (media), negative control (media and cells) and experimental (DMSO concentrations).

ii) Evaluation of Cell Viability Following Exposure to Free BetA

Free BetA concentrations (5-2 µg/ml) were prepared as previously described (Damle *et al*., 2013). BetA was dissolved in DMSO in order to prepare a stock solution of 5 mg/ml and diluted in DMEM (1% penicillin and streptomycin and 10% FBS) to obtain concentrations of

5 µg/ml, 10 µg/ml, 15 µg/ml and 20 µg/ml of free BetA. The stock solution of BetA was sterile filtered (0.2 µm filter) before being used to prepare 5-20 µg/ml free BetA. The stock solution and working solution were stored at 4 ˚C (Faujan *et al*., 2010).

A 100 µl of cells were seeded into 96-well plates (where n = 6 for each column treated) while 100 µl of PBS was added to the outer rows and columns to avoid evaporation. Cells were seeded at a cell density of 1 x 10^3 and 5 x 10^3 for SK-N-BE(2) and KELLY NB cells respectively. Cells were allowed 24 hours for attachment in a water jacketed CO_2 incubator at 37 °C with 5% CO_2 after which the media was removed and replaced with a range of 5-20µ g/ml of free BetA and placed back into the incubator for 24, 48 and 72 hours. Following incubation, the WST-1 colorimetric assay was performed as described above (section 2.4.3.2, i). After incubation, the plates was gently shaken for a minute and read with a spectrophotometer (BMG labotec, Germany) with an absorbance wavelength set at 450 nm and the reference absorbance wavelength set at 620 nm. The parameters for the plates were set as follows: Blank (media), negative control (media and cells) and experimental (free BetA concentrations).

iii) Evaluation of Cell Viability in SK-N-BE(2) and KELLY NB Cell Lines Following Exposure to Liposomal Formulations and Free γ-CD

BetAL concentrations was prepared as free BetA by diluting the prepared BetAL (in PBS solution) with DMEM (1% penicillin and streptomycin and 10% FBS) in order to obtain increasing concentrations of 5 µg/ml, 10 µg/ml, 15 µg/ml, 20 µg/ml and 50 µg /ml BetAL. Free γ-CD was prepared based on the initial amount used in the preparation of γ-CD-BetAL. A stock concentration of 2.84 mg/ml of γ-CD was prepared in PBS and diluted in DMEM (1% penicillin and streptomycin and 10% FBS) in order to obtain increasing concentrations of 5 µg/ml, 10 µg/ml, 15 µg/ml, 20 µg/ml and 50 µg/ml free γ-CD. The γ-CD-BetAL concentration was selected based on the cell viability results obtained from free γ-CD exposure (5-50 µg/ml).

A 100 µl of cells were seeded into 96-well plates as described above (where n = 6 for each column treated). Cells were seeded at a cell density of 1 x 10^3 and 5 x 10^3 for SK-N-BE(2) and KELLY NB cells respectively and cells were allowed 24 hours to attach in a water jacketed CO_2 incubator at 37 °C with 5% CO_2 after which the media was removed and replaced with a 100 µl of EL, BetAL (5-50 µg/ml) and free γ-CD (5-50 µg/ml) for 24, 48 and

72 hours. The γ-CD-BetAL concentrations were selected based on free γ-CD results (5-50 μg/ml for 24 hours and 5-15 μg/ml for 48-72 hours for KELLY NB cell line and 5-50 μg/ml for 24 hours, 5-15 μg/ml for 48 hours and 5-10 μg/ml for SK-N-BE(2) NB cell line). Following incubation, the WST-1 colorimetric assay was performed as described above (section 2.4.3.2, i). Plates were gently shaken for a minute after incubation and read with a spectrophotometer (BMG labotec, Germany) with an absorbance at 450 nm and the reference absorbance at 620 nm. The parameters for the plate were set as follows: Blank (media), negative control (media and cells) and experimental (EL, conventional BetAL, free γ-CD and γ-CD-BetAL).

2.5 Statistical Analysis

2.5.1 Liposome data was analysed using GraphPad Prism (version 5)

- Two-way Anova and T-test for grouped data
- Data represented as the mean ± standard deviation (SD)
- A probability of $P < 0.05$, $P < 0.01$ and $P < 0.001$ indicates level of statistical significance (annotated by one, two and three asterisks respectively)

2.5.2 Cell culture data was analysed using Medcalc Statistics Programme (version 11.6.1)

- Student T-test was selected for parametric data
- Data represented as the mean ± SD
- A probability of $P < 0.05$ indicates statistical significance (annotated by one asterisk)

2.5.3 IC_{50} concentration values was determined using the linear regression analyses feature after plotting a X-Y graph on GraphPad Prism (version 5)

CHAPTER 3

PHYSIO-CHEMICAL CHARACTERISATION OF LIPOSOMES GENERATED FROM THIN FILM HYDRATION METHOD

Numerous methods of synthesising liposomes have been proposed since their discovery in the 1960's, however the most widely employed and convenient method for research scale liposome production still remains the thin film hydration method (Kraft *et al*., 2014). In this study, different liposome formulations were prepared using the thin film hydration method as described in Chapter 2, section 2.3.1. BetA containing liposomes (BetAL and γ-CD-BetAL) were synthesized using the passive drug encapsulation technique as previously described (Mullauer *et al*., 2011). Two BetAL batches were prepared with different BetA concentrations, while the lipid concentration remained constant: Batch 1 (B1) (50 mg DPPC: 2.5 mg BetA) and Batch 2 (B2) (50 mg DPPC: 5 mg BetA). In order to enhance BetA loading into liposomes, BetA was complexed with γ-CD to produce a γ-CD-BetA inclusion complex (γ-CD-BetA) (Dehelean *et al*., 2011a; Şoica *et al*., 2014), subsequently double loading of BetA and γ-CD-BetA occurred to produce the novel γ-CD-BetAL liposomes (section 2.3.2 and 2.3.2, Chapter 2). Empty liposomes (EL) (50 mg DPPC: 10 mg Chol) containing no BetA were also prepared and compared to BetAL formulations. Liposomal formulations were characterized based on size, polydispersity index (PI) and zeta-potential (ζ-potential) using photon correlation spectroscopy (Zetasizer NanoZS instrument). Shape and size characteristic were studied using high resolution scanning electron microscopy (HR-SEM). The concentration (in mg/ml) of BetA entrapped in liposomes and the percent entrapment efficiency (% EE) was determined using ultra-high pressure liquid chromatography (UHPLC). Thin film hydration method yields multilamellar vesicles (MLVs) in the μm size range; therefore liposomes were downsized using an Avanti-mini extruder above phase transition temperature (Tc = 55 ˚C) to produce liposomes in the nm size range. Un-extruded liposomes were compared to the extruded liposomes for each liposomal formulation. The data was obtained in triplicates and analysed using GraphPad Prism 5 in order to construct bar graphs (mean ± standard deviation, n = 3 ± SD). The error bars were calculated standard error of the means and the level of statistically significant differences are annotated by asterisk(s) (* $P < 0.5$; ** $P < 0.01$; *** $P < 0.001$).

3.1 Size Analysis of the Liposomes

When a large multilamellar vesicle (MLV) suspension created after thin film hydration is forced through filters with defined pore sizes above Tc, concentric layers of the MLVs deform to pass through the pore. The destruction of the lipid bilayer membranes occurs as liposomes are reduced in size to produce unilamellar vesicles (ULVs) or small unilamellar vesicles (SUVs) (Mokhtarieh *et al*., 2013). If a liposome suspension is continually cycled through a filter with a specific pore size, this process will produce liposome populations with a mean diameter that reflects that of the filter (Hinna *et al*., 2015). In this study the prepared liposomes were extruded 11 times through a 200 nm polycarbonate membrane followed by 5 times through a 100 nm polycarbonate membrane at 55 ˚C (section 2.3.4, Chapter 2).

Figure 3.1 (p. 67), shows the size distribution of un-extruded liposomes (A), extruded liposomes (B) and the comparison of the two (C). Un-extruded EL (4194 nm ± 2260) is noticeably larger when compared to the other un-extruded BetA loaded liposomal formulations, while γ-CD-BetAL showed the smallest size (1367 nm ± 190.5). Liposomes loaded with BetA (B1, B2 and γ-CD-BetAL) showed a decrease in size as the concentration of BetA was increased. However, statistically significant differences were only noted upon comparison of the un-extruded EL with un-extruded B1 (BetAL) (2387 nm ± 249.2) and un-extruded EL with un-extruded γ-CD-BetAL (* $P < 0.05$).

Following extrusion (Figure 3.1, B), extruded B2 (BetAL) (179 nm ± 9.45) was visibly larger when compared to the other liposomal formulations, while extruded γ-CD-BetAL (116.7 nm ± 0.95) showed the smallest size. Statistically significant differences were reported upon comparison of the extruded EL (149.3 nm ± 21.84) with extruded γ-CD-BetAL, extruded B1 (BetAL) (159 nm ± 15.50) with extruded γ-CD-BetAL and extruded B2 (BetAL) with extruded γ-CD-BetAL (** $P < 0.01$ and * $P < 0.05$).

As shown in Figure 3.1 (C), the un-extruded EL is noticeably larger when compared to extruded EL. Statistically significant differences was noted upon comparison of the un-extruded liposomal formulations with its extruded counterpart (*** $P < 0.001$). The average size of EL before extrusion was 4194 nm and was reduced to 149.3 nm after extrusion. The average size of un-extruded B1 (BetAL) was 2387 nm and was reduced to 159 nm, while un-extruded B2 (BetAL) was 1742 nm and decreased to 179 nm after extrusion (refer to Appendix, Table 7.1). The smallest average size before and after extrusion can be observed for un-extruded γ-CD-BetAL (1367 nm ± 190.5) and extruded γ-CD-BetAL (116.7 nm ±

1.65). Thus extrusion was successful in reducing large liposomes in the µm size range to a size range of less than 200 nm.

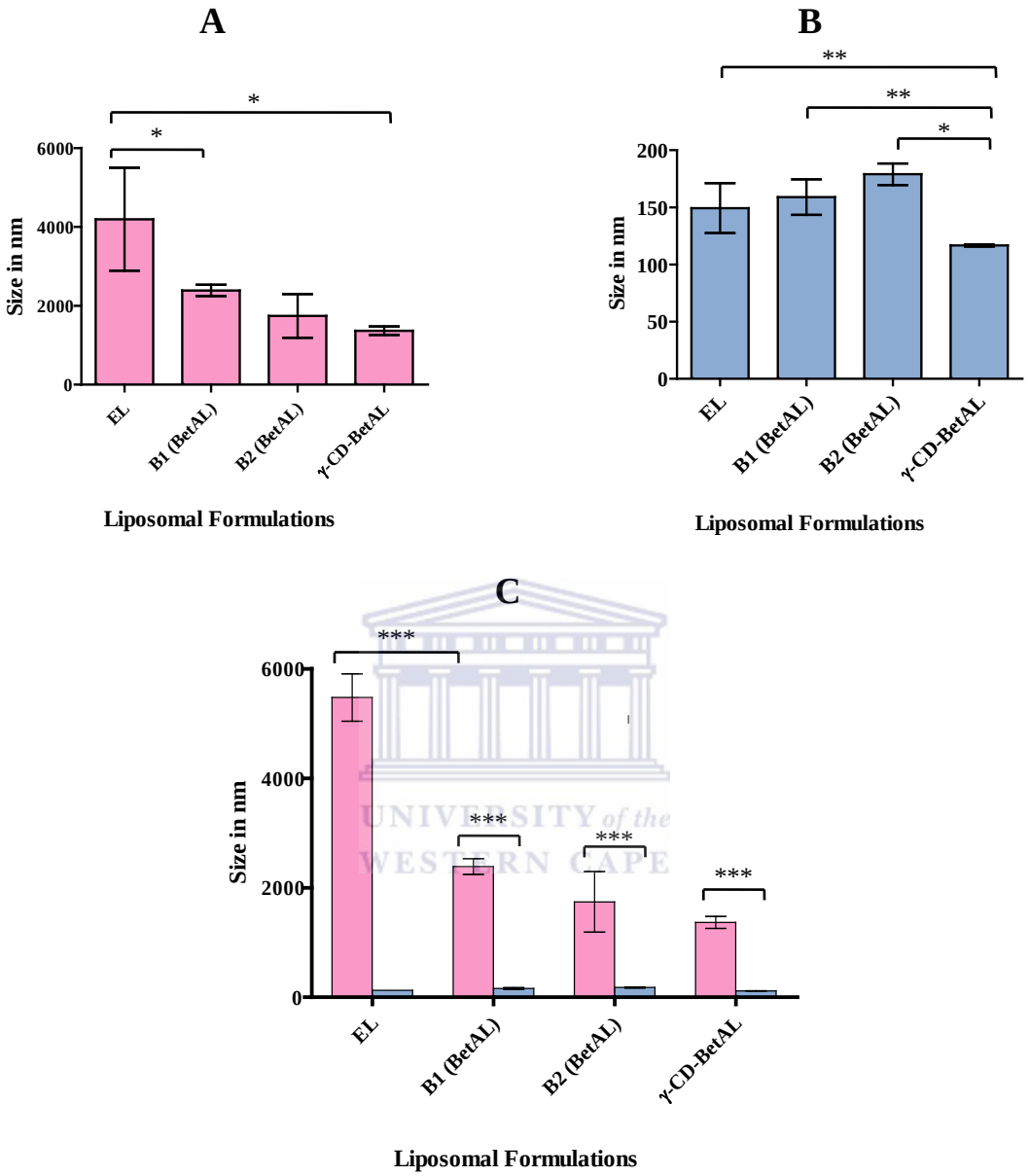

Figure 3.1 The size (diameter) distribution of different liposomal formulations before (A) and after extrusion (B) was determined and compared (C). *The size distribution of liposomal formulations was measured at 25 ºC using dynamic light scattering (DLS) at an angle of 173 ˚C to the laser beam on a Malvern Zetasizer NanoZs instrument (Malvern instruments, Ltd., UK). Data was obtained in triplicates and used to construct bar graphs (mean ± standard deviation, n = 3 ± SD). Error bars represent calculated standard error of the means. Level of statistically significant differences are annotated by asterisk(s) (* P < 0.05; ** P < 0.01 and *** P < 0.001).*

3.2 Polydispersity Index (PI) of Liposomes

The PI is the width parameter derived from the cumulants analyses and is used to evaluate the homogeneity of colloidal particles in solution (Iqbal *et al.*, 2012). A PI in a range of 0.1-

0.25 indicates uniformity in the liposome size distribution and a more monodisperse solution, while a PI above 0.5 and closer to 1 suggests that the sample is too polydisperse and may have a non-uniform size distribution (Kale *et al*., 2012 and Sabeti *et al*., 2014).

Figure 3.2, shows the PI of un-extruded liposomes (A), the PI of extruded liposomes (B) and the comparison of the two (C).

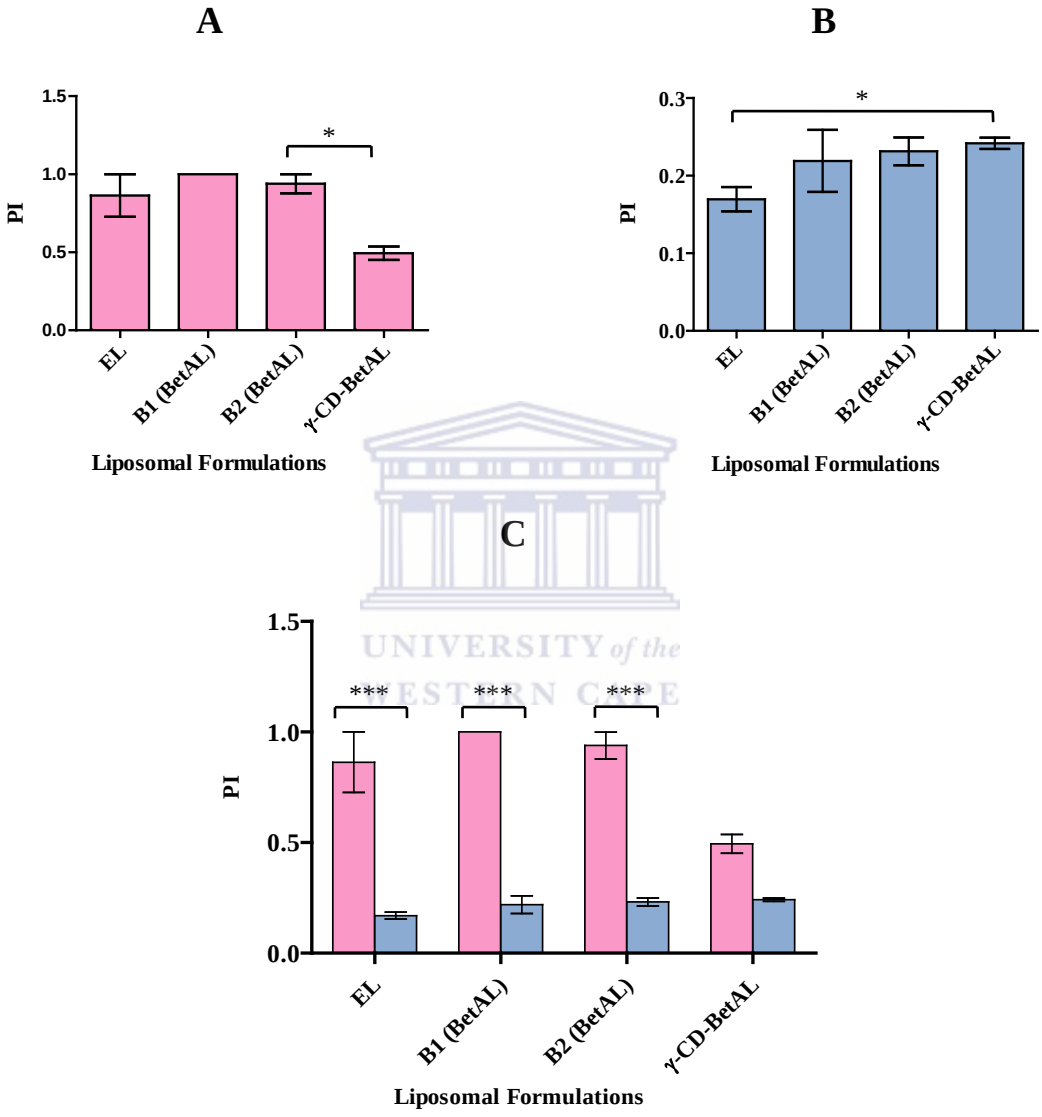

Figure 3.2 The polydispersity index (PI) of different liposomal formulations before (A) and after extrusion (B) was determined and compared (C). *The PI of liposomal formulations was measured at 25 ºC using dynamic light scattering (DLS) at an angle of 173 ˚C to the laser beam on a Malvern Zetasizer NanoZs (Malvern instruments, Ltd., UK) Data was obtained in triplicates and used to construct bar graphs (mean ± standard deviation, n = 3 ± SD). Error bars represent calculated standard error of the means. Level of statistically significant differences are annotated by asterisk(s) (* P < 0.05 and *** P < 0.001).*

Un-extruded EL (0.86 ± 0.13), un-extruded B1 (BetAL) (1 ± 0.0), un-extruded B2 (BetAL) (0.94 ± 0.1) and un-extruded γ-CD-BetAL (0.49 ± 0.07) showed PI values in a range of 0.5-1 (Figure 3.2, A). Statistically significance difference were only observed upon comparison of un-extruded B2 (BetAL) and un-extruded γ-CD-BetAL (* $P < 0.05$).

After extrusion (Section 2.3.4, Chapter 2), extruded EL had the lowest PI (0.17 ± 0.03) while extruded γ-CD-BetAL had the highest PI. There is a noticeable increase in the PI of BetA loaded liposomes as the concentration of BetA increases (extruded B1: 0.22 ± 0.04, extruded B2: 0.23 ± 0.01 and extruded γ-CD-BetAL: 0.24 ± 0.01). Statistically significance difference were observed when extruded EL were compared to extruded γ-CD-BetAL (* $P < 0.05$).

The results for the PI of liposomal formulations before extrusion was closer to 1 and after extrusion the PI was reduced to less than 0.3 (Figure 3.2, C). There were statistically significant differences recorded when un-extruded liposomal formulations were compared to its extruded counterpart (*** $P < 0.001$) (Figure 3.2, C). In summary, the high PI generated after thin film hydration method showed a liposome solution with a high degree of non-uniformity in size distribution and extrusion was successful in producing liposomes with a uniform size distribution in solution.

3.3 Zeta-potential (ζ-potential) of Liposomes

The potential that exists at the slipping plane of a particle in an aqueous solution is called the ζ-potential (Domingues *et al*., 2008; Kaszuba *et al*., 2010). It is a physical property which is exhibited by any particle in suspension and measurements of ζ-potential are commonly used to assess the stability of colloidal systems (Freire *et al*., 2011).

The ζ-potential before extrusion of EL (-1.205 mV ± 0.74), B1 (BetAL) (-2.25 mV ± 0.1), B2 (BetAL) (-2.52 mV ± 0.18) and γ-CD-BetAL (-2.02 mV ± 0.21) produced negative ζ-potential values as seen in Figure 3.3 (A), p. 70. Inclusion of BetA into un-extruded liposomes showed a higher negative ζ-potential when compared to un-extruded EL, with un-extruded B2 (BetAL) demonstrating the highest negative ζ-potential. Statistically significant difference were noted upon comparison of EL with B1 (* $P < 0.05$) (Figure 3.3, A).

After extrusion, EL showed a positive ζ-potential value close to 0 (1.05 mV ± 0.05) indicating a neutral surface charge on the DPPC lipid (Figure 3.3, B). Extruded B1 (BetAL) (-1.24 mV ± 0.04), extruded B2 (BetAL) (-1.29 mV ± 0.01) and extruded γ-CD-BetAL (-1.47 mV ± 0.03) remained in the negative zeta range. The γ-CD-BetAL showed the highest

negative zeta-potential after extrusion. Statistically significant difference can be observed when EL is compared to all liposomal formulations (*** P < 0.001) (Figure 3.3, B).

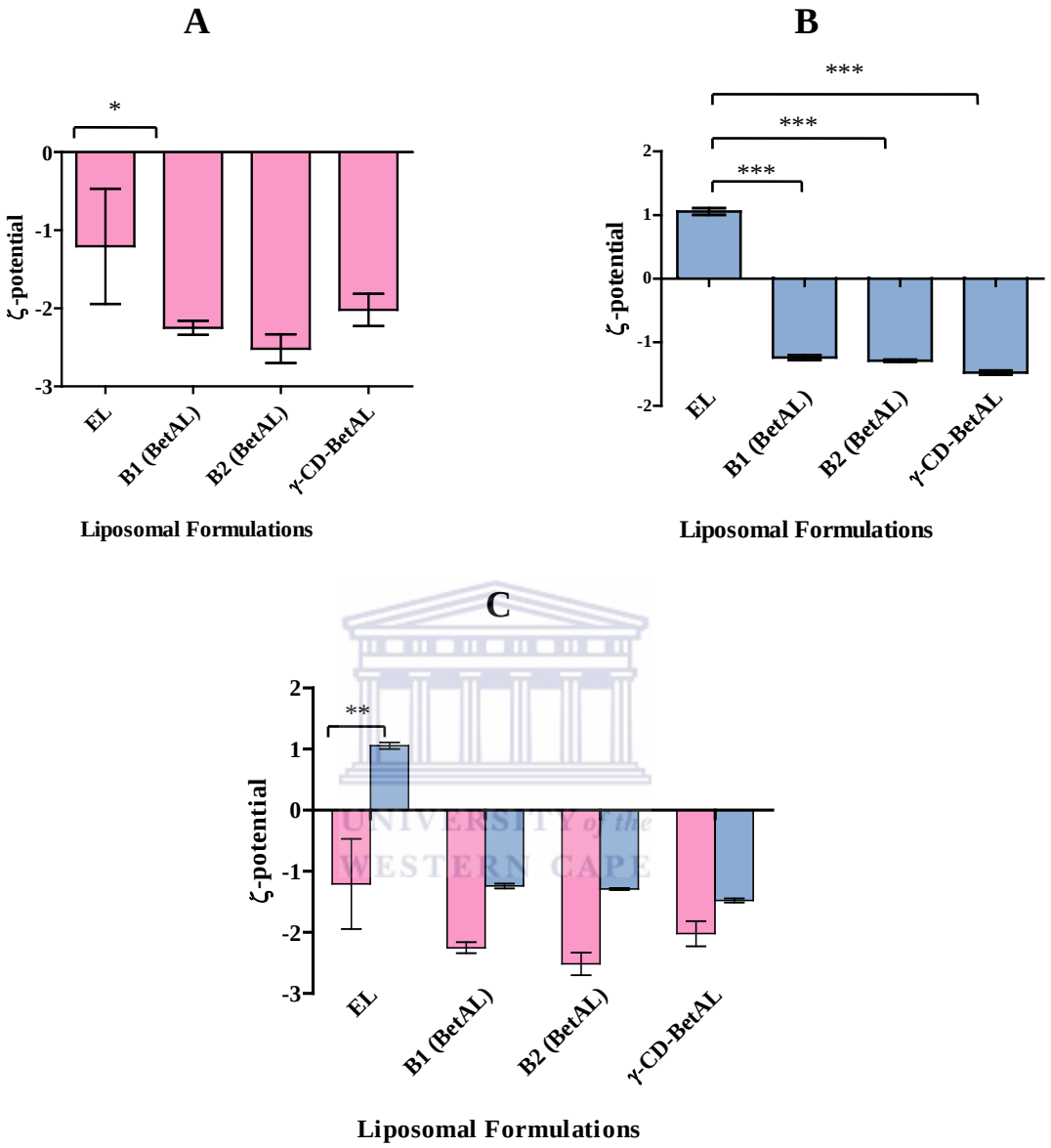

Figure 3.3 The zeta potential (ζ-potential) of different liposomal formulations before (A) and after extrusion (B) was determined and compared (C). *The ζ-potential of liposomal formulations was measured using a voltage of 4 mV on a Malvern Zetasizer NanoZs (Malvern instruments, Ltd., UK) at 25 ºC using dynamic light scattering (DLS) at an angle of 173 ˚C to the laser beam. Data was obtained in triplicates and used to construct bar graphs (mean ± standard deviation, n = 3 ± SD). Error bars represent calculated standard error of the means. Level of statistically significant differences are annotated by asterisk(s) (* P < 0.05; ** P < 0.01 and *** P < 0.001).*

The ζ-potential of BetA loaded liposomal formulations before extrusion was in the negative range and became slightly less negative after extrusion (Figure 3.3, C). Statistically, significant differences were only observed for un-extruded EL compared to extruded EL (**

P < 0.01) (Figure 3.3, C). Therefore changes in ζ-potential are related to size and BetA loading.

3.4 Physical Morphology of Liposomes

Size distribution (diameter) studies of liposomes from the Zetasizer nanoZS instrument uses dynamic light scattering (DLS) which provides statistical information about the size distribution of liposomes in solutions only. DLS does not yield information about the shape morphology of NPs; hence other techniques are usually applied for this purpose. SEM is often used to study surface morphology and shape characteristics of NPs (Charurvedi and Dave, 2012). In this study, the investigation of size and shape morphology was studied using HR-SEM.

Figure 3.4 (p. 72) are HR-SEM micrographs of the prepared liposomes. Figure 3.4 shows the size and physical morphology of un-extruded EL (A and B), extruded B1 (BetAL) (C and D) and extruded γ-CD-BetAL (E and F). Un-extruded EL revealed a non-uniform size distribution of spherical like vesicles in a size range of ± 300 nm (different sizes of vesicles indicated by white arrows in A and B). Extruded B1 (BetAL) and extruded γ-CD-BetAL showed a more narrow uniform size distribution of spherical-like vesicles in a size range of less than 200 nm (indicated by arrows in C, D and F). Black arrows in un-extruded EL (A and B) and γ-CD-BetAL (F) indicate aggregation of liposomes as electrostatic forces present on the surface of liposomes are low and cannot prevent clumping of particles together, relating to the low negative ζ-potential results obtained. Un-extruded EL size analyses from Malvern Zetasizer NanoZs showed a size distribution of > 4000 nm (4194 nm ± 2260); this does not correlate with the size distribution of un-extruded EL using HR-SEM analyses (vesicles are < 4000 nm). The uniform vesicles in extruded B1 (BetAL) (indicated by white arrows in C and D) and extruded γ-CD-BetAL (indicated by the white arrow in F) correlates with the PI study in a range of less than 0.25 for extruded B1 (BetAL) (0.22 ± 0.04) and extruded γ-CD-BetAL (0.24 ± 0.01), indicating uniformity in the liposome size distribution and a monodisperse solution after extrusion.

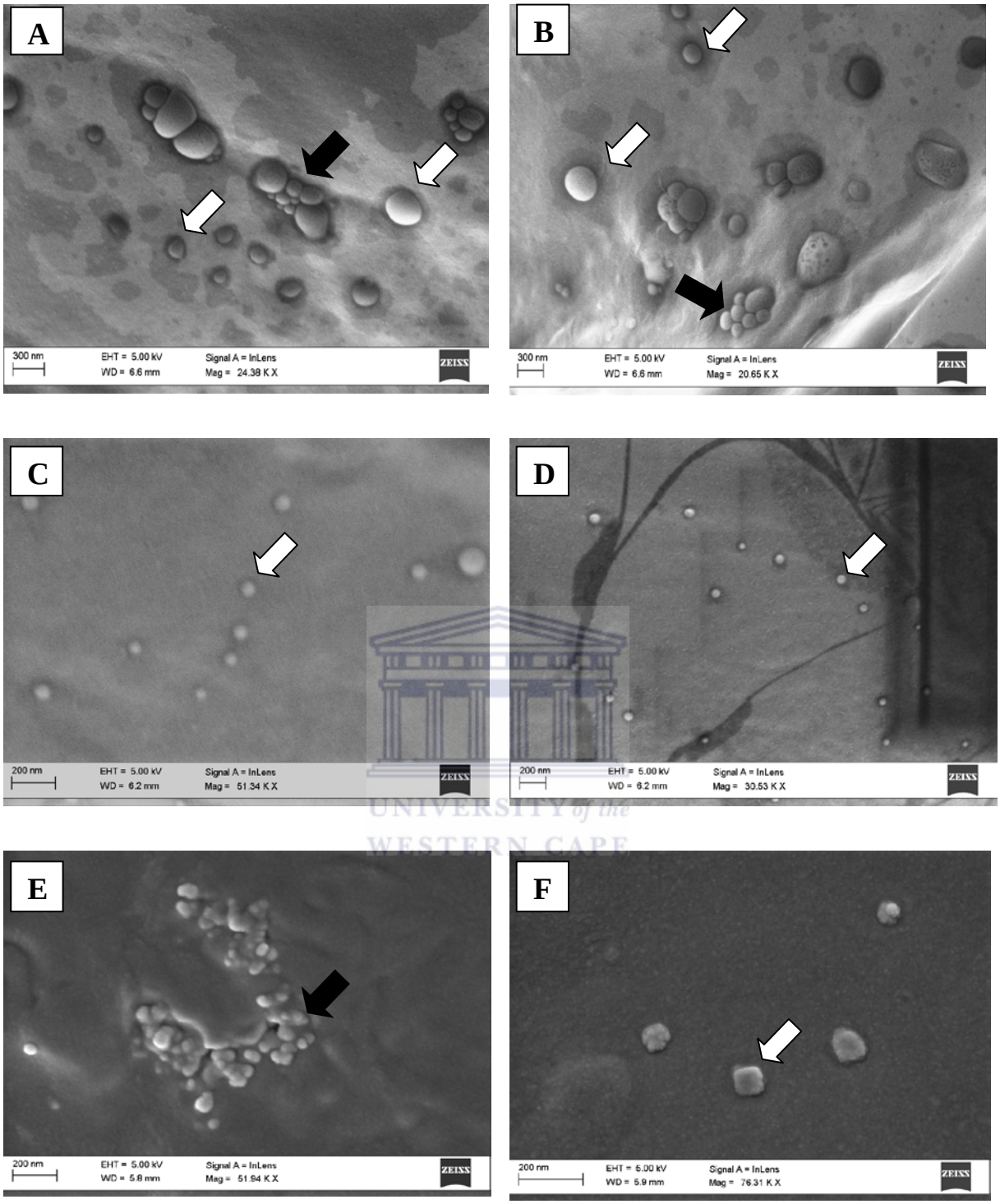

Figure 3.4 HR-SEM micrographs of un-extruded EL (A and B), extruded B1 (BetAL) (C and D) and extruded γ-CD-BetAL (E and F). *A drop of un-extruded or extruded liposomes was dispersed on carbon adhesive tape applied on an aluminium stub and then left overnight to completely dry under fume hood. The dried liposomes were coated with gold palladium for 30 seconds using Emitech K550X (England) sputter coater and viewed with the Auriga HR-SEM F50 (Zeiss, South Africa) at a voltage of 5 KV. A scale-bar in nm, Extra high tension (EHT), Working distance (WD) and Magnification (Mag) is provided for each image. Black arrows indicate features of aggregation and white arrows show different sizes of un-extruded and extruded vesicles.*

3.5 Determination of the Concentration of BetA Entrapped in Liposomes and the Percentage Entrapment Efficiency (% EE) of BetA in Liposomes

The % EE refers to the total amount of drug or compound entrapped within liposomes (in mg/ml) divided by the total starting concentration (in mg/ml) multiplied by 100. Several factors such as the affinity of the drug to the lipid membrane, the lipid composition of the membrane, the volume of internal aqueous phase and the lipid bilayer, the concentration of the liposomes formed, drug-to-lipid ratio and the method of downsizing of liposomes have influences on the % EE of liposomes (Muppidi *et al*., 2012). In this study it was important to evaluate the amount of BetA entrapped within the liposomes in order to select the most appropriate liposomal formulations for further biological characterization of prepared liposomes.

The concentration in mg/ml of BetA and the % EE of BetA in liposomes was determined using a UHPLC system (Flexar FX-20 UHPLC) (as described in section 2.4.2.1, Chapter 2). BetA was dissolved in methanol in order to prepare standards (0.005-1 mg) (section 2.4.2.1, Chapter 2). A calibration curve with standards plotted against the area under the peak/curve was constructed (Figure 2.4, Chapter 2). The linear equation was obtained to determine the concentration (in mg/ml) of BetA entrapped in the liposomes. From this, the % EE of BetA in liposomes was calculated using the following equation:

$$\% \text{ Entrapment efficiency} = \frac{\text{Amount of drug in liposomes (pellet) (mg/ml)}}{\text{Total amount of drug used (mg/ml)}} \times 100$$

The amount of BetA entrapped in the formulations was dependent on the amount of BetA added while the DPPC remained constant. Table 3.1 shows the concentration of BetA in mg/ml entrapped in the different liposomal formulations. Thin film hydration method yielded a low entrapment of BetA before and after extrusion as seen in Table 3.1

Table 3.1 The concentrations (in mg/ml) of BetA entrapped in liposomes (in mg/ml) (n = 3)

	B1 (BetAL)	**B2 (BetAL)**	**γ-CD-BetAL**
Starting concentration of BetA	0.5 mg/ml	1 mg/ml	1 mg/ml
Total entrapped BetA before extrusion	0.17 mg/ml	0.22 mg/ml	0.31 mg/ml
Total entrapped BetA after extrusion	0.04 mg/ml	0.05 mg/ml	0.13 mg/ml

Table 3.2 shows the % EE of BetA in different liposomal formulations before and after extrusion. B1 (BetAL) shows the highest % EE (34.14% ± 2.86), while B2 (BetAL) shows the lowest % EE (22.78% ± 2.83). Incorporation of γ-CD-BetA into liposomes showed a decrease in γ-CD-BetAL (30.57% ± 1.74) when compared to B1 (BetAL). Statistically significant differences were observed when the % EE of un-extruded B1 (BetAL) was compared to the % EE of un-extruded B2 (BetAL) (* $P < 0.05$). This indicates that the lowest starting concentration of BetA loaded into liposomes (0.5 mg/ml) produced the highest entrapment before extrusion and employing a starting concentration of 1 mg/ml BetA (Table 3.1) could not entrap more than 30% BetA.

The % EE of BetA in different liposomal formulations after extrusion (section 2.3.4, Chapter 2) showed a noticeable decrease. Extruded γ-CD-BetAL (13.20% ± 4.58) showed the highest % EE of BetA when compared to extruded B1 (BetAL) (8.50% ± 1.22) and extruded B2 (BetAL) (5.14% ± 1.12), however no statistically significant differences were reported upon comparison of the % EE of different extruded liposomal formulations.

Table 3.2 The percentage entrapment efficiency (% EE) of different liposomal formulations before extrusion and after extrusion (n = 3)

	B1 (BetAL)	B2 (BetAL)	γ-CD-BetAL
% EE of BetA before extrusion	34.14% ± 2.86	22.78% ± 2.83	30.57% ± 1.74
% EE of BetA after extrusion	8.50% ± 1.22	5.14% ± 1.12	13.24% ± 4.58

Figure 3.5 (p. 75) shows the comparison of % EE of BetA in liposomes before and after extrusion. The % EE of un-extruded B1 (BetAL) was higher than the % EE of un-extruded B2 (BetAL), therefore in this case BetA loaded liposomes decreased with an increase in BetA concentration as the phospholipid composition remained the same ($P < 0.05$). Since B1 (BetAL) showed a higher % EE than B2 (BetAL), this batch was selected to load γ-CD-BetA to form the γ-CD-BetAL. The incorporation of γ-CD-BetA into B1 (BetAL) liposomal formulation showed no increase in % EE of un-extruded γ-CD-BetAL when compared to un-extruded B1 (BetAL), however an increase in % EE of extruded γ-CD-BetAL was noticeable when compared to both extruded B1 (BetAL) and extruded B2 (BetAL). Statistically significantly differences were not reported when the % EE of extruded γ-CD-BetAL was

compared with the % EE of extruded B1 (BetAL) and extruded B2 (BetAL). Statistically significant differences were observed upon comparison of un-extruded liposomal formulations with its extruded counterpart (Figure 3.5) (** P < 0.01 and * P < 0.05). In summary, the size of liposomes formed using thin film hydration method influenced the initial entrapment of BetA in liposomes and BetA loss after extrusion was significant.

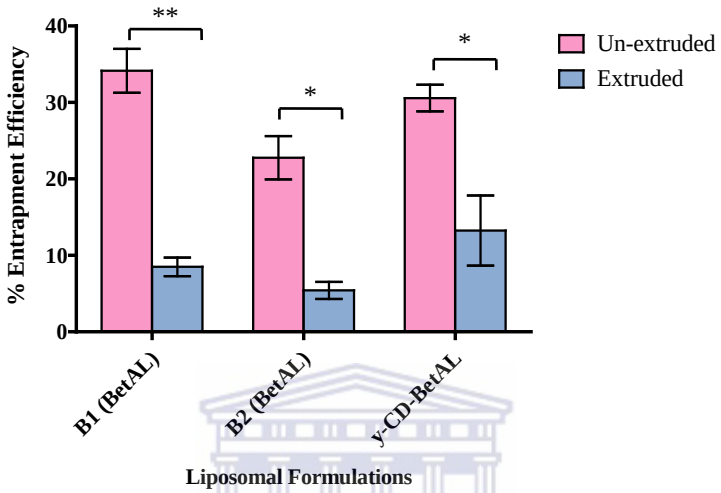

Figure 3.5 The percentage entrapment efficiency (% EE) of different liposomal formulations before extrusion and after extrusion was determined and compared. *The % EE of BetA and γ-CD-BetA into liposomes was obtained using Ultra High Performance Liquid Chromatography (UHPLC) (Perkin Elmer Flexar FX-15 UHPLC, USA). UHPLC conditions were as follows: C-18 (4.5 mm x 150. 5µm) column (Phenomenex Kinetex, USA), mobile phase of acetonitrile: methanol (80:20 v/v), triplicate injections with an injection volume of 10 µl and 0.5 ml/min flow rate. Detection occurred at 2.5 minutes using a wavelength of 205 nm. Data were obtained in triplicates and used to construct bar graphs (mean ± standard deviation, n = 3 ± SD). Error bars represent calculated standard error of the means. Level of statistically significant differences are annotated by asterisk(s) (** P < 0.01 and * P < 0.05).*

CHAPTER 4

CYTOTOXICITY STUDIES OF THE SELECTED LIPOSOMAL FORMULATIONS ON NEUROBLASTOMA BRAIN CANCER CELL LINES

For liposomes to be considered as a drug-delivery system, they must be evaluated *in vitro* for cytotoxicity on cell cultures and, subsequently, *in vivo* in pre-clinical and clinical trials. *In vitro* evaluation could assist in establishing the biocompatibility of the liposomal design, optimal liposomal formulation and reveal mechanisms of cell-liposome interaction. There are numerous methods used to analyze the cytotoxicity, which involve different aspects of cell function, such as cell viability and proliferation, cell morphology, loss of membrane integrity, decrease in cell adhesion etc. Following the physio-chemical characterization of liposomes (Chapter 3), B1 (BetAL) and γ-CD-BetAL was selected to evaluate their effect on the cell viability of two NB cell lines. This Chapter presents the results on the effects of free BetA (non-liposomal BetA), BetAL, γ-CD-BetAL and free γ-CD (non-liposomal γ-CD) on the viability of SK-N-BE(2) and KELLY NB cells *in vitro*. It is known from literature that certain concentrations of DMSO and γ-CD induce cytotoxicity into cell cultures. Free BetA was prepared from a working stock solution of 5 mg/ml BetA dissolved in DMSO. Therefore a DMSO tolerance test was conducted at concentrations of 0.1 to 2% in order to establish the final concentration of DMSO that is tolerable in both cell lines. In order to evaluate the cytotoxicity of free γ-CD in cells, treatment with 5-50 μg/ml free γ-CD occurred in both cell lines and based on this results, the concentration range of γ-CD-BetAL to treat SK-N-BE(2) and KELLY NB cells was selected. Cells were subjected with treatment of free BetA at a concentration range of 5-20 μg/ml, while BetAL treatment was performed at a concentration range of 5-50 μg/ml. The concentration of BetAL was increased due to the low entrapment of BetA in BetAL (section 3.5, Chapter 3). Empty liposomes (liposomes not containing BetA) were used as a control to evaluate the effect of the DPPC lipid and cholesterol (Chol) in both NB cell lines. The cell viability was evaluated using the WST-1 colorimetric cell viability assay. Control cells were untreated cells represented as 100% viability. The data was obtained and analysed using Medcalc Statistics Programme (version 11.6.1) in order to construct bar graphs (mean ± SD; n = 6). Error bars represent calculated standard error of the means. A probability of $P < 0.05$ indicates statistical significance (annotated by one asterisk). The % cell viability values and P values are included (refer to Appendixes). The half maximal inhibitory concentration (IC_{50}) values, represents the drug concentration required for 50% inhibition of cell viability *in vitro*. IC_{50} concentration values was obtained using

linear regression analyses feature on GraphPad Prism 5 for SK-N-BE(2) and KELLY NB cell lines exposed to free BetA, BetAL and γ-CD-BetAL after 24, 48 and 72 hours exposure.

4.1 DMSO Tolerance Test for SK-N-BE(2) and KELLY NB Cell Lines

DMSO is usually used as a cryo-protective agent for storing cells as it is added to cell freezing media to prevent the formation of ice crystals during the freezing process (Chen and Thibeault, 2013). It is also often used as a delivery vehicle for most non-soluble compounds and drugs and is usually tolerated with little or no observable effects at 0.1% final concentration (v/v) (Chen and Thibeault, 2013). At 1% or higher concentrations, depending on the cell line, its effects *in vitro* on cell viability have been reported to be selectively cytotoxic (Kim *et al*., 2001; Da Violante *et al*., 2002; Kvasnica *et al*., 2005; Qi *et al*., 2008; Chen and Thibeault, 2013; Galvao *et al*., 2014). DMSO tolerance test for SK-N-BE(2) and KELLY NB cell lines using the WST-1 cell viability assay is not reported in literature, therefore a DMSO tolerance test was performed on these two cell lines before treatment with free BetA as the free BetA concentrations (5-20 μg/ml) was prepared from a stock solution of 5 mg/ml BetA (dissolved in DMSO).

Figure 4.1 (p. 78) illustrates the DMSO tolerance test for SK-N-BE(2) (A) and KELLY (B) NB cell lines with control (untreated cells) represented as 100% cell viability. For DMSO treatment of SK-N-BE(2) NB cell line for all exposure time points, there was a general increase in cell viability above control at 0.1-0.4% DMSO exposure and a sharp linear decrease in cell viability from 1-2% DMSO exposure showing a noticeable trend (Figure 4.1, A and refer to Appendixes, Table 7.3.1). When compared to control, there was a 23% increase in cell viability at 72 hours for 0.1% DMSO treatment (123% cell viability), showing the highest increase while the 2% DMSO treatment at 72 hours produced the lowest cell viability (53% cell viability).

The DMSO tolerance test for KELLY NB cell line (Figure 4.1, B, p. 78) did not show a noticeable trend as the cell viability showed variations across the exposure durations. At 24 hours for 0.1-2% DMSO treatment, cell viability remained similar to controls and then decreased slightly from 0.4-2% DMSO exposure (Table 7.3.4, refer to Appendixes) as observed in the general trend with SK-N-BE(2) NB cells exposed to DMSO (Figure 4.1, A). Treatment with 0.1-2% DMSO showed a decrease below controls at 48 hours. Cell viability at 0.2-0.4% DMSO exposure for 72 hours showed a slight increase with the highest cell viability being reported at 1% DMSO treatment (111% cell viability). At 24 hours exposure

to 2% DMSO, cell viability decreased by 29%, showing the lowest cell viability (71% cell viability) (Table 7.3.4, refer to Appendixes).

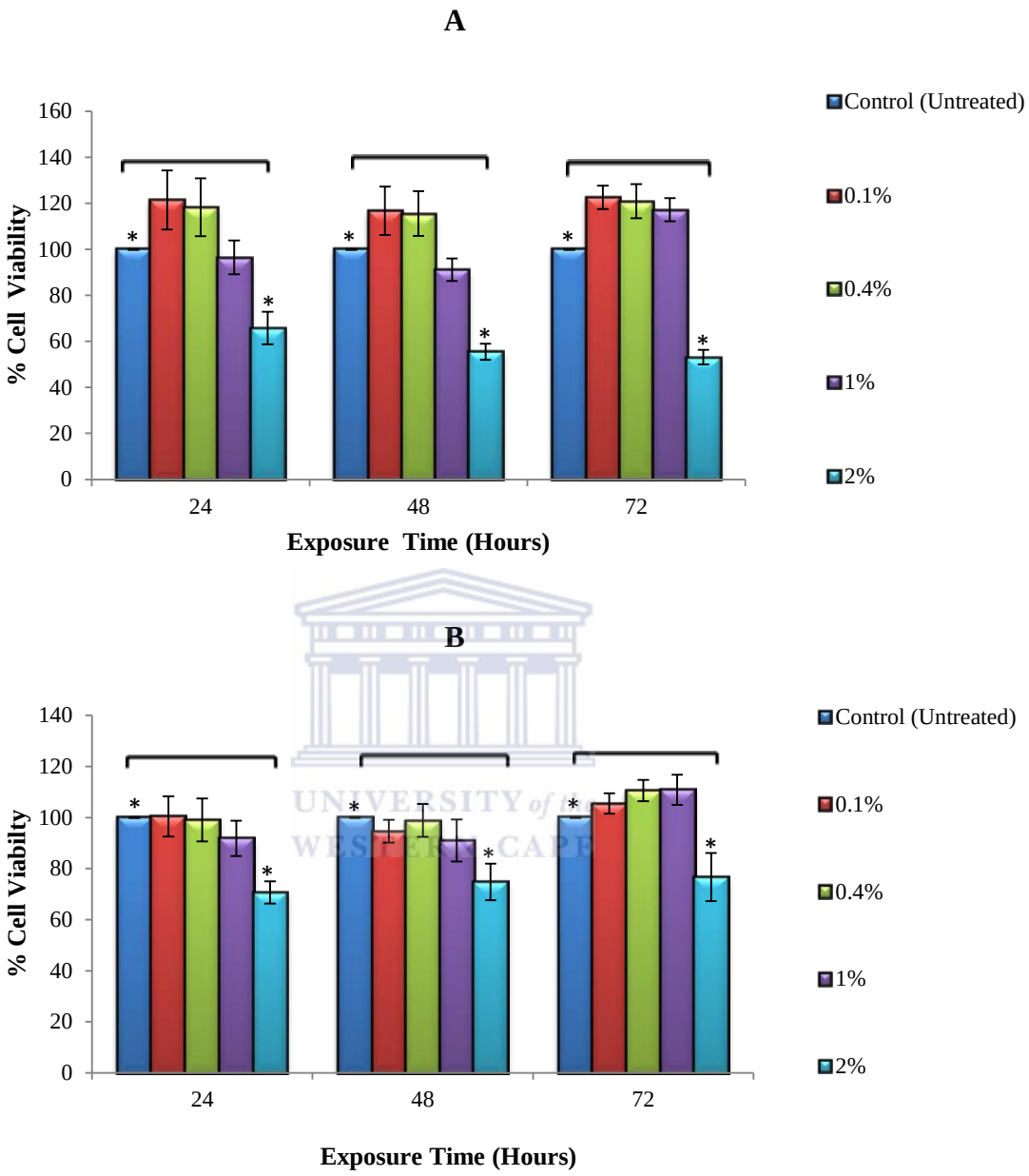

Figure 4.1 DMSO tolerance test for SK-N-BE(2) (A) and KELLY (B) NB cell lines. *Cells were subjected to treatment with 0.1-2% DMSO for 24-72 hours. Control cells are untreated cells represented as 100% cell viability. Cell viability was evaluated using the WST-1 colorimetric cell viability assay. The data was obtained and used to construct bar graphs (mean ± SD, n = 6). Error bars represent calculated standard error of the means. Statistically significant differences are annotated by asterisks (* P < 0.05).*

For both cell lines, no statistically significant differences were reported upon comparison of untreated cells with 0.1-1% DMSO treated cells for all exposure durations. However, cells treated with 2% DMSO showed statistically significant differences (annotated by one

asterisk) when compared to controls for all exposure durations ($P < 0.05$) (Figure 4.1, Table 7.3.2 and Table 7.3.5, refer to Appendixes). No statistically significant differences were reported for NB cells treated with 0.1-2% DMSO compared between the selected time intervals (24 hours compared to 48 hours, 48 hours compared to 72 hours and 24 hours compared to 72 hours) as seen in Table 7.3.3 and Table 7.3.6 (refer to Appendixes). In general, DMSO at low concentrations (0.1 and 0.4%) promoted cell growth in SK-N-BE(2) NB cells at 24-72 hours exposure while in KELLY NB cells it promoted cell growth only at 72 hours with no statistically significant differences being reported when compared to controls. DMSO exposure at high concentrations (1% and 2%) was toxic to both cell lines. Therefore these results reveal that DMSO kept below 0.4% as a final concentration will not be toxic to SK-N-BE(2) and KELLY NB cells.

4.2 Evaluation of Cytotoxicity for Free BetA and BetAL treatment in SK-N-BE(2) and KELLY NB Cell Lines

BetA has demonstrated anti-cancer capabilities *in vitro* for numerous cancer cell lines with established IC_{50} concentration values reported to fall in the rage of 0.5–17 µg/ml depending on the type of cell lines and cell viability assay methods used (Faujan *et al*., 2010; Suresh *et al*., 2012). The sensitivity of neuroectodermal derived tumour cells to free BetA was established previously with IC_{50} concentration values for human NB cell lines starting at 14-17 µg/ml and the underlying molecular apoptotic pathways were also studied (Fulda *et al*., 1997 and Schmidt *et al*., 1997). Other brain tumour cell lines sensitive to free BetA (such as glioblastoma and medulablastoma) have also been reported to show IC_{50} concentration values at 3-13.5 µg/ml and 2-17 µg/ml, respectively whereas no cytotoxic signs in non-malignant murine neuronal cells were observed (Wick *et al*., 1999 and Fulda *et al*., 1999). Head and neck squamous cellular carcinoma cells were also reported to be sensitive to BetA (Thurnher *et al*., 2003).

The high lipophilic character associated with BetA shows that it cannot be dissolved and administered in most aqueous solutions, posing a difficulty in its efficacy *in vivo* and hampering a pharmaceutical formulation. Studies have modified BetA derivatives in an attempt to increase their solubility to address this issue (Liu *et al*., 2004; Huang *et al.*, 2007; Rajendran *et al.*, 2008), however it seems as though the lipophilic character of BetA is important in its pluripotent mechanism of action, which is responsible for its broad activity

profile (Mullauer *et al.,* 2010). Therefore different liposomal formulations of BetA were prepared.

Originally synthesized large BetAL (> 1 μm) was downsized (< 200 nm) for treatment of SK-N-BE(2) and KELLY NB cell lines, thus leading to a decrease in the total percentage entrapment efficiency (% EE) of BetA. Therefore the concentration of extruded BetAL (% EE: 8.50 % ± 1.22) and extruded γ-CD-BetAL (% EE: 13.24 % ± 4.58) was increased from 5-20 μg/ml used in free BetA to 5-50 μg/ml due to the low entrapment of BetA and to evaluate if higher concentrations would have a statistically significant effect on cell viability.

Figure 4.2.1 (p. 81) demonstrates the sensitivity of SK-N-BE(2) NB cell line subjected to 5-20 μg/ml free BetA treatment (A) and 5-50 μg/ml BetAL (B) treatment when compared to control (untreated cells). For all exposure durations to free BetA, there appeared to be a noticeable time and concentration dependent decrease in the cell viability (Figure 4.2.1, A). This is evident for 5-20 μg/ml treatment at 24 hours exposure and 5-15 μg/ml treatment at both 48 and 72 hours exposure. The lowest cell viability can be observed at 72 hours exposure at 15 μg/ml (7% cell viability), while the highest cell viability was observed at 5 μg/ml treatment with free BetA at 48 hours exposure (83% cell viability). Cell viabilities at 48 hours and 72 hours showed a decrease at 5-10 μg/ml and then an increase at 15-20 μg/ml (Figure 4.2.1 and Table 7.4.1, refer to Appendixes). The estimated IC_{50} values for SK-N-BE(2) NB cells treated with free BetA were reported as follows: 13.10 μg/ml (24 hours exposure); 14.03μg/ml (48 hours exposure) and 7.85 μg/ml (72 hours exposure) (Table 4.1, Chapter 4, p. 91).

SK-N-BE(2) NB cells treated with BetAL compared to control (untreated cells) showed a similar trend in viability when compared to free BetA treatment as cells exposed to BetAL showed a concentration (5-50 μg/ml) and time (24-72 hours) dependent decrease for all hours of exposure (Figure 4.2.1, B, p. 81). The lowest cell viability can be observed at treatment with 50 μg/ml BetAL at 72 hours exposure (31% cell viability). EL (liposomes without BetA) showed a viability similar to untreated cells at 24 hours exposure (99% cell viability), but increased at 48 and 72 hours (110% cell viability and 102% cell viability, respectively). The estimated IC_{50} values for SK-N-BE(2) NB cells treated with BetAL were reported as follows: 53.45 μg/ml (24 hours exposure); 38.73 μg/ml (48 hours exposure) and 18.30 μg/ml (72 hours exposure) (Table 4.2, Chapter 4, p. 91).

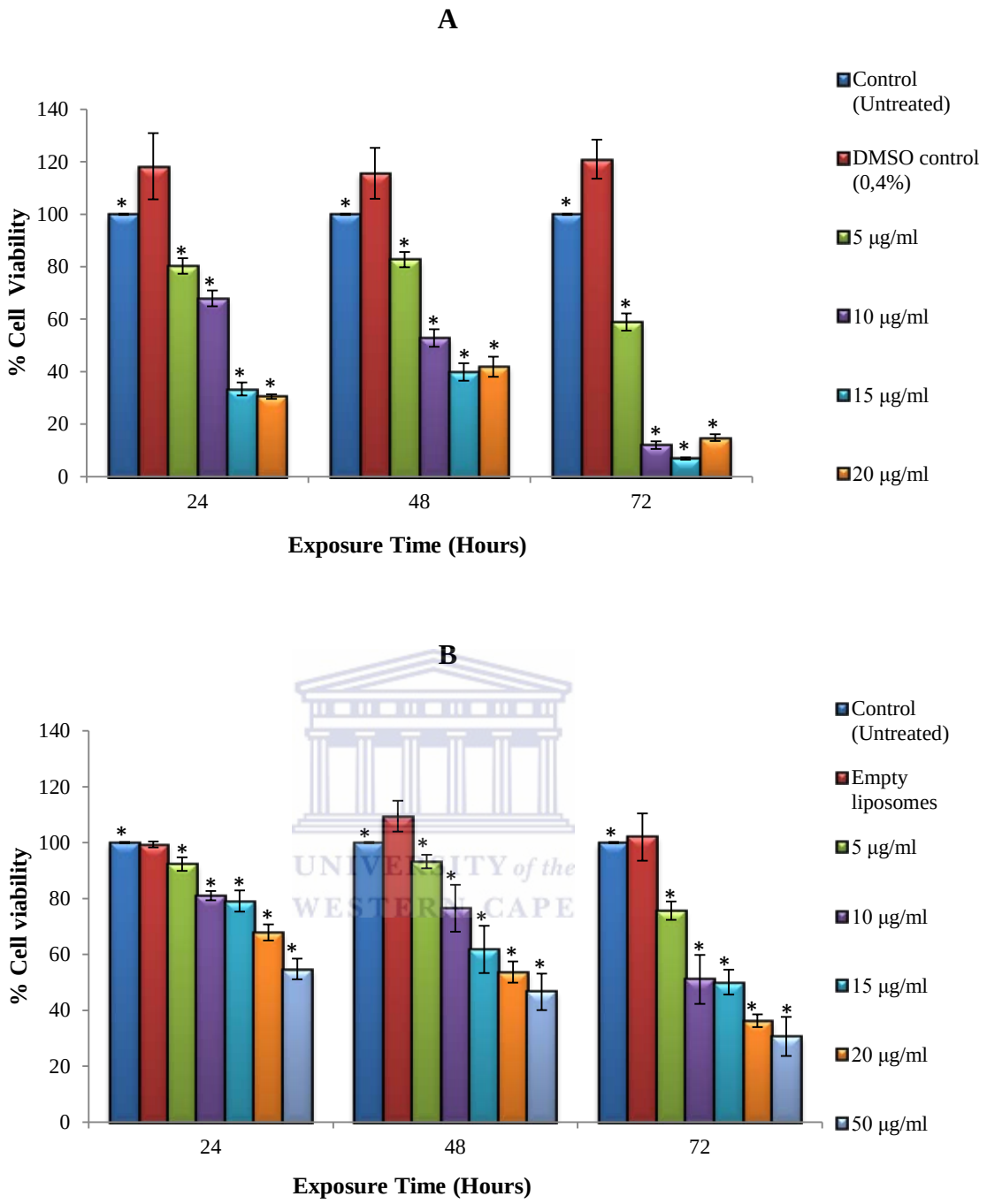

Figure 4.2.1 The evaluation of SK-N-BE(2) NB cell viability following exposure to free BetA (A) and BetAL (B) for 24-72 hours. *Cells were subjected to treatment with 5-20 µg/ml free BetA and 5-50 µg/ml BetAL for 24-72 hours. Control cells are as follows: untreated cells (100% cell viability), DMSO control (0.4%) and empty liposomes (EL). Cell viability was measured using the WST-1 cell viability assay. The data was obtained and used to construct bar graphs (mean ± SD, n = 6). Error bars represent calculated standard error of the means. Statistically significant differences are annotated by asterisks (* P < 0.05)*

Statistically significant differences (annotated by the asterisks) were noted upon comparison of controls with 5-20 µg/ml free BetA treated cells (Figure 4.2.1, A) and with 5-50 µg/ml BetAL treated cells (Figure 4.2.1, B) ($P < 0.05$). Statistically significant differences were also

evident across time points for both free BetA and BetAL (refer to Appendixes, Table 7.4.3 and Table 7.5.3). This suggests that treatment with 5-20 µg/ml free BetA for 24-72 hours and 5-50 µg/ml exposure of BetAL for 24-72 hours induces cytotoxicity in SK-N-BE(2) NB cells in a time and concentration dependent manner. DMSO control (Figure 4.2.1, A) and EL control (Figure 4.2.1, B) for 24-72 hours exposure showed no statistically significant differences when compared to untreated cells, indicating its safety profile in NB cells (Table 7.5.2, refer to Appendixes).

The sensitivity of KELLY NB cell line exposed to 5-20 µg/ml free BetA (Figure 4.2.2, A) and 5-50 µg/ml BetAL (Figure 4.2.2, B) for 24-72 hours compared to controls (untreated cells) represented as 100% cell viability was determined (p. 83). When compared to the controls, for all exposure durations, there appeared to be a noticeable time and concentration dependent decrease in the cell viability of KELLY NB cells exposed to free BetA (Figure 4.2.2, A). This is evident at 5-20 µg/ml free BetA treatment for 24-48 hours exposure. The lowest cell viability was observed at 72 hours exposure to 10 µg/ml free BetA (14% cell viability) (Table 7.4.4, refer to Appendixes). Cell viability at 72 hours exposure to free BetA showed a decrease from 5-10 µg/ml and then a slight increase at 15-20 µg/ml suggesting that cells are starting to recover at the highest concentrations; however it was still lower than 50% cell viability. The estimated IC_{50} concentration values for KELLY NB cells treated with free BetA were reported as follows: 24.00 µg/ml (24 hours exposure); 14.50 µg/ml (48 hours exposure) and 76.05 µg/ml (72 hours exposure) (Table 4.2, p. 91).

The effect of BetAL exposure (5-50µg/ml) to KELLY NB cells compared to untreated cells showed variations in cell viability across the exposure time points, however there seems to be a trend as cell viability decreases with an increase in exposure time (Figure 4.2.2, B, p. 83). This can be observed at 10-50 µg/ml BetAL treatment at 24 hours and 5-20 µg/ml exposure at 48 and 72 hours. The lowest cell viability was reported at 15 µg/ml BetAL treatment at 72 hours (41% cell viability). Cells treated with EL showed a 5% increase in cell viability at 24 hours (105% cell viability) and a slight decrease at 48 and 72 hours (98% cell viability) (Table 7.5.4, refer to Appendixes). The estimated IC_{50} values for KELLY cells treated with BetAL were reported as: 68.65 µg/ml (24 hours exposure), 61.52µg/ml (48 hours exposure) and 21.42µg/ml (72 hours exposure) (Table 4.2, p. 91).

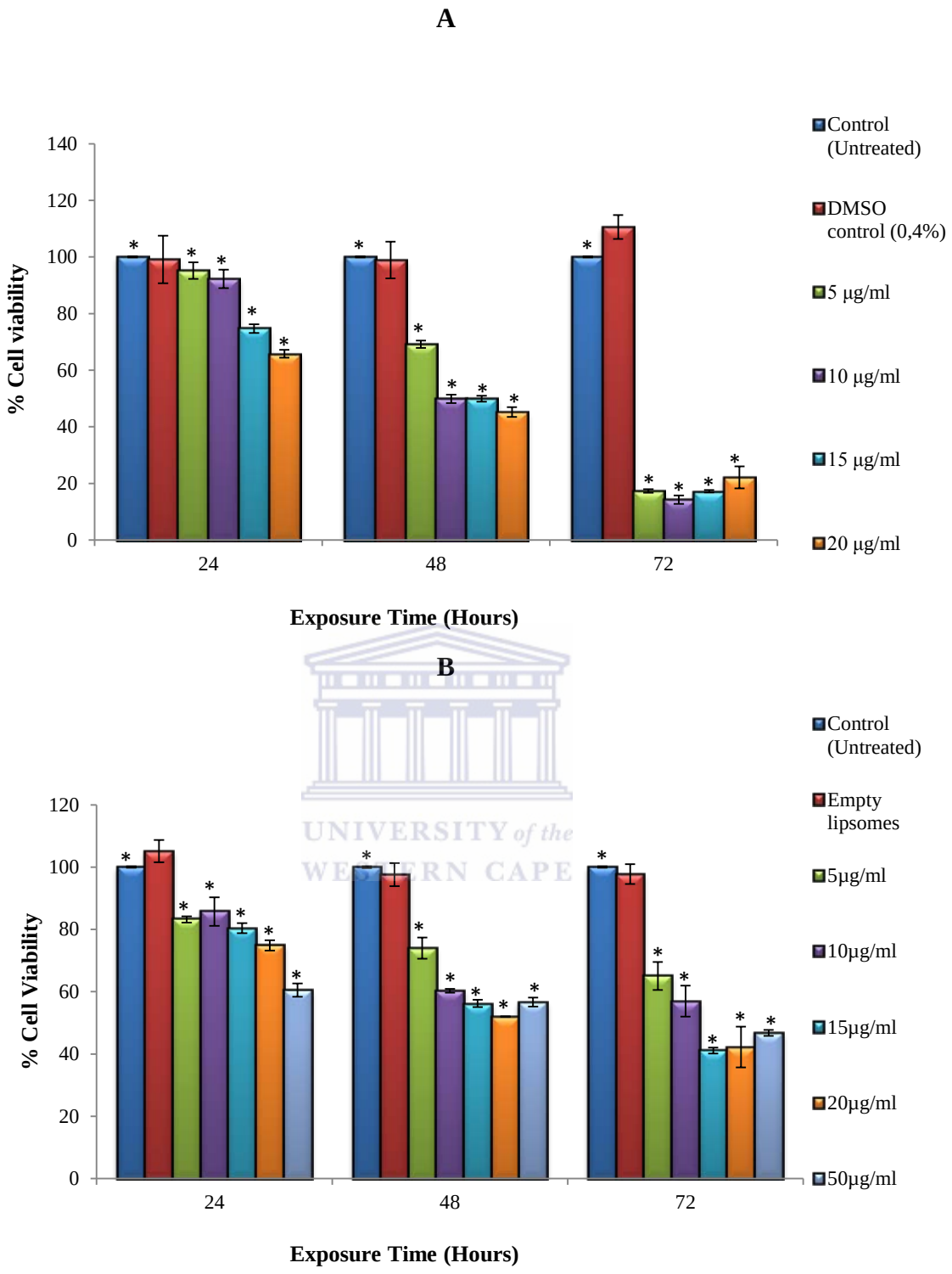

Figure 4.2.2 The evaluation of KELLY NB cell viability following exposure to free BetA (A) and BetAL (B) for 24-72 hours. *Cells were subjected to treatment with 5-20 µg/ml free BetA and 5-50 µg/ml BetAL for 24-72 hours. Control cells are as follows: untreated cells (100% cell viability), DMSO control (0.4%) and EL. Cell viability was measured using the WST-1 cell viability assay. The data was obtained and used to construct bar graphs (mean ± SD, n = 6). Error bars represent calculated standard error of the means. Statistically significant differences are annotated by asterisks (* P < 0.05)*

Statistically significant differences (annotated by the asterisks) for KELLY NB cells were observed upon comparison of untreated cells and cells treated with 5-20 μg/ml free BetA (Figure 4.2.2, A, p. 83) and 5-50 μg/ml BetAL (Figure 4.2.2, B, p. 83) ($P < 0.05$). Statistically significant differences were also evident across time points for both free BetA and BetAL (refer to Appendixes, Table 7.4.6 and Table 7.5.6). This suggests that treatment with 5-20 μg/ml free BetA for 24-72 hours and treatment with 5-50 μg/ml BetAL for 24-72 hours induces cytotoxic effects in KELLY NB cells. DMSO control (Figure 4.2.2, A) and EL control can be considered safe as they had (Figure 4.3, B) no statistically significant effect on cell viability compared to untreated cells (Table 7.5.5, refer to Appendixes).

4.3 Evaluation of Cytotoxicity For Free γ-CD and γ-CD-BetAL Exposure in SK-N-BE(2) and KELLY NB Cell Lines

It was reported in literature that certain cyclodextrin (CD) groups demonstrate toxicity such as α-CD, β-CD and a number of alkylated CDs are known to show renal toxicity and disruption of biological membranes, while γ-CD and some of its derivatives (HP-γ-CD), as well as HP-β-CD and SBE-β-CD, appear to be much safer (Stella and He *et al*., 2008; Hanumegowda *et al*., 2014). A limited amount of studies have been done on the effect of γ-CD interaction with brain cancer cell lines, however studies have shown the effect of different CD including γ-CD on an *in vitro* BBB model (Monnaert *et al.*, 2004). Monnaert *et al*., (2004) studied the toxicity and endothelial permeability for α-, β- and γ-CDs on the blood-brain barrier (BBB). The study revealed that the α-CD series is the most toxic, closely followed by β-CD series, whereas the γ-CD presents the lowest toxicities. As more products using CDs are approved or undergoing evaluation by regulatory agencies for use in pharmaceuticals, toxicity studies become essential in establishing their safety profile especially for neuroscience research.

Incorporation of γ-CD-BetA into liposomes did enhance the % EE in extruded liposomes (13.24 % ± 1.22) and therefore the free γ-CD was prepared based on the initial amount used in the preparation of γ-CD-BetAL. A stock concentration of 2.84 mg/ml of γ-CD was prepared (dissolved in PBS) and diluted in DMEM (1% penicillin and streptomycin and 10% FBS) in order to obtain concentrations of 5-50 μg/ml free γ-CD. The γ-CD-BetAL concentration was selected based on the cytotoxicity results obtained from free γ-CD exposure (5-50 μg/ml).

Figure 4.3.1 (p. 86) shows the effects on the cell viability of SK-N-BE(2) NB cell line when exposed to free γ-CD (A) and γ-CD-BetAL (B) for 24-72 hours. The cell viability of SK-N-BE(2) cells with treatment of 5-50 μg/ml free γ-CD showed variation in cell viability across the exposure time points (24-72 hours) when compared to controls (untreated cells) (Figure 4.3.1, A and Table 7.6.1, refer to Appendixes). At 48 hours, statistically significant differences were noted at 20 μg/ml and 50 μg/ml free γ-CD exposure compared to controls (85% cell viability and 87% cell viability, respectively) ($P < 0.05$) (refer to Appendixes: Table 7.6.1 and Table 7.6.2, refer to Appendixes). At 72 hours, it is evident that free γ-CD exposure causes an increase in cell proliferation above controls with exposure to 15 μg/ml free γ-CD showing the highest increase in cell viability (121% cell viability), while at 20 μg/ml and 50 μg/ml free γ-CD exposure cell viability decreased to below 50% (48% and 40% cell viability, respectively) (Figure 4.3.1, A, p. 86 and refer to Appendixes: Table 7.6.2). No statistically significant differences were reported for 24 hours exposure with 5-50 μg/ml free γ-CD when compared to controls, however statistically significant differences were observed when compared across different time points (Table 7.6.3, refer to Appendixes). Therefore free γ-CD at 24 hours exposure to 5-50 μg/ml, at 48 hours exposure to 5-15 μg/ml and at 72 hours exposure to 5-10 μg/ml did not induce cytotoxicity into SK-N-BE(2) NB cells and was safe to use in γ-CD-BetAL cell viability experiments.

Figure 4.3.1 (B) shows the sensitivity of the SK-N-BE(2) NB cell line to γ-CD-BetAL exposure concentrations. The cell viability of SK-N-BE(2) cells with treatment of γ-CD-BetAL showed a concentration dependent decrease in viability for all exposure times with statistically significant differences being reported (annotated by the asterisks) ($P < 0.05$) (Figure 4.3.1 and refer to Appendixes: Table 7.7.1 and Table 7.7.2). SK-N-BE(2) NB cells treated with γ-CD-BetAL showed estimated IC_{50} concentration values at: 44.90 μg/ml (24 hours exposure); 32.10 μg/ml (48 hours exposure) and 12.12 μg/ml (72 hours exposure) (Table 4.3, p.91.).

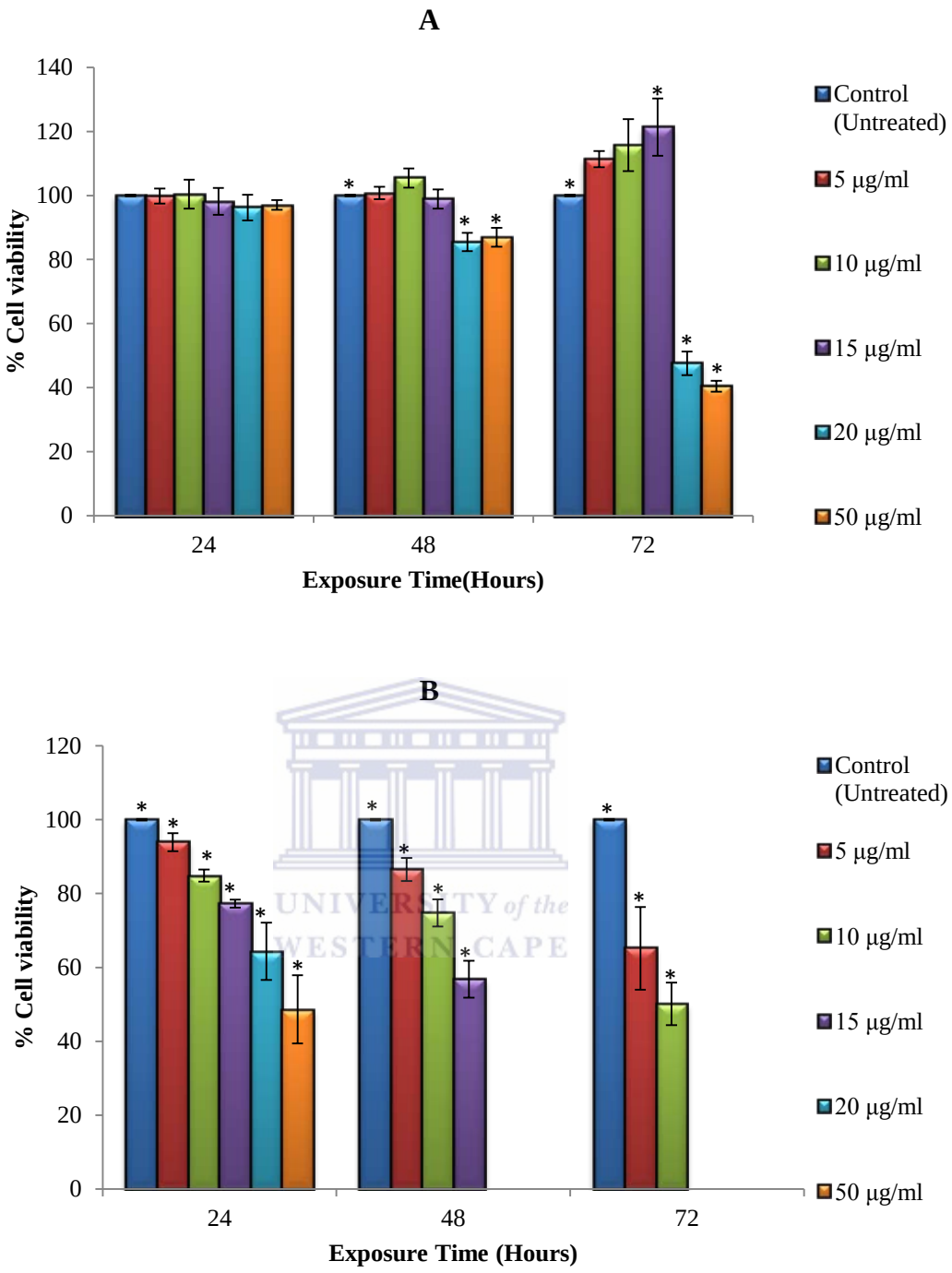

Figure 4.3.1 The evaluation of SK-N-BE(2) NB cell viability following exposure to free γ-CD (A) and γ-CD-BetAL (B) for 24-72 hours. *Cells were subjected to treatment with: 5-50 µg/ml free γ-CD for 24-72 hours, 5-50 µg/ml γ-CD-BetAL for 24 hours, 5-15 µg/ml γ-CD-BetAL for 48 hours and 5-10 µg/ml γ-CD-BetAL for 72 hours. Control cells are untreated cells represented as 100% cell viability. Cell viability was evaluated using the WST-1 cell viability assay. The data was obtained and used to construct bar graphs (mean ± SD, n = 6). Error bars represent calculated standard error of the means. Statistically significant differences are annotated by asterisks (* P < 0.05)*

Figure 4.3.2 (A) shows the sensitivity of KELLY NB cell line to free γ-CD (5-50 μg/ml) exposure with controls represented as 100% cell viability. Similarly to the SK-N-BE(2) cells, the cell viability of KELLY cells with treatment of free γ-CD showed variation in cell viability across the exposure time (24-72 hours) (Figure 4.3.2, p.88 and Table 7.6.4, refer to Appendixes). At 24 hours exposure to 5-50 μg/ml free γ-CD, statistically significant differences was only reported at 50 μg/ml free γ-CD compared to controls (untreated cells), however at 48 and 72 hours statistically significant differences were noted at 20 μg/ml (94.65% and 94.94% cell viability, respectively viability) and 50 μg/ml (86.42% and 91.94% cell viability, respectively) when compared to controls ($P < 0.05$) (Figure 4.3.2, B, and Table 7.6.5, refer to Appendixes). No statistically significant differences were reported when the different time points were compared (Table 7.6.6, refer to Appendixes). Therefore treatment with 5-20 μg/ml free γ-CD at 24 hours and 5-15 μg free γ-CD treatment at 48 and 72 hours did not confer cytotoxicity into KELLY NB cells and was safe to use in γ-CD-BetAL cell viability experiments.

KELLY NB cells treated with γ-CD-BetAL (Figure 4.3.2, B) showed a concentration dependent decrease in viability for all exposure times similar to γ-CD-BetAL treated SK-N-BE(2) cells (Figure 4.3.1, B). At 24 hours cells were subjected to treatment with 5-20 μg/ml γ-CD-BetAL and at 48 and 72 hours cells were subjected to treatment with 5-15 μg/ml γ-CD-BetAL. Statistically significant differences were reported for all concentrations ($P < 0.05$) (Table 7.7.5, refer to Appendixes). KELLY NB cells exposed to γ-CD-BetAL showed estimated IC_{50} concentration values to be: 49.17 μg/ml (24 hours), 40.63 μg/ml (48 hours) and 38.25 μg/ml (72 hours) (Table 4.3, p. 91).

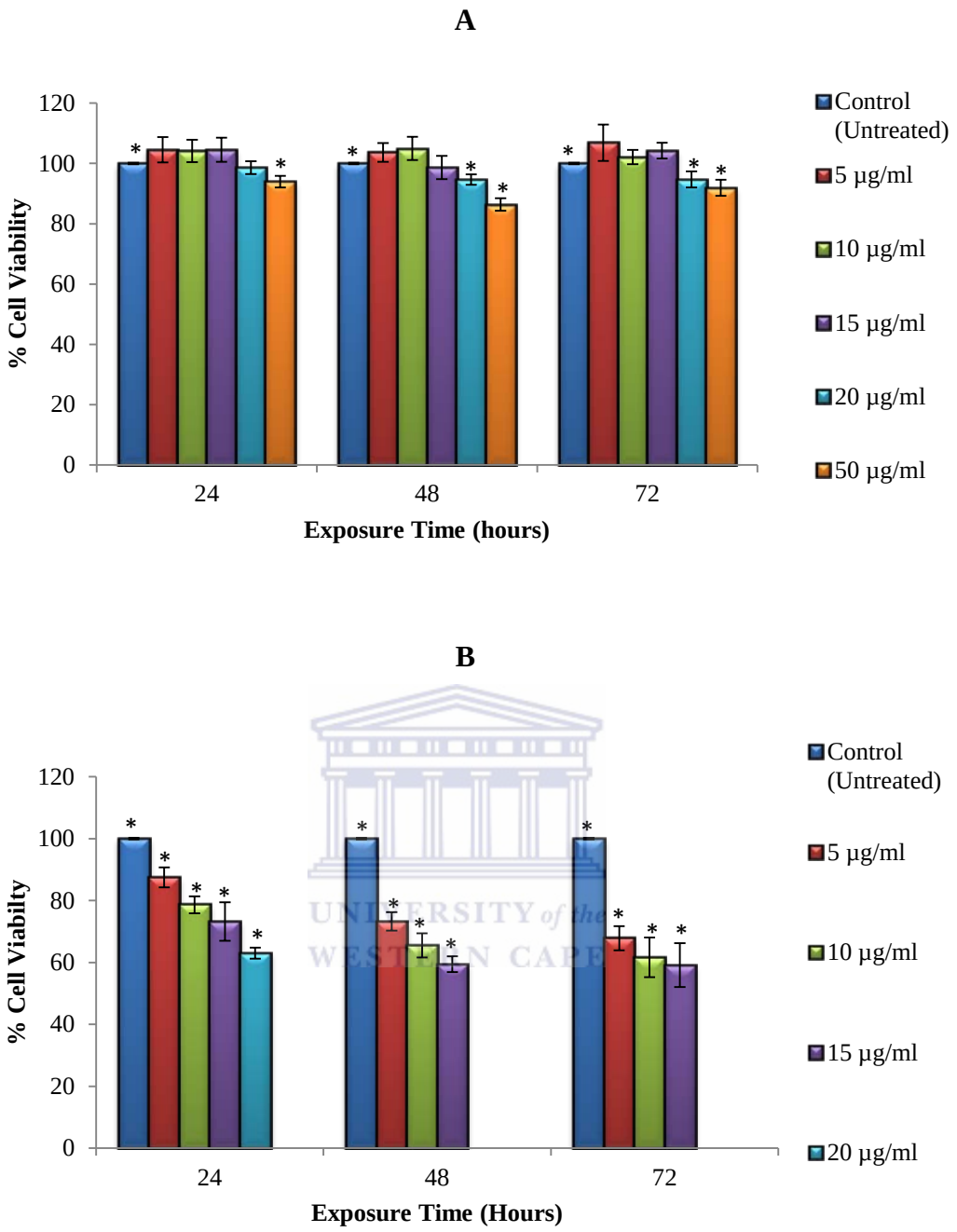

Figure 4.3.2 The evaluation of KELLY NB cell viability following exposure to free γ-CD (A) and γ-CD-BetAL (B) for 24-72 hours. *Cells were subjected to treatment with: 5-50 µg/ml free γ-CD for 24-72 hours, 5-20 µg/ml γ-CD-BetAL for 24 hours and 5-15 µg/ml γ-CD-BetAL for 48-72 hours. Control cells are untreated cells represented as 100% cell viability. Cell viability was evaluated using the WST-1 cell viability assay. The data was obtained and used to construct bar graphs (mean ± SD, n = 6). Error bars represent calculated standard error of the means. Statistically significant differences are annotated by one asterisk (* P < 0.05)*

4.4 Comparison of Selected Concentrations of Free BetA, BetAL and γ-CD-BetAL at Specific Time Points in SK-N-BE(2) and KELLY NB Cell Lines

Figure 4.4 (A), p. 90, shows the comparison of free BetA, BetAL and γ-CD-BetAL at the same concentrations and exposure time points in the SK-N-BE(2) NB cell line. For all concentrations and exposure durations, cell viability showed a significant drop for free BetA when compared to BetAL and γ-CD-BetAL. The γ-CD-BetAL was more effective in reducing the cell viability when compared to BetAL at all hours and concentrations, except at 24 hours, 5-10 μg/ml treatment. Statistically significant differences were noted when the same concentrations of free BetA was compared to BetAL (i.e. 5 μg/ml free BetA compared to 5 μg/ml BetAL etc.) for all concentrations at 24 and 72 hours exposure (Figure 4.1, A, Table 7.8.1, refer to Appendixes). This was also noted for free BetA compared to γ-CD-BetAL (Figure 4.1, A, Table 7.8.2, refer to Appendixes) for all concentrations being compared at 24 and 72 hours exposure. At 48 hours exposure, statistically significant differences can be observed when 5 μg/ml free BetAL was compared to 5 μg/ml γ-CD-BetAL and at 72 hours at 5 μg/ml free BetA treatment compared to 5 μg/ml BetAL.

The comparison of free BetA, BetAL and γ-CD-BetAL at the same concentrations and exposure time points in KELLY NB cell line was studied (Figure 4.4, B). Free BetA showed the lowest cell viabilities when compared to the same concentrations of BetAL and γ-CD-BetAL for all hours, except at 24 hours treatment with 5-10 μg/ml free BetA. Free BetA was also reported to show statistically significant differences when compared to liposomal formulations for all hours ($P < 0.05$) (Figure 4.1, B, Table 7.8.4 and Table 7.8.5, refer to Appendixes). The γ-CD-BetAL was more effective in reducing the cell viability when compared to BetAL at all hours and concentrations, except at 24 hours, 5-10 μg/ml treatment.

In summary, both cell lines show a noticeable concentration dependent decrease in cell viability for exposure durations. Free BetA is more effective in inducing cytotoxicity when compared to the same concentrations of BetAL and γ-CD-BetAL for both NB cell lines. Treatment with-γ-CD-BetAL induced a higher cytotoxicity than BetAL in SK-N-BE(2) as seen at 24 hours (15-20 μg/ml), 48 hours (5-15 μg/ml) and 72 hours (5-10 μg/ml). KELLY cells were more sensitive to treatment with BetAL at 48 hours (5-20 μg/ml) and 72 hours (5-20 μg/ml), except at 24 hours (10-20 μg/ml) when compared γ-CD-BetAL. SK-N-BE(2) NB cells appear to be more sensitive to free BetA at 24 hours when compared to KELLY NB cells, however they show a similar decrease in cell viability at 72 hours (10-20 μg/ml).

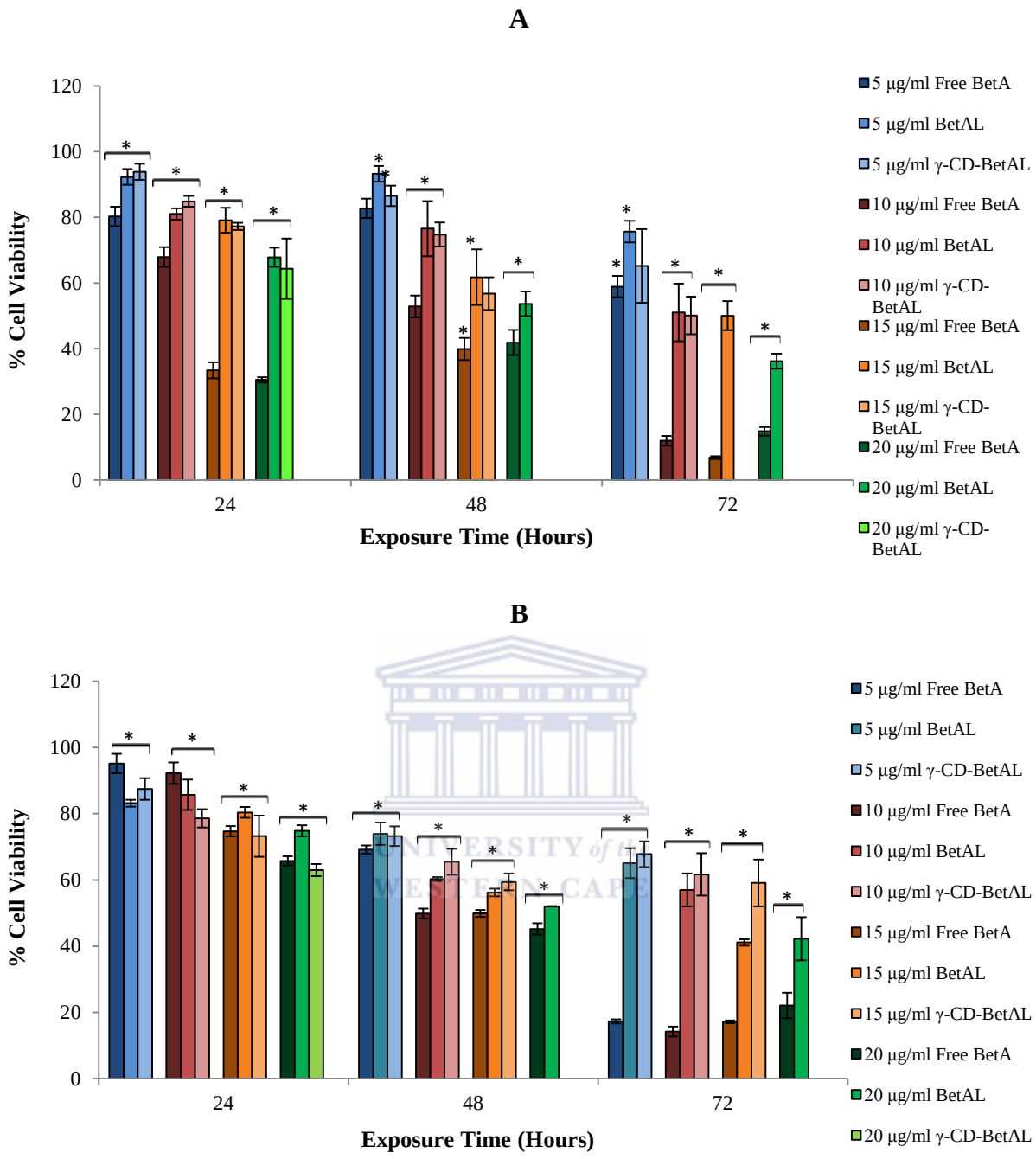

Figure 4.4 Comparison of the same concentrations of free BetA, BetAL and γ-CD-BetAL at 24-72 hours treatment in SK-N-BE(2) (A) and KELLY NB (B) NB cell lines*. SK-N-BE(2) and KELLY NB cells were subjected to treatment with free BetA, BetAL and γ-CD-BetAL. Cell viability was measured using the WST-1 cell viability assay. The data was obtained and used to construct bar graphs (mean ± SD, n = 6). Error bars represent calculated standard error of the means. Statistically significant differences are annotated by one asterisk (* P < 0.05)*

Table 4.1: Estimated half maximal inhibitory concentration values (IC_{50}) for free BetA.

Cell line	Time (Hours)	IC_{50} values (µg/ml)
SK-N-BE(2)	24	13.10
	48	14.03
	72	7.85
KELLY	24	24.00
	48	14.50
	72	76.05

Table 4.2: Estimated half maximal inhibitory concentration values (IC_{50}) for BetAL.

Cell line	Time (Hours)	IC_{50} values (µg/ml)
SK-N-BE(2)	24	53.45
	48	38.73
	72	18.30
KELLY	24	68.65
	48	61.52
	72	21.42

Table 4.3: Estimated half maximal inhibitory concentration values (IC_{50}) for γ-CD-BetAL.

Cell line	Time (Hours)	IC_{50} values (µg/ml)
SK-N-BE(2)	24	44.90
	48	32.10
	72	12.12
KELLY	24	49.17
	48	40.63
	72	38.25

CHAPTER 5

DISCUSSION

5.1 Introduction

More than half of children diagnosed with high-risk NB will either not respond to conventional therapies or relapse after treatment (London *et al*., 2011). There are various complicating factors associated with the treatment of NS and CNS cancers. The delivery of drugs in CNS cancers is mainly limited by the presence of anatomical barriers: the blood–brain barrier (BBB), blood–cerebrospinal fluid barrier (BCSFB) and the cerebrospinal fluid brain barrier (CSF) (Engelhardt and Sorokin, 2009). These barriers are highly selective and regulate the passage of certain substances into the brain. The crossing of any molecule through these barriers is dependent upon its physicochemical properties, and pharmacokinetic profile in plasma and therefore, a large number of drugs with low vesicular transport and high metabolic activity or molecules such as nucleic acids, peptides, proteins and antibiotics cannot cross the BBB (Balda and Matter, 1998). In addition to the anatomical barriers presented by the CNS, normal brain vasculature differs when compared to tumour vasculature of the brain, as tumour vasculature comprises abnormal blood vessels; distended capillaries with leaky walls, leading to inconsistent drug delivery at the tumour site (Van Meir, *et al.,* 2010). The diminished therapeutic value of many potent anticancer drugs is also greatly impacted by the lack of specificity of anticancer drugs to pathological diseased sites, resulting in very low amounts of administered drug that can ultimately reach the brain (Begley and Brightman, 2003). This is responsible for the systemic toxicity associated with chemotherapeutic agents. The long term toxic side effects of chemotherapeutic drugs to adjacent healthy brain structures usually include cognitive deficits and epilepsy due to neuronal damage (Wen and Kesari, 2008), as neurons present in the CNS do not present regenerative capacity, therefore damaged neurons are not capable of dividing and replacing themselves under normal circumstances (Buga *et al*., 2011), this compromises the CNS greatly. Growth reduction, thyroid function disorders, learning difficulties and an increased risk of secondary cancers continue to affect survivors of high-risk NB (Trahair *et al*., 2007). It has been proposed that one of the mechanisms contributing to the aggressive behaviour of advanced-stage NB in older children is resistance to the extrinsic apoptosis pathway activation (George *et al.,* 2010). Hence, research in recent years has focused on the activation of apoptosis via the mitochondrial pathway (Ferrin *et al*., 2011; Posadas *et al*., 2012).

The medicinal use of plant-derived bioactive compounds for the treatment of many disease conditions including cancer predates recorded human history. BetA, a natural plant-derived compound belonging to the prominent class of triterpenoids, has emerged as a highly promising anti-cancer compound due to its ability to directly target the mitochondrial pathway of apoptosis (Mullauer *et al*., 2010). Its efficacy in many *in vitro* and *in vivo* systems has been widely studied with minimal to no cytotoxic effects in healthy cells and rodents (Zuco *et al*., 2002; Fulda and Kroemer 2009; Mullauer *et al.,* 2010). However, the formulation of a pharmaceutical product from this compound has been hampered by its highly lipophilic character and weak hydrosolubility (Mullauer *et al*., 2011). Many studies have tried to modify BetA derivatives to enhance their solubility such as modifications at the C-3 and C-28 positions which were found to be promising in addressing the solubility issues (Lui *et al.,* 2004; Huang *et al.,* 2007; Rajendran *et al.,* 2008). However, since the lipophilic character of BetA is likely to be crucially involved in its pluripotent mechanism of action, which is responsible for its broad activity profile, novel formulations of BetA are needed. Owing to the challenges faced with BetA and drug delivery to the brain, advancement in science has lead to the discovery of specialized drug delivery techniques using nanotechnology.

Nanotechnology utilizes particles in the 1-100 nm size range in at least one dimension; this allows them to cross biological barriers through small capillaries into individual cells, thereby permitting efficient drug accumulation at the target site and reducing the residual toxicity imposed by most chemo-therapeutic agents (Fisher and Ho, 2002, Lockman *et al*., 2002; Peer *et al.,* 2007). This offers numerous novel possibilities for the treatment of cancer.

Liposomes, a class of NPs, were discovered by Dr Bangham and colleagues in 1965 and have generated much enthusiasm due to their unique potential to improve the efficacy of current drugs (Paliwal *et al*., 2011). They are considered to be self-assembled closed colloidal structures composed of one or more concentric lipid bilayers surrounding a central aqueous core (Parveen *et al*., 2012). The unique ability of liposomes to entrap hydrophilic molecules into the core and hydrophobic molecules into the bilayers renders them attractive for drug delivery systems (Akbarzadeh *et al*., 2013). Cyclodextrins (CDs) are non-reducing cyclic oligosaccharides with features of a hydrophilic outer surface and lipophilic interior cavity, allowing for the improvement of poorly water soluable molecules by entrapping guest molecules (lipophilic molecules) inside the internal cavity and acting as complexing agents (Laza-Knoerr *et al.,* 2010; Nasir *et al*., 2012). CDs and liposomes have recently gained

interest as novel drug delivery vehicles by forming complexes that can be incorporated into the aqueous core of liposomes, hence improving therapeutic load, bioavailability and efficacy of many poorly water-soluble drugs (Arun *et al.*, 2008; Li *et al.*, 2011; Nasir *et al.*, 2012; Chordiya and Senthilkumaran, 2012; Vafaei *et al*., 2014). This present study focuses on a novel drug delivery system for BetA using liposomes and γ-CDs and applying it for the treatment of human NB cancer cells.

5.2 Size Analysis of the Liposomes

The effects on size distribution of the EL, BetAL (B1 and B2) and γ-CD-BetAL generated from thin film hydration, before and after extrusion was studied (Figure 3.1, Chapter 3). In this study thin film hydration generated multilamellar vesicles (MLVs) (> 0.1μm). Thin film hydration is known to yield MLVs; liposomes with a diameter of approximately 0.1-20 μm with more than 4 bilayers present (Elhissi *et al*., 2006; Raman *et al*., 2007; Al-Zubaidi *et al*., 2014). As shown in Figure 3.1, A (Chapter 3), the size of un-extruded EL (4194 nm ± 2260) was larger than un-extruded BetAL (B1 and B2) (2387 nm ± 249.2 and 1742 nm ± 959.9, respectively) and γ-CD-BetAL (1367 nm ± 190.5). As the concentration of BetA was increased, the size of the un-extruded BetA liposomal formulations decreased. Statistically significant differences were noted upon comparison of the un-extruded EL with un-extruded B1 (BetAL) and un-extruded γ-CD-BetAL (* $P < 0.05$). This suggests that cholesterol (Chol) might be included in the bilayer of liposomes more efficiently than BetA which allowed for larger size distribution of un-extruded liposomes. The presence of the hydroxyl group (OH) attached to the end of the Chol makes that part weakly hydrophilic therefore it inserts itself in the bilayer with its OH-group towards the aqueous core, and the rigid hydrophobic tail toward the phospholipid bilayers (Cooper and Hausman; 2009; Perrie and Rades, 2010). It could also be attributed to the high hydrophobicity of the long acyl chains present in DPPC phospholipid and repulsive interactions between water molecules at the interface; causing them to aggregate (Zhao and Feng, 2004; Zhao and Feng, 2005), therefore DLS could have measured these agglomerated particles as singular large particles. It is also important to note that 2 mg/ml of Chol was used in EL preparation, 0.5 and 1 mg/ml of BetA were used in BetAL preparations while the DPPC lipid remained constant. Increasing the concentration of BetA did not however cause the size of liposomes to increase (Figure 3.1, A, Chapter 3). The size of liposomes appears to depend largely on the interaction of DPPC lipids with either Chol or BetA during the formation process of liposomes and it seems as though Chol has a higher affinity for the DPPC bilayers than BetA.

It is suggested in the literature that the incorporation of both cholesterol (Chol) and BetA into liposome bliayers worked together to contribute to a highly rigid bilayer, a phenomenon of cooperative membrane rigidification also observed for Chol together with carotenoids (Reddy and Couvreur, 2008; Mullauer *et al.*, 2011). BetAL was prepared without Chol to avoid rigidification and allow for easier extrusion (Mullauer *et al.*, 2011) however, extrusion in this study was still difficult due to the viscosity of the liposome solution after thin film hydration and the desired SUVs (small unlamellar vesicles) in a range of less than 100 nm was therefore not achieved when studied with DLS (Figure 3.1, B). However, DLS measurements from Zetasizer NanoZS reveal that extrusion was successful in reducing MLVs in the μm size range, to large unilamellar vesicles (LUVs) in a size range of less than 200 nm (Figure 3.1.3, Chapter 3). Extrusion through a 100 nm filter did not work initially; therefore a 200 nm filter was used first and then a 100 nm filter (Section 2.3.4, Chapter 2). This could explain why the size distribution after extrusion for BetAL (B1 and B2) was larger when compared to EL as these two batches had a very viscous whitish medium after hydration making extrusion particularly difficult in both 200 nm and 100 nm filters (Figure 3.1.2, Chapter 3). A recent study revealed that extrusion through different sized filter pores and increasing the amount of passes through filters when extruding is more effective in achieving smaller liposomes (Hinna *et al*., 2015). Therefore it's possible that increasing the amount of passes through the filter during extrusion and employing a smaller filter size (80 nm) in this study could have resulted in liposomes with a size of less than 100 nm.

5.3 Polydispersity Index (PI) of liposomes

PI for all liposomes before extrusion (Figure 3.2, A, Chapter 3) was closer to 1 and after extrusion PI was reduced to less than 0.3 (Figure 3.2, B, Chapter 3) indicating that the process of extrusion generated liposomes with a relatively narrow size distribution irrespective of BetA loading. The PI of B1 (BetAL) (1 ± 0.0) and B2 (BetAL) (0.94 ± 0.1) before extrusion shows a relationship with the large size distribution obtained for un-extruded B1 (BetAL) (2387 nm ± 143.9) and un-extruded B2 (BetAL) (1742 nm ± 959.9). After the hydration step, the lipid suspension should contain a heterogeneous mixture of MLVs, LUVs and SUVs (Laouini *et al*., 2012). This was noted in this study by the turbid whitish viscous lipid suspension before extrusion and therefore after extrusion this lipid suspension became more transparent. The low PI (0.1-0.24) after extrusion correlates to the nm size range obtained after extrusion, indicating that the transparent liposome solution observed after extrusion is monodisperse with a narrow uniform size distribution of liposomes in solution.

This also relates to previous studies where reported PI range of 0.2-0.4, yielded uniform sized liposomes in the nm size range (Cabral *et al*., 2004; Saha *et al*., 2011).

5.4) ζ-potential of Liposomes

The ζ-potential of EL (-1.205 mV ± 0.74), B1 (BetAL) (-2.25 mV ± 0.1), B2 (BetAL) (-2.52 mV ± 0.18) and γ-CD-BetAL (-2.02 mV ± 0.21) before extrusion was in the negative range (3.3, A, Chapter 3). The average un-extruded BetAL (B1 and B2) and un-extruded γ-CD-BetAL showed a higher negative ζ-potential upon comparison to the extruded liposomes (Figure 3.3, C, and Chapter 3). When BetA was loaded into liposomes, the ζ-potential was more negative than EL (Figure 3.3, A) and remained in the negative range even after extrusion (Figure 3.3, C). BetA has a hydroxyl group which makes the compound slightly negative, which could explain why the ζ-potential remains negative after BetA loading and extrusion, as the BetA contributes to the negative ζ-potential of liposomes. This low ζ-potential for BetA does not correlate to previous studies, BetA incorporated in flax-seed oil containing a nanoemulsion formulation showed higher negative ζ-potential values (−39.1 ± 1.2), however this could be due to a different nanoparticle drug delivery system (Dehelean *et al*., 2011b). EL showed a positive ζ-potential value before extrusion (Figure 3.3, A) and a low negative ζ-potential after extrusion (Figure 3.3, B), with both values being closer to 0 mV, thus indicating a neutral surface charge. The surface charge of the EL was influenced by the 1,2-Dipalmitoyl-*sn*-glycero-3-phosphocholine (DPPC) phospholipid used in the liposome preparation. DPPC lipid consists of a hydrophilic head group with a quaternary ammonium moiety choline, which is linked to a glycerol via a phosphoric ester (Brandl, 2001). The permanent positive charge on the choline of the head group counteracts the negative charge of the phosphate to give a neutral hydrophilic head group (Philippot and Schuber, 1994).

The size of un-extruded BetAL (B1 and B2) was larger than un-extruded γ-CD-BetAL (Figure 3.1, A, Chapter 3) and higher negative ζ-potential values was evident when comparing the ζ-potential of un-extruded BetAL (B1 and B2) with un-extruded γ-CD-BetAL (Figure 3.3, A, Chapter 3). B2 (BetAL), which had a higher BetA loading compared to B1 (BetAL), showed the highest ζ-potential before extrusion. These support the suggestion by Howard and Levi (2010) that the ζ-potential is related to size and drug loading. Higher BetA concentrations made the surface charge on the DPPC liposomes more intense before extrusion but when extruded, the intensity of the BetAL (B1 and B2) and γ-CD-BetAL was similar to that of un-extruded EL, suggesting that the stability of liposomes decreases as the

size decreases (Figure 3.3, C, Chapter 3). According to literature, liposomes with a ζ-potential in a range of > +30 mV or < −30 mV are normally considered stable for biological applications (Hunter *et al*., 2001; Laouini *et al*., 2012; Monteiro *et al*., 2014; Sabeti *et al*., 2014); however the lipid-to-drug ratio used will influence the ζ-potential values (Honary and Zahir, 2013). The lipid-to-drug ratio of the neutral charged DPPC lipid and the slightly negatively charged BetA contributed to the low ζ-potential observed in this study. Liposomal formulations with ± 30 mV is superior in dispersion stability than the reported ranges in this study due to the fact that such formulations will have stronger electrostatic repulsion interaction forces present, thereby preventing aggregation of liposomes. This could explain the low ζ-potential values of liposomal formulations as the electrostatic repulsion is weak causing agglomeration. Furthermore ζ-potential with ± 30 mV has been shown to have higher drug encapsulation efficiency, due to stronger ζ-potential contributing to unilamellar liposome formation (Sou *et al.*, 2011). Surface potential plays an important role in the behaviour of liposomes *in vivo* and *in vitro*. The ζ-potential of liposomes will affect the interaction with cells as most cancer cells are negatively charged due to the translocation of negatively charged constituents of the inner layer of the cell membrane to the cell surface (Ran *et al*., 2002). The BBB has also been reported to be negatively charged due to anionic sites located on the luminal surfaces of brain capillaries (Béduneau *et al*., 2007). More positively charged NPs could facilitate in crossing biological membranes and the BBB (Honary and Zahir, 2013). Therefore even though liposomal formulations in this study revealed low negative ζ-potential values, this could assist in the mechanism of liposome-cell-interaction and drug delivery to cells.

5.5 Size and Physical Morphology of Liposomes

HR-SEM micrographs of un-extruded EL, extruded B1 (BetAL) and extruded γ-CD-BetAL revealed spherical-shaped vesicles (Figure 3.4, Chapter 3). The spherical shape was maintained even after the incorporation of BetA into liposomes. Un-extruded EL had a heterogeneous size distribution of spherical vesicles as some were in the size range of less than 300 nm and a few vesicles were larger than 300 nm (A and B). This did not correlate with the size results obtained from the Zetasizer NanoZs instrument which showed a size distribution of more than 4000 nm for un-extruded EL (4194 nm ± 2260). However it did relate to the PI studies of un-extruded EL, as the PI was above 0.5, indicating a heterogeneous solution, suggesting that liposomes in solution are non-uniform in shape. Extruded B1 (BetAL) (C and D) and extruded γ-CD-BetAL (E and F) showed a more

homogeneous size distribution, thus extrusion was successful in converting large liposomes into a uniform and narrow liposome population. This also corresponds with the PI results obtained from the Zetasizer NanoZs instrument for extruded B1 (BetA) (0.22 ± 0.04) and extruded y-CD-BetAL (0.24 ± 0.01) as the PI was in a range of less than 0.25, indicating a monodisperse solution. The reported size distribution of extruded B1 (BetAL) and extruded γ-CD-BetAL after analyses with the Zetasizer NanoZs was larger when compared with the sizes observed in the HR-SEM micrographs (Figure 3.4, Chapter 3). This is largely related to the different techniques used in the analysis of size. The Zetasizer NanoZs instrument uses dynamic light scattering (DLS) techniques to measure particles in solution undergoing Brownian motion and hydrodynamic size whereas in HR-SEM analyses, the sample requirement is smaller and must be completely dried under a fume hood prior to analyses (Elsayed and Cevc, 2011). Liposomes dispersed in liquid would have different properties compared to the liposomes that are air-dried. It is possible that the larger sizes reported in un-extruded EL (Figure 3.1, A) using DLS was attributed to aggregation of liposomes as seen in un-extruded EL HR-SEM micrographs (black arrows in Figure 3.4, A, B and E). This relates to the low ζ-potential reported for un-extruded EL (Figure 3.3, A) observed as electrostatic repulsion forces prevent NPs from agglomerating and low ζ-potential values have been reported to result in agglomeration of NPs (Hunter *et al*., 2001, Jiang *et al*., 2009; Sabeti *et al*., 2014). In this study, the repulsive forces present was weak and forces of agglomeration prevailed causing the clumping together of vesicles as observed in Figure 3.4 (A, B and E). Aggregation of liposomes may contribute to leakage of entrapped agents (Torchilin *et al*., 1992; Matteucci and Thrall, 2000; Pedroso de Lima *et al*., 2003) which was evident in the low % EE in this study and the significant loss of BetA after extrusion (Figure 3.5.2, Chapter 3). Colloidal particles (size range of 1 μm) in solution often pose challenges in accurate characterization and measurement as they are constantly transitioning between Brownian movement and the fluid-induced movement (Elimelech, 1995). HR-SEM could give accurate information about size of liposomes, but the size of liposomes is also important in solution as this is the medium used to treat cells.

SEM is less frequently used to image liposomes as the sample must be air dried/ freeze dried/ fixed before imaging and these prior steps cause liposomal vesicles to collapse during drying stages and burst or crack under the intensity of the electron beam as the magnification is increased (Ruozi *et al*., 2011). Liposomes in this study suffered structural perturbations as a result of the high-vacuum conditions of the HR-SEM instrument (images not shown) and

many vesicles collapsed during the air-drying step. The intensity of the electron beam caused the destruction of liposomes at higher magnifications; therefore images had to be taken quickly. This also explains why some images may seem out of focus (Figure 3.4, C and F). Liposomes, unlike cells, do not have pumps to enable the transfer of water out and therefore liposomes cannot tolerate a high osmotic pressure. When samples are diluted excessively during the sample preparation, the osmotic pressure could cause the liposomes to swell and burst. Freeze drying of samples using cryo-transmission electron microscopy (Cryo-TEM) could assist in improving the quality of images (Fox *et al*., 2014). Cryo-TEM imaging could also provide lamellarity characteristics (Farhang *et al*., 2012). However we were successful in imaging liposomes that are spherical in shape, as most liposomes imaged using SEM reported in literature are spherical (Nirale *et al*., 2009; Yousefi *et al*., 2009; Ramana *et al*., 2010; Odeh *et al*., 2012). Smooth external surfaces of liposomes in SEM images have been reported to demonstrate that the structure is a self-assembled and a closed membrane of lipid bilayers in contrast to agglomeration of lipids or fragments of lipid bilayers (Stamm *et al*., 2012). Smooth surfaces of un-extruded EL and extruded BetAL can be observed on the surfaces of spherical vesicles (white arrows in Figure 3.4, A and D). The shape and size morphology is an essential component in understanding and elucidating the mechanisms involved in drug release from liposomes and the biological analyses of liposome-cell-interaction.

5.6 The Concentration (mg/ml) and the Percentage Entrapment Efficiency (% EE) of BetA in Liposomes

The results presented in Table 3.1, Table 3.2 and Figure 3.5 (Chapter 3) indicates that BetA loading achieved using the thin film hydration method was poor and BetA loss in the extrusion process was significant (*** $P < 0.01$ and * $P < 0.05$). Statistically significant differences was reported when the % EE of un-extruded B1 (BetAL) was compared with the % EE of un-extruded B2 (BetAL) (* $P < 0.05$) but did not differ statistically when compared to un-extruded γ-CD-BetAL (Table 3.2, Chapter 3). This suggests that loading low amounts of BetA (0.5 mg/ml) was more effective in entrapping higher amounts of BetA in the DPPC bilayers. It's possible that DPPC bilayers may have reached a limit in the capacity to entrap BetA at higher concentrations (1 mg/ml). Since the concentration of DPPC remained the same, increasing DPPC concentrations could have enhanced drug loading as shown by Chorachoo *et al*., (2013). The initial entrapment of BetA in un-extruded liposomes was generally low (Table 3.2 and Figure 3.5, Chapter 3); indicating that passive loading using thin film hydration method produced a poor entrapment of BetA as a lipophilic molecule (Figure

3.5, Chapter 3). This relates to previous studies which reported on the low entrapment of non-polar derivatives and hydrophilic molecules into liposomes using thin film hydration method (Patel *et al*., 2010; Vyas *et al*., 2011; Muppidi *et al*., 2012).

The initial size of liposomes generated from thin film hydration and liposomes subjected to extrusion shows a relationship with the % EE of BetA. It's possible if the size of BetA loaded liposomes was increased, the % EE could be increased as shown by Mullauer *et al*., (2011) where large liposomes (1.5µm), assembled without Chol, contained a fivefold-enhanced BetA incorporation (approximately 6 mg/ml) (Mullauer *et al*., 2011). The researchers did conclude that the larger liposomes would not be feasible for human application. Extrusion has also been reported to decrease drug entrapment in liposomes (Jousma *et al*., 1987; Berger *et al*., 2001, Mokhtarieh *et al*., 2013) as observed in this study. Previous studies suggested that BetA orients itself in the bilayer of liposomes (Mullauer *et al*., 2011). As extrusion took place, it appears that BetA was being discarded as the bilayers were being destroyed, thus the extruded liposome had an even lower % EE (Figure 3.5, Chapter 3). This resulted in less than 1 mg/ml BetA in extruded B1 (BetAL), extruded B2 (BetAL) and extruded γ-CD-BetAL (Table 3.2).This finding corroborated a previous study by Mullauer *et al*., (2011), where they prepared long circulating liposomes in the size range of 100-200 nm which entrapped less than 1 mg/ml BetA. In the current study, long circulating liposomes (< 200 nm) was prepared because of their small size and prolonged circulatory half-life that could potentially enter into the tumour tissue by virtue of the local enhanced permeability retention (EPR) effect, thereby delivering BetA to the tumour tissue (Maeda *et al.*, 2000).

Chol is known to improve membrane stability for liposome formulations and hydrophobicity in the bilayers, especially for non-polar molecules. Chol does this by inserting itself into the membrane with its hydroxyl groups oriented towards the aqueous core and aliphatic chain aligned parallel to the acyl chains in the centre of the bilayer (Perrie and Rades, 2010). However Chol was not added to BetAL (B1 and B2) and γ-CD-BetAL in this study in order to avoid rigidification. The incorporation of Chol and BetA in the bilayer of liposomes renders an extremely rigid membrane, causing difficulty in downsizing of liposomes and slow or sustained drug release, as reported previously (Mullauer *et al*., 2011),

Previous studies showed that there are variations in the % EE of molecules due to the increasing or decreasing amount of Chol, in some cases increasing the amount of Chol showed an increasing drug encapsulation efficiency, as reported by Bhatia *et al*., (2004)

where 30% Chol addition lead to an increased % EE of tamoxifen from 45.2% to 57.5%. There is variation in the % EE of hydrophobic molecules due to the increasing or decreasing amount of Chol. These effects may be due to molecular interaction between the phospholipids, Chol and drug. Chol enhances the hydrophobicity region of the bilayered membrane which may favour the entrapment of hydrophobic molecules (Subczynski *et al*., 1994; Pasenkiewicz-Gierula *et al.*, 2000). Addition of Chol in this study could have enhanced BetA loading and prevented BetA leakage; however considering the conflicting fact that Chol may favour incorporation into the limited hydrophobic bilayer, there might be a competition for space between the alkyl chains of DPPC, cholesterol and BetA resulting in an overall lower encapsulation with an increasing Chol content.

It is known from literature that employing a lipid with a long alkyl chain length, increases partitioning of the non-polar or lipophilic derivatives into the bilayer and could help to avoid poor encapsulation and retention of drug which is one of the common disadvantages associated with liposomal drug delivery systems prepared using natural phospholipid such as the commonly used soy derived EPC (1,2-dioleoyl-*sn*-glycero-3-ethylphosphocholine) (Begum *et al*., 2012). In this study, a synthetic EPC lipid called DPPC, a 16 alkyl chain lipid, was used due to its reported high entrapment of hydrophobic drugs (Begum *et al.*, 2012 and Odeh *et al*., 2012), however the % EE of BetA was still low. Using heating (above Tm) and cooling cycles in the hydration step was suggested as a means to increase the entrapment of BetA in the bilayer of liposomes, as this induced opening and closing of liposomes which would entrap more BetA. It is suggested in literature that after forming a thin film of lipids on a 250 ml round bottom flask, purging with nitrogen can reduce lipid oxidation (Achim *et al*., 2009; Popovska *et al*., 2013). It is possible that some form of lipid peroxidation prevented BetA loading in the final prepared liposomes as no nitrogen purging for thin films with nitrogen was done, but stored immediately at -4˚C and cooling and heating cycles took place in the hydration step which was suppose to enhance BetA loading. Changes in temperature is one of the factors that can cause lipid peroxidation in DPPC liposomes as these changes can alter certain properties of lipids and the way in which they arrange themselves in order to enclose molecules and form liposomes during the hydration step (Cubillos *et al.*, 2006). It is known from literature that the % EE of lipophilic molecules in liposomes depends largely on the affinity of drug to the lipid membrane (Muppidi *et al.,* 2012).Therefore in this study, the ability of BetA to entrap in liposomes depended largely on the interaction and affinity of BetA in the DPPC bilayers of liposomes.

The interaction between BetA and DPPC lipid could be seen as non-specific as it is dependent on the hydrophobic (or van der Waals) force (Mullauer *et al.*, 2011). Upon analyses of the molecular structure of BetA and DPPC lipid, low % EE of BetA in DPPC liposomes could be attributed to the absence or weakness of the van der Waals forces between the two compounds, hence hindering and acting as a physical barrier for the movement of BetA into the bilayers and forming unstable systems at the air/water interface during preparation. In chemistry, van der Waals forces are defined as the sum of the attractive or repulsive forces between molecules (or between parts of the same molecule) other than those due to covalent bonds, or the electrostatic interaction of ions with one another, with neutral molecules, or with charged molecules. There are three types of van der Waals' forces-dipole-dipole forces, dispersion forces and hydrogen bonding. Chol could have been better oriented in the DPPC lipid bilayer than BetA, since it can form a hydrogen bond with 3β-hydroxyl and the sn-2 carbonyl of DPPC (Sankaram and Thompson, 1991), this also correlates to the large sizes reported for un-extruded EL and the smaller un-extruded sizes for BetA loaded liposomes in this study. Partitioning of molecules into DPPC bilayers of liposomes is attributed to increasing hydrophobicity (Ojogun *et al.*, 2010); hence it is possible that with BetA and DPPC having weak van der Waals forces between them, there are no strong electrostatic forces retaining BetA within DPPC bilayers. This correlates with the low negative ζ-potential values reported in this study before and after extrusion and the significant loss in BetA observed after extrusion. Further work using differential scanning calorimetry (DSC) is required to elucidate this. It could be assumed that some sort of adsorption took place inside the bilayers, where BetA incorporated in the bilayer of liposomes are in between the alkly chain lengths of DPPC and not held in place by electrostatic forces, as retention within the bilayers of BetA was weak. These factors could have contributed to BetA leakage from the liposome.

The γ-CD-BetA did enhance BetA loading in γ-CD-BetAL but it was not statistically significant when compared to B1 (BetAL), BetA might have been entrapped in the core of liposomes when complexed with γ-CD but it was a very low amount as it only differed from B1 (BetAL) by 5% (Table 3.2, Chapter 3). Forces such as van der Waals, hydrogen bonds and hydrophobic effects contribute to the formation of a stable complex of drugs in the non-polar cavity of CDs (Nasir *et al.*, 2012). These forces could have been really poor or complexation was weak, therefore contributing to poor loading of γ-CD-BetA into liposomes.

The % EE of BetA loading in DPPC liposomes reported in this study was dependent on size and ζ-potential. Decreasing the size of liposomes caused a decrease in BetA entrapment and therefore a decrease in ζ-potential of liposomes. This gives an indication that the accommodation of BetA within the liposome bilayers could be responsible for the slight negative ζ-potential values. The ζ-potential values with ± 30 mV has been shown to have higher drug encapsulation efficiency, due to stronger ζ-potential contributing to the formation of unilamellar stable liposomes (Sou *et al.*, 2011). The low ζ-potential in this study matches with the low % EE. The ζ-potential for extruded γ-CD-BetAL showed the highest negative ζ-potential after extrusion and the highest % EE after extrusion.

The selected method and drug-to-lipid ratio were two important factors considered when analyzing the low entrapment of BetA in DPPC liposomes for this study as optimization of drug-to-lipid ratios will influence the entrapment of drugs in liposomes (Muppidi *et al.*, 2012). Thin film hydration method is the oldest and simplest method for preparing liposomes and usually yields poor entrapment efficiency (Gubernator, 2011; Prathyusha *et al.,* 2013). The method of BetA loading used in this study is known as the passive loading method where BetA was included during the preparation of liposomes. Recently, active loading methods for producing liposomes have become more popular, as they demonstrate higher % EE (Sur *et al.*, 2014). In this method, empty liposomes are first created and then the drug/compound is loaded using transmembrane pH gradients where drugs can cross membrane layers to enter into the liposome. This method however seem to increase the % EE of hyrophilihc drugs more than hydrophobic/lipophilic drugs. Particulate-based proliposome technology is becoming more synonymous with improving hydrophobic and lipophilic drugs entrapped in liposomes. The method involves carbohydrates as soluble carrier materials layered with phospholipids to form MLVs upon addition of the aqueous phase above Tc (Payne *et al*., 1986). Liposomes are prepared by attaching a flask containing carrier particles to a rotary evaporator followed by the addition of the organic solution in a portion wise manner through a feed-line under reduced pressure to coat the carrier particles. Evaporation of the organic solvent under vacuum using rotary evaporation causes the formation of particulate based proliposome (Payne *et al*., 1986; Elhissi *et al*., 2006). Lipophilic drugs incorporated in liposomes prepared from this method demonstrated high entrapment efficiency such as Amphotericin B (100%) (Payne *et al*., 1987), Nimodipine (84.70%) (Sun *et al.,* 2013), CM3 peptide (100%) and Ciprofloxacin (96%) (Desai *et al*., 2002).

The amount of hydrophobic/ lipophilic drug that can be introduced in a liposome is highly dependent on packing restrictions in the lipid bilayers and, as a result, liposomal formulations for this type of drug may differ significantly from one drug to the next (Mayer *et al*., 1986). Packaging restrictions of liposomes are influenced by factors such as the technique used and drug-to-lipid ratio. The water solubility of lipophilic drugs or hydrophobic compounds incorporated into the conventional liposome bilayer is often limited in terms of drug-to-lipid ratio (Dhule *et al*., 2012). It has also been reported that some lipophilic drugs may interfere with the formation of the liposome bilayer, limiting the dose which can be incorporated into the liposome (Chordiya and Senthilkumaran *et al.,* 2012). This could have occurred when higher starting concentrations of BetA (1 mg/ml) loaded into liposomes were unable to be entrapped efficiently and therefore lower starting concentrations of BetA (0.5 mg/ml) was more efficient in entrapping BetA. In addition, both incomplete and rapid release and have been reported for lipophilic drugs entrapped within liposomes (Otero-Espinar *et al*., 2010), therefore we proceeded to evaluate the effect of B1 (BetAL) liposomes and γ-CD-BetA liposomes in two NB cell lines.

5.7) DMSO Tolerance Test for SK-N-BE(2) and KELLY NB Cell Lines

The results of this study revealed that DMSO at low concentrations (0.1 and 0.4%) promoted cell growth in SK-N-BE(2) NB cells for 24-72 hours while in KELLY NB cells, it promoted cell growth only at 72 hours with no statistically significant difference reported when compared to controls. It is evident that exposure to 1-2% DMSO is toxic in both cell lines ($P < 0.05$). It has been reported that different reagents generally dissolved with a final DMSO concentration in a range of 0.1-0.6% and less than 1% did not have significant effects on the viability of NB cancer cell lines, in some cases even up to 72 hours exposure (Jadhav *et al*., 2007; Ponthan *et al*., 2007; Wickstro *et al*., 2007; Xia *et al*., 2008; Fallarini *et al*., 2009; Götte *et al*., 2010; More *et al*., 2011; Frumm *et al*., 2013; Tsutsumimoto *et al*., 2014). Therefore, in this study, the highest concentration of free BetA (5-20 μg/ml) prepared from a stock solution of 5 mg/ml BetA (dissolved in DMSO) contained 0.4% DMSO.

5.8) Evaluation of Cytotoxicity for Free BetA and BetAL Treatment in SK-N-BE(2) and KELLY NB Cell Lines

In this study, free BetA treatment (5-20 μg/ml) induced cytotoxic effects on SK-N-BE(2) (Figure 4.2.1, A and B) and KELLY NB (Figure 4.2.2, A and B) cell lines. SK-N-BE(2) NB cells subjected to 5-20 μg/ml free BetA treatment, demonstrated a time and concentration

dependent decrease in the cell viability for all exposure hours (Figure 4.2.1, A, Chapter 4). KELLY NB cells treated with free BetA only showed a concentration dependent decrease at 24 hours exposure (Figure 4.2.2, A, Chapter 4). The lowest cell viability for SK-N-BE(2) NB cell line were observed at 15 µg/ml exposure at 72 hours (7% cell viability) and in KELLY NB cell line at 10 µg/ml (14% cell viability) ($P < 0.05$, annotated by asterisks). Statistically significant differences were noted for treated cells compared to untreated cells. Estimated IC_{50} concentration values for treatment with free BetA were reported to be 13.10 µg/ml (24 hours), 14.03 µg/ml (48 hours) and 7.85 µg/ml (72 hours) for SK-N-BE(2) NB cells and 24 µg/ml (24 hours), 14.50 µg/ml (48 hours) and 76.05 µg/ml (72 hours) for KELLY NB cells (Table 4.1, Chapter 4). Therefore the reported IC_{50} concentration values for this study corresponded to the established IC_{50} values for NB and other brain cancer cell lines reported in literature (Fulda *et al*., 1997; Schmidt *et al*., 1997; Steele *et al*., 1999; Wick *et al*., 1999; Thurnher *et al*., 2003; Moghaddam *et al*., 2012; Suresh *et al*., 2012).

SK-N-BE(2) NB cells treated with BetAL (Figure 4.2.1, B, Chapter 4) showed a time and concentration dependent decrease in the cell viability, similar to the treatment of SK-N-BE(2) NB cells with free BetA (Figure 4.2.1, A). However cell viability results reported for free BetA were lower when compared to BetAL treated cells as concentration and exposure duration increased (Table 7.4.1 and Table 7.5.1, refer to Appendix). The estimated IC_{50} concentration values for SK-N-BE(2) cells treated with BetAL (53.45 µg/ml for 24 hours 38.73 µg/ml for 48 hours and 18.30 µg/ml for 72 hours) was higher when compared to the IC_{50} concentration values reported for free BetA exposure (Table 4.1 and Table 4.2, Chapter 4). KELLY cells treated with BetAL shows variability in the cell viability across concentrations, this is seen at 48 hours as viability decreases from 5-20 µg/ml (74%, 60%, 56% and 52% cell viability, respectively) and then an increase at 50 µg/ml (57% cell viability) (Figure 4.3.2, Chapter 4). This could suggest that KELLY NB cells demonstrate recovery at higher concentrations and exposure times. The estimated IC_{50} concentration values for KELLY NB cells treated with BetAL were higher at 24 and 48 hours (68.65 µg/ml and 61.52 µg/ml, respectively) but lower at 72 hours (21.42 µg/ml) when compared to the reported IC_{50} concentration values for free BetA. The estimated IC_{50} concentration values for SK-N-BE(2) and KELLY NB cell line reported in this study suggests that free BetA is more effective in inhibiting cell growth *in vitro* at lower concentrations and shorter exposure durations than BetAL. The cytotoxic activity of free drug might have been more effective in

reducing the proliferation of NB cells; however BetAL was still successful in reducing the cell viability even if the BetA entrapment was poor.

For all hours with EL exposure in both cell lines, no statistically significant differences was observed when compared to untreated cells, suggesting that EL did not confer any cytotoxic effects on the cell viability which is in agreement with previous studies (Mitsopoulos and Suntres 2011; Dhule *et al*., 2012; Venegas *et al*., 2012). This may be due to the phospholipid and Chol used in the preparation of EL, which are major components found in biological membranes and essential for cellular functions. Liposomes are usually composed of biocompatible and biodegradable lipids and should not have any cytotoxic effects in cell culture at concentrations up to 200 µM final lipid concentration (Puapermpoonsiri *et al*., 2005). This could also be due to the fact that the lipids used exhibited a neutral charge.

5.9) Evaluation of Cytotoxicity for Free γ-CD and γ-CD-BetAL Treatment in SK-N-BE(2) and KELLY NB Cell Lines

Treatment with free γ-CD did not show any statistically significant difference when compared to the control at 24 hours for SK-N-BE(2) NB cells, however statistically significant differences were noted in KELLY NB cells at 50 µg/ml. Both cell lines showed statistically significant differences at 48 and 72 hours exposure to 20 and 50 µg/ml free γ-CD suggesting that free γ-CD induces cytotoxicity only after 24 hours exposure at higher concentrations. Studies reporting on the *in vitro* toxicity of free CDs are contradictory as some studies report that free CD is toxic and others report no toxicity, however the toxicity seems to be related to the type of CDs molecule. CDs are classified based on the amount of glucose units present: α-, β-, and γ-CDs (with 6, 7 or 8 glucose units respectively) (Das *et al*., 2013) subsequently relating to how they would interact with cells *in vitro*. The β-CD series is the most widely studied CD type and has revealed that it can modulate Chol in cell membranes due to their high affinity for Chol, affecting the structure of the cell membrane (Zidovetzki and Levitan, 2007), α-CD are most efficient in extracting phospholipids from cells (Monnaert *et al*., 2004) and γ-CD is less lipid selective compared to the other two CDs (Monnaert *et al*., 2004). This is noted in a study investigating CD toxicity in an *in vitro* endothelial BBB model, where the researchers concluded that the α-CD and β-CD series are the most toxic CDs whereas the γ-CD series are less toxic (Monnaert *et al.*, 2004). CDs have also demonstrated cell toxicity in fibroblasts (Pitha *et al*., 1988). Abu-Dahab *et al*., (2013) synthesized thymoquine-β-CD self assembling NPs and demonstrated that free CDs (which

was the control) had no cytotoxic effects on MCF-7 cells after 72 hours exposure. In this study for both cell lines, as the concentration increased from 10-50 μg/ml free γ-CD, the cell proliferation decreased. This was observant for both cell lines of 24 and 72 hours. This could be due to the aggregation of CD molecules, as previous studies demonstrated that higher CDs concentrations, including γ-CDs, have been reported to form aggregates with a diameter of 100 nm in solution which contributes to toxicity *in vitro* (Arun *et al*., 2008; Messner *et al*., 2010; Messner *et al*., 2011). The cytotoxicity induced by free γ-CD was an important factor to consider when preparing γ-CD-BetAL, especially in the SK-N-BE(2) NB cell line at 20-50 μg/ml treatment for 72 hours . Therefore concentrations where the final amount of γ-CD in γ-CD-BetAL were below 20 μg/ml for 48 and 72 hours exposure in KELLY cell and SK-N-BE(2) cells was prepared.

SK-N-BE(2) NB cells treated with γ-CD-BetAL (Figure 4.3.1, Chapter 4) showed a time and concentration dependent decrease in cell viability, similar to the trend noticed in both free BetA and BetAL exposure. The cell viability was moderately lower in SK-N-BE(2) with γ-CD-BetAL treatment when compared with BetAL for the same concentrations and time points. The estimated IC_{50} concentration values for γ-CD-BetAL exposure in SK-N-BE(2) cells for 24-72 hours were lower when compared to BetAL treated cells for 24-72 hours, suggesting that γ-CD-BetAL was more effective in inhibiting cell growth at lower concentrations when compared to BetAL as demonstrated by the lower cell viabilities. This corresponds to γ-CD-BetAL having a 5% higher BetA entrapment than BetAL, however free BetA was still more effective than both liposomal formulations in reducing cell growth (Table 4.1, Table 4.2 and Table 4.3, Chapter 4). Similar results were observed in KELLY cells treated with γ-CD-BetAL (Figure 4.3.2, Chapter 4), as the cell viability showed a time and concentration dependent decrease. KELLY cells treated with γ-CD-BetAL showed estimated IC_{50} concentration values for 24 and 48 hours that were lower than BetAL, however free BetA is the most effective in producing lower IC_{50} concentration values.

5.10) Conclusive Findings of Liposomal BetA Formulations Compared to Free BetA in SK-N-BE(2) and KELLY NB Cell Lines

BetA is insoluble in most aqueous solutions, hence it was prepared as previously described (Damle *et al*., 2013) by dissolving BetA in DMSO to produce a stock concentration of 5 mg/ml BetA and further diluted in media to obtain 5-20 μg/ml free BetA concentrations. BetAL and γ-CD-BetAL concentrations were prepared in the same manner in defined cell

culture media (Section 4.2.3.2, Chapter 2). The amount of BetA in the final concentrations of BetAL and γ-CD-BetAL were not equivalent to the amount of BetA found in free BetA even though the concentrations were the same (e.g. 5 μg/ml free BetA and 5 μg/ml BetAL/ γ-CD-BetAL). This is due to the fact that liposomes were subjected to extrusion to produce a final concentration of 0.04 mg/ml BetA entrapped in BetAL (B1) and 0.13 mg/ml BetA entrapped in γ-CD-BetAL. This is significantly lower when compared to the 1 mg/ml free BetA prepared in DMSO. Concentrations were prepared in the same manner from these working stock solutions; however the 5-20 μg/ml used in free BetA was increased to 5-50 μg/ml for BetAL. This could be the main reason that free BetA conferred a higher cytotoxicity in NB cells when compared to BetAL and γ-CD-BetA. The entrapment of BetA in liposomes was poor (< 1 mg/ml BetA entrapped in extruded liposome) and therefore did not match the cytotoxicity induced by free BetA treatment (Figure 4.4, Chapter 4). Free BetA compared to the same concentration of BetAL and γ-CD-BetAL showed statistically significant differences ($P < 0.05$), suggesting that free BetA is more effective in decreasing cell proliferation and inducing cytotoxicity into NB cells, especially at 72 hours (10-20 μg/ml) (Figure 4.4, Chapter 4). Treatment with-γ-CD-BetAL induced a higher cytotoxicity than BetAL in SK-N-BE(2), while treatment with BetAL in KELLY cells induced higher cytotoxicity than γ-CD-BetAL as the exposure duration increased. The estimated IC_{50} values for free BetA was lower when compared to BetAL and γ-CD-BetAL, however the IC_{50} values for γ-CD-BetAL was lower when compared to BetAL suggesting that γ-CD-BetAL was more toxic than BetAL. This could be attributed to the higher BetA entrapment in γ-CD-BetAL.

Additionally, the less cytotoxic nature of liposomes could also be attributed to sustained drug release upon using liposomes, especially in the case of the γ-CD-BetAL as there is double loading of BetA and γ-CD. This could have a delayed release of BetA as seen at 48 and 72 hours in Figure 4.3.2 (Chapter 4). CDs have been reported to demonstrate a delayed release of drugs referred to as 'sustained' or 'controlled' drug release (Sotthivirat *et al*., 2007; Sotthivirat *et al*., 2009; Daoud-Mahammed *et al*., 2008; Weifen *et al*., 2008; Otero-Espinar *et al*., 2012, Mignet *et al*., 2013). This is especially noticed in CD liposome drug delivery systems (Singh *et al*., 2010; Cui *et al*., 2011; Nasir *et al*., 2012; Vafaei *et al*., 2014). Lipophilic plant derivatives within the bilayer of liposomes may cause rigidity of the bilayers, resulting in the decreased release of the contents or uptake of liposome by the cell *in vitro* (Gao *et al*., 2012; Odeh *et al*., 2012). The nutritional value of the phospholipids of the

liposomes could also account for the low cytotoxicity induced by the liposomal formulations (Crosasso *et al*., 2000).

It is a known fact that the cytoplasmic membranes of cancer cells are more fluid when compared to normal cells (Leth-Larsen *et al*., 2010) and this could be one of the mechanisms to facilitate liposome-cell interaction. Although the mechanism of liposome cell interaction was not ascertained in this study, previous studies have shown mechanisms in which cells would internalize liposomes and other nanoparticles (NPs) through receptor-mediated endocytosis. The entire liposome enters the cell via an endosome and then into the lysosome or the liposome can cause endosome destabilization resulting in drug liberation into the cell cytoplasm (Torchilin, 2005; Dobrovolskaia and McNeil, 2007; Hess and Tseng 2007). In the event where the liposome does not enter the cell, liposomes come into close proximity with the cell surface and liposome-cell-lipid exchange could occur and the contents are automatically released into the cytoplasm (Torchilin, 2005). Low ζ-potentials reported in this study indicate low stability in BetAL and γ-BetAL and the fact that BetA was not strongly retained within the bilayer by strong van der Waals forces, undesirable BetA leakage might have occurred impacting on the results obtained. Therefore cytotoxicity could also be due to low concentrations of free BetA uptake that leaked from liposomes. As observed in the SEM micrographs of liposomes (Figure 3.4, A and E), aggregation could have also contributed to the low cytotoxicity induced by the BetA liposomes. The presence of electrolytes and high ionic strength of biological media can result in aggregation of NPs and this may influence their ability to interact with or enter cells (Vesaratchanon *et al*., 2007; Alkilany and Murphy, 2010).

Regardless of the delayed effect of BetAL and γ-CD-BetAL on the SK-N-BE(2) and KELLY NB cells, the cell viability showed a noticeable concentration and time decrease in cell proliferation, similar to free BetA. The cytotoxicity exhibited by BetAL and γ-CD-BetAL correlates with the % EE studies. Increasing the amount of BetA in liposomes through complexing BetA with γ-CD for enhanced entrapment into γ-CD-BetAL was more effective in decreasing cell viability at higher concentrations when compared to BetAL. However both BetAL and γ-CD-BetAL could not measure up to the cytotoxicity induced by free BetA treatment for both cell lines, suggesting that liposomal formulation were both weak when compared to free BetA treatment. This is also seen with the lower estimated IC_{50} concentration values for free BetA in both cell lines when compared to BetAL and γ-CD-BetAL.

CHAPTER 6

CONCLUSION AND FUTURE RECOMMENDATIONS

6.1) CONCLUSION

This study was conducted in order to develop a novel drug delivery system in addressing the solubility issues associated with the lipophilic anti-cancer plant extract BetA. This was done by preparing BetAL and improving the % EE through double entrapment of BetA and γ-CD-BetA inclusion complex forming a novel γ-CD-BetAL. The drug delivery system was then characterized based on physio-chemical characteristics and evaluated in two NB cancer cell lines, compared to free BetA treatment in order to investigate cytotoxicity.

In this study, liposomal formulations: EL, BetAL (B1 and B2) and γ-CD-BetAL, were prepared using the thin film hydration method. Liposomal formulations yielded a heterogeneous size distribution of approximately 1-4 μm and manual extrusion was successful in reducing the size of liposomes to less than 200 nm for biological systems application. HR-SEM images revealed aggregated vesicles of different sizes before extrusion and a uniform size distribution of spherical-like vesicles in a size range of less than 200 nm after extrusion, matching with size distribution and PI studies obtained from Zetasizer NanoZS instrument. HR-SEM micrographs of un-extruded EL did not match with results obtained from Zetasizer NanoZS instrument, as HR-SEM images revealed a smaller size distribution of liposomes. This was suggested to be due to the differences in techniques and aggregated liposomes being measured as large single particles by DLS. Extrusion of liposomes caused a decrease in size, PI and ζ-potential. Increasing the concentration of BetA into liposomes did not cause an increase in size or ζ-potential before extrusion; however as the size decreased the ζ-potential decreased contributing to a less stable liposomal formulation. The EL showed a ζ-potential close to 0 mV, indicating that the lipid is neutral; this suggested that incorporation of BetA in the lipid bilayers contributed to the negative ζ-potential values reported for BetA loaded liposomes.

The % EE results indicate that passive loading of BetA using the thin film hydration method was poor and BetA loss after extrusion process was significant. Partitioning of BetA into DPPC bilayers of liposomes was dependent upon the hydrophobicity induced by the DPPC bilayers and the affinity of BetA to the membrane bilayers. Hence it is possible that with BetA and DPPC having weak van der Waals forces between them as no hydrogen bond can

be formed, there are no strong electrostatic forces retaining BetA in the DPPC bilayers, causing drug leakage. This correlates with the low negative ζ-potential values reported in this study before and after extrusion and the significant loss in BetA observed during the preparation process. Inclusion of low starting concentrations of BetA (0.5 mg/ml) was more effective in entrapping higher amounts of BetA in the DPPC bilayers. Incorporation of γ-CD-BetA inclusion complex into liposomes to form γ-CD-BetAL did enhanced the % EE by 5% when compared to B1 (BetA); however this was not statistically significant. Nevertheless the therapeutic efficacy of EL, BetAL (Batch 1) and γ-CD-BetAL in SK-N-BE(2) and Kelly NB cell lines was still substantiated. A DMSO tolerance test (0.1%-2%) was performed and the sensitivity of free BetA and free γ-CD in both cell lines was determined. Cell viability was evaluated using the WST-1 colorimetric cell viability assay.

DMSO tolerance test revealed that 0.4% DMSO as a final concentration used in free BetA preparation did not confer any cytotoxic effects on cell viability. Treatment with free γ-CD at 20-50 μg/ml at 48 hours and 72 hours in both cell lines showed cytotoxicity. The EL had no cytotoxic effects on both cell lines for all exposure durations. Free BetA, BetAL and γ-CD-BetAL showed a time and concentration dependent decreases in the cell viability of SK-N-BE(2) NB cell line. The estimated IC_{50} concentration values in SK-N-BE(2) and KELLY NB cell lines for free BetA were lower when compared to BetAL and γ-CD-BetAL. This is noticeable with the higher cytotoxicity induced by free BetA when compared with BetAL and γ-CD-BetAL. BetA was more effective in inhibiting cell proliferation at lower concentrations and at earlier exposure durations. This could be due to the low % EE of BetA into liposomes, poor liposomal stability, weak γ-CD-BetA complexion, sustained drug release, liposome-cell-interaction and the nutritional value of phospholipids of the liposomes.

In conclusion, the estimated IC_{50} concentration values for free BetA produced from this study matched with established IC_{50} concentration values reported in previous studies. The objectives of preparing and characterizing different liposomal formulations of BetA and the novel γ-CD-BetAL were achieved. In this study, the loading of γ-CD-BetA into BetAL to produce the novel γ-CD-BetAL exhibited the highest % EE when compared to the other liposomal formulations in line with the hypothesis of the study. However, owing to the overall low % EE of BetA (< 1 mg/ml), low ζ-potential after extrusion and aggregation the liposomal designs became unstable. Weak electrostatic forces were unable to retain BetA in liposomes, therefore drug leakage and loss was significant in the preparation of liposomes.

These results influenced the evaluation of liposomal formulations in SK-N-BE(2) and Kelly NB cell lines. BetAL and γ-CD-BetAL did not measure up to the cytotoxicity induced by free BetA. However, γ-CD-BetAL was more effective in reducing cell viability in SK-N-BE(2) NB cells than BetAL and BetAL was more effective than γ-CD-BetAL in KELLY NB cells at 48-72 hours. Pronounced decrease in cell viability of SK-N-BE(2) and Kelly NB cells treated with free BetA, BetAL and γ-CD-BetAL still provides a basis for new hope for the effective management of NB using BetA.

6.2) FUTURE WORK AND RECOMMENDATIONS

Despite the many advantages posed by liposomes, the main drawback experienced in this study was the poor % EE of BetA, as drug loading was poor and drug loss in the initial preparation process was significant. Future studies aimed at investigating an active method or particulate-based proliposome technology for entrapping BetA as an alternative to the passive method used in this study are recommended. Previous studies have shown that these methods are more advantageous in promoting a higher % EE than passive loading (Akbarzadeh *et al*., 2013; Sun *et al*., 2013). Extrusion has also been reported to decrease drug entrapment in liposomes (Jousma *et al*., 1987; Berger *et al*., 2001, Mokhtarieh *et al*., 2013). Therefore creating liposomes of a specific size range first and then optimizing drug loading for efficient entrapment into liposomes is also recommended.

Drug-to-lipid optimization and the use of a longer alkyl chain length lipid instead of DPPC (a 16 alkyl chain length) are recommended (e.g., 18 alkyl chain length) as this could enhance the % EE. The use of different lipids in combination or alone could facilitate more strongly the retention of BetA in the bilayer of liposomes through strong electrostatic forces/ van der Waals forces. To improve BetA entrapment within the DPPC bilayers of liposomes, it was recommended to increase the electrostatic forces or van der Waals force by employing hydrogen bonding. This could be achieved by preserving the positive charge on the DPPC lipid, through increasing the carbon chain between the phosphoric group and amine group, the amine group could still have a positive charge and could assist in maintaining BetA in the bilayer. The amine group in DPPC could also be substituted with a stronger negatively charged group to form van der Waals forces between the BetA and the DPPC lipid.

Modification of liposomal surfaces with phosphatidylinositol or polyethylene glycol (PEG) has been known to improve the stability of liposomes and prevent aggregation (Goa *et al*., 2012). The addition of charged lipids to the neutral DPPC such as phosphatidylglycerol (PG)

or phosphatidylserine (PS) that is negatively charged could also enhance drug loading and increase negative ζ-potential values thereby increasing stability properties of liposomes.

Drug release kinetics studies are recommended, a drug release study over 24-72 hours would be ideal in investigating whether sustained drug release occurred and whether or not γ-CD hampered the release of BetA from liposomes, providing further insight into the mechanism of liposome-cell-interaction. Differential scanning calorimetry (DSC) would be performed in order to evaluate the complexation of BetA with γ-CD. Cryo-TEM for lamellarity structure analyses would provide insight into the amount of bilayers present in prepared liposomes and further insight into drug loss after the extrusion process.

Futher cell viability studies to evaluate the effects of the liposomal formulations in non-malignant human or murine neuronal cell line are recommended. Further investigation of estimated IC_{50} concentration values and determining the selectivity index for free BetA and liposomal BetA is also recommended. The integrity of the blood-brain barrier can be evaluated *in vitro* before and after treatment of liposomal formulations using transendothelial electrical resistance (TEER). An apoptosis study to evaluate the cytochrome C release could validate whether apoptosis is occurring via the intrinsic pathway as reported in literature (Fulda and Debatin, 2000, Fulda *et al*, 2010).

Chlorotoxin (CTX) is a 36-amino acid peptide found in the venom of the deathstalker scorpion (*Leiurus quinquestriatus*) which blocks small-conductance chloride channels (DeBin and Strichartz, 1991) and has emerged as a promising targeting agent due to its ability to specifically recognize over expressed tumour receptors in a broad spectrum of cancers including tumours of neuroectodermal origin such as human NB and some glioblastoma cell lines (Kievit *et al*., 2010). Future studies for improving the liposomal BetA would investigate the development of a targeted drug delivery BetAL system using CTX.

Animal model of NB are recommended to investigate the *in vivo* effects of liposomes, in terms of drug release, clearance and biodistribution to ascertain whether there is a correlation with *in vitro* findings.

APPENDIXES: SUPPLEMENTARY DATA

7.1 Liposome Results

Table 7.1 Average size (diameter) distribution, PI and ζ-potential analyses of liposomal formulations (n = 3 ± SD) from Malvern Instruments' Zetasiser Nano Zs

	EL	Batch 1	Batch 2	Un-extruded γ-CD-BetA L
Average size before extrusion	4194 nm ± 2260	2387 nm ± 249.2	1742 nm ± 959.9	1367 nm ± 190.5
Average size after extrusion	149.30 nm ± 37.82	159.0 nm ± 26.85	179.0 nm ± 16.37	116.70 nm ± 1.650
PI before extrusion	0.86 ± 0.2361	1.00 ± 0.0	0.94 ± 0.11	0.49 ± 0.07
PI after extrusion	0.17 ± 0.03	0.22 ± 0.07	0.23 ± 0.03	0.24 ± 0.01
ζ-potential before extrusion	-1.21 mV ± 1.28 mV	-2.25 mV ± 0.16 mV	-2.52 mV ± 0.32 mV	-2.02 mV ± 0.36 mV
ζ-potential after extrusion	1.06 mV ± 0.09 mV	-1.24 mV ± 0.07 mV	-1.29 mV ± 0.03 mV	-1.48 mV ± 0.06 mV

7.2 UHPLC Chromatographs

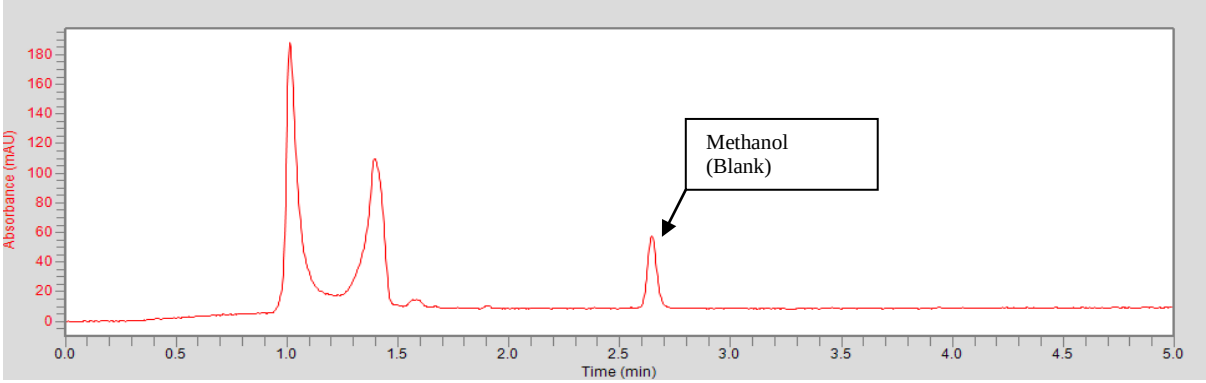

Figure 7.2.1 UHPLC chromatogram of methanol (blank) detected at wavelength of 205 nm. *Retention time was 2.6 minutes and separation was achieved at 35 °C using the following chromatographic conditions: C-18 (4.5 mm x 150.5 µm) column (Phenomenex Kinetex, USA), mobile phase of acetonitrile: methanol (80:20 v/v), an injection volume of 10 ul and 0.5 ml/min flow rate.*

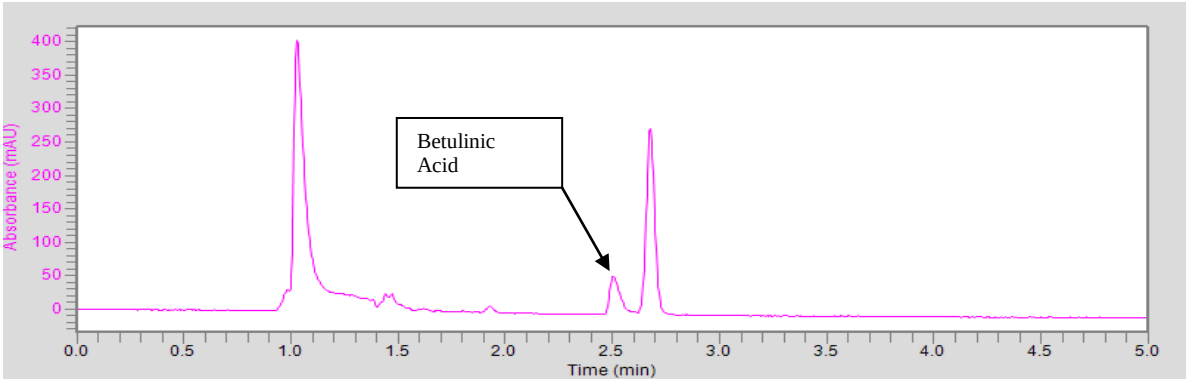

Figure 7.2.2 UHPLC chromatogram of Betulinic acid standard (0.0625 mg/ml) detected at wavelength of 205 nm. *Retention time was 2.5 minutes and separation was achieved at 35 °C using the following chromatographic conditions: C-18 (4.5 mm x 150.5µm) column (Phenomenex Kinetex, USA), mobile phase of acetonitrile: methanol (80:20 v/v), an injection volume of 10 ul and 0.5 ml/min flow rate.*

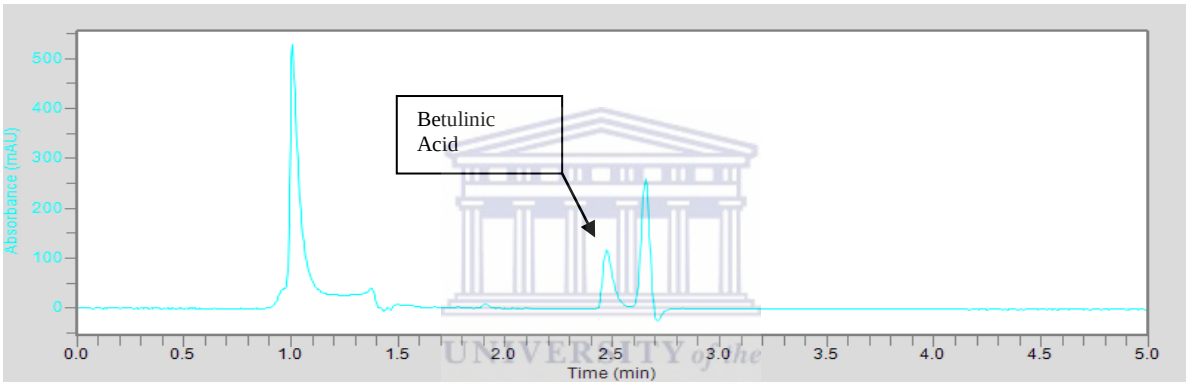

Figure 7.2.3 UHPLC chromatogram of Betulinic acid standard (0.125 mg/ml) detected at wavelength of 205 nm. *Retention time was 2.5 minutes and separation was achieved at 35 °C using the following chromatographic conditions: C-18 (4.5 mm x 150.5 µm) column (Phenomenex Kinetex, USA), mobile phase of acetonitrile: methanol (80:20 v/v), an injection volume of 10 ul and 0.5 ml/min flow rate*

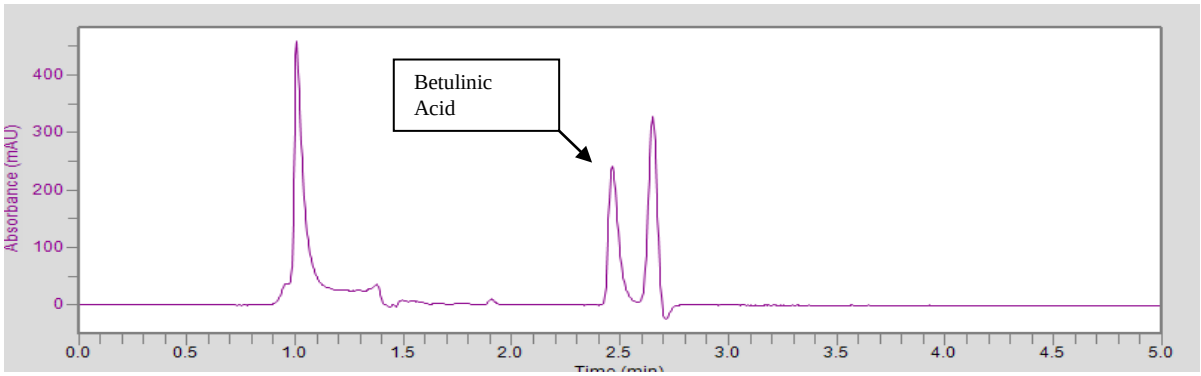

Figure 7.2.4 UHPLC chromatogram of Betulinic acid standard (0.250 mg/ml) detected at wavelength of 205 nm. *Retention time was 2.5 minutes and separation was achieved at 35 °C using the following chromatographic conditions: C-18 (4.5 mm x 150.5µm) column (Phenomenex Kinetex. USA), mobile phase of acetonitrile: methanol (80:20 v/v), an injection volume of 10 ul and 0.5 ml/min flow rate.*

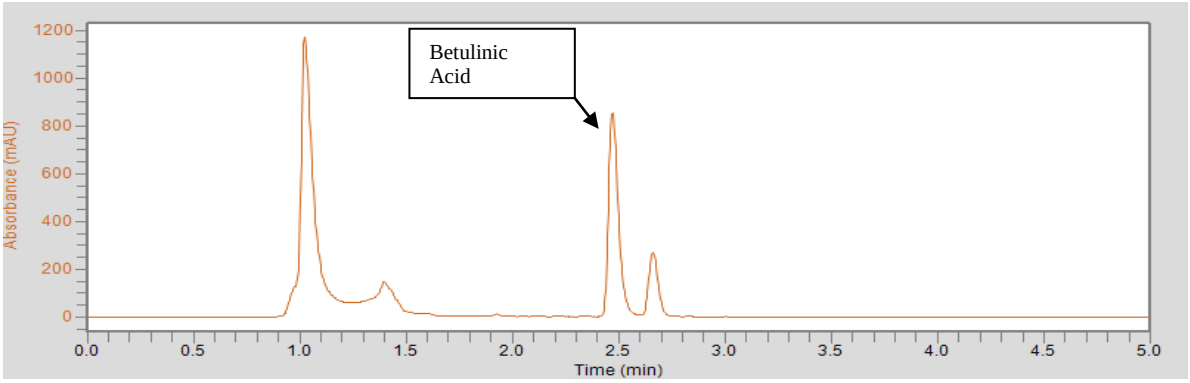

Figure 7.2.5 UHPLC chromatogram of Betulinic acid standard (1 mg/ml) detected at wavelength of 205 nm. *Retention time was 2.5 minutes and separation was achieved at 35 °C using the following chromatographic conditions: C-18 (4.5 mm x 150.5µm) column (Phenomenex Kinetex, USA), mobile phase of acetonitrile: methanol (80:20 v/v), an injection volume of 10 ul and 0.5 ml/min flow rate.*

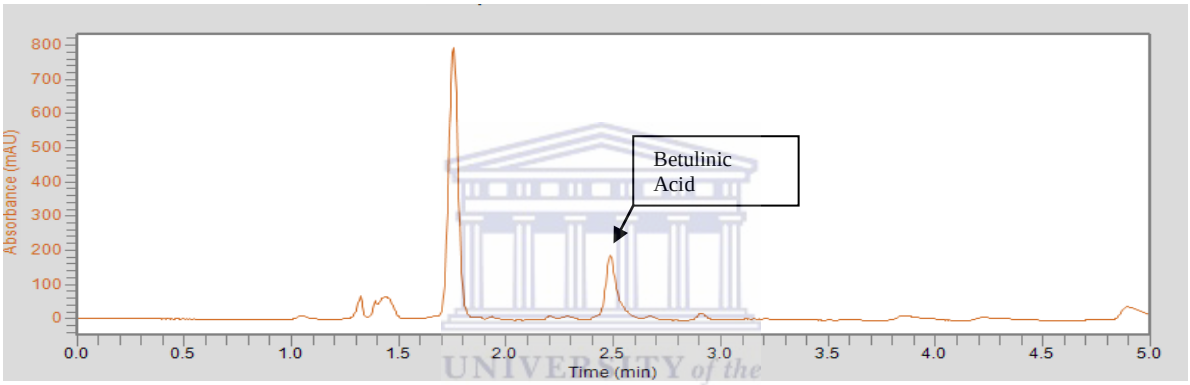

Figure 7.2.6 UHPLC chromatogram of BetAL detected at wavelength of 205 nm. *Retention time was 2.5 minutes and separation was achieved at 35 °C using the following chromatographic conditions: C-18 (4.5 mm x 150.5µm) column (Phenomenex Kinetex, USA), mobile phase of acetonitrile: methanol (80:20 v/v), an injection volume of 10 ul and 0.5 ml/min flow rate.*

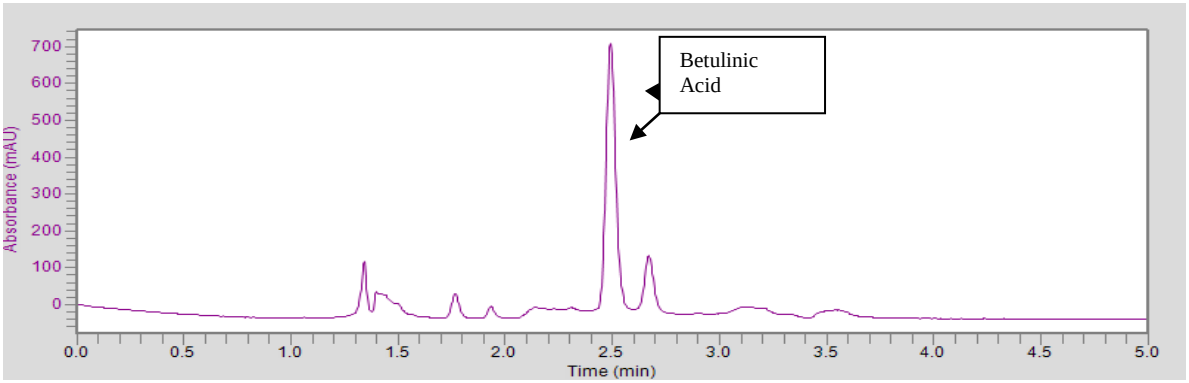

Figure 7.2.7 UHPLC chromatogram of γ-CD-BetAL detected at wavelength of 205 nm. *Retention time was 2.5 minutes and separation was achieved at 35 °C using the following chromatographic conditions: C-18 (4.5 mm x 150.5µm) column (Phenomenex Kinetex, USA), mobile phase of acetonitrile: methanol (80:20 v/v), an injection volume of 10 ul and 0.5 ml/min flow rate.*

7.3 DMSO Tolerance Test of SK-N-BE(2) and KELLY NB Cells

Table 7.3.1 Percentage cell viability of SK-N-BE(2) NB cells exposed to 0.1-2% DMSO concentrations at the selected time intervals (24-72 hours) compared to control (untreated cells, represented as 100% cell viability).

Cell viability of DMSO tolerance test for SK-N-BE(2) NB cells (n = 6)					
Hours	**Control (Untreated)**	**0.1% DMSO**	**0.4% DMSO**	**1% DMSO**	**2% DMSO**
24	100%	122%	118%	97%	66%
48	100%	117%	116%	91%	56%
72	100%	123%	121%	117%	53%

Table 7.3.2 P values (* P < 0.05) for SK-N-BE(2) NB cells exposed to 0.1-2% DMSO compared to control (untreated cells) at the selected time intervals (24-72 hours).

P values (* P < 0.05) of DMSO tolerance test for SK-N-BE(2) NB cells (n = 6)				
Hours	**0.1% DMSO**	**0.4% DMSO**	**1% DMSO**	**2% DMSO**
24	P = 0.1211	P = 0.1695	P = 0.6789	P = 0.0008
48	P = 0.0947	P = 0.0921	P = 0.2724	P < 0.0001
72	P = 0.2164	P = 0.5159	P = 0.2164	P < 0.0001

Table 7.3.3 P values (* P < 0.05) for SK-N-BE(2) NB cells exposed to 0.1-2% DMSO compared between the selected time intervals (24-72 hours).

P values (* P < 0.05) of DMSO tolerance test for SK-N-BE(2) NB cells (n = 6)				
Comparison between hours	**0.1% DMSO**	**0.4% DMSO**	**1% DMSO**	**2% DMSO**
24 & 48	P = 0.7996	P = 0.8680	P = 0.554	P = 0.8805
48 & 72	P = 0.7780	P = 0.7408	P = 0.1172	P = 0.0957
24 & 72	P = 0.9329	P = 0.8827	P = 0.3917	P = 0.0594

Table 7.3.4 Percentage cell viability of KELLY NB cells exposed to 0.1-2% DMSO concentrations at the selected time intervals (24-72 hours) compared to control (untreated cells represented as 100% cell viability).

Cell viability of DMSO tolerance test for KELLY NB cells (n = 6)					
Hours	**Control**	**0.1% DMSO**	**0.4% DMSO**	**1% DMSO**	**2% DMSO**
24	100%	100%	99%	92%	71%
48	100%	95%	99%	91%	75%
72	100%	106%	111%	111%	77%

Table 7.3.5 P values (* P < 0.05) for KELLY NB cells exposed to 0.1-2% DMSO compared to control (untreated cells) at the selected time intervals (24-72 hours).

P values (* P < 0.05) of DMSO tolerance test for KELLY NB cells (n = 6)				
Hours	**0.1% DMSO**	**0.4% DMSO**	**1% DMSO**	**2% DMSO**
24	P = 0.9323	P = 0.9424	P = 0.2774	P < 0.0001
48	P = 0.2809	P = 0.9007	P = 0.3090	P = 0.0045
72	P = 0.5749	P = 0.3268	P = 0.6349	P = 0.0006

Table 7.3.6 P values (* P < 0.05) for KELLY NB cells exposed to 0.1-2% DMSO compared between the selected time intervals (24-72 hours).

P values (* P < 0.05) of DMSO tolerance test for KELLY NB cells (n = 6)				
Comparison between hours	**0.1% DMSO**	**0.4% DMSO**	**1% DMSO**	**2% DMSO**
24 & 48	P = 0.5367	P = 0.9848	P = 0.9367	P = 0.6362
48 & 72	P = 0.6372	P = 0.7024	P = 0.5744	P = 0.2002
24 & 72	P = 0.7689	P = 0.7413	P = 0.5875	P = 0.2568

7.4 Free BetA Exposure to SK-N-BE(2) and KELLY NB Cells

Table 7.4.1 Percentage cell viability of SK-N-BE(2) NB cells exposed to 5-20 µg/ml free BetA concentrations at the selected time intervals (24-72 hours) compared to control (untreated cells, represented as 100% cell viability

Cell viability of SK-N-BE(2) NB cells exposed to free BetA (5-20 µg/ml) for 24-72 hours (n = 6)					
Hours	**Control**	**5 µg/ml BetA**	**10 µg/ml BetA**	**15 µg/ml BetA**	**20 µg/ml BetA**
24	100%	80%	68%	33%	31%
48	100%	83%	53%	40%	42%
72	100%	59%	12%	7%	15%

Table 7.4.2 P values (* P < 0.05) for SK-N-BE(2) NB cells exposed to 5-20 µg/ml free BetA compared to control (untreated cells) at the selected time intervals (24-72 hours).

P values (* P < 0.05) for SK-N-BE(2) NB cells exposed to free BetA (5-20 µg/ml) (n = 6)				
Hours	**5 µg/ml BetA**	**10 µg/ml BetA**	**15 µg/ml BetA**	**20 µg/ml BetA**
24	P < 0.0001	P < 0.0001	P < 0.0001	P < 0.0001
48	P < 0.0001	P < 0.0001	P < 0.0001	P < 0.0001
72	P < 0.0010	P < 0.0001	P < 0.0001	P < 0.0001

Table 7.4.3 P values (* P < 0.05) for SK-N-BE(2) NB cells exposed to 5-20 µg/ml free BetA compared between the selected time intervals (24-72 hours).

P values (* P < 0.05) for SK-N-BE(2) NB cells exposed to free BetA (5-20 µg/ml) (n = 6)				
Hours	**5 µg/ml BetA**	**10 µg/ml BetA**	**15 µg/ml BetA**	**20 µg/ml BetA**
24 & 48	P = 0.1484	P = 0.0051	P = 0.1767	P = 0.0305
48 & 72	P = 0.5122	P < 0.0001	P < 0.0001	P = 0.0003
24 & 72	P = 0.0841	P < 0.0001	P < 0.0001	P < 0.0001

Table 7.4.4 Percentage cell viability of KELLY NB cells exposed to 5-20 µg/ml free BetA concentrations at the selected time intervals (24-72 hours) compared to control (untreated cells, represented as 100% cell viability).

Cell viability of KELLY NB cells exposed to free BetA (5-20 µg/ml) for 24-72 hours (n = 6)					
Hours	**Control**	**5 µg/ml BetA**	**10 µg/ml BetA**	**15 µg/ml BetA**	**20 µg/ml BetA**
24	100%	95%	92%	75%	66%
48	100%	69%	50%	50%	45%
72	100%	17%	14%	17%	22%

Table 7.4.5 P values (* $P < 0.05$) for KELLY NB cells exposed to 5-20 µg/ml free BetA compared to control (untreated cells) at the selected time intervals (24-72 hours).

P values (* P < 0.05) for KELLY NB cells exposed to free BetA (5-20 µg/ml) (n = 6)				
Hours	**5 µg/ml BetA**	**10 µg/ml BetA**	**15 µg/ml BetA**	**20 µg/ml BetA**
24	P = 0.0031	P = 0.0362	P = 0.0011	P = 0.0003
48	P = 0.0294	P < 0.0001	P < 0.0001	P < 0.0001
72	P < 0.0001	P < 0.0001	P < 0.0001	P < 0.0001

Table 7.4.6 P values (* $P < 0.05$) for KELLY NB cells exposed to 5-20 µg/ml free BetA compared between the selected time intervals (24-72 hours).

P values (* P < 0.05) for KELLY NB cells exposed to free BetA (5-20 µg/ml) (n = 6)				
Hours	**5 µg/ml BetA**	**10 µg/ml BetA**	**15 µg/ml BetA**	**20 µg/ml BetA**
24 & 48	P = 0.0009	P < 0.0001	P = 0.0267	P < 0.0001
48 & 72	P < 0.0001	P < 0.0001	P < 0.0001	P = 0.0002
24 & 72	P < 0.0001	P < 0.0001	P < 0.0001	P < 0.0001

7.5 BetAL Exposure to SK-N-BE(2) and KELLY NB Cells

Table 7.5.1 Percentage cell viability of SK-N-BE(2) NB cells exposed to EL and 5-50 µg/ml BetAL at the selected time intervals (24-72 hours) compared to control (untreated cells, represented as 100% cell viability).

Cell viability of SK-N- BE (2) NB cells exposed to BetAL (5-50 µg/ml) for 24-72 hours (n = 6)							
Hours	**Control**	**EL**	**5 µg/ml BetAL**	**10 µg/ml BetAL**	**15 µg/ml BetAL**	**20 µg/ml BetAL**	**50 µg/ml BetAL**
24	100%	99%	92%	81%	79%	68%	55%
48	100%	110%	93%	77%	62%	54%	47%
72	100%	102%	76%	51%	50%	36%	31%

Table 7.5.2 P values (* P < 0.05) for SK-N-BE(2) NB cells exposed to EL and 5-50 µg/ml BetAL compared to control (untreated) cells at the selected time intervals (24-72 hours).

P values (* P < 0.05) for SK-N-BE(2) NB cells exposed to BetAL (5-50 µg/ml) (n = 6)						
Hours	**EL**	**5 µg/ml BetAL**	**10 µg/ml BetAL**	**15 µg/ml BetAL**	**20 µg/ml BetAL**	**50 µg/ml BetAL**
24	P = 0.5062	P < 0.0001	P < 0.0001	P = 0.0090	P = 0.0002	P < 0.0001
48	P = 0.1062	P = 0.0124	P = 0.0306	P = 0.0114	P < 0.0001	P < 0.0001
72	P = 0.1836	P < 0.0001	P = 0.0002	P < 0.0001	P < 0.0001	P < 0.0001

Table 7.5.3 P values (* P < 0.05) for SK-N-BE(2) NB cells exposed to EL and 5-50 µg/ml BetAL compared between the selected time intervals (24-72 hours).

P values (* P < 0.05) for SK-N-BE(2) NB cells exposed to BetAL (5-50 µg/ml) (n = 6)						
Hours	**EL**	**5 µg/ml**	**10 µg/ml**	**15 µg/ml**	**20 µg/ml**	**50 µg/ml**
24 & 48	P = 0.1065	P = 0.8898	P = 0.6420	P = 0.2380	P = 0.0203	P = 0.0006
48 & 72	P = 0.0522	P = 0.3170	P = 072200	P = 0.3980	P = 0.0002	P = 0.7030
24 & 72	P = 0.2002	P = 0.0022	P = 0.0073	P = 0.0053	P = 0.0001	P = 0.0120

Table 7.5.4 Percentage cell viability of KELLY NB cells exposed to EL and 5-50 µg/ml BetAL at the selected time intervals (24-72 hours) compared to control (untreated cells, represented as 100% cell viability).

Cell viability of KELLY NB cells exposed to BetAL (5-50 µg/ml) for 24-72 hours (n = 6)							
Hours	**Control**	**EL**	**5 µg/ml BetAL**	**10 µg/ml BetAL**	**15 µg/ml BetAL**	**20 µg/ml BetAL**	**50 µg/ml BetAL**
24	100%	105%	83%	86%	80%	75%	61%
48	100%	98%	74%	60%	56%	52%	57%
72	100%	98%	65%	57%	41%	42%	47%

Table 7.5.5 P values (* P < 0.05) for KELLY NB cells exposed to 5-50 µg/ml BetAL compared to control (untreated) cells at the selected time intervals (24-72 hours).

P values (* P < 0.05) for KELLY NB cells exposed to BetAL (5-50 µg/ml) (n = 6)						
Hours	**EL**	**5 µg/ml BetAL**	**10 µg/ml BetAL**	**15 µg/ml BetAL**	**20 µg/ml BetAL**	**50 µg/ml BetAL**
24	P = 0.1604	P < 0.0001	P = 0.0125	P = 0.0001	P < 0.0001	P < 0.0001
48	P = 0.5818	P = 0.0003	P < 0.0001	P < 0.0001	P < 0.0001	P < 0.0001
72	P = 0.05613	P < 0.0001	P < 0.0001	P < 0.0001	P < 0.0001	P < 0.0001

Table 7.5.6 P values (* P < 0.05) for KELLY NB cells exposed to 5-50 µg/ml BetAL compared between the selected time intervals (24-72 hours).

P values (* P < 0.05) for KELLY NB cells exposed to BetAL (5-50 µg/ml) (n = 6)						
Hours	**EL**	**5 µg/ml**	**10 µg/ml**	**15 µg/ml**	**20 µg/ml**	**50 µg/ml**
24 & 48	P = 0.1604	P = 0.1731	P = 0.4342	P < 0.0001	P < 0.0001	P = 0.1661
48 & 72	P = 0.9656	P = 0.1357	P = 0.4593	P < 0.0001	P = 0.1667	P = 0.0002
24 & 72	P = 0.1547	P = 0.0759	P = 0.0017	P < 0.0001	P = 0.0007	P = 0.0002

7.6 Free γ-CD Exposure to SK-N-BE(2) and KELLY NB Cells

Table 7.6.1 Percentage cell viability of SK-N-BE(2) NB cells exposed to 5-50 µg/ml free γ-CD at the selected time intervals (24-72 hours) compared to control (untreated cells, represented as 100% cell viability). Values are rounded off to two decimal places.

Cell viability of SK-N- BE (2) NB cells exposed to free γ-CD (5-50 µg/ml) for 24-72 hours (n = 6)						
Hours	**Control**	**5 µg/ml γ-CD**	**10 µg/ml γ-CD**	**15 µg/ml γ-CD**	**20 µg/ml γ-CD**	**50 µg/ml γ-CD**
24	100%	100%	100%	98%	96%	97%
48	100%	101%	105%	99%	85%	87%
72	100%	111%	116%	121%	48%	40%

Table 7.6.2 P values (* P < 0.05) for SK-N-BE NB (2) cells exposed to 5-50 µg/ml free γ-CD compared to control (untreated) cells at the selected time intervals (24-72 hours).

P values (* P < 0.05) for SK-N-BE(2) NB cells exposed to free γ-CD (5-50 µg/ml) (n = 6)					
Hours	**5 µg/ml γ-CD**	**10 µg/ml γ-CD**	**15 µg/ml γ-CD**	**20 µg/ml γ-CD**	**50 µg/ml γ-CD**
24	P = 0.9534	P = 0.8704	P = 0.7225	P = 0.4125	P = 0.1148
48	P = 0.5794	P = 0.0821	P = 0.7945	P = 0.0006	P = 0.0002
72	P = 0.2820	P = 0.0773	P = 0.0353	P < 0.0001	P < 0.0001

Table 7.6.3 P values (* P < 0.05) for SK-N-BE(2) NB cells exposed to 5-50 µg/ml free γ-CD compared between the selected time intervals (24-72 hours).

P values (* P < 0.05) for SK-N-BE(2) NB cells exposed to free γ-CD (5-50 µg/ml) (n = 6)					
Hours	**5 µg/ml γ-CD**	**10 µg/ml γ-CD**	**15 µg/ml γ-CD**	**20 µg/ml γ-CD**	**50 µg/ml γ-CD**
24 & 48	P = 0.7564	P = 0.3727	P = 0.8914	P = 0.5763	P = 0.8498
48 & 72	P = 0.6380	P = 0.2639	P = 0.0379	P < 0.0001	P < 0.0001
24 & 72	P = 0.4901	P = 0.1311	P = 0.0400	P < 0.0001	P < 0.0001

Table 7.6.4 Percentage cell viability of KELLY NB cells exposed to 5-50 µg/ml free γ-CD at the selected time intervals (24-72 hours) compared to control (untreated cells, represented as 100% cell viability). Values are rounded off to two decimal places.

Cell viability of KELLY NB cells exposed to free γ-CD (5-50 µg/ml) for 24-72 hours (n = 6)						
Hours	**Control**	**5 µg/ml γ-CD**	**10 µg/ml γ-CD**	**15 µg/ml γ-CD**	**20 µg/ml γ-CD**	**50 µg/ml γ-CD**
24	100%	105%	104%	105%	99%	94%
48	100%	104%	105%	99%	95%	86%
72	100%	107%	102%	104%	95%	92%

Table 7.6.5 P values (* P < 0.05) for KELLY NB cells exposed to 5-50 µg/ml free γ-CD compared to control (untreated) cells at the selected time intervals (24-72 hours).

P values (* P < 0.05) for KELLY NB cells exposed to free γ-CD (5-50 µg/ml) (n = 6)					
Hours	**5 µg/ml γ-CD**	**10 µg/ml γ-CD**	**15 µg/ml γ-CD**	**20 µg/ml γ-CD**	**50 µg/ml γ-CD**
24	P = 0.2855	P = 0,2753	P = 0,2673	P = 0,5908	P = 0,0112
48	P = 0.2327	P = 0,7913	P = 0,7913	P = 0,01169	P = 0.0001
72	P = 0.2585	P = 0,3319	P = 0,1161	P = 0,00932	P = 0.0153

Table 7.6.6 P values (* P < 0.05) for KELLY NB cells exposed to 5-50 µg/ml free γ-CD compared between the selected time intervals (24-72 hours).

P values (* P < 0.05) for KELLY NB cells exposed to free γ-CD (5-50 µg/ml) (n = 6)					
Hours	**5 µg/ml γ-CD**	**10 µg/ml γ-CD**	**15 µg/ml γ-CD**	**20 µg/ml γ-CD**	**50 µg/ml γ-CD**
24 & 48	P = 0.8577	P = 0.8502	P = 0.9604	P = 0.1785	P = 0.0224
48 & 72	P = 0.5826	P = 0.3791	P = 0.9999	P = 0.9935	P = 0.1300
24 & 72	P = 0.7018	P = 0.6589	P = 0.9469	P = 0.2748	P = 0.5472

7.7 γ-CD-BetAL Exposure to SK-N-BE(2) and KELLY NB Cells

Table 7.7.1 Percentage cell viability of SK-N-BE(2) NB cells exposed to 5-50 µg/ml γ-CD-BetAL at the selected time intervals (24-72 hours) compared to control (untreated cells, represented as 100% cell viability).

Cell viability of SK-N- BE (2) NB cells exposed to γ-CD-BetAL (5-50 µg/ml) for 24-72 hours (n = 6)						
Hours	**Control**	**5 µg/ml γ-CD-BetA L**	**10 µg/ml γ-CD-BetA L**	**15 µg/ml γ-CD-BetA L**	**20 µg/ml γ-CD-BetA L**	**50 µg/ml γ-CD-BetA L**
24	100%	94%	85%	77%	64%	49%
48	100%	87%	75%	57%	-	-
72	100%	65%	50%	-	-	-

Table 7.7.2 P values (* P < 0.05) for SK-N-BE(2) NB cells exposed to 5-50 µg/ml γ-CD-BetAL compared to control (untreated) cells at the selected time intervals (24-72 hours).

P values (* P < 0.05) for SK-N-BE(2) NB cells exposed to γ-CD-BetAL (5-5 µg/ml) (n = 6)					
Hours	**5 µg/ml γ-CD-BetA L**	**10 µg/ml γ-CD-BetA L**	**15 µg/ml γ-CD-BetA L**	**20 µg/ml γ-CD-BetA L**	**50 µg/ml γ-CD-BetA L**
24	P = 0.0406	P < 0.0001	P < 0.0001	P = 0.0010	P = 0.0003
48	P = 0.0010	P = 0.0001	P < 0.0001	-	-
72	P = 0.0117	P < 0.0001	-	-	-

Table 7.7.3 P values (* P < 0.05) for SK-N-BE(2) NB cells exposed to 5-5 µg/ml γ-CD-BetAL compared between the selected time intervals (24-72 hours).

P values (* P < 0.05) for SK-N-BE(2) NB cells exposed to γ-CD-BetAL (5-50 µg/ml) (n = 6)					
Hours	**5 µg/ml γ-CD-BetA L**	**10 µg/ml γ-CD-BetA L**	**15 µg/ml γ-CD-BetA L**	**20 µg/ml γ-CD-BetA L**	**50 µg/ml γ-CD-BetA L**
24 & 48	P = 0.1288	P = 0.0018	P = 0.0025	P = 0.0757	P = 0.3669
48 & 72	P = 0.1598	P = 0.0309	P = 0.0436	-	-
24 & 72	P = 0.0314	P = 0.0002	-	-	-

Table 7.7.4 Percentage cell viability of KELLY NB cells exposed to 5-50 µg/ml γ-CD-BetAL at the selected time intervals (24-72 hours) compared to control (untreated cells, represented as 100% cell viability).

Cell viability of KELLY NB cells exposed to γ-CD-BetAL (5-50 µg/ml) for 24-72 hours (n = 6)					
Hours	**Control**	**5 µg/ml γ-CD-BetA L**	**10 µg/ml γ-CD-BetA L**	**15 µg/ml γ-CD-BetA L**	**20 µg/ml γ-CD-BetA L**
24	100%	87%	79%	73%	63%
48	100%	73%	66%	59%	-
72	100%	68%	62%	59%	-

Table 7.7.5 P values (* P < 0.05) for KELLY NB cells exposed to 5-50 µg/ml γ-CD-BetAL compared to control (untreated) cells at the selected time intervals (24-72 hours).

P values (* P < 0.05) for KELLY NB cells exposed to γ-CD-BetAL (5-50 µg/ml) (n = 6)				
Hours	**5 µg/ml γ-CD-BetA L**	**10 µg/ml γ-CD-BetA L**	**15 µg/ml γ-CD-BetA L**	**20 µg/ml γ-CD-BetA L**
24	P = 0.0038	P < 0.0001	P = 0.0017	P < 0.0001
48	P < 0.0001	P < 0.0001	P < 0.0001	-
72	P < 0.0001	P = 0.0001	P = 0.0002	-

Table 7.7.6 P values (* P < 0.05) for KELLY NB cells exposed to 5-50 µg/ml γ-CD-BetAL compared between the selected time intervals (24-72 hours).

P values (* P < 0.05) for KELLY NB cells exposed to γ-CD-BetAL (5-50 µg/ml) (n = 6)				
Hours	**5 µg/ml γ CD-BetAL**	**10 µg/ml γ CD-BetAL**	**15 µg/ml γ CD-BetAL**	**20 µg/ml γ CD-BetAL**
24 & 48	P = 0.0089	P = 0.0024	P = 0.2755	P = 0.1952
48 & 72	P = 0.2924	P = 0.7707	P = 0.0590	-
24 & 72	P = 0.0030	P = 0.0351	P = 0.0308	-

7.8 Comparison of Selected Concentrations of Free BetA, BetAL and γ-CD-BetAL at Specific Time Points in SK-N-BE(2) and KELLY NB Cell Lines

Table 7.8.1 P values (* P < 0.05) for SK-N-BE(2) NB cells exposed to 5-20 µg/ml free BetA compared to 5-20 µg/ml free BetAL at the selected time intervals (24-72 hours).

P values (* P < 0.05) for the comparison of free BetA with BetAL in SK-N-BE(2) NB (n = 6)				
Hours	**5 µg/ml γ-CD**	**10 µg/ml γ-CD**	**15 µg/ml γ-CD**	**20 µg/ml γ-CD**
24	P = 0.0133	P = 0.006	P = 0.0001	P < 0.0001
48	P = 0.3457	P = 0.038	P = 0.1372	P = 0.0543
72	P = 0.0075	P = 0.001	P < 0.0010	P < 0.0001

Table 7.8.2 P values (* P < 0.05) for SK-N-BE(2) NB cells exposed to 5-20 µg/ml free BetA compared to 5-20 µg/ml free γ-CD-BetAL at the selected time intervals (24-72 hours).

P values (* P < 0.05) for the comparison of free BetA with γ-CD-BetAL in SK-N-BE(2) NB (n = 6)				
Hours	**5 µg/ml γ-CD**	**10 µg/ml γ-CD**	**15 µg/ml γ-CD**	**20 µg/ml γ-CD**
24	P = 0.0061	P = 0.0008	P < 0.0001	P = 0.0016
48	P = 0.4815	P = 0.0180	P = 0.0302	-
72	P = 0.0471	P < 0.0001	-	-

Table 7.8.3 P values (* P < 0.05) for SK-N-BE(2) NB cells exposed to 5-20 µg/ml BetAL compared to 5-20 µg/ml free γ-CD-BetAL at the selected time intervals (24-72 hours).

P values (* P < 0.05) for the comparison of BetAL with γ-CD-BetAL in SK-N-BE(2) NB (n = 6)				
Hours	**5 µg/ml γ-CD**	**10 µg/ml γ-CD**	**15 µg/ml γ-CD**	**20 µg/ml γ-CD**
24	P = 0.6550	P = 0.1354	P = 0.7824	P = 0.0792
48	P < 0.0001	P = 0.4630	P = 0.7131	-
72	P = 0.3894	P < 0.0001	-	-

Table 7.8.4 P values (* P < 0.05) for KELLY NB cells exposed to 5-20 µg/ml free BetA compared to 5-20 µg/ml free BetAL at the selected time intervals (24-72 hours).

P values (* P < 0.05) for the comparison of free BetA with BetAL in KELLY NB (n = 6)				
Hours	**5 µg/ml γ-CD**	**10 µg/ml γ-CD**	**15 µg/ml γ-CD**	**20 µg/ml γ-CD**
24	P < 0.0001	P = 0.0030	P = 0.0002	P < 0.0001
48	P = 0.0042	P = 0.0185	P < 0.0001	P < 0.0001
72	P = 0.0003	P < 0.0001	P < 0.0001	P = 0.0239

Table 7.8.5 P values (* P < 0.05) for KELLY NB cells exposed to 5-20 µg/ml free BetA compared to 5-20 µg/ml free γ-CD-BetAL at the selected time intervals (24-72 hours).

P values (* P < 0.05) for the comparison of free BetA with γ-CD-BetAL in KELLY NB (n = 6)				
Hours	**5 µg/ml γ-CD**	**10 µg/ml γ-CD**	**15 µg/ml γ-CD**	**20 µg/ml γ-CD**
24	P = 0.0003	P < 0.0001	P = 1.0000	P < 0.0001
48	P = 0.0001	P = 0.0365	P = 0.0001	-
72	P < 0.0001	P < 0.0001	P = 0.0005	-

Table 7.8.6 P values (* P < 0.05) for KELLY NB cells exposed to 5-20 µg/ml BetAL compared to 5-20 µg/ml free γ-CD-BetAL at the selected time intervals (24-72 hours).

P values (* P < 0.05) for the comparison of BetAL with γ-CD-BetAL in KELLY NB (n = 6)				
Hours	**5 µg/ml γ-CD**	**10 µg/ml γ-CD**	**15 µg/ml γ-CD**	**20 µg/ml γ-CD**
24	P = 0.5015	P = 0.2115	P = 0.2901	P = 0.0007
48	P = 0.0843	P = 0.6840	P = 0.0063	-
72	P = 0.7835	P = 0.5769	P = 0.1751	-

References

1) Abbott, N.J., Rönnbäck, L and Hansson, E. (2006) 'Astrocyte-endothelial interactions at the blood-brain barrier'. *Nature Reviews Neuroscience*, 7(1), 41-53.
2) Abu-Dahab, R., Odeh, F., Ismail, S.I., Azzam, H and Al Bawab, A. (2013) 'Preparation, characterization and antiproliferative activity of thymoquinone-beta-cyclodextrin self assembling nanoparticles'. *Die Pharmazie*, 68(12), 939–944.
3) Achim, M., Precup C, Gonganaunitu, D., Barbu-Tudoran, L., Porfire, A.S., Scurtu, R and Ciuce, C. (2009) 'Thermosensitive liposomes containing doxorubicin. Preparation and in vitro evaluation'. *Farmacia*, 57 (6), 703-710.
4) Acosta, S., Lavarino, C., Paris, R., Garcia, I., Torres, C., Rodriguez, E., Beleta, H and Mora, J. (2009) 'Comprehensive characterization of neuroblastoma cell line subtypes reveals bilineage potential similar to neural crest stem'. *BMC Developmental Biology*, 9(12), 1-14.
5) Adams, M.L., Lavasanifar, A and Kwon, G.S. (2003) 'Amphiphilic block copolymers for drug delivery'. *Journal of Pharmaceutical Sciences*, 92(7), 1343-1355.
6) Ait-Oudhia, S., Mager, D. E and Straubinger, R. M. (2014) 'Application of pharmacokinetic and pharmacodynamic analysis to the development of liposomal formulations for oncology'. *Pharmaceutics*, 6(1), 137–174.
7) Akbarzadeh, A., Rezzaei-Sadabady, R., Davaran, S., Joo, S.W., Zarghami, N., Hanifehpour, Y., Samiei, M., Kouhi, M and Nejati-Koshki, K. (2013) 'Liposome: classification, preparation ad applications'. *Nanoscale Research Letters*, 8(1), 1-9.
8) Al-Zubaidi, I.A., Al-Rubaie, M.S and Abdullah, T.S. (2014) 'Multi lamellar vesicles (MLVs) liposomes preparation by thin film hydration technique'. *Journal of Engineering and Technology*, 32(3), 550-560.
9) Alakurtti, S., Mäkelä, T., Koskimies, S and Kauha-luoma, Y.J. (2006) 'Pharmacological properties of the ubiquitous natural product betulin'. *European Journal of Pharmaceutical Sciences: Official Journal of the European Federation for Pharmaceutical Sciences*, 29(1), 1-13.
10) Alexander-Bryant, A. A., Vanden Berg-Foels, W. S and Wen, X. (2013) 'Bioengineering strategies for designing targeted cancer therapies'. *Advances in Cancer Research*, 118, 1–59.

11) Alkilany, A.M and Murphy, M.C.J. (2010) 'Toxicity and cellular uptake of gold nanoparticles: what we have learned so far?' *Journal of Nanoparticle Research: An Interdisciplinary Forum for Nanoscale Science and Technology*, 12(7), 2313–233.

12) Allen, T.M and Cullis. (2013) 'Advanced Liposomal drug delivery systems: From concept to clinical applications'. *Advanced Drug Delivery Reviews*, 65(1), 36–48.

13) Althoff, K., Beckers, A., Bell, E., Nortmeyer, M., Thor, T., Sprüssel, A., Linder, S., De Preter, K., Florin, A., Heukamp, L.C., Klein-Hitpass, L., Astrahantseff, K., Kumps, C., Speleman, F., Eggert, A., Westermann, F., Schramm, A and Schulte, J.H. (2015) 'A cre-conditional MYCN-driven neuroblastoma mouse model as an improved tool for pre-clinical studies'. *Oncogene*, 34(26), 3357-68.

14) Alvarado, C.S., London, W.B., Look, A.T., Brodeur, G.M., Altmiller, D.H., Thorner, P.S., Joshi, V.V., Rowe, S.T., Nash, M.B., Smith, E.I., Castleberry, R.P and Cohn, S.L. (2000) 'Natural history and biology of stage A neuroblastoma: A pediatric oncology group study'. *Journal of Pediatric Hematology/Oncology*, 22(3), 197–205.

15) Amstad, E., Kohlbrecher, J., Muller, E., Schweizer, T., Textor, M and Reimhult, E. (2011) 'Triggered release from liposomes through magnetic actuation of iron oxide nanoparticle containing membranes'. *Nano Letters*, 11(4), 1664-1670.

16) Anjana. M.N., Nair, S.C and Joseph, J. (2013) 'An updated review of cyclodextrins –an enabling technology for challenging pharmaceutical formulations'. *International Journal of Pharmacy and Pharmaceutical Sciences*, 5(3), 54-58.

17) Arun, R., Ashok, K and Sravanthi, V.V.N.S.S. (2008) 'Cyclodextrins as drug carrier molecule: A review'. *Scientia Pharmaceutica*, 76, 567-598.

18) Astraya, G., Gonzalez-Barreirob, C., Mejutoa, J.C., Rial-Oterob, R and Simal-Gándarab, J. (2009) 'A review on the use of cyclodextrins in foods'. *Food Hydrocolloids*, 23(7), 1631–1640.

19) Audouy, S.A.L., de Leij, L.F.H., Hoekstra, D and Mlema, G. (2002) 'In vivo characteristics of cationic liposomes as delivery vectors for gene therapy'. *Pharmaceutical Research*, 19(11), 1599-1605.

20) Avanti® Mini-Extruder. Available at: http://www.avantilipids.com/index.php?option=com_content&view=article&id=533&Itemid=297 [Accessed 17 March 2015].

21) Azevedo, F.A., Carvalho, L.R., Grinberg, L.T., Farfel, J.M., Ferretti, R.E., Leite, R.E., Jacob Filho, W., Lent, R and Herculano-Houzel, S. (2009) 'Equal numbers of neuronal

and non-neuronal cells make the human brain an isometrically scaled-up primate brain'. *The Journal of Comparative Neurology*, 513(5), 532-541.

22) Baban, D.F and Seymour, L.W. (1998) 'Control of tumour vascular permeability'. *Advanced Drug Delivery Reviews*, 34(1), 109-119.

23) Bachetti, T., Di Paola, D., Di Lascio, S., Mirisola, V., Brignole, C., Bellotti, M., Caffa, I., Ferraris, C., Fiore, M., Fornasari, D., Chiarle, R., Borghini, S., Pfeffer, U., Ponzoni, M., Ceccherini, I and Perri, P. (2010) 'PHOX2B-mediated regulation of ALK expression: in vitro identification of a functional relationship between two genes involved in neuroblastoma'. *PLOS one*, 5(10), 1-15.

24) Bagatell, R., London, W.B., Wagner, L.M., Voss, S.D., Stewart, C.F., Maris, J.M., Kretschmar, C and Cogh, S.L. (2011) 'Phase II study of irinotecan and temozolomide in children with relapsed or refractory neuroblastoma: a Children's Oncology Group study'. *Journal of Clinical Oncology: Official Journal of the American Society of Clinical Oncology*, 29(2), 208-213.

25) Baik, J., Kwon, H., Kim, K., Jeong, Y., Cho, Y and Lee, Y. (2012) 'Cordycepin induces apoptosis in human neuroblastoma SK-N-BE(2)-C and melanoma SK-MEL-2 cells'. *Indian Journal of Biochemistry and Biophysics*, 49 (2), 86-91.

26) Balda, M.S and Matter, K. (1998) 'Tight junctions'. *Journal of cell science*, 111(5), 541-547.

27) Banerjee, T., Mitra, Singh, A.K., Shrma, R.K and Maitra, A. (2002) 'Preparation, characterization and biodistributon of ultrafine chitosan nanoparticles'. *International Journal of Pharmaceutics*, 243(1-2), 93-105.

28) Bear, M.F., Connors, B.W and Paradiso, M.A. (2006) *Neuroscience: Exploring the Brain*. 3rd Edition. London: Williams and Wilkins.

29) Béduneau, A., Saulnier, P and Benoit, J.P. (2007) 'Active targeting of brain tumors using nanocarriers'. *Biomaterials*, 28(33), 4947–4967.

30) Begley, D.J and Brightman, M.W. (2003) 'Structural and functional aspects of the blood-brain barrier'. *Progress in Drug Research*, 61, 39-78.

31) Begum, M.Y., Abbulu, K and Sudhakar, M. (2012) 'Celecoxib-encapsulated liposomes of long alkyl chain lipids: Formulation, characterization and in vitro performance'. *Der Pharmacia Sinica*, 3(1), 117-125.

32) Beierle, E.A., Trujillo, A., Nagaram, A., Kurenova, E.V., Finch, R., Ma, X., Vella, J., Cance, W.G and Golubovskaya, V.M. (2007) 'N-MYC regulates focal adhesion kinase

expression in human neuroblastoma'. *The Journal of Biological Chemistry*, 282(17), 12503-12516.

33) Berger, N., Sachse, A., Bender, J., Schubert, R and Brandl, M. (2001) 'Filter extrusion of liposomes using different devices: comparison of liposome size, encapsulation efficiency, and process characteristics'. *International Journal of Pharmaceutics*, 223(1-2), 55-68.

34) Bhatia, A., Kumar, R and Katare, O.P. (2004) 'Tamoxifen in topical liposomes: development, characterization and in-vitro evaluation'. *Journal of Pharmacy and Pharmaceutics Sciences*: *A Publication of the Canadian Society for Pharmaceutical Sciences, Societe Canadienne des Sceiences Pharmaceutiques*, 7(2), 252-259.

35) Bhatt, S., Diaz, R and Trainor, P., A. (2013) 'Signals and Switches in Mammalian Neural Crest Cell Differentiation'. *Cold Spring Harbor Perspectives Biology*, 5(2), 1-20.

36) Bishayee, A., Ahmed, S., Brankov, N and Perloff, M. (2011) 'Triterpenoids as potential agents for the chemoprevention and therapy of breast cancer'. *Frontiers in Bioscience : A Journal and Virtual Library*, 16, 980–996.

37) Birch Bark Extract Powder (Betulin/Betulinic ACID 98%). Available at: http://plantextract8988.en.ec21.com/Birch_Bark_Extract_Powder_Betulin--5520266_5520364.html [Acessed 26 February 2015].

38) Blanford, W.J. (2014) 'Model of phase distribution of hydrophobic organic chemicals in cyclodextrin–water–air–solid sorbent systems as a function of salinity, temperature, and the presence of multiple CDs'. *Journal of inclusion Phenomena and Macrocyclic Chemistry*, 79(1), 57-64.

39) Blasi, P., Giovangioli, S., Schoubben, A., Ricci, M and Rossi, C. (2007) 'Solid lipid nanoparticles for targeted barin drug delivery'. *Advances in Drug Delivery Reviews*, 59(6), 454-477.

40) Borst, P., Evers, R., Kool, M and Wijnholds. (2000) 'A family of drug transporters: the multidrug resistance associated proteins'. *Journal of the National Cancer Institute*, 92(16), 1295–1302.

41) Bouillet, P., Metcalf, D., Huang, D.C., Tarlinton, D.M., Kay, T.W., Kontgen, F., Adams, J.M and Strasser, A. (1999) 'Proapoptotic Bcl-2 relative Bim required for certain apoptotic responses, leukocyte homeostasis, and to preclude autoimmunity'. *Science (New York, N.)*, 286(5445), 1735-1738.

42) Bragagni, M., Maestrelli, F., Mennini, N., Ghelardini, C and Mura, P. (2010) 'Liposomal formulations of prilocaine: effect of complexation with hydroxypropyl-β-cyclodextrin on drug anesthetic efficacy'. *Journal of Liposome Research*, 20(4), 315-322.

43) Brandl, M. (2001) 'Liposomes as drug carriers: A technological approach'. *Biotechnology Annual Reviews*, 7, 59-85.

44) Bratton, S.B., Walker, G., Srinivasula, S.M., Sun, X.M., Butterworth, M., Alnemri, E.S and Cohen, G.M. (2001) 'Recruitment, activation and retention of caspases-9 and -3 by Apaf-1 apoptosome and associated XIAP complexes'. *The EMBO Journal*, 20(5), 998–1009.

45) Bringmann, G., Saeb, W., Assi, L.A., Francios, G., Sankara Narayanan, A.S., Peters, K and Peters, E.M. (1997) 'Betulinic Acid: Isolation from Triphyophyllum peltatum and Ancistro- cladus heyneanus, Antimalarial Activity, and Crystal Structure of the Benzyl Ester'. *Planta Medica*, 63(3), 255-257.

46) Brodeur, G. M. (2003) 'Neuroblastoma: biological insights into a clinical enigma'. *Nature Reviews Cancer*, 3(3), 203–216.

47) Brodeur, G.M., Hogarty, M.D., Mosse, Y.P and Maris, J.M. (2011) *Neuroblastoma. In: Pizzo PA, Poplack DG (eds). Principles and Practice of Pediatric Oncology*. 6th Edition: Philadelphia: Lippincott Williams and Wilkins.

48) Brodeur, G.M., Seeger, R.C., Barrett, A., Berthold, F., Castleberry, R.P., D'Angio, G., De Bernadi, B., Evans, A.E., Favrot, M and Freeman, A. I., Hartmann, G.H.O., Hayes, F.A., Helson, L., Kemshead, J., Lampert, F., Ninane, J., Ohkawa, H., Philip, T., Pinkerton, C.R., Pritchard, J., Sawada, T., Siegel, S., Smith, E.I., Tsuchida, Y and Voute P.A. (1988) 'International criteria for diagnosis, staging, and response to treatment in patients with neuroblastoma'. *Jounal of Clinical Oncology*: *Official Journal of the American Society of Clinical Oncology*, 6(12), 1874-1881.

49) Buga, A.M., Vintilescu, R., Pop, O.T and Popa-Wagner, A. (2011) 'Brain aging and regeneration after injuries: an organismal approach'. *Aging and Disease*, 2(1), 64-79.

50) Burke, M., Langer, R and Brim, H. (1999) *Central Nervous System Drug Delivery to Treat*. New York: John Wiley and Sons.

51) Butt, A.M., Jones, H.C and Abbott, N.J. (1990) 'Electrical resistance across the blood-brain barrier in anaesthetized rats: a developmental study'. *Journal Physiology*, 429, 47-62.

52) Cabral, M., Zollner, R.L and Santana, M.H.A. (2004) 'Preparation and characterization of liposomes entrapping allergenic proteins'. *Brazilian Journal of Chemical Engineering*, 21(2), 137-146.

53) Castleberry, R.P., Pritchard, J., Ambros, P., Berthold, F., Brodeur, G.M., Castel, V., Cohn, S.L., De, B.B., Cks-Mireaux, C., Frappaz, D., Haase, G.M., Haber, M., Jones,

D.R., Joshi, V.V., Kaneko, M., Kemshead, J.T., Kogner, P., Lee, R.E.J., Matthay, K.K., Michon, J.M., Monclair, R., Roald, B.R., Seeger, R.C., Shaw, P.J and Shimada, H., Shuster, J.J. (1997) 'The International Neuroblastoma Risk Groups (INRG): A preliminary report'. *European Journal of Cancer (Oxford : 1990)*. 33(12), 2113–2116.

54) Suresh, C., Zhao, H., Gumbs, A., Chetty, C. S and Bose, H. S. (2012) 'New ionic derivatives of betulinic acid as highly potent anti-cancer agents'. *Bioorganic & Medicinal Chemistry Letters*, 22(4), 1734–1738.

55) Chandramu, C., Manohar, R.D., Krupadanam, D.G and Dashavantha, R.V. (2003) 'Isolation, characterization and bio- logical activity of betulinic acid and ursolic acid from vitex negundo l'. *Phytotherapy Research : PTR*, 17(2), 129-134.

56) Characteristic cellular changes that normally occur during apoptosis image. Available at Promega, 200-2011: https://www.promega.com/resources/product-guides-and-selectors/protocols-and-applications-guide/apoptosis/ [Accessed 28 April 2015].

57) Charurvedi, S and Dave, P.N. (2012) 'Microscopy in nanotechnology. Microscopy contributions to advances in science and technology'. *Microscopy: advances in scientific research and education*, 946-952.

58) Chemical structure of Cholestrol. Available at: http://www.sigmaaldrich.com/catalog/product/sigma/c8667?lang=en&region=ZA [Accessed 21 April 2015].

59) Chen, X and Thibeault, S. (2013) 'Effect of DMSO concentration, cell density and needle gauge on the viability of cryopreserved cells in three dimensional hyaluronan hydrogel'. *Conference proceedings: ...Annual International Conference of the IEEE Engineering in Medicine and Biology Society. IEEE Engineering in Medicine and Biology Society. Annual Conference*, 2013, 6228–6231.

60) Cheng, Y., Shao, Yundong and Yan, Weidong. (2011) 'Solubilities of Betulinic acid in thirteen organic solvents at different temperature'. *Journal of Chemical Engineering*, 56(12), 4587–4591.

61) Cheung, N.V and Deyer, A. (2013) 'Neuroblastoma: developmental biology, cancer genomics and immunotherapy'. *Nature Reviews Cancer*, 13(6), 397-411.

62) Chien, P.Y., Wang, J., Carbonaro, D., Lei, S., Miller, B., Sheikh, S., Ali, S.M., Ahmad, M.U and Ahmad, I. (2005) 'Novel cationic cardiolipin analogue-based liposome for efficient DNA and small interfering RNA delivery in vitro and in vivo'. *Cancer Gene Therapy*, 12(3), 321-328.

63) Chinnaiyan, A.M. (1999) 'The apoptosome: heart and soul of the cell death machine'. *Neoplasia (New York, N.Y.)*, 1(1), 5–15.

64) Chintharlapalli, S., Papineni, S., Ramaiah, S.K and Safe, S. (2007) 'Betulinic acid inhibits prostate cancer growth through inhibition of specificity protein transcription factors'. *Cancer Research*, 67(6), 2816-2823.

65) Chipuk, J.E., Kuwana, T., Bouchier-Hayes, L., Droin, N.M., Newmeyer, D.D., Schuler, M and Green, D.R. (2004) 'Direct activation of Bax by p53 mediates mitochondrial membrane permeabilization and apoptosis'. *Science (New York, N.Y.)*, 303(5660), 1010-1014.

66) Cho, S.J., Maysinger, D., Jain, M., Röder, B., Hackbarth, S and Winnik, F.M. (2007) 'Long-term exposure to CdTe quantum dots causes functional impairments in live cells'. *Langmuir*, 23(4), 1974-1980.

67) Chorachoo, J., Amnuaikit, T and Voravuthikunchai, S.P. (2013) 'Liposomal encapsulated rhodomyrtone: A novel anticancer drug'. *Evidence-Based Complementary and Alternative Medicine : eCAM*, 2013, 1-7.

68) Chordiya, M and Senthilkumaran, K. (2012) 'Cyclodextrin in drug delivery: a review research and reviews: journal of pharmacy and pharmaceutical sciences'. *Research & Reviews in Pharmacy and Pharmaceutical Sciences*, 1(1), 19-29.

69) Chuang, Y.C, Tyagi, P., Huang, H.Y., Yoshimura, N., Wu, M and Kaufman, J. (2011) 'Chancellor, M.B. Intravesical immune suppression by liposomal tacrolimus in cyclophosphamide-induced inflammatory cystitis'. *Neurourology and Urodynamics*, 30(3):421-427.

70) Cichewicz, R.H and Kouzi, S.A. (2004) 'Chemistry, biological activity, and chemotherapeutic potential of betulinic acid for the prevention and treatment of cancer and HIV infection'. *Medicinal Research Reviews*, 24(1), 90-114.

71) Cohn, S.L., Pearson, A.D., London, W.B., Monclair, T., Ambros, P.F., Brodeur, G.M., Faldum, A., Hero, B., Iehara, T., Machin, D., Mosseri, V., Simon, T., Garventa, A., Castel, V., Matthay, K.K., INRG Task Force. (2009) 'The International Neuroblastoma Risk Group (INRG) classification system: an INRG Task Force report'. *Journal of Clinical Oncology: Official Journal of the American Society of Clinical Oncology*, 27(2), 289-297.

72) Cooper, G.M. (2000) *The Cell: A molecular Approach.* 2nd Edition. Sunderland (Massachusetts, U.S.A): Sinauer Associates.

73) Cooper, G. M and Hausman, R. E. (2009) *The Cell: A molecular Approach*. 5th Edition. Sunderland (Massachusetts, U.S.A): Sinauer Associates.

74) Copp, A. J. (2005) 'Neurulation in the cranial region-normal and abnormal'. *Journal of Anatomy*, 207(5), 623–635.

75) Cornell, S. (2000) *Membrane Structure in Disease and Drug Therapy*. 1st Edition. New York: Marcel Dekker, Inc.

76) Cory, S and Adams, J.M. (2002) 'The Bcl2 family: regulators of the cellular life-or-death switch'. Nature *Reviews Cancer*, 2(9), 647–656.

77) Cretney, E., Takeda, K and Smyth, M.J (2007) 'Cancer: novel therapeutic strategies that exploit the TNF-related apoptosis-inducing ligand (TRAIL)/TRAIL receptor pathway'. *International Journal of Biochemistry Cell Biology*, 39(2), 280-286.

78) Crosasso, P., Ceruti, M., Brusa, P., Arpicco, S., Dosio, F and Cattel, L. (2000) 'Preparation, characterization and properties of sterically stabilized paclitaxel-containing liposomes'. *Journal of Controlled Release: Official Journal of the Controlled Release Society*, 63(1-2), 19–30.

79) Csuk, R., Barthel, A., Sczepek, R., Siewert, B and Schwarz, S. (2011) 'Synthesis, Encapsulation and Antitumor Activity of New Betulin Derivatives'. *Archiv de Pharmaize*, 344(1), 37-49.

80) Cubillos, M., lissi, E and abuin, E. (2006) 'Lipid peroxidation rates of DPPC liposomes containing different amounts of oxidable lipids show opposite dependence with the temperature'. *Journal of Chilean Chemical Society*, 51(1), 839–842.

81) Cui, J., Li, C., Wang, C., Li, Y., Zhang, L., Zhang, L., Xiu, X., Li, Y and Wei, N. (2011) 'Development of pegylated liposomal vincristine using novel sulfobutyl ether cyclodextrin gradient: is improved drug retention sufficient to surpass DSPE-PEG-induced drug leakage?'. *Journal of Pharmaceutical Sciences*, 100(7), 2835–2848.

82) CytoSelect™ WST-1 Cell Proliferation Assay Reagent Product Manual, 2013-214. Available at: http://www.cellbiolabs.com/sites/default/files/CBA-253-cell-proliferation-assay-colorimetric.pdf [Accessed 16 March 2015].

83) Da Violante, G., Zerrouk, N., Richard, I, Provot, G., Chaumeil, J.C and Arnaud, P. (2002) 'Evaluation of the cytotoxicity effect of dimethyl sulfoxide (DMSO) on Caco2/TC7 colon tumor cell cultures'. *Biological and Pharmaceutical Bulletin*, 25(12), 1600-1603.

84) Damle, A.A., Pawar, Y.P and Narkar, A.A. (2013) 'Anicancer activity of betulinic acid on MCF-7 tumours in nude mice'. *Indian Journal of Experimental Biology*, 51(7), 485-491.

85) Dang, Z., Lai, W., Qian, K., Ho, P., Lee, K.H., Chen, C.H and Huang, L. (2009) 'Betulinic Acid Derivatives as Human Immunodeficiency Virus Type 2 (HIV-2) Inhibitors (parallel)'. *Journal of Medicinal Chemistry*, 52(23), 7887-7891.

86) Danhier, F., Feron, O and Préat, V. (2010) 'To exploit the tumor microenvironment: Passive and active tumor targeting of nanocarriers for anti-cancer drug delivery'. *Journal of Controlled Release: Official Journal of the Controlled Release Society*, 148(2), 135-146.

87) Daoud-Mahammed, S., Grossiord, J.L., Bergua, T., Amiel, C., Couvreur, P and Gref, R. (2008) 'Self-assembling cyclodextrin based hydrogels for the sustained delivery of hydrophobic drugs'. *Journal of Biomedical Materials Research*, 86(3), 736-748.

88) Das, S.K., Rajabalaya, R., David, S., Gani, N., Khanam, J and Nanda, A. (2013) 'Cyclodextrins-the molecular container'. *Research Journal of Pharmaceutical, Biological and Chemical Sciences*, 4(2), 1694-1720.

89) DeBin, J.A and Strichartz, G.R. (1991) 'Chloride channel inhibition by the venom of the scorpion Leiurus quinquestriatus'. *Toxicon: Official Journal of the International Society on Toxinology*, 29(11), 1403-1408.

90) De Jong, W.H and Borm, P.J.A. (2008) 'Drug delivery and nanoparticles: applications and hazards'. *International Journal of Nanomedicine*, 3(2), 133-149.

91) de Sá, M.S., Costa, J.F., Krettli, A.U., Zalis, M.G., Maia, G.L., Sette, I.M., Câmara Cde, A., Filho, J.M., Giulietti-Harley, A.M., Ribeiro Dos Santos, R and Soares M.B. (2009) 'Antimalarial activity of betulinic acid and derivatives in vitro against Plasmodium falciparum and in vivo in P. berghei-infected mice'. *Parasitology Research*, 105(1), 275-279.

92) Dehelean, C.A., Soica, C., Peev, C., Ciurlea, S., Feflea, S and Kasa, P. (2011a) 'A pharmaco-toxicological evaluation of betulinic acid mixed with hydroxipropilgamma cyclodextrin on in vitro and in vivo models'. *Farmaci*, 59(1), 51-59.

93) Dehelean, C.A., Feflea, S., Ganta, S and Amiji, M. (2011b) 'Anti-angiogenic effects of betulinic acid administered in nanoemulsion formulation using chorioallantoic membrane assay'. *Journal of Biomedical Nanotechnology*, 7(2), 317–324.

94) Dehelean, C., Şoica, C., Peev, C., Gruia, A.T and Şeclaman, E. (2008) 'Physico-chemical and molecular analysis of antitumoral pentacyclic triterpenes in complexation with gamma-cyclodextrin'. *Revista de Chimie -Bucharest- Original Edition-*, 59(8), 887–890.

95) Dehelean, C.A., Şoica, C., Ledeţi, L., Aluaş, M., Zupko, I., Găluşcan, A., Cinta-Pinzaru S and Munteanu, M. (2012) 'Study of the betulin enriched birch bark extracts effect on human carcinoma cells and ear inflammation'. *Chemistry Central Journal*, 6(137), 1-9.

96) Desai, N. (2012) 'Challenges in Development of NP-Based Therapeutics'. *The AAPS Journal*, 14(2), 282-295.

97) Desai, T.R., Wong, J.P., Hancock, R.E.W and Finlay, W.H. (2002) 'A novel approach to the pulmonary delivery of liposomes in dry powder forms to eliminate the deleterious effects of milling'. *Journal of Pharmaceutical Sciences*, 91(2), 482-491.

98) Deveraux, Q.L and Reed, J.C. (1999) 'IAP family proteins—suppressors of apoptosis'. *Genes and Development*, 13(3), 239–252.

99) Dhule, S.S., Penfornis, P., Frazier, T., Walker, R., Feldman, J., Tan, G., He, J., Alb, A., John, V and Pochampally, R. (2012) 'Curcumin-loaded γ-cyclodextrin liposomal nanoparticles as delivery vehicles for osteosarcoma'. *Nanomedicine: Nanotechnology, Biology and Medicine. Nanomedicine*, 8(4), 440-451.

100) Dobrovolskaia, M.A and McNeil, S.E. (2007) 'Immunological properties of engineered nanomaterials'. *Nature Nanotechnology*, 2(8), 469-478.

101) Dokka, S., Toledo, D., Shi, Z., Castranova, V and Rojanasakul, Y. (2000) 'Oxygen radical-mediated pulmonary toxicity induced by some cationic liposomes'. *Pharmaceutical Research*, 17(5), 521-525.

102) Domingues, M.M., Santiago, P.S., Castanho, M.A.R.B and Santos, N.C. (2008) 'What can light scattering spectroscopy do for membrane-active peptide studies?' *Journal of Peptide Science: An Official Publication of the European Peptide Society*, 14(4), 394-400.

103) Drummond, D. C., O. Meyer, Hong, K., Kirpotin, D.B and Papahadjopoulos, D. (1999) 'Optimizing Liposomes for Delivery of Chemotherapeutic Agents to Solid Tumors'. *Pharmacological Reviews*, 51(4), 691-743.

104) D'Souza, S. (2014) 'A Review of In Vitro Drug Release Test Methods for Nano-Sized Dosage Forms'. *Advances in Pharmaceutics*, 2014, 1-12.

105) Du, C., Fang, M., Li, Y., Li, L and Wang, X. (2000) 'Smac, a mitochondrial protein that promotes cytochrome c-dependent caspase activation by eliminating IAP inhibition'. *Cell*, 102(1), 33–42.

106) Dua, J.S., Rana, A.C and Bhandari, A.K. (2012) 'Liposome: methods of preparation and application'. *International Journal of Pharmaceutical Studies and Research*, 3(2), 14-20.

107) Duan, H.W., Kuang, M., Wang, X.X., Wang, Y.A., Mao, H and Nie, S.M. (2008) 'Re-examining the effects of particle size and surface chemistry on the magnetic properties of iron oxide nanocrystals: New insights into spin disorder and proton relaxivity'. *The Journal of Physical Chemistry*, 112(22), 8127–8131.

108) DuBois, S.G., Chesler, L., Groshen, S., Hawkins, R., Goodarzian, F., Shimada, H., Yanik, G., Tagen, M., Stewart, C., Mosse, Y.P., Maris, J.M., Tsao-Wei D, Marachelian, A.,Villablanca, J.G and Matthay, K.K. (2012) 'Phase I study of vincristine, irinotecan, and ^{131}I-metaiodobenzylguanidine for patients with relapsed or refractory neuroblastoma: A new approaches to neuroblastoma therapy trial'. *Journal of Clinical Oncology: Official Journal of the American Society of Clinical Oncology*, 18(9), 2679-2686.

109) Dudley, A. C. (2012) 'Tumor Endothelial Cells'. *Cold Spring Harbor Perspectives in Medicine*, 2(3), 1-18.

110) Dupin, E., Calloni, G., Real, C., Gonçalves-Trentin, A and Le Douarin, N. M. (2007) 'Neural crest progenitors and stem cells'. *Comptes Rendus Biologies*, 330(2007), 521-529.

111) Dykstra, K.H., Arya, A., Arriola, D.M., Bungay, P.M., Morrison, P.F and Dedrick, R.L. (1993) 'Microdialysis study of zidovudine (AZT) transport in rat brain'. *Journal of Pharmacology and Experimental Therapeutics*, 267(3), 1227–1236.

112) Ehrhardt, H., Fulda, S., Fuhrer, M., Debatin, K.M and Jeremias, I. (2004) 'Betulinic acid-induced apoptosis in leukemia cells'. *Leukemia*, 18(8), 1406-1412.

113) Eiznhamer, D.A and Xu, Z.Q. (2004) 'Betulinic acid: a promising anticancer candidate'. *ID Drugs :* The Investigational Drugs Journal, 7(4), 359–373.

114) Elhissi, A.M.A., Karnam, K.K., Danesh, M.R., Gill, H.S and Taylor, K.M.G. (2006) 'Formulations generated from ethanol-based proliposome formulations for delivery via medical nebulisers'. *The Journal of Pharmacy and Pharmacology*, 58(7), 887-894.

115) Elimelech, M., Gregory, J., Jia, X and Williams R.A (1995) *Particle Deposition and Aggregation*. Woburn, MA: Butterworth – Heinemann.

116) Elmore, S. (2007) 'Apoptosis: A review of programmed cell death'. *Toxicologic Pathology*, 35(4), 495–516.

117) Elsayed, M.M and Cevc, G. (2011) 'Turbidity spectroscopy for characterization of submicroscopic drug carriers, such as nanoparticles and lipid vesicles: size determination'. *Pharmaceutical Research*, 28(9), 2204-2222.

118) Emadi, A., Jones, R.J and Brodsky, R.A. (2009) 'Cyclophosphamide and cancer: golden anniversary'. *Nature Reviews Clinical Oncology*, 6(11), 638–647.

119) Enari, M., Sakahira, H., Yokoyama, H., Okawa, K., Iwamatsu, A and Nagata, S. (1998) 'A caspase-activated DNase that degrades DNA during apoptosis, and its inhibitor ICAD'. *Nature*, 391(6662), 43–50.

120) Engelhardt, B and Sorokin, L. (2009) 'The blood-brain and the bloodcerebrospinal fluid barriers: function and dysfunction'. *Semininars in Immunopathology*, 31(4), 497-511.

121) Enwerem, N.M., Okogun, J.I., Wambebe, C.O., Okori, D.A and Akah, P.A. (2001) 'Anthelmintic activity of the stem bark extracts of Berlina grandiflora and one of its active principles, Betulinic acid'. *Phytomedicine*, 8(2), 112-114.

122) Fallarini, G., Miglio, T., Paoletti, A., Minassi, A., Amoruso, C., Bardelli, S., Brunelleschi and Lombardi, G. (2009) 'Clovamide and rosmarinic acid induce neuroprotective effects in vitro models of neuronal death'. *British Journal of Pharmacology*, 157(6), 1072–1084.

123) Farhang, B., Kakuda, Y and Corredig, M. (2012) 'Encapsulation of ascorbic acid in liposomes prepared with milk fat globule membrane-derived phospholipids'. *Dairy Science and Technology*, 92(4), 353-366.

124) Faujan, N.H., Alitheen, N.B., Yeap, S.K., Ali, A.M., Muhajir, A.H and Ahmad, F.B.H. (2010) 'Cytotoxic effect of betulinic acid and betulinic acid acetate isolated from Melaleuca cajuput on human myeloid leukemia (HL-60) cell line'. *African Journal of Biotechnology*, 9(38), 6387-6396.

125) Ferrin, G., Linares, C.I and Muntané, J. (2011) 'Mitochondrial drug targets in cell death and cancer'. *Current Pharmaceutical Design*, 17(20), 2002–2016.

126) Fischer, U and Schulze–Osthof, K. (2005) 'New approaches and therapies targeting apoptosis in disease'. *Pharmacological Reviews*, 57(2), 187–215.

127) Fisher, R.S and Ho, J. (2002) 'Potential new methods for antiepileptic drug delivery'. *CNS Drugs*, 16(9), 579-593.

128) Flowchart representing the divisions and sub-divisions of the NS. Available at: http://classconnection.s3.amazonaws.com/420/flashcards/1094420/jpg/nervous_system_organization1328056081853.jpg [Accessed 29 April 2015].

129) Fontanay, S., Grare, M., Mayer, J., Finance, C and Duval, R.E. (2008) 'Ursolic, oleanolic and betulinic acids: antibacterial spectra and selectivity indexes'. *Journal of Ethnopharmacology*, 120(2), 272-276.

130) Freire, J. M., Domingues, M. M., Matos, J., Melo, M. N., Veiga, A. S., Santos, N. C and Castanho, M. A. R. B. (2011) 'Using zeta-potential measurements to quantify peptide partition to lipid membranes'. *European Biophysics Journal*, 40(4), 481–487.

131) French, S., DuBois, S.G., Horn, B., Granger, M., Hawkins, R., Pass, A., Plummer, E and Matthay, K. (2013) '131I-MIBG followed by consolidation with busulfan, melphalan and autologous stem cell transplantation for refractory neuroblastoma'. *Pediatriac Blood and Cancer*, 60(5), 879-884,

132) Frumm, S.M., Fan, Z.P., Ross, K.N., Duvall, J.R., Gupta, S., VerPlank, L., Suh, B., Holsen, E., Wanger, F.F., Smith, W.B., Paranal, R.M., Bassil, C.F., Qi, J., Roti, G., Kung, A.L., Bradner, J.E., Tolliday, N and Stegmaier, K. (2013) 'Selective HDAC1/HDAC2 Inhibitors Induce Neuroblastoma Differentiation'. *Chemistry and Biology*, 20(5), 713-725.

133) Fulda, S. (2008) 'Betulinic Acid for Cancer Treatment and Prevention'. *International Journal of Molecular Sciences*, 9(6), 1096–1107.

134) Fulda, S and Debatin, K. M. (2000) 'Betulinic acid in duces apoptosis through a direct effect on mitochondria in neuroectodermal tumors'. *Medical and Paediatric Oncology*, 35(6), 616-618.

135) Fulda, S and Kroemer, G. (2009) 'Targeting mitochondrial apoptosis by betulinic acid in human cancers'. *Drug Discovery Today*, 14(17-18), 885-890.

136) Fulda, S., Friesen, C., Los, M., Scaffidi, C., Mier, W., Benedict, M., Nuñez, G., Krammer, P. H., Peter, M. E and Debatin, K. M. (1997) 'Betulinic acid triggers CD95 (APO-1/Fas) and p53-independent apoptosis via activation of caspases in neuroectodermal tumors'. *Cancer Research*, 57(21), 4956-4964.

137) Fulda, S., Gorman, A.M., Hori, O and Samali, A. (2010) 'Cellular Stress Responses: Cell Survival and Cell Death'. *International Journal of Cell Biology*, 2010, 1-23.

138) Fulda, S., Jeremias, I., Steiner, H. H., Pietsch, T and Debatin, K. M. (1999) 'Betulinic acid: a new cytotoxic agent against malignant brain-tumor cells'. *International Journal of Cancer*, 82(3), 435-441.

139) Fulda, S., Scaffidi, C., Susin, S.A., Krammer, P.H., Kroemer, G., Peter, M.E and Debatin, K.M. (1998) 'Activation of mitochondria and release of mitochondrial apoptogenic factors by betulinic acid'. *The Journal of Biological Chemistry*, 273(51), 33942-33948.

140) Fuller, G.N. (2008) 'The WHO Classification of Tumours of the Central Nervous System, 4th Edition'. *Archives of Pathology & Laboratory Medicine*, 132(6), 906-906.

141) Folkman, J and Shing, Y. (1992) 'Angiogenesis'. *Journal of Biological Chemistry*, 267(10), 10931-10934.

142) Fox, C. B., Mulligan, S. K., Sung, J., Dowling, Q. M., Fung, H. W. M., Vedvick, T. S and Coler, R. N. (2014) 'Cryogenic transmission electron microscopy of recombinant tuberculosis vaccine antigen with anionic liposomes reveals formation of flattened liposomes'. *International Journal of Nanomedicine*, 9, 1367–1377.

143) Galvao, J., Davis, B., Tilley, M., Normando, E and Dunchen, M.R. (2014) 'Unexpected low-dose toxicity of the universal solvent DMSO'. *FASEB Journal: Official Publication of the Federation of American Societies for Experimental Biology*, 28(3), 1317-1330.

144) Gammill, L.S and Bronner-Fraser, M. (2003) 'Neural crest specification: migrating into genomics'. *Nature Reviews Neurosciences*, 4(10), 795-805.

145) Gao, J., Yu, Y., Zhang, Y., Song, J., Chen, H., Li, W., Qian, W., Deng, L., Kou, G., Chen, J and Guo, Y. (2012) 'EGFR-specific PEGylated immunoliposomes for active siRNA delivery in hepatocellular carcinoma'. *Biomaterials*, 33(1), 270-282.

146) Garrido, C., Galluzzi, L., Brunet, M., Puig, P.E., Didelot, C and Kroemer, G. (2006) 'Mechanisms of cytochrome c release from mitochondria'. *Cell Death and Differentiation*, 13(9), 1423–1433.

147) George, R.E., Diller, L and Bernstein, M.L. (2010) 'Pharmacotherapy of neuroblastoma'. *Expert Opinion on Pharmacotherapy*, 11(9), 1467–1478.

148) Goel, S., Wong, A.H.K and Jain, R., K., (2012) 'Vascular Normalization as a Therapeutic Strategy for Malignant and Nonmalignant Disease'. *Cold Spring Harbor Perspectives in Medicines*, 2(3), 1-24.

149) Gogolin, S., Ehemann, V., Becker, G., Brueckner, L.M., Dreidax, D., Bannert, S., Nolte, I., Savelyeva, L., Bell, E and Westermann, F. (2013) 'CDK4 inhibition restores G(1)-S arrest in MYCN-amplified neuroblastoma cells in the context of doxorubicin-induced DNA damage'. *Cell Cycle (Georgetown, Tex.)*, 12(7), 1091-104.

150) Götte, M., Hofmann, G., Michou-Gallani, A., Glickman, F.J., Wishart, W and Gabriel, D. (2010) 'An imaging assay to analyze primary neurons for cellular neurotoxicity'. *Journal of Neuroscience Methods*, 192(1), 7-16.

151) Gotter, T. G. (2009) 'Apoptosis and cancer: the genesis of a research field'. *Nature Reviews: Cancer*, 9(7), 501–507.

152) Green, D.R and Kroemer, G. (2009) 'Cytoplasmic functions of the tumour suppressor p53'. *Nature*, 458(7242), 1127-1130.

153) Gregoriadis, G. (2007) *Liposome Technology, Liposome Preparation and Related Techniques*. 3rd Edition. USA: Taylor and Francis Group.

154) Grimmer, M.R and Weiss, W.A. (2006) 'Childhood tumors of the nervous system as disorders of normal development'. *Current Opinion in Pediatrics*, 18(6), 634-638.

155) Gubernator, J. (2011) 'Active methods of drug loading into liposomes: recent strategies for stable drug entrapment and increased in vivo activity'. *Expert Opinion on Drug Delivery*, 8(5), 565–580.

156) Gupta, A.K and Gupta, M. (2005) 'Synthesis and surface engineering of iron oxide nanoparticles for biomedical applications'. *Biomaterials*, 26(18), 3995-4021.

157) Gupta, R. B and Kompella, U.B. (2006) *Nanoparticle technology for drug delivery*. New York: Taylor and Francis.

158) Guo, S and Huang, L. (2011) 'Nanoparticles escaping res and endosome: challenges for siRNA delivery for cancer therapy'. *Journal of Nanomaterials*, 1(1), 1-12.

159) Hagtvet, E., Evjen, T., Olsen, D.R., Fossheim, S and Nilssen, E.A. (2011) 'Ultrasound enhanced antitumor activity of liposomal doxorubicin in mice'. *Journal of Drug Targeting*, 19(8), 701-708.

160) Hakkarainen, B., Fujita, K., Immel, S., Kenne, L and Sandström, C. (2005) '1H NMR studies on the hydrogen-bonding network in mono-altro-beta-cyclodextrin and its complex with adamantane-1-carboxylic acid'. *Carbohydrate Research*, 340(8), 1539-1545.

161) Haley, B and Frenkel, E. (2008) 'Nanoparticles for drug delivery in cancer treatment'. *Urologic Oncology*, 26(1), 57-64.

162) Hanahan, D and Weinberg, R.A. (2000) 'The hallmarks of cancer'. *Cell*, 100(1), 57-70.

163) Hanahan, D and Weinberg, R.A. (2011) 'Hallmarks of cancer: the next generation'. *Cell*, 144(5), 646-674.

164) Hanumegowda, U.M., Wu, Y and Adams, S.P. (2014) 'Potential Impact of Cyclodextrin Containing Formulations in Toxicity Evaluation of Novel Compounds in Early Drug Discovery'. *Journal of Pharmaceutical Pharmacology*, 2(1), 1-5.

165) Hess, H and Tseng, Y. (2007). 'Active intracellular transport of nanoparticles: opportunity or threat'. *American Chemical Society Nano*, 1(5), 390-392.

166) Hill, M.M., Adrain, C., Duriez, P.J., Creagh, E.M and Martin, S.J. (2004) 'Analysis of the composition, assembly kinetics and activity of native Apaf-1 apoptosomes'. *The EMBO Journal*, 23(10), 2134–2145.

167) Hill, R.A and Connolly, J.D. (2013) 'Triterpenoids'. *Natural Products Report*, 30(7), 1028-1065.

168) Hinna, A., Steiniger, F., Hupfeld, S., Stein, P., Kuntsche, J and Brandl, M. (2015) 'Filter-extruded liposomes revisited: a study into size distributions and morphologies in relation to lipid-composition and process parameters'. *Journal of Liposome Research*, 26(1), 11-20.

169) Honary, S and Zahir, F. (2013) 'Effect of zeta potential on the properties of nano-drug delivery systems - a review (part 1)'. *Tropical Journal of Pharmaceutical Research*, 12(2), 255-264.

170) Howard, F.B and Levin, I. (2010) 'Lipid vesicle aggregation induced by cooling'. *International Journal of Molecular Science*, 11(2), 754-761.

171) Hsu, T.I., Wang, M.C., Chen, S.Y., Huang, S.T., Yeh, Y.M., Su, W.C., Chang, W.C and Hung, J.J. (2012) 'Betulinic acid decreases specificity protein 1 (Sp1) level via increasing the sumoylation of sp1 to inhibit lung cancer growth'. *Molecular Pharmacology*, 82(6), 1115-1128.

172) Huang, L., Ho, P and Chen, C.H. (2007) 'Activation and inhibition of the proteasome by betulinic acid and its derivatives'. *FEBS Letters*, 581(25), 4955-4959.

173) Huber, K. (2006) 'The sympathoadrenal cell lineage: specification, diversification, and new perspectives'. *Devepmental Biolology*, 298(2), 335-343.

174) Hunter, R.J. (1981) *Zeta Potential in Colloids Science.* New York: Academic Press.

175) Hunter, R.J., Midmore, B.R and Zang, H.J. (2001) 'Zeta potential of highly charged thin double layered systems'. *Journal of Colloid and Interface Science*, 237(1), 147-149.

176) Ilinskaya, A. N and Dobrovolskaia, M. A. (2013) 'Nanoparticles and the blood coagulation system. Part II: safety concerns'. *Nanomedicine (London, England)*, 8(6), 969–981.

177) Immordino, M.L., Dosio, F and Cattel, L. (2006) 'Stealth liposomes: review of the basic science, rationale, and clinical applications, existing and potential'. *International Journal of Nanomedicine*, 1(3), 297–315.

178) International Neuroblastoma Staging System (INSS) for NB based on anatomical presence. Available at: http://www.nant.org/Patients_and_Families/neuroblastoma.php [Accessed 1 March 2015].

179) Iqbal, M.A., Md S., Sahni, J.k., Baboota, S., Dang, S and Ali, J. (2012) 'Nanostructured lipid carriers system: recent advances in drug delivery'. *Journal of Drug Targeting*, 20(10), 813-830.

180) Jadhav, U., Ezhilarasan, R., Vaughn, S.F., Berhow, M.A and Mohanam, S. (2007) 'Cell Cycle Arrest and Apoptosis in Human Neuroblastoma Cells'. *International Journal of Molecular Medicine*, 19(3), 353-361.

181) Jäger, S., Winkler, K., Pfüller, U and Scheffler, A. (2007) 'Solubility studies of oleanolic acid and betulinic acid in aqueous solutions and plant extracts of Viscum album L'. *Planta Medica*, 73(2), 157-162.

182) Ji, H.-F., Li, X.-J and Zhang, H.Y. (2009) 'Natural products and drug discovery. Can thousands of years of ancient medical knowledge lead us to new and powerful drug combinations in the fight against cancer and dementia?' *EMBO Reports*, 10(3), 194–200.

183) Jiang, J., Oberdörster, G and Biswas, P. (2009) 'Characterization of size, surface charge, and agglomeration state of nanoparticle dispersions for toxicological studies'. *Journal of Nanoparticle Research*, 11(1), 77–89.

184) Jiang, M., Stanke, J and Lahti, J. M. (2011) 'The Connections between Neural Crest Development and Neuroblastoma'. *Current Topics in Developmental Biology*, 94, 77–127.

185) Johanson, C. E., Duncan, J. A., Klinge, P. M., Brinker, T., Stopa, E. G and Silverberg, G. D. (2008) 'Multiplicity of cerebrospinal fluid functions: New challenges in health and disease'. *Cerebrospinal Fluid Research*, 5(10), 1-32.

186) Johnson, S.M., Bangham, A.D., Hill, M.W and Korn E.D. (1971) 'Single bilayer liposomes'. *Biochimica et Biophysica Acta*, 233(3), 820-826.

187) Johnstone, R.W., Ruefli, A.A and Lowe, S.W. (2002) 'Apoptosis: a link between cancer genetics and chemotherapy'. *Cell*, 108(2), 153-164.

188) Jousma, H., Talsma, H., Spies, F., Joosten, J.G.H., Junginger, H.E and Crommelin, D.J.A. (1987) 'Characterization of liposomes. The influence of extrusion of multilamellar

vesicles through polycarbonate membranes on particle size, particle size distribution and number of bilayers'. *International of Journal of Pharmaceutics*, 35(3), 263-274.

189) Joza, N., Susin, S.A., Daugas, E., Stanford, W.L., Cho, S.K., Li, C.Y., Sasaki, T., Elia, A.J., Cheng, H.Y., Ravagnan, L., Ferri, K.F., Zamzami, N., Wakeham. A., Hakem, R., Yoshida, H., Kong, Y.Y., Mak, T.W., Zuniga- Pflucker, J.C., Kroemer, G and Penninger, J.M. (2001) 'Essential role of the mitochondrial apoptosis-inducing factor in programmed cell death'. *Nature*, 410(6828), 549–554.

190) Kaatsch, P. (2010) 'Epidemiology of childhood cancer'. *Cancer Treatment Reviews*, 36(4), 277– 285.

191) Kale, M., Suruse, P., Singh, R., Malhotra, G and Raut, P. (2012) 'Effect of size reduction techniques on doxorubicin hydrochloride loaded liposomes'. *International Journal of Biological and Pharmaceutical Research*, 3(3), 308-316.

192) Kalluri, R and Neilson, E.G. (2003) 'Epithelialmesenchymal transition and its implications for fibrosis'. *The Journal of Clinical Investigation*, 112(12), 1776–1784.

193) Kalluri, R and Weinberg, R. (2009) 'The basics of epithelial-mesenchymal transition'. *The Journal of Clinical Investigation*, 119(6), 1420-1428.

194) Kamijo, T. (2012) 'Role of stemness-related molecules in neuroblastoma'. *Pediatric Research*, 71(4 Pt 2), 511–515.

195) Kandel, E., R., Schwartz, J., H and Jessell, T., M. (1995) *Essentials of Neural Science and Behavior*. 1rst Edition. Stamford: Appleton and Lange.

196) Kasperczyk, H., Ferla-Bruhl, K., Westhoff, M.A., Behrend, L., Zwacka, R.M., Debatin, K.M and Fulda, S. (2005) 'Betulinic acid as new activator of NF-kappaB: molecular mechanisms and implications for cancer therapy'. *Oncogene*, 24(46), 6945–6956.

197) Kaszuba, M., Corbett, J., Watson, F.M and Jones, A. (2010) 'High-concentration zeta potential measurements using light-scattering techniques'. *Philosophical Transactions. Series A, Mathematical, Physical, and Engineering Science*s, 368(1927), 4439– 4451.

198) Kelly, C., Jefferies, C and Cryan, S.A. (2011) 'Targeted liposomal drug delivery to monocytes and macrophages'. *Journal of Drug Delivery*, 11(2011), 1-11.

199) Kent, C. (1995) 'Eukaryotic Phospholipid Biosynthesis'. *Annuals Review of Biochemistry*, 64, 315-343.

200) Khanbabaie, R and Jahanshahi, M. (2012) 'Revolutionary impact of nanodrug delivery on neuroscience'. *Current Neuropharmacology*, 10(4), 370-392.

201) Kievit, F.M., Veiseh, O., Fang, C., Bhattarai, N., Lee, D., Ellenbogen, R.G and Zang, M. (2010) 'Chlorotoxin labeled magnetic nanovectors for targeted gene delivery to glioma'. *ACS Nano Letters*, 4(8), 4587–4594.

202) Kim, J.Y., Koo, H.M and Kim, D.S.H.L. (2001) 'Development of C-20 modified Betulinic acid derivatives as antitumor agents'. *Bioorganic and Medicinal Chemistry Letters*, 11(17), 2405-2408.

203) Kinoshita, K., Akiba, M., Saitoh, M., Ye, Y., Koyama, K., Takahashi, T., Kondo, N and Yuasa, H. (1998) 'Antinociceptive effect of triterpenes from cacti'. *Pharmaceutical Biology*, 36(1), 50-57.

204) Kraft, J. C., Freeling, J. P., Wang, Z and Ho, R. J. Y. (2014) 'Emerging research and clinical development trends of liposome and lipid nanoparticle drug delivery systems'. *Journal of Pharmaceutical Sciences*, 103(1), 29–52.

205) Kramer, K., Kushner, B., Heller, G and Cheung, N.K. (2001) 'Neuroblastoma metastatic to the central nervous system. The memorial sloan-kettering cancer center experience and a literature review'. *Cancer*, 91(8), 1510-1519.

206) Kulesa, P.M., Lefcort, F and Kasemeier-Kulesa, JC. (2009) 'The migration of auntonomic precursor cells in the embryo'. *Autonomic Neuroscience: Basic & Clinical*, 151(1), 3-9.

207) Kumar, C.S and Mohammad, F (2011) 'Magnetic Nanomaterials for Hyperthermia-based Therapy and Controlled Drug Delivery'. *Advanced drug delivery reviews*, 63(9), 789-808.

208) Kumar, S., Marfatia, R., Tannenbaum, S., Yang, C and Avelar, E. (2012) 'Doxorubicin-induced cardiomyopathy 17 years after chemotherapy'. *Texas Heart Institute Journal*, 39(3), 424–427.

209) Kushner, B.H., Kramer, K., Modak, S., Qin, L.X and Cheung, N.K. (2010) 'Differential impact of high-dose cyclophosphamide, topotecan, and vincristine in clinical subsets of patients with chemoresistant neuroblastoma'. *Cancer*, 116(12), 3054-3060.

210) Kushner, B.H., Modak, S., Kramer, K., Basu, E.M., Roberts, S.S and Cheung, N.K. (2013) 'Ifosfamide, carboplatin, and etoposide for neuroblastoma: a high-dose salvage regimen and review of the literature'. *Cancer*, 119(3), 665-671.

211) Kvasnica, M., Sarek, J., Klinotova, E., Dzubak, P and Hajduch, M. (2005) 'Synthesis of phthalates of betulinic acid and betulin with cytotoxic activity'. *Bioorganic and Medicinal Chemistry Letters*, 13(10), 3447–3454.

212) LaConte, L.E.W., Nitin, N., Zurkiya, O., Caruntu, D., O'Connor, C.J., Hu, X.P and Bao, G. (2007) 'Coating thickness of magnetic iron oxide nanoparticles affects R-2 relaxivity'. *Journal of Magnetic Resonance Imaging*, 26(6), 1634–1641.

213) Laouini, A., Jaafar-Maalej, C., Blouza, L., Sfar, S., Charcosset, C and Fessi, H. (2012) 'Preparation, characterization and applications of liposomes: state of the art'. *Journal of colloid science and biotechnology*, 1(2), 147-168.

214) Laza-Knoerr, A.L., Gref, R and Couvreur, P. (2010) 'Cyclodextrins for drug delivery'. *Journal of drug target*, 18(9), 645-656.

215) Lee, J.H and Kim, K.T. (2004) 'Induction of cyclin-dependent kinase 5 and its activator p35 through the extracellular-signal-regulated kinase and protein kinase A pathways during retinoic-acid mediated neuronal differentiation in human neuroblastoma SK-N-BE(2)C cells'. *Journal of Neurochemistry*, 91(3), 634-647.

216) Lee, S.C., Lee, K., E., Kim, J., J and Lim, S., H. (2005) 'The Effect of Cholesterol in the Liposome Bilayer on the Stabilization of incorporated Retinol'. *Journal of Liposome Research*, 15(3-4), 157-166.

217) Leth-Larsen, R., Lund, R. R and Ditzel, H. J. (2010) 'Plasma Membrane Proteomics and its Application in Clinical Cancer Biomarker Discovery'. *Molecular & Cellular Proteomics : MCP*, *9*(7), 1369–1382.

218) Li, C and Wallace, S. (2008) 'Polymer-drug conjugates: recent development in clinical oncology'. *Advanced Drug Delivery Reviews*, 60(8), 886-898.

219) Li, C.L., Cui, J.X., Wang, C.X., Li, Y.H., Zang, L., Xiu, X., Li, Y.F., Wei, N., Zang, Li and Wang, P. (2011) 'Novel sulfobutyl ether cyclodextrin gradient leads to highly active liposomal irinotecan formulation'. *The Journal of Pharmacy and Phamacology*, 63(6), 765-773.

220) Li, L.Y., Luo X and Wang X. (2001) 'Endonuclease G is an apoptotic DNase when released from mitochondria'. *Nature*, 412(6842), 95–9.

221) Li, Z and Vance. D. E. (2008) 'Phosphatidylcholine and Choline Homeostasis'. *Journal of Lipid Research*, 49(6), 1187-94.

222) Liu, D., Liu, F and Song, Y. K (1995) 'Recognition and Clearance Of liposomes Containing Phosphatidylserine are mediated by serum opsonin'. *Biochemica et Biophysica Acta*, 1235(1), 140-6.

223) Liu, W.K., Ho, J.C., Cheung, F.W., Liu, B.P., Ye, W.C and Che, C.T. (2004) 'Apoptotic activity of betulinic acid derivatives on murine melanoma B16 cell line'. *European Journal of Pharmacology*, 498(1-3), 71-78.

224) Lockman, P.R., Mumper, R.J., Khan, M.A and Allen, D.D. (2002) 'Nanoparticle technology for drug delivery across the blood-brain barrier'. *Drug Devolopment and Industrial Pharmacy Journal*, 28(1), 1-13.

225) Lodish H, Berk A, Zipursky, S.L., Matsudaira, P., Balitimore, D and Darnell, J. (2000) *Molecular Cell Biology*. 4th Edition. New York: W. H. Freeman.

226) London, W.B., Castel, V., Monclair, T., Ambros, P.F., Pearson, A.D.J., Cohn, S.L., Berthold, F., Nakagawara, A., Ladenstein, R.L., Iehara, T and Matthay, K.K. (2011) 'Clinical and biological features predictive of survival after relapse of neuroblastoma: a report from the international neuroblastoma risk group project'. *Journal of Clinical Oncology : Official Journal of the American Society of Clinical Oncology* 29(24), 3286-3292.

227) Lopes, S.C.A., Giuberti, C.S., Rocha, T.G.R., Ferreira, D.S., Leite, E.A and Oliveir, M.O (2013) 'Liposomes as Carriers of Anticancer Drugs'. *Cancer Treatment-Conventional and Innovative*, 86-124.

228) Maccauro, G., Spinelli, M., S., Mauro, S., Perisano, C., Graci, C and Ros, M., A. (2011) 'Physiopathology of spine metastasis'. *International Journal of Surgical Oncology*, 2011, 1-8.

229) Maeda, H., Wu, J., Sawa, T., Matsumura, Y and Hori, K. (2000) 'Tumor vascular permeability and the EPR effect in macr omolecular therapeutics: a review'. *Journal of Controlled Release: Official Journal of the Controlled Release Society*, 65(1-2), 271-284.

230) Maestrelli, F., Gonzalez-Rodriguez, M.L., Rabasco, A.M., Ghelardini, C and Mura, P. (2010) 'New drug-in cyclodextrin-in deformable liposomes formulations to improve the therapeutic efficacy of local anaesthetics'. *International Journal of Pharmaceutics*, 395(1-2), 222-231.

231) Maherani, B., Arab-Tehranyl, E., Mozafari, C., Gaianil, C and Linder, M. (2011) 'Liposomes: A review of manufacturing techniques and targeting strategies'. *Current Nanoscience*, 7(3), 436-452.

232) Mai, W.X and Meng, H. (2013) 'Mesoporous silica nanoparticles: A multifunctional nano therapeutic system'. *Integrative Biology: quantitative biosciences from nano to macro*, 5(1), 19-28.

233) Mak, M., Fung, L and Strasser, J.F. (1995) 'Distribution of drugs following controlled delivery to the brain interstitium'. *Journal of Neuro-oncology*, 26(2), 91–102.

234) Malik, N., Evagorou, E.G and Duncan, R. (1999) 'Dendrimer- platinate: a novel approach to cancer chemotherapy'. *Anticancer Drugs*, 10(8), 767-76.

235) Mamo, T., Moseman, E. A., Kolishetti, N., Salvador-Morales, C., Shi, J., Kuritzkes, D. R and Farokhzad, O. C. (2010) 'Emerging nanotechnology approaches for HIV/AIDS treatment and prevention'. *Nanomedicine (London, England)*, 5(2), 269–285.

236) Maris, J. (2010) 'Recent advances in neuroblastoma'. *The New England Journal of Medicine*, 362(23), 2202-2211.

237) Maris, J.M., Hogarty, M.D., Bagatell, R and Cohn, S.L. (2007) 'Neuroblastoma'. *The Lancet*, 369(9579), 2106-2120.

238) Maris, J.M and Matthay, KK. (1999) 'Molecular biology of neuroblastoma'. *Journal of Clinical Oncology*, 17(7), 2264-2279.

239) Maris, J.M., Weiss, M., J., Mosse, Y., Hii, G., Guo, C., White, P. S., Hogarty, M.D., Mirensky, T., Brodeur, G., M., Rebbeck, T. R., Urbanek, M and Shusterman, S. (2002) 'Evidence for a hereditary neuroblastoma predisposition locus at chromosome 16p12-13'. *Cancer Research*, 62(22), 6651-6658.

240) Markovsky, E., Baabur-Cohen, H., Eldar-Boock, A., Omer, L., Tiram, G., Ferber, S., Ofek, P., Polyak, D., Scomparin, A and Satchi-Fainaro, R. (2012) 'Administration, distribution, metabolism and elimination of polymer therapeutics'. *Journal of Controlled Release: Official Journal of the Controlled Release Society*, 161(2), 446-460.

241) Martinez-Morales, J.R., Del Bene, F., Nica, G., Hammerschmidt, M., Bovolenta, P and Wittbrodt, J (2005) 'Differentiation of the vertebrate retina is coordinated by an FGF signalling center'. *Developmental Cell*, 8(4), 565-574.

242) Martini, F., H. (2006) *Fundamentals of Anatomy and physiology*. 7th Edition. San Francisco: Pearson Education Inc.

243) Marshall, G.M., Carter, D.R., Cheung, B.B., Liu, T., Mateos, M.K., Meyerowitz, J.G and Weiss, W.A. (2014) 'The prenatal origins of cancer'. *Nature Reviews Cancer*, 14(4), 277-289.

244) Massing, U and Fuxius, S. (2000) 'Liposomal formulations of anticancer drugs: selectivity and effectiveness'. *Drug Resistance Updates*, 3(3), 171-177.

245) Matteucci, M.L and Thrall, D.E. (2000) 'The role of liposomes in drug delivery and diagnostic imaging: a review'. *Veterinary Radiology and Ultrasound*, 41(2), 100-107.

246) Matthay, K.K. (1995) 'Neuroblastoma: A clinical challenge and biologic puzzle'. *CA: A Journal for Clinicians*, 45(3), 179–192.

247) Matthay, K., K., Brisse, H., Couanet, D., Couturier, J., Bénard, J., Mosseri, V., Edeline, V., Lumbroso, J., Valteau-Couanet, D and Michon, J. (2003) 'Central nervous

system metastasis in neuroblastoma: radiologic, clinical, and biological features in 23 patients'. *Cancer*, 98(1), 155-165.

248) Matthay, K.K., Villablanca, J.G., Seeger, R.C., Stram, D.O., Harris, R.E., Ramsay, N.K., Swift, P., Shimada, H., Black, C.T., Brodeur, G.M., Gerbing, R.B and Reynolds, C.P. (1999) 'Treatment of high-risk neuroblastoma with intensive chemotherapy, radiotherapy, autologous bone marrow transplantation, and 13-cis-retinoic acid'. Children's Cancer Group'. *The New England Journal of Medicine*, 341(16), 1165–1173.

249) Maurer, N., Fenske, D. B and Cullis, P. R. (2001) 'Developments in liposomal drug delivery systems'. *Expert Opinion in Biological Therapy*, 1(6), 923-947.

250) Mayer, L., Balley, M.B., Hope, M.J and Cullis, P.R. (1986) 'Techniques for encapsulating bioactive agents into liposomes'. *Chemistry and Physics of Lipids*', 40(2-4), 333-345.

251) McChesney, J.D., Venkataraman, S.K and Henri, J.T. (2007) 'Plant natural products: back to the future or into extinction?'. *Phytochemistry*, 68(14), 2015-2022.

252) McCorry, L. K. (2007) 'Physiology of the autonomic nervous system'. *American Journal of Pharmaceutical Education*, 71(4), 1-11.

253) Medina, O.P, Zhu, Y and Kairemo, K. (2004) 'Targeted liposomal drug delivery in cancer'. *Current Pharmaceutical Design*, 10(24), 2981-2989.

254) Messner, M, Kurkov SV, Brewster ME, Jansook P and Loftsson T. (2011) 'Self-assembly of cyclodextrin complexes: aggregation of hydrocortisone/cyclodextrin complexes'. *International Journal of Pharmaceutics*, 407(1-2), 174–183.

255) Messner, M., Kurkov, S.V., Jansook, P and Loftsson, T. (2010) 'Self-assembled cyclodextrin aggregates and nanoparticles'. *International Journal of Pharmaceutics*, 387(1-2), 199–208.

256) Mignet, N., Seguin, J and Chabot, G,G. (2013) 'Bioavailability of Polyphenol Liposomes: A Challenge Ahead'. *Pharmaceutics*, 5(3), 457-471.

257) Misra, A., Ganesh, S., Shahiwala, A and Shah, S.P. (2003) 'Drug delivery to the central nervous system: a review'. *Journal of Pharmacy and Pharmaceutical Sciences* : *A Publication of the Canadian Society for Pharmaceutical Sciences, Societe Canadienne des Sceiences Pharmaceutiques*, 6(2), 252–273.

258) Mitsopoulos, P and Suntres, Z.E. (2011) 'Protective effects of liposomal n-acetylcysteineagainst paraquat-induced cytotoxicity and gene expression'. *Journal of Toxicology*, 2011, 1-14.

259) Modak, S and Cheung, N.V. (2010) 'Neuroblastoma: Therapeutic strategies for a clinical enigma'. *Cancer Treatment Reviews*, 36(4), 307–317.

260) Mody, V.V., Cox, A., Shah, S., Singh, A., Bevins, W and Parihar, H. (2014) 'Magnetic nanoparticle drug delivery systems for targeting tumor'. *Applied Nanoscience*, 1(4), 385-392.

261) Moghaddam, M.G., Ahmed, B.H and Kermani, A.S. (2012) 'Biological activity of betulinic acid: A review'. *Pharmacology and Pharmacy*, 3(2), 119-123.

262) Moghimi, S.M., Hunter, A.C and Murray, J.C. (2001) 'Long-circulating and target-specific nanoparticles: Theory to practice'. *Pharmacological Reviews*, 53(2), 283–318.

263) Mokhtarieh, A. A., Davarpanah, S. J and Lee, M. K. (2013) 'Ethanol treatment a Non-extrusion method for asymmetric liposome size optimization'. *DARU Journal of Faculty of Pharmacy, Tehran University of Medical Sciences*, 21(1), 1-4.

264) Molecular structure of β-cyclodextrin. Available at: http://www.chemiedidaktik.uni-wuppertal.de/disido_cy/cyen/info/03_physical_cy.htm [Accessed 22 April 2015].

265) Monnaert, V., Betbeder, D., Fenart, L., Bricout, H., Lenfant, A.M., Landry, C., Cecchelli, R., Monflier, E and Tilloy, S. (2004) 'Effects of γ-and Hydroxypropyl-γ-cyclodextrins on the transport of doxorubicin across an in vitro model of blood-brain barrier'. *The Journal of Pharmacology and Experimental Therapeutics*, 311(3), 1115-1120.

266) Monteiro, N., Martins, A., Reis, R. L and Neves, N. M. (2014) 'Liposomes in tissue engineering and regenerative medicine'. *Journal of the Royal Society Interface*, 11(101), 1-24.

267) Mora, J and Gerald, W., L. (2004) 'Origin of neuroblastic tumors: clues for future therapeutics'. *Expert Review of Molecular Diagnostics*, 4(3), 293–302.

268) More, S. S., Itsara, M., Yang, X., Geier, E. G., Tadano, M. K., Seo, Y Vanbrocklin, H.F., Weiss, W.A., Mueller, S., Haas-Kogan, D.A., Dubois, S.G., Matthay, K.K and Giacomini, K. M. (2011) 'Vorinostat increases expression of functional norepinephrine transporter in neuroblastoma in vitro and in vivo model systems'. *Clinical Cancer Research : An Official Journal of the American Association for Cancer Research*, 17(8), 2339–2349.

269) Morell, P and Quarles, R.H. (1999) *The Myelin Sheath, Basic Neurochemistry: Molecular, Cellular and Medical Aspects*. 6th Edition. Philadelphia: Lippincott-Raven.

270) Morimoto, Y., Kobayashi, N., Shinohara, N., Myojo, T., Tanaka, I and Nakanishi, J. (2010) 'Hazard assessments of manufactured nanomaterials'. *Journal of Occupational Health*, 52(6), 325-334.

271) Mosse, Y. P., Laudenslager, M., Khazi, D., Carlisle, A.J., Winter, C.L., Rappaport, E and Maris, J.M. (2004) 'Germline PHOX2B mutation in hereditary neuroblastoma'. *American Journal of Human Genetics*, 75(4), 727-730.

272) Mosse, Y. P., Laudenslager, M., Longo, L., Cole, K. A., Wood, A., Attiyeh, E. F., Laquaglia, M. J., Sennett, R., Lynch, J. E., Perri, P., Laureys, G., Speleman, F., Kim, C., Hou, C., Hakonarson, H., Torkamani, A., Schork, N.J., Brodeur, G.M., Tonini, G.P., Rappaport, E., Devoto, M and Maris, J.M. (2008) 'Identification of ALK as a major familial neuroblastoma predisposition gene'. *Nature*, 455(7215), 930-935.

273) Motegi, A., Fujimoto, J., Kotani, M., Sakuraba, H and Yamamoto, T. (2004) 'ALK receptor tyrosine kinase promotes cell growth and neurite outgrowth'. *Journal of Cell Science*, 117(Pt 15), 3319–3329.

274) Motoyama, K., Nakashima, Y., Aramaki, Y., Hirayama, F., Uekama, K and Arima, H. (2011) '*In Vitro* Gene Delivery Mediated by Asialofeutin-Appended Cationic Liposomes Associated with γ-Cyclodextrin into Hepatocytes'. *Journal of Drug Delivery*, 2011, 1-13.

275) Mozafari, M., Z., Johnson, C., Hatziantoniou, S and Demetzos, C. (2008) 'Nanoliposomes and their applications in food nanotechnology'. *Journal of Liposome Research*, 18(4), 309-327.

276) Mufamadi, M.S., Pillay, V., Choonara, Y.E., Du Toit, L.C., Modi, G., Naidoo, D and Ndesendo, V.M.K. (2011) 'A Review on Composite Liposomal Technologies for Specialized Drug Delivery'. *Journal of Drug Delivery*, 2011, 1-19.

277) Mullauer, F.B., van Bloois, L., Daalhuisen, J.B., Ten Brink, M.S, Storm, G., Mefema, J.P., Schiffelers, R and Kessler, J.H. (2011) 'Betulinic acid delivered in liposomes reduces growth of human lung and colon cancers in mice without causing systemic toxicity'. *Anticancer Drugs*, 22(3), 223-233.

278) Mullauer, F.B., Kessler, J.H and Medema, J.P. (2010) 'Betulinic acid, a natural compound with potent anticancer effects'. *Anticancer Drugs*, 21(3), 215-227.

279) Muppidi, K., Pumerantz, A., S., Wang, J and Betageri, G. (2012) 'Development and stability studies of novel liposomal vancomycin formulations'. *ISRN Pharmaceutics*, (2012), 1-8.

280) Nakanishi, T., Fukushima, S., Okamoto K, Suzuki, M., Matsumura, Y., Yokoyama, M., Okano, T., Sakurai, Y and Kataoka, K. (2001) 'Development of the polymer micelle

carrier system for doxorubicin'. *Journal of Controlled Release: Official Journal of the Controlled Release Society*, 74(1-3), 295-302.

281) Nallamothu, R., Wood, G.C., Kiani. M.F., Moore, B.M., Horton, F.P and Thoma, L.A. (2006) 'A targeted liposome delivery system for combretastatin A4: formulation optimization through drug loading and in vitro release studies'. *PDA Journal of Pharmaceutical Science and Technology*, 60(3), 144-55.

282) Nappini, S., Kayal, T.A., Berti, D., Nordèn, B and Baglioni, P. (2011) 'Magnetically triggred release from giant unilamellar vesicles: Visualization by means of confocal microscopy'. *Journal of Physical Chemistry Letters*, 2(7):713-718.

283) Nasir, A., Harikumar S.L and Kaur A. (2012) 'Cyclodextrins: An excipients tool in drug delivery'. *International Research Journal of Pharmacy*, 3(4), 44-50.

284) Nasongkla, N., Bey, E., Ren, J., Ai, H., Khemtong, C and Guthi, J.S., Chin , S., Sherry , A.D., Boothman, D.A and Gao, J (2006) 'Multifunctional polymeric micelles as cancer-targeted, MRI-ultrasensitive drug delivery systems'. *Nano Letters*, 6(11), 2427-2430.

285) Navid, F., Santana, V. M and Barfield, R. C. (2010) 'Anti-GD2 antibody therapy for gd2-expressing tumors'. *Current Cancer Drug Targets*, 10(2), 200–209.

286) Nirale, N. M., Vidhate, R. D and Nagarsenker, M. S. (2009) 'Fluticasone propionate liposomes for pulmonary delivery'. *Indian Journal of Pharmaceutical Sciences*, 71(6), 709–711.

287) Nuchtern, J.G., London, W.B., Barnewolt, C.E., Naranjo, A., McGrady P. W., Geiger, J.D., Diller, L., Schmidt, M.L., Maris, J.M., Cohn, S.L and Shamberger, R.C. (2012) 'A prospective study of expectant observation as primary therapy for neuroblastoma in young infants: a children's oncology group study'. *Annals of Surgery*, 256(4), 573–580.

288) Odeh, F., Ismail S., I., Abu-Dahab, R., Mahmoud, I. S and Al Bawab., A. (2012) 'Thymoquinone in liposomes: a study of loading efficiency and biological activity towards breast cancer'. *Drug Delivery*, 19(8), 371–377.

289) Ogihara, T., Kagawa, H., Gao, Q and Mori, K (2010) 'A study of the molecular structure of phospholipids and the aggregation of liposomes using the molecular orbital method'. *Journal of Computer Chemistry Japapn*, 9(1), 43-46.

290) Ojogun, V., Vyas, S.M., Lehmler, H.J and Knutson, B.L (2010) 'Partitioning of homologous nicotinic acid ester prodrugs (nicotinates) into dipalmitoylphosphatidylcholine (dppc) membrane bilayers'. *Colloids and Surfaces. B, Biointerfaces*, 78(1), 75–84.

291) Ola, M.S., Nawaz, M and Ahsan, H. (2011) 'Role of Bcl-2 family proteins and caspases in the regulation of apoptosis'. *Molecular Cell Biology*, 351(1-2), 41-58.

292) Ong, W., Yang, Y., Cruciano, A. C and McCarley, R. L. (2008) 'Redox-triggered contents release from liposomes'. *Journal of the American Chemical Society*, 130(44), 14739–14744.

293) Orr, G.A., Verdier-Pinard, P., McDaid, H and Horwitz, S.B. (2003) 'Mechanisms of taxol resistance related to microtubules'. *Oncogene*, 22(47), 7280-7295.

294) Otero-Espinar, F.J., Torres-Labandeira, J.J. Alvarez-Lorenzo, C and Blanco- Méndez, J. (2010) 'Cyclodextrins in drug delivery systems'. *Journal of Drug Science and Technology*, 20(4), 289-301.

295) Palai, T.K and Mishra, S., R. (2015) 'Caspases: An apoptosis mediator'. *Journal of Advanced Veterinary Animal Research*, 2(1), 18-22.

296) Paliwal, S.R., Paliwal, R., Agrawal, G.P and Vyas, S.P. (2011) 'Liposomal nanomedicine for breast cancer therapy'. *Nanomedicine (London, England)*, 6(6), 1085-1100.

297) Pandey, M.K., Sung, B and Aggarwal, B.B. (2010) 'Betulinic acid suppresses STAT3 activation pathway through induction of protein tyrosine phosphatase SHP-1 in human multiple myeloma cells'. *International Journal of Cancer*, 127(2), 282-292.

298) Pardridge, W. M., (2005) 'The blood-brain barrier: bottleneck in brain drug development'. *NeuroRx : The Journal of the American Society for Experimental NeuroTherapeutics*, 2(1), 3–14.

299) Park J.R., Eggert, A and Caron, H. (2008) 'Neuroblastoma: biology, prognosis, and treatment'. *Pediatriac Clinics of North America*, 55(1), 97-120.

300) Parveen, S., Misra, R and Shao, S.K. (2012) 'Nanoparticles: a boon to drug delivery, therapeutics, diagnostics and imaging'. *Nanomedicine: Nanotechnology, Biology, and Medicine*, 8(2), 147–166.

301) Pasenkiewicz-Gierula, M., Róg, T., Kitamura, K and Kusumi, A (2000) 'Cholesterol effects on the phosphatidylcholine bilayer polar region: a molecular simulation study'. *Biophysical Journal*, 78(3), 1376–1389.

302) Patel, N and Panda, Subhranshu. 2012. Liposome drug delivery system: a critic review. *Journal of Pharmaceutical Science and Bioscientific Research (JPSBR)*, 2(4), 169-175.

303) Patel, S.S., Patel, M.S., Salampure, S., Vishwanath, B and Patel, N.M. (2010) 'Development and evaluation of liposomes for topical delivery of tacrolimus (Fk-506)'. *Journal of Scientific Research*, 2(3), 585-596.

304) Payne, N.I., Cosgrove, R.F., Green, A.P and Liu, L., (1987) 'In-vivo studies of amphotericin B liposomes derived from proliposomes: Effect of formulation on toxicity and tissue disposition of the drug in mice'. *The Journal of Pharmacy and Pharmacology*, 39(1) 24-28.

305) Payne, N.I., Timmins, P., Ambrose, C.V., Ward, M.D and Ridgway, F. (1986) 'Proliposomes: a novel solution to an old problem'. *Journal of Pharmaceutical Sciences*, 75(4), 325-329.

306) Pearson, A.D., Pinkerton, C.R., Lewis, I.J., Imeson, J., Ellershaw, C., Machin, D., European Neuroblastoma Study Group; Children's Cancer and Leukaemia Group (CCLG formerly United Kingdom Children's Cancer Study Group). (2008) 'High-dose rapid and standard induction chemotherapy for patients aged over 1 year with stage 4 neuroblastoma: A randomised trial'. *The Lancet Oncology*, 9(3), 247–256.

307) Pedroso de Lima, M.C., Neves, S., Filipe, A., Düzgüneş, N and Simões, S. (2003) 'Cationic liposomes for gene delivery: from biophysics to biological applications'. *Current Medicinal Chemistry*, 10(14), 1221-1231.

308) Peer, D., Karp, M.K., Hong, S., Farokhzad, O.C., Margalit, R and Langer, R. (2007) 'Nanocarriers as an emerging platform for cancer therapy'. *Nature Nanotechnology*, 2, 751-760.

309) Perche, F and Torchili, V.P. (2013) 'Recent trends in multifunctional liposomal nanocarriers for enhanced journal of drug delivery tumor targeting'. *Journal of Drug Delivery*, 2013, 1-32.

310) Perrie, Y and Rades, T. (2010) *Pharmaceutics: Drug Delivery and Targeting*. 2nd Edition. London: Pharmaceutical Press.

311) Philippot, J.R and Schuber, F. (1994) *Liposomes as tools in basic research and industry*. Florida: CRS Press.

312) Pisha, E., Chai, H., Lee, I.S., Chagwedera, T.E., Farnsworth, N.R., Cordell, G.A., Beecher, C.W.W., Fong, H.H.S., Kinghorn, A.D., Brown, D.M., Wani, M.C., Wall, M.E., Hieken, T.J., Gupta, T.K.D and Pezzuto, J.M. (1995) 'Discovery of betulinic acid as a selective inhibitor of human melanoma that functions by induction of apoptosis'. *Nature Medicine*, 1(10), 1046-1051.

313) Pitha, J., Irie, T., Sklar, P.B and Nye, J.S. (1988) 'Drug solubilizers to aid pharmacologists: Amorphous cyclodextrin derivatives'. *Life Sciences*, 43(6), 493-502.

314) Ponce, A.M., Vujaskovic, Z., Yuan, F., Needham, D and Dewhirst, M.W. (2006) 'Hyperthermia mediated liposomal drug delivery'. *International Journal of Hyperthermia: The Official Journal of European Society for Hyperthermic Oncology, North American Hyperthermia Group*, 22(3), 205–213.

315) Ponthan, F., Wickström, M., Gleissman, H., Fuskevåg, O.M., Segerström, L., Sveinbjörnsson, B., Redfern, C.P., Eksborg, S., Kogner, P and Johnsen, J.I. (2007) 'Celecoxib prevents neuroblastoma tumor development and potentiates the effect of chemotherapeutic drugs in vitro and in vivo'. *Clinical Cancer Research : An Official Journal of the American Association for Cancer Research*, 13(3), 1036-1044.

316) Popovska, O., Simonovska, J., Kavrakovski, Z and Rafajlovska, V. (2013) 'An overview: methods for preparation and characterization of liposomes as drug delivery systems'. *International Journal of Pharmaceutical and Phytopharmacological Research*, 3(2), 13-20.

317) Posadas, I., Santos, P and Ceña, V. (2012) 'Acetaminophen induces human neuroblastoma cell death through nfkb activation'. *PLOS One*, 7(11), 1-13.

318) Prathyusha, K., Muthukumaran, M and Krishnamoorthy, B. (2013) 'Liposomes as targeted drug delivery systems present and future prospective: a review'. *Journal of drug delivery and therapeutics*, 3(4), 195-201.

319) Puapermpoonsiri, U., Lipipun, V and Vardhanabhuti. (2005) 'Synergistic Effect of Phospholipid-Based Liposomes and Propylthiouracil on U-937 Cell Growth'. *Journal of Liposomes Research*, 15(3-4), 215-227.

320) Purves, D., Augustine, G.J., Fitzpatrick, D., Katz, L.C., LaMantia, A., McNamara and Williams, S.M. (2001) *Neuroscience*. 2nd Edition. Sunderland (Massachusetts U.S.A.): Sinauer Associates.

321) Puthalakath, H., Huang, D.C., O'Reilly, L.A., King, S.M and Strasser A. (1999) 'The proapoptotic activity of the Bcl-2 family member Bim is regulated by interaction with the dynein motor complex'. *Molecular Cell*, 3(3), 287-296.

322) Qi, W., Ding, D and Salvi, R.J. (2008) 'Cytotoxic effects of dimethyl sulphoxide (DMSO) on cochlear organotypic cultures'. *Hearing Research*, 236(1-2), 52-60.

323) Quail, D., F and Joyce, J.A. (2013) 'Microenvironmental regulation of tumor progression and metastasis'. *Nature Medicine*, 19(11), 1423-1437.

324) Raabe, E. H., Laudenslager, M., Winter, C., Wasserman, N., Cole, K., LaQuaglia, M., Maris, D.J., Mosse, Y.P and Maris, J.M. (2008) 'Prevalence and functional consequence of PHOX2B mutations in neuroblastoma'. *Oncogene*, 27(4), 469–476.

325) Radomski, A., Jurasz, P., Alonso-Escolano, D., Drews, M., Morandi, M., Malinski, T and Radomski, M.W. (2005) 'Nanoparticle-induced platelet aggregation and vascular thrombosis'. *British Journal of Pharmacology*, 146(6), 882-893.

326) Raghuvar Gopal, D.V., Narkar, A.A., Badrinath, Y., Mishra, K.P and Joshi, D.S. (2005) 'Betulinic acid induces apoptosis in human chronic myelogenous leukemia (CML) cell line K562 without altering the levels of Bcr-Abl'. *Toxicology Letters*, 155(3), 343-351.

327) Rajendran, P., Jaggi, M., Singh, M.K., Mukherjee, R and Burman, A.C. (2008) 'Pharmacological evaluation of C-3 modified Betulinic acid derivatives with potent anticancer activity'. *Investigational New Drugs*, 26(1), 25-34.

328) Ramana, L.N., Sethuraman, S., Ranga, U and Krishnan, U.M. (2010) 'Development of a liposomal nanodelivery system for nevirapine'. *Journal of Biomedical Science*, 17(1), 1-9.

329) Ran, S., Downes, A and Thorpe, P.E. (2002) 'Increased exposure of anionic phospholipids on the surface of tumor blood vessels'. *Cancer Research*, 62(21), 6132-6140.

330) Rastogi, V., Yadav, P., Bhattacharya, S.S., Mishra, A.K., Verma, N., Verma, A and Pandit, J.K. (2014) 'Carbon Nanotubes: An Emerging Drug Carrier for Targeting Cancer Cells'. *Journal of Drug Delivery*, 2014, 1-23.

331) Reddy, L.H and Couvreur, P. (2008) 'Novel approaches to deliver gemcitabine to cancers'. *Current Pharmaceutical Design*, 14(11), 1124-1137.

332) Redzic, Z. (2011) 'Molecular biology of the blood-brain and the blood-cerebrospinal fluid barriers: similarities and differences'. *Fluids and Barriers of the CNS*, 8(1), 1-23.

333) Reiner, T., Parrondo, R., de Las Pozas, A., Palenzuela, D and Perez-Stable, C. (2013) 'Betulinic acid selectively increases protein degradation and enhances prostate cancer-specific apoptosis: possible role for inhibition of deubiquitinase activity'. *PLoS One*. 8(2), 1-11.

334) Risinger, A.L., Giles, F.J and Mooberry, S.L. (2009) 'Microtubule dynamics as a target in oncology'. *Cancer Treatment Reviews*, 35(3), 255-261.

335) Rohrer, T., Trachsel, D., Engelcke, G and Hammer, J. (2002) 'Congenital central hypoventilation syndrome associated with Hirschsprung's disease and neuroblastoma: case of multiple neurocristopathies'. *Pediatric Pulmonology*, 33(1), 71-76.

336) Rong, Y., Durden, D.L., Van Meir, E.G and Brat, D.J. (2006) 'Pseudopalisading necrosis in glioblastoma: a familiar morphologic feature that links vascular pathology, hypoxia, and angiogenesis'. *Journal of Neuropathology and Experimental Neurology*, 65(6), 529-539.

337) Rubio-Moscardo, F., Blesa, D., Mestre, C., Siebert, R., Balasas, T., Benito, A., Rosenwald, A., Climent, J., Martinez, J.I., Schilhabe, l.M., Karran, E.L., Gesk, S., Esteller, M., de Leeuw, R., Staudt, L.M., Fernandez-Luna, J.L., Pinkel, D., Dyer, M.J and Martinez-Climent, J.A. (2005) 'Characterization of 8p21.3 chromosomal deletions in Bcell lymphoma: TRAIL-R1 and TRAIL-R2 as candidate dosage-dependent tumor suppressor genes'. *Blood*, 106(9), 3214–3222.

338) Ruozi, B., Belletti, D., Tombesi, A., Tosi, G., Bondioli, L., Forni, F and Vandelli, M.A. (2011) 'AFM, ESEM, TEM, and CLSM in liposomal characterization: a comparative study'. *International Journal of Nanomedicine*, 6, 557-563.

339) Sabeti, B., Noordin, M.I., Mohd, S., Hashim, R., Dahlan, A and Javar, H.A. (2014) 'Development and characterization of liposomal doxorubicin hydrochloride with palm oil'. *BioMedical Research International*, 2014, 1-6.

340) Saelens, X., Festjens, N., Walle, L.V., van Gurp, M., van Loo, G and Vandenabeele, P. (2004) 'Toxic protiens released from mitochondria in cell death'. *Oncogene*, 23(16), 2861-2874.

341) Saha, R., Verma, P.K., Mitra, R.K and Pal, S.K. (2011) 'Structural and dynamical characterization of unilamellar AOT vesicles in aqueous solutions and their efficacy as potential drug delivery vehicle'. *Colloids and Surfaces. B, Biointerfaces*, 88(1), 345-353.

342) Sahoo, S.K and Labhasetwar, V. (2005) 'Enhanced antiproliferative activity of transferrin-conjugated paclitaxel-loaded nanoparticles is mediated via sustained intracellular drug retention'. *Molecular Pharmaceutics*, 2(5), 373-383.

343) Saim, M. (2012) *Cerebral Spinal Fluid and Intracranial pressure* [PowerPoint Presentation]. Available at: http://www.slideshare.net/saim_18/cerebrospinal-fluid-and-intracranial-pressure [Accessed 21 April 2015].

344) Saito, Y and Wright, E.M. (1983) 'Bicarbonate transport across the frog choroid plexus and its control by cyclic nucleotides'. *The Journal of Physiology*, 336, 635-648.

345) Sanchis, J., Canal, F., F., Lucas, R and Vicent, M.J. (2010) 'Polymer-drug conjugates for molecular targets'. *Nanomedicine (London, England)*, 5(6), 915-935.

346) Sankaram, M.B and Thompson, T.E. (1991) 'Cholesterol-induced fluid-phase immiscibility in membranes (magic-ange spinning NMR/bralcals/hydrogen bonding/^{13}C relaaion rates)'. *Proceedings of the National Academy of Sciences*, 88, 8686-8690.

347) Sankari, S.L., Masthan, K.M.K., Babu, N., A., Bhattacharjee, T and Elumalai, M. (2012) 'Apoptosis in Cancer- An Update'. *Asian Pacific Journal of Cancer Prevention*, 13(10), 4873-4878.

348) Santaguida, S., Janigro, D., Hossain, M., Oby, E., Rapp, E and Cucullo, L. (2006) 'Side by side comparison between dynamic versus static models of blood-brain barrier in vitro: a permeability study'. *Brain Research*, 1109(1), 1-13.

349) Schacht, J., Talaska, A. E and Rybak, L. P. (2012) 'Cisplatin and aminoglycoside antibiotics: hearing loss and its prevention'. *Anatomical Record (Hoboken, N.J. : 2007)*, 295(11), 1837–1850.

350) Scheinfeld, N and Bangalore, S. (2006) 'Facial edema induced by isotretinoin use: a case and a review of the side effects of isotretinoin'. *Journal of Drugs in Dermatology : JDD*, 5(5), 467–468.

351) Schimmer, A.D. (2004) 'Inhibitor of apoptosis proteins: translating basic knowledge into clinical practice'. *Cancer Research*, 64(20), 7183–7190.

352) Schmidt, M.L., Kuzmanoff, K.L., Ling-Indeck, L and Pezzuto, J.M. (1997) 'Betulinic acid induces apoptosis in human neuroblastoma cell lines'. *European Journal of Cancer (Oxford, England: 1990)*, 33(12), 2007-2010.

353) Schmidt, M.L., Lukens, J.N., Seeger, R.C., Brodeur, G.M., Shimada, H., Gerbing, R.B., Stram, D.O., Perez, C., Haase, G.M and Matthay, K.K. (2000) 'Biologic factors determine prognosis in infants with stage IV neuroblastoma: A prospective Children's Cancer Group study'. *Journal of Clinical Oncology: Official Journal of the American Society of Clinical Oncology*, 18(6), 1260–1268.

354) Schneider, C., Wicht, H., Enderich, J., Wegner, M and Rohrer, H. (1999) 'Bone morphogenetic proteins are required in vivo for the generation of sympathetic neurons'. *Neuron*, 24(4), 861-870.

355) Schneider, P and Tschopp, J. (2000) 'Apoptosis induced by death receptors'. *Pharmaceutica Acta Helvetiae*, 74(2-3), 281-286.

356) Schönherr, C., Yang, H.L, Vigny, M., Palmer, R.H and Hallberg, B. (2010) 'Anaplastic lymphoma kinase activates the small GTPase Rap1 via the Rap1-specific GEF C3G in both neuroblastoma and PC12 cells'. *Oncogene*, 29(19), 2817–2830.

357) Schulz, M and Engelhardt, B. (2005) 'The circumventricular organs participate in the immunopathogenesis of experimental autoimmune encephalomyelitis'. *Cerebrospinal Fluid Research*, 30, 2-8.

358) Shahi, M.H., A. Lorente and Castresana, J.S (2008) 'Hedgehog signalling in medulloblastoma, glioblastoma and neuroblastoma'. *Oncology Reports*, 19(3), 681-688.

359) Shalaby, T., Fiaschetti, G., Baumgartner, M and Grotzer, M.A. (2014) 'MicroRNA signatures as biomarkers and therapeutic target for CNS embryonal tumors: The pros and the cons'. *International Journal of Molecular Science*, 15(11), 21554-21586.

360) Shanmugam, M.K., Nguyen, A.H., Kumar, A.P., Tan, B.K., Sethi, G. (2012) 'Targeted inhibition of tumor proliferation, survival, and metastasis by pentacyclic triterpenoids: potential role in prevention and therapy of cancer'. *Cancer Letters*, 320(2), 158–170.

361) Sharp, S.E., Gelf, M.J and Shulkin, B.L. (2011) 'Pediatrics: diagnosis of neuroblastoma'. *Seminars in Nuclear Medicine*, 41(5), 345-353.

362) Shepherd, G.M. (1987) *Neurobiology*. 2nd Edition. Oxford: Oxford University Press.

363) Siegal, R., Ma, J., Zou, Z and Jemal, A. (2014) 'Cancer Statistics, 2014'. *CA: A Cancer Journal for Clinicians*, 64(1), 9-29.

364) Silke, J., Hawkins, C.J., Ekert, P.G., Chew, J., Day, C.L., Pakusch, M., Verhagen, A.M and Vaux, D.L. (2002) 'The anti-apoptotic activity of XIAP is retained upon mutation of both the caspase-3- and caspase-9-interacting sites'. *The Journal Cell Biology*, 157(1), 115–24.

365) Simões-Costa, M and Bronner, M. (2013) 'Insights into neural crest development and evolution from genomic analysis'. *Genome Research*, 23(7), 1069-1080.

366) Simões, S., Moreira, J.N., Fonseca, C., Duzgunes, N and de Lima, M.C. (2004) 'On the formulation of pH-sensitive liposomes with long circulating times'. *Advanced Drug Delivery Reviews*, 56(7), 947-965.

367) Simon, T., Längler, A., Harnischmacher, U., Frühwald, M.C., Jorch, N., Claviez, A., Berthold, F and Hero, B. (2007) 'Topotecan, cyclophosphamide, and etoposide (TCE) in the treatment of high-risk neuroblastoma. Results of a phase-II trial'. *Journal of Cancer Research and Clinical Oncology*, 133(9), 653-661.

368) Simon, T., Spitz, R., Faldum, A., Hero, B and Berthold, F. (2004) 'New definition of low-risk neuroblastoma using stage, age, and 1p and MYCN status'. *Journal of Pediatric Hematology/Oncology*, 26(12), 791–796.

369) Singh, H.P., Tiwary, A.K and Jain, S. (2010) 'Preparation and *in vitro, in vivo* characterisation of elastic liposomes encapsulating cyclodextrin-colchine complexes for topical delivery of colchicine'. *Yakugaku Zasshi: Journal of Pharmaceutical Society of Japan*, 130(3), 397-407.

370) Small, D.M. (1986) *The Physical Chemistry of Lipids: From Alkanes to Phospholipids*. 1st Edition. New York: Plenum Press.

371) Şoica, C., Danciu, C., Savoiu-Balint, G., Borcan, F., Ambrus, R., Zupko, I., Bojin, F., Coricovac, D., Ciurlea, S., Avram, S., Dehelean, C.A., Olariu, T and Matusz, P. (2014) 'Betulinic acid in complex with a gamma-cyclodextrin derivative decreases proliferation and in vivo tumor development of non-metastatic and metastatic B164A5 cells'. *International Journal of Molecular Sciences*, 15(5), 8235-8255.

372) Şoica, C., Dehelean, C., Danciu, C., Wang, H., M., Wenz, G., Ambrus, R., Bojin, F and Anghe, M. (2012) 'Betulin complex in γ-Cyclodextrin derivatives: Properties and antineoplasic activities in vitro and in vivo tumor models'. *International Journal of Molecular Sciences*, 13(11), 14992-15011.

373) Sonawane, P., Cho, H.E., Tagde, A., Verlekar, D, Yu, A.L., Reynolds, C.P and Kang, M.H. (2014) 'Metabolic characteristics of 13-cis-retinoic acid (isotretinoin) and anti-tumour activity of the 13-cis-retinoic acid metabolite 4-oxo-13-cis-retinoic acid in neuroblastoma'. *British Journal of Pharmacology*, 171(23), 5330-5344.

374) Sotthivirat, S., Haslam J.L and Stella V.J. (2007) 'Controlled porosity-osmotic pump pellets of a poorly water-soluble drug using sulfobutyl ether-beta-cyclodextrin, (SBE) (7M)-b-CD, as a solubilizing and osmotic agent'. *Journal of Pharmaceutical Sciences*, 96(6), 2364-2374.

375) Sotthivirat, S., Haslam, J.L., Lee, P.I., Rao, V.M and Stella, V.J. (2009) 'Release mechanisms of a sparingly water-soluble drug from controlled porosity-osmotic pump pellets using sulfobutyletherb-cyclodextrin as both a solubilizing and osmotic agent'. *Journal of Pharmaceutical Sciences*, 98(6), 1992-2000.

376) Sou, K., Goins, B., Oyajobi, B. O., Travi, B. L and Phillips, W. T. (2011) 'Bone marrow-targeted liposomal carriers'. *Expert Opinion on Drug Delivery*, 8(3), 317–328.

377) Stahl, S., M. (2008) *Stahl's Essential Psychopharmacology: Neuroscientific Basis and Practical Application*. 3rd Edition. New York: Cambridge University Press.

378) Stamatovic, S. M., Keep, R. F and Andjelkovic, A. V. (2008) 'Brain endothelial cell-cell junctions: how to "open" the blood brain barrier'. *Current Neuropharmacology*, 6(3), 179–192.

379) Stamm, M.T., Zha, Z., Jiang, L., Dai, Z and Zohar, Y. (2012) 'Functionalization of Ceramic Liposomal Nanoparticles, Cerasomes, with Antibodies'. *Physical Chemistry and Biophysics*, 2(1), 1-5.

380) Steele, J.C., Warhurst, D.C., Kirby, G.C and Simmonds, M.S. (1999) '*In vitro* and *in vivo* evaluation of betulinic acid as an antimalarial'. *Phytotherapy Research : PTR*, 13(2), 115-119.

381) Stella, V.J and He, Q. (2008) 'Cyclodextrins'. *Toxicologic Pathology*, 36(1), 30-42.

382) Stiller, A., C. (2004) 'Epidemiology and genetics of childhood cancer'. *Oncogene*, 23(38), 6429–6444.

383) Subczynski, W. K., Wisniewska, A., Yin, J. J., Hyde, J. S and Kusumi, A. (1994) 'Hydrophobic barriers of lipid bilayer-membranes formed by reduction of water penetration by alkyl chain unsaturation and cholesterol'. *Biochemistry*, 33(24), 7670–7681.

384) Sun, C., Wang, J., Liu, J., Qiu, L., Zhang, W and Zhang, L. (2013) 'Liquid proliposomes of nimodipine drug delivery system: preparation, characterization, and pharmacokinetics'. *AAPS PharmSciTech*, 14(1), 332–338.

385) Suntres, Z.E. (2011) 'Liposomal Antioxidants for Protection against Oxidant-Induced Damage'. *Journal of Toxicology*, 2011, 1-16.

386) Sur, S., Fries, A.C., Kinzler, K.W., Zhou, S and Vogelstein, B. (2014) 'Remote loading of preencapsulated drugs into stealth liposomes'. *Proceedings of the National Academy of Sciences of the United States of America*, 111(6), 2283-2288.

387) Susin, S.A., Daugas, E., Ravagnan, L., Samejima, K., Zamzami, N., Loeffler, M., Costantini, P., Ferri, K.F., Irinopoulou, T., Prevost, M.C., Brothers, G., Mak, T.W., Penninger, J, Earnshaw, W.C and Kroemer, G. (2000) 'Two distinct pathways leading to nuclear apoptosis'. *Journal of Experimental Medicine*, 192(4), 571–580.

388) Svenson, S and Tomalia, DA. (2005) 'Dendrimers in biomedical applications-reflections on the field'. *Advanced Drug Delivery Reviews*, 57(15), 2106-2129.

389) Swaaya, D.V and deMello, A. (2013) 'Microfluidic methods for forming liposome'. *Lab on a Chip*, 13(5), 752-767.

390) Szente, L and Szejtli, J. (1999) 'Highly soluble cyclodextrin derivatives: Chemistry, properties, and trends in development'. *Advances in Drug Delivery Reviews*, 36(1), 17-28.

391) Szejtli, J. (1998) ‘Introduction and general overview of cyclodextrin chemistry’. *Chemistry Reviews*, 98(5), 1743–1754.

392) Szoka, F., Jr and Papahajopoulos, D. (1980) ‘Comparative properties and methods of preparation of lipid vesicles (liposomes)’. *Annual Review of Biophysics and Bioengineering*, 9, 467-508.

393) Takada, Y and Aggarwal, B.B. (2003) ‘Betulinic acid suppresses carcinogen-induced NF-kB activation through inhibition of I kBα kinase and p65 phosphorylation: Abrogation of clyclooxigenase-2 and matrix metalloprotienase 9’. *Journal of Immunology*, 171(6), 3278-86.

394) Takeuchi, H., Kojima, H., Yamamoto, H and Kawashima Y. (2001) ‘Passive targeting of doxorubicin with polymer coated liposomes in tumor bearing rats’. *Biological and Pharmaceutical Bulletin*, 24(7), 795–799.

395) Taneyhill, L.A. (2008) ‘To adhere or not to adhere: the role of Cadherins in neural crest development’. *Cell Adhesion and Migration*, 2(4), 223-230.

396) Taralkar, S., V and Chattopahyay, S. (2012) ‘A HPLC Method for Determination of Urosolic Acid and Betulinic Acids from their Methanol Extracts of Vitex Negundo Linn’. *Journal of Analytical and Bioanalytical Techniques*, 3(3), 1-6.

397) Theveneau, E and Mayor, R. (2012) ‘Neural crest delamination and migration: From epithelium-to-mesenchyme transition to collective cell migration’. *Developmental Biology*, 366(1), 34–54.

398) Thornberry, N. A and Lazebnik, Y. (1998) ‘Caspases: enemies within’. *Science*, 281(5381), 1312– 1316.

399) Thorpe PE. (2004) ‘Vascular targeting agents as cancer therapeutics’. *Clinical Cancer Research : An Official Journal of the American Association for Cancer Research*, 10(2), 415-427.

400) Three of the most common types of cyclodextrins (CDs) image. Available at: http://unam.bilkent.edu.tr/~uyar/images/Research_fig2.png [Accessed 14 April 2015].

401) Thuerauf, N and Fromm, M.F. (2006) ‘The role of the transporter P-glycoprotein for disposition and effects of centrally acting drugs and for the pathogenesis of CNS diseases’. *European Archives of Psychiatry and Clinical Neuroscience*, 256(5), 281-286.

402) Thurnher, D., Turhani, D., Pelzmann, M., Wannemacher, B., Knerer, B., Formanek, M., Wacheck, V and Selzer, E. (2003) ‘Betulinic acid: a new cytotoxic compound against malignant head and neck cancer cells’. *Head and Neck*, 25(9), 732-740.

403) Tiwari, G., Tiwari, R and Rai, A.K. (2010) 'Cyclodextrins in delivery systems: Applications'. *Journal of Pharmacy and Bioallied Sciences*, 2(2), 72-79.

404) Tiwari, G., Tiwari, R., Sriwastawa, B., Bhati, L., Pandey, S., Pandey, P and Bannerjee, S. K. (2012) 'Drug delivery systems: An updated review'. *International Journal of Pharmaceutical Investigation*, 2(1), 2–11.

405) Tolstikov, G., Flekhter, O., Schultz, E., Baltina, L and Tolstikov, A. (2005) 'Betulin and its derivatives. Chemistry and biological activity'. *Chemistry for Sustainable Development*, 13, 1-29.

406) Torchilin, V.P. (2005) 'Recent advances with liposomes as pharmaceutical carriers'. *Nature Reviews Drug Discovery*, 4(2):145-160.

407) Torchilin, V.P. (2010) 'Passive and active drug targeting: drug delivery to tumour as an example'. *Handbook of experimental pharmacology*, 2010(197), 3-35.

408) Torchilin, V.P and Weissig, V. (2003) *Liposomes: A practical approach*. 2nd Edition. New York: Oxford University Press.

409) Torchilin, V.P., Omelyanenko, V.G and Lukyanov, A.N. (1992) 'Temperature-dependent aggregation of pH-sensitive phosphatidyl ethanolamine-oleic acid-cholesterol liposomes as measured by fluorescent spectroscopy'. *Analytical Biochemistry*, 207(1), 109-113.

410) Trahair, T.N., Vowels, M.R., Johnston, K., Cohn, R.J., Russell, S.J., Neville, K.A., Carroll, S., Marshall, G.M. (2007) 'Long-term outcomes in children with high-risk neuroblastoma treated with autologous stem cell transplantation' *Bone Marrow Transplant*, 40(8), 741–746.

411) Trochet, D., Bourdeaut, F., Janoueix-Lerosey, I., Deville, A., de Pontual, L., Schleiermacher, G., Coze, C., Philip, N., Frébourg, T., Munnich, A., Lyonnet, S., Delattre, O and Amiel, J. (2004) 'Germline mutations of the paired-like homeobox 2B (PHOX2B) gene in neuroblastoma'. *American Journal of Human Genetics*, 74(4), 761–764.

412) Troutman, T. S., Leung, S. J and Romanowski, M. (2009) 'Light-Induced Content Release from Plasmon Resonant Liposomes'. *Advanced Materials (Deerfield Beach, Fla.)*, 21(22), 2334–2338.

413) Tsutsumimoto, T., Williams, P and Yoneda, T. (2014) 'The SK-N-AS human neuroblastoma cell line develops osteolytic bone metastases with increased angiogenesis and COX-2 expression'. *Journal of Bone Oncology*, 3(3-4) 67–76.

414) Upadhyay, R.K. (2014) ‘Drug delivery system, CNS Protection, and the blood brain barrier’. *BioMed Research International*, 2014, 1-37.

415) Vafaei, S.Y., Dinarvand, R., Esmaeili, M., Mahjub, R and Toliyat, T. (2014) ‘Controlled-release drug delivery system based on fluocinolone acetonide-cyclodextrin inclusion complex incorporated in multivesicular liposomes’. *Pharmaceutical development and technology*, 26, 1-7.

416) van Loo, G., van Gurp, M., Depuydt, B., Srinivasula, S.M., Rodriguez, I., Alnemri, E.S., Gevaert, K., Vandekerckhove, J., Declercq, W and Vandenabeele, P. (2002) ‘The serine protease Omi/HtrA2 is released from mitochondria during apoptosis. Omi interacts with caspase-inhibitor XIAP and induces enhanced caspase activity’. *Cell Death Differentiation*, 9(1), 20–26.

417) Van Meir, E.G., Hadjipanayis, C.G., Norden, A.D., Shu, H.K., Wen, P.Y and Olson, JJ. (2010) ‘Exciting new advances in neuro-oncology: the avenue to a cure for malignant glioma’. *CA: A Cancer Journal for Clinicians*, 60(3), 166–193.

418) van Noesel, M.M and Versteeg, R. (2004) ‘Pediatric neuroblastomas: Genetic and epigenetic danse macabre’. *Gene*, 325, 1–15.

419) Veal, G.J., Errington, J., Rowbotham, S.E., Illingworth, N.A., Malik, G., Cole, M., Daly, A.K., Pearson, A.D and Boddy, A.V. (2013) ‘Adaptive dosing approaches to the individualization of 13-cis-retinoic acid (isotretinoin) treatment for children with high-risk neuroblastoma’. *Clinical cancer research : an official journal of the American Association for Cancer Research*, 19(2), 469-479.

420) Veiseh, O., Gunn, J and Zhang, M. (2010) ‘Design and fabrication of magnetic nanoparticles for targeted drug delivery and imaging’. *Advanced Drug Delivery Reviews*, 62(3), 284-304.

421) Venegas, B., Zhu, W., Haloupek, N. B., Lee, J., Zellhart, E., Sugár, I. P., Kiani, M.F and Chong, P. L. (2012) ‘Cholesterol Superlattice Modulates CA4P Release from Liposomes and CA4P Cytotoxicity on Mammary Cancer Cells’. *Biophysical Journal*, 102(9), 2086–2094.

422) Vesaratchanon, S., Nikolov, A and Wasan, D.T. (2007) ‘Sedimentation in nano-colloidal dispersions: effects of collective interactions and particle charge’. *Advances in Colloid and Interface Science*, 134-135, 268–278.

423) Villunger, A., Michalak, E.M., Coultas, L., Mullauer, F., Böck, G., Ausserlechner, M.J., Adams, J.M and Strasser, A (2003) ‘p53- and drug-induced apoptotic responses

mediated by BH3-only proteins puma and noxa'. *Science (New York, N.Y.)*, 302(5647), 1036-1038.

424) Visser, C. C., Stevanović, S., Voorwinden L. H., van Bloois, L., Gaillard, P. J., Danhof, M., Crommelin, D. J. A and de Boer, A. G. (2005) 'Targeting liposomes with protein drugs to the blood-brain barrier in vitro'. *European Journal of Pharmaceutical Sciences: Official Journal of the European Federation for Pharmaceutical Sciences*, 25(2-3), 299-305.

425) Vyas, J., Vyas, P and Krutika, S. (2011) 'Formulation and evaluation of topical niosomal gel of erythromycin'. *International Journal of Pharmacy and Pharmaceutical Sciences*, 3(1), 122-126.

426) Vyas, S.P and Khar, R.K. (2002) *Targeted and controlled drug delivery*. 1rst Edition. New Delhi: CBS publishers.

427) Wagner, A and Vorauer-Uhl, K. (2011) 'Liposome Technology for Industrial Purpose'. *Journal of Drug Delivery*, 2011, 1-9.

428) Wagner, M.K., Li, F., Li, J., Li, X-F and Chris, X. (2010) 'Use of quantum dots in the development of assays for cancer biomarkers'. *Analytical and Bioanalytical Chemistry*, 397(8), 3213–3224.

429) Wakamatsu, Y., Watanabe, Y., Nakamura, H and Kondoh, H. (1997) 'Regulation of the neural crest cell fate by N-myc: promotion of ventral migration and neuronal differentiation'. *Development (Cambridge, England)*, 124(10), 1953-1962.

430) Wang, K. Zhang, H., Attiyeh, E.F., Winter, C., Hou, C., Schnepp, R.W., Diamond, M., Bosse, K., Mayes, P.A., Glessner, J., Kim, C., Frackelton, E., Garris, M., Wang, Q., Glaberson, W., Chiavacci, R., Nguyen, L., Jagannathan, J., Saeki, N., Sasaki, H., Grant, S.F., Iolascon, A., Mosse, Y.P., Cole, K.A., Li, H., Devoto, M., McGrady, P.W., London, W.B.,Capasso, M., Rahman, N., Hakonarson and H., Maris, J.M (2011) 'Integrative genomics identifies LMO1 as a neuroblastoma oncogene'. *Nature*, 469(7329), 216-220.

431) Wang, Q., Zhu, Y and Yang, P. (2013) 'Is Mda-7/IL-24 a Potential Target and Biomarker for Enhancing Drug Sensitivity in Human Glioma U87 Cell Line?'. *The Anatomical Record*, 296(8), 1154-1160.

432) Wang, W.S., Chiou, T.J., Liu, J.H., Fan, F., F.S., Yen, C.C and Chen, P. (2000) 'Vincristine-induced Dysphagia Suggesting Esophageal Motor Dysfunction: A Case Report'. *Japanese Journal of Clinical Oncology*, 30(11), 515-518.

433) Weifen, Z., Xiguang, C., Piwu, L., Qiangzhi, H., Huiyun, Z and Dongsu, C. (2008) 'Chitosan and β-cyclodextrin microspheres as pulmonary sustained delivery systems'. *Journal of Wuhan University of Technology-Materials Science Edition*, 23(4), 541-546.

434) Wen, P.Y and Kesari, S. (2008) 'Malignant gliomas in adults'. *The New England Journal of Medicine National*, 359(5), 492-507.

435) Westphal, M and Lamszus, K. (2011) 'The neurobiology of gliomas: from cell biology to the development of therapeutic approaches'. *Nature Reviews Neuroscience*, 12(9), 495–508.

436) Wick, W., Grimmel, C., Wagenknecht, B., Dichgans, J and Weller, M. (1999) 'Betulinic acid-induced apoptosis in glioma cells: A sequential requirement for new protein synthesis, formation of reactive oxygen species, and caspase processing'. *The Journal of Pharmacology and Experimental Therapeutics*, 289(3), 1306-1312.

437) Wickström, M., Johnsen, J.I., Ponthan, F., Segerström, L., Sveinbjörnsson, B., Lindskog, M., Lövborg, H., Viktorsson, K., Lewensohn, R., Kogner, P., Larsson, R., Gullbo, J. (2007) 'The novel melphalan prodrug J1 inhibits neuroblastoma growth in vitro and in vivo'. *Molecular Cancer Therapeutics*, 6(9), 2409–2417.

438) Wislet-Gendebien, S., Laudet, E., Neirinckx, V and Rogister, B. (2012) 'Adult bone marrow: which stem cells for cellular therapy protocols in neurodegenerative disorders?'. *Journal of Biomedicine and Biotechnology*, 2012, 1-10.

439) Wong, R.S.Y. (2011) 'Apoptosis in cancer: from pathogenesis to treatment'. *Journal Experimental and Clinical Cancer Research*, 30(1), 1-14.

440) Wu, J., Liu, L., Yen, R.D., Catana, A., Nantz, M.H and Zern, M.A. (2004) 'Liposome-mediated extracellular superoxide dismutase gene delivery protects against acute liver injury in mice'. *Hepatology (Balitimore, Md.)*, 40(1), 195-204.

441) Xia, M., Huang, R., Witt, K. L., Southall, N., Fostel, J., Cho, M.H, Jadhav, A., Smith, C.S., Inglese, J., Portier, C.J., Tice, R.R and Austin, C. P. (2008) 'Compound cytotoxicity profiling using quantitative high-throughput screening'. *Environmental Health Perspectives*, 116(3), 284–291.

442) Xu, T., Pang, Q., Zhou, D., Zhang, A., Luo, S., Wang, Y and Yan, X. (2014) 'Proteomic investigation into betulinic acid-induced apoptosis of human cervical cancer Hela cells'. *PLoS ONE*, 9(8), 1-11.

443) Yang, F., Jin, C., Jiang, Y., Li, J., Di, Y., Ni, Q and Fu, D. (2011) 'Liposome based delivery systems in pancreatic cancer treatment: From bench to bedside'. *Cancer Treatment Reviews*, 37(8), 633-642.

444) Yang, R. K and Sondel, P. M. (2010) 'Anti-GD2 Strategy in the Treatment of Neuroblastoma'. *Drugs of the Future*, 35(8), 1-15.

445) Yariş, N., Yavuz, M.N., Reis, A., Yavuz, A.A., Okten, A. (2004) 'Primary cerebral neuroblastoma: a case treated with adjuvant chemotherapy and radiotherapy'. *The Turkish Journal of Pediatrics*, 46(2), 182-185.

446) Yigit, M.V., Moore, A and Medarova, Z. (2012) 'Magnetic nanoparticles for cancer diagnosis and therapy'. *Pharmaceutical Research*, 29(5), 1180-1188.

447) Yogeeswari, P and Sriram, D. (2005) 'Betulinic acid and its derivatives: a review on their biological properties'. *Current Medicinal Chemistry*, 12(6), 657-666.

448) Yong, K-T., Wang, Wang, Y., Roy, I., Rui, H., Swihart, M., Law, W-C., Kwak, S.K., Ye, L., Liu, J., Mahajan, S.D and Reyonds, J.L. (2012) 'Preparation of Quantum Dot/Drug Nanoparticle Formulations for Traceable Targeted Delivery and Therapy'. *Theranostics*, 2(7), 681-694.

449) Yoo, S., Y and Kwon, S. M. (2013) 'Angiogenesis and its therapeutic opportunities'. *Mediators of Inflammation*, 2013, 1-11.

450) Yousefi, A., Esmaeili, F., Rahimian, S., Atyabi, F and Dinarvand, R. (2009) 'Preparation and *In Vitro* Evaluation of a Pegylated Nano-Liposomal Formulation Containing Docetaxel'. *Scientica Pharmaceutica*, 77, 453-464.

451) Zage, P.E., Kletzel, M., Murray, K., Marcus, R., Castleberry, R., Zhang, Y., London, W.B., Kretschmar, C.; Children's Oncology Group C. (2008) 'Outcomes of the POG 9340/9341/9342 trials for children with high-risk neuroblastoma: A report from the Children's Oncology Group'. *Pediatriac Blood and Cancer*, 51(6), 747–753.

452) Zhao, L and Feng, S. (2004) 'Effects of lipid chain length on molecular interactions between paclitaxel and phospholipid within model biomembrane'. *Journal of Colloid and Interface Science*, 274(1) 55-68.

453) Zhao, L and Feng, S. (2005) 'Effects of lipid chain unsaturation and headgroup type on molecular interactions between paclitaxel and phospholipid within model biomembrane'. *Journal of Colloid and Interface Sci*ence, 285(1), 326-335.

454) Zidovetzki, R and Levitan, I. (2007) 'Use of cyclodextrins to manipulate plasma membrane cholesterol content: evidence, misconceptions and control strategies'. *Biochimica et Biophysica Acta*, 1768(6), 1311–1324.

455) Zou, H., Henzel, W.J., Lui, X., Lutschg, A and Wang, X. (1997) ‘Apaf-1, a human protein homologous to C.elegans CED-4, participates in cytochrome c-dependent activation of caspase-3’. *Cell*, 90(3), 405-413.

456) Zuco, V., Supino, R., Righetti, S.C., Cleris, L., Marches,i E and Gambacorti-Passerini, C., Fromelli, F. (2002) ‘Selective cytotoxicity of betulinic acid on tumor cell lines, but not on normal cells’. *Cancer Letters*, 175(1), 17-25.